
# *In-vitro* investigation of factors affecting the fate of dry powders in the lung

Emanuela Cingolani
MSc (Hons)

Thesis submitted to the University of Nottingham
for the degree of Doctor of Philosophy

September 2016

# Acknowledgements

First and foremost, I would like to thank my supervisors Dr. Cynthia Bosquillon (University of Nottingham), Dr. Snow Stolnik (University of Nottingham) and Dr. Robyn Sadler (GlaxoSmithKline) for their endless and invaluable support, and for being friendly and motivating at all times.

Special thanks go to the technical team in Boots Science Building: Mrs. Christine Grainger-Boultby, Mr. Paul Cooling, Mr. Thomas Boots and Mrs Tammy Lydamore. In particular, infinite thanks to Mr. Paul Cooling who, on top of the countless times he helped me when something went wrong in the lab, also drilled a hole in the rubber stopper to secure the PennCentury™ device, thus improving the quality of the deposition system.

Many thanks to Dr. Catherine Ortori and Dr. Sarir Sarmad for their invaluable and constant support on the use of the mass spectrometry suite, and for allowing me to use their centrifuge, multiple shaker and calibrated (!) pipettes.

Many thanks to Dr. Richard Argent for his help in cell culture lab, and to Dr. Andrew Hook for helping me every time the Imstar was "actively refusing" to work.

Thanks to Matthew Pike in Computer Science for helping in writing the ImageJ macro.

Additional thanks go to the Centre for Doctoral Training team at the University of Nottingham, Prof. Cameron Alexander, Dr. Maria Marlow and in particular to Dr. Claudia Matz for managing such a great PhD programme.

***Acknowledgements***

Many thanks to all the administrative staff, but in particular to Julia Crouch for being so kind and friendly, always putting a smile on my face with the biscuits she bought at the Italian week in the local Lidl.

Thanks to all the people (PhD students and non) that I met in the various labs I ended up working in, certain days would have not been the same without your company.

Special thanks also go my friends. The old ones, that I left in Italy, but it never felt like we were apart; and the new ones, that I met during these four years, for sharing with me the great times but also keeping me sane in the most difficult ones. No need to name you all, you know who you are!

Last but not least, I would like to express my greatest gratitude to my Mum and Dad who have always unconditionally supported and guided me.

I am also very grateful to the funding bodies, EPSRC (grant n. EP/I01375X/1) and GlaxoSmithKline, for supporting the project.

# Abstract

The popularity of dry powder inhalers (DPIs) to deliver drugs to the lungs is constantly increasing thanks to their advantages over nebulisers and pressurised metered dose inhalers (pMDIs), including the high stability of dry powders, avoidance of propellant gases and ease of use. DPIs generate dry powder aerosols that deposit on the lung mucosa upon inhalation. In order to achieve the desired therapeutic outcome, drug particles must first dissolve in the lung lining fluids, then diffuse across these fluids to reach the epithelium and be absorbed.

The fate of inhaled particles once deposited on the lung surfaces has not been yet fully understood. However, the particle physicochemical properties are believed to play a role on their dissolution, interaction with lung lining fluids and permeability across the lung epithelium.

The main aim of this doctoral thesis was a better understanding of the relationships between drug particle physicochemical properties and their fate in the lung tissue in terms of dissolution and drug absorption. Increased knowledge in this area would indeed assist the development of novel and more effective inhaled medications.

The first objective was the development and validation of a simple and low cost deposition system to apply aerosolised dry powder particles in a narrow size range and a controlled dose to both epithelial and non-epithelial lung models (Calu-3 cells grown at the air-liquid interface (ALI) and airway mucus) for *in-vitro* studies.

***Abstract***

The deposition system consisted of a vacuum desiccator fitted with a PennCentury Dry Powder Insufflator™ – Model DP-4 without the needle but equipped with a PennCentury Air Pump™ – Model AP-1 (Penn-Century. Inc. Wyndmoor, PA). We demonstrated that it was able to homogeneously disperse different types of dry powders (micronised and spray dried), and consistently deliver controlled doses of drug in a narrow particle size range (3-5 μm). However, the system presented a major limitation as no real separation between respirable (<10 μm) and non-respirable (>10 μm) particles could be achieved.

The system was then exploited to investigate the effect of the formulation on drug absorption across Calu-3 cell layers. Salbutamol sulfate and indomethacin, respectively in class III (high solubility, low permeability) and II (low solubility and high permeability) of the Biopharmaceutical Classification System (BCS), were chosen as model dry powders.

It was demonstrated that for both drugs, a dry powder formulation led to a faster absorption across Calu-3 layers than their solution counterpart. Indomethacin was more permeable than salbutamol in either case, proving that our system was capable of discriminating between drugs with different permeability profiles according to the BCS. Indomethacin low water solubility did not limit its absorption.

Accordingly, the potential of novel indomethacin formulations produced by colleagues at University College London (UCL) as platforms to improve the absorption of poorly soluble drugs could not be appreciated.

In the case of salbutamol, we attempted to gain a better understanding of its mechanism of absorption through the lung epithelium, particularly when delivered as a dry powder. The data showed that Organic Cation Transporters (OCT) are likely to contribute to salbutamol absorption when applied in solution, but no valid conclusions

could be drawn when the drug was delivered as dry powder due to Calu-3 cell layers being disrupted during the course of the experiment.

Finally, the role of mucus on salbutamol and indomethacin particle dissolution and drug absorption was investigated. A system consisting of a thin mucus layer coating Transwell® insert membranes was developed. Drug permeation across the mucus layer was monitored and compared with that across the Calu-3 cell layers. The rate of permeation of salbutamol sulfate and indomethacin across the three barriers investigated (clean Transwell® inserts, mucus layer and Calu-3 cell layers) followed an opposite order (clean insert > mucus layer > Calu-3 cell layer for salbutamol sulfate, Calu-3 cell layer > mucus layer > clean insert for indomethacin), demonstrating that the mucus was acting as a barrier in the case of salbutamol, but conversely promoted dissolution of indomethacin particles.

A contribution to the clarification of the role of the mucus was made with the identification of some of the parameters that affect drug-mucus interaction: ionisation and lipophilicity. Solubility in water did not seem to have the same impact as for oral delivery. In this respect, we showed that the BCS, which only takes into account drug solubility and permeability, was a non-adequate description for the prediction of the behaviour of indomethacin in the lungs.

# Table of contents

# List of abbreviations

| | |
|---|---|
| A→B | Apical-to-Basolateral |
| ABC | ATP-Binding Cassette |
| ACI | Andersen Cascade Impactor |
| AcN | Acetonitrile |
| AFM | Atomic Force Microscopy |
| ALI | Air Liquid Interface |
| ALICE | Air-Liquid Interface Cell Exposure |
| ASL | Airway Surface Liquid |
| ATI | Alveolar cell Type I |
| ATII | Alveolar cell Type II |
| API | Active Pharmaceutical Ingredient |
| AR | Adrenoreceptor |
| ASM | Airway Smooth Muscle |
| ATP | AdenosynTriPhosphate |
| ATCC | American Type Culture Collection |
| B→A | Basolateral-to-Apical |
| BCS | Biopharmaceutical Classification System |
| BP | British Pharmacopoeia |
| CC | Cascade Centripeter |
| CDT | Centre for Doctoral Training |

| | |
|---|---|
| CF | Cystic Fibrosis |
| CI | Cascade Impactor |
| COPD | Chronic Obstructive Pulmonary Disease |
| CULTEX-RFS | CULTEX - Radial Flow System |
| CV | Coefficient of Variation [%] |
| DMEM:F-12 | Dulbecco's Modified Eagle's Medium: F-12 |
| DMSO | Dimethyl Sulfoxide |
| DPI | Dry Powder Inhaler |
| EDTA | Ethylenediaminetetraacetic Acid |
| EtOH | Ethanol |
| F68 | Pluronic F-68 |
| FBS | Foetal Bovine Serum |
| GI | Gastrointestinal |
| GSK | GlaxoSmithKline |
| HBSS | Hank's Balanced Salt Solution |
| HFA | Hydrofluoroalkanes |
| HPH | High-Pressure Homogenisation |
| HPLC | High Performance Liquid Chromatography |
| HPLC-MS/MS | High Performance Liquid Chromatography-tandem Mass Spectrometry |
| IMS | Industrial Methylated Spirits |
| IPA | Isopropyl Alcohol |
| IUPAC | International Union Of Pure and Applied Chemistry |
| LPS | Lipopolysaccharide |
| LY | Lucifer Yellow VS dilithium salt |

| | |
|---|---|
| MDI | Metered Dosed Inhaler |
| MeOH | Methanol |
| MF | Matrix Formers |
| MMAD | Mass Median Aerodynamic Diameter |
| MRM | Multi Reaction Monitoring |
| MSLI | Multi Stage Liquid Impinger |
| NAC | N-Acetyl Cysteine |
| NGI | Next Generation Impactor |
| NHBE | Normal Human Bronchial Epithelial cells |
| NSAID | Non-Steroidal Anti-Inflammatory Drug |
| OAT | Organic Anion Transporters |
| OCT | Organic Cationic Transporter |
| OCTN | Organic Zwitterions/Cation Transporters OR Organic Carnitine Transporter |
| PADDOCC | Pharmaceutical Aerosol Deposition Device on Cell Culture |
| PAS | Periodic Acid Schiff |
| pBCS | pulmonary Biopharmaceutical Classification System |
| PBS | Phosphate Buffer Saline solution |
| PEG | Poly-Ethylene Glycol |
| P-gp | P-glycoprotein |
| pMDI | Pressurised Metered Dose Inhalers |
| PSD | Particle Size Distribution |
| SAECs | Small Airways Epithelial Cells |
| SC% | Surface Coverage Percentage |
| SD | Standard Deviation |

| | |
|---|---|
| SDS | Sodium Dodecyl Sulfate |
| SEM | Scanning Electron Microscope |
| sem | Standard Error of Mean |
| SLC | Solute Carrier |
| TEA | Tetraethylammonium |
| TEER | Transepithelial Electrical Resistance |
| TJ | Tight Junctions |
| TPGS | D-α-Tocopherol polyethylene glycol 1000 succinate |
| UCL | University College London |
| UK | United Kingdom |
| USA | United States of America |
| VOC | Volatile Organic Compounds |

# List of equations

# List of figures

# List of tables

# Chapter 1
# Introduction

## 1.1. Pulmonary drug delivery

Targeting the lungs to deliver active principles in order to ease several symptoms dates back to more than 4000 years, when *Atropa Belladonna* leaves were smoked for the treatment of cough (Gonda 2000; Patton & Byron 2007).

Since then, especially in the last 60 years, a great effort has been put in the discovery and formulation of new drugs suitable for lung delivery. Nowadays, more than 30 Active Pharmaceutical Ingredients (APIs) are effectively delivered to the respiratory tract (Hou *et al.* 2015; Forbes *et al.* 2011). Currently, pulmonary delivery represents the best option for the treatment of lung diseases such as asthma, chronic obstructive pulmonary disease (COPD) and cystic fibrosis (CF), but it has proven to be an interesting and convenient administration route for systemic therapy as well, especially for drugs like peptides and proteins that are unsuitable for oral delivery due to their quick degradation by the enzymes in the gastrointestinal (GI) tract (Patton *et al.* 2004; Agu *et al.* 2001).

Pulmonary delivery presents several advantages in comparison to other administration routes. It is non-invasive and the lungs provide a large surface area for absorption (about 140 $m^2$ in the alveolar area and 1-2 $m^2$ in the conducting airways (Weibel & Gomez 1962)), high solute permeability and avoidance of the first-pass metabolism (Schanker 1978; Patton 1996). Also, the alveolar region is characterised by an extensive vasculature and high blood flow (5 L/min) and a thin diffusion path to the

bloodstream (150 μm) (Ducreux & Vanbever 2007). In addition, the high drug concentrations achievable at the site of action allows for the administration of lower doses, significantly reducing the side effects (Labiris & Dolovich 2003).

## 1.2. The lung physiological barriers to pulmonary drug delivery

The human respiratory system is complex and has evolved in such a way to guarantee the organism the proper exchange of gases essential for survival, but at the same time prevent foreign material (e.g. particulate, bacteria, pollen, tobacco smoke) to penetrate the system. The anatomy of the respiratory system is particularly important in this respect, presenting a number of barriers to inhaled materials including the lung structure, the epithelium and non-epithelial barriers. Drug delivery systems for inhalation will have to overcome these barriers in order to penetrate the respiratory system, reach the targeted tissues and obtain the desired therapeutic outcome.

### 1.2.1. Anatomy of the human respiratory system

The lungs are complex organs, usually described as a dichotomous branched system of tubes in which the number of branches increases moving from the trachea to the bronchi and the alveoli (Figure 1.1). The branching develops into up to 23 generations (Z), from the trachea (Z=0) to the alveolar sacs (Z=23). The two "daughter" airways deriving from the same branch belong to the same generation. The diameter of the tubes constantly decreases with the generation number (Weibel & Gomez 1962).

Two different areas can be distinguished in the human respiratory system: the conducting area (trachea, bronchi and bronchioles) where the inhaled air flows through, but no gaseous exchange process occurs; and the respiratory zone (respiratory bronchioles and alveolar sacs) where the actual gaseous exchange takes place (Bérubé *et al*. 2010).

## *1. Introduction*

The respiratory system intimately interacts with the circulatory system by means of an extensive vasculature, especially in the alveolar region, and work together in order to guarantee the organism the correct gas exchange required for survival. Inhaled oxygen is transported from the lungs to the cells, whereas the metabolic product carbon dioxide is transported from the cells to the lungs to be eventually eliminated by exhalation. This process is known as respiration, the combination of two distinct movements, namely the inspiration and the expiration. Healthy lungs intake about 500-600 mL of air at a rate of about 5-6 L/min (Hughes 2010). The respiration movements are regulated by the contraction and relaxation of the diaphragm. The bronchomotor tone is also modulated by the airway smooth muscle (ASM), an additional tissue that is found attached to cartilage at the back of the trachea in the upper airways, and surrounding the bronchi in the lower airways. ASM main function is to contract thus modulating the bronchomotor tone, but also taking part in inflammation events in clinical conditions such as asthma, CF and chronic bronchitis (Panettieri *et al*. 2008; Amrani & Panettieri 2003; Mitchell 2009).

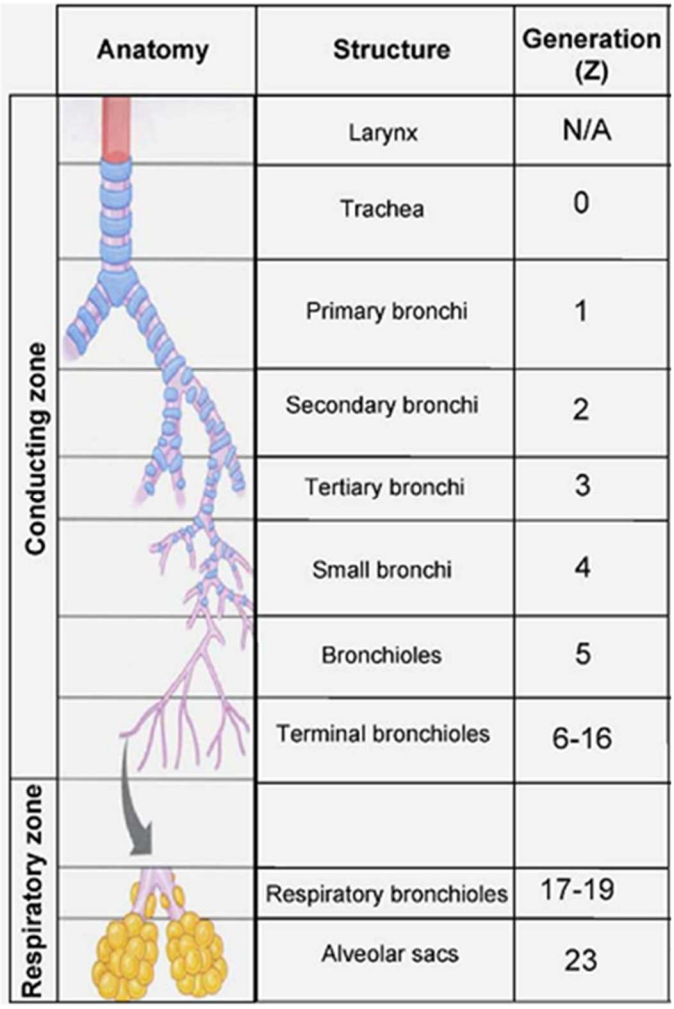


**Figure 1.1: conducting and respiratory zones of the human respiratory system. Adapted from Bérubé *et al.* (2010)**

## 1.2.2. Airway epithelium

A continuous layer of epithelial cells lines the entire respiratory tract. The lung epithelium is a dynamic tissue undergoing continuous renewal, with a turnover of 30-50 days. It plays a key role in preserving the normal functionality of the lungs, maintaining the conduit of air to and from the alveoli, and also represents a barrier to foreign materials (e.g. pollen, bacteria, tobacco smoke and particles) with the combined action of secretory and ciliated cells (Crystal *et al*. 2008).

About 50 different cell types have been found in the lungs. The main types of cells are basal, columnar, secretory, ciliated and undifferentiated, although there are also other less frequent types such as neural and neuroendocrine cells (Crystal *et al*. 2008).

Moving from the conducting to the respiratory zone, the cell types vary to adapt to the functions and defence mechanisms typical of each region (Figure 1.2). The upper airway epithelium is pseudo-stratified and mainly consists of basal cells, tall (≈60 µm) secretory goblet cells and ciliated cells, the latter two being responsible for the mucociliary clearance mechanism. The bronchiolar epithelium is characterised by thinner cuboidal cells and secretory Clara cells. Finally, the alveolar zone contains extremely thin (<0.1 µm) alveolar cell type I and II (ATI and ATII). The air-side of the alveoli is patrolled by alveolar macrophages (phagocytes) (Bérubé *et al.* 2010; Crystal *et al.* 2008; Patton & Byron 2007).

As mentioned before, one of the lung epithelium functions is to protect the respiratory system from external insults. It does so by means of a number of defence mechanisms including the regulation of the volume of fluids on the airway surface, secretion of ions as well as anti-inflammatory, antibacterial and antioxidant molecules, and the mucociliary clearance.

A second line of defence against external insults is determined by the intercellular junctions that create a tight and efficient selective barrier against intrusions from the external environment. The permeability of the barrier is modulated by tight junctions (TJs) that regulate the flow of molecules between the apical and the basolateral sides (Patton & Byron 2007; Bérubé *et al.* 2010). Measurement of the potential difference across the airways in animal models and patients reported variations in the tightness across the respiratory system (Schneeberger *et al.* 1980; Boucher *et al.* 1981; Alton *et al.* 1991).

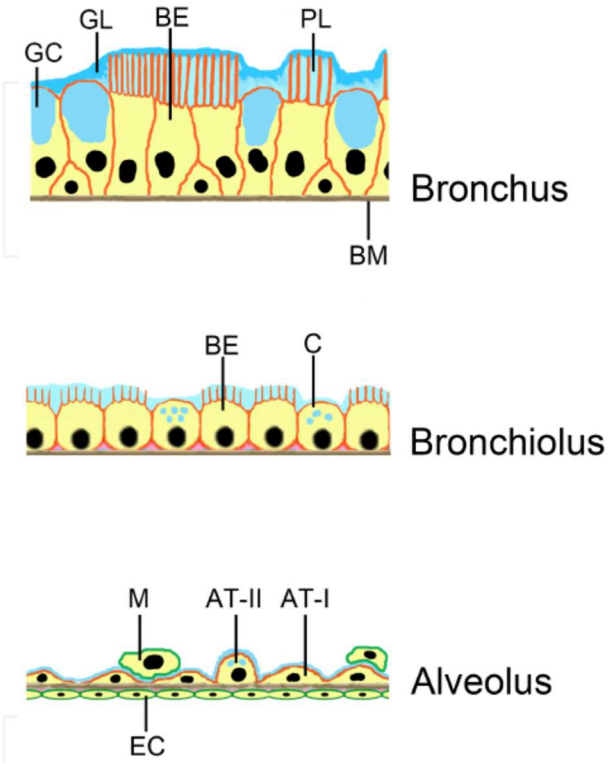


**Figure 1.2: barriers of the respiratory system. Major cell types in the lung epithelium: mucus-producing goblet cells (GC); columnar bronchial epithelial cells with cilia (BE); basement membrane cells (BM); Clara cells (C); AT-I cells (AT-I); AT-II cells (AT-II); endothelial cells (EC). Non-epithelial barriers: periciliary layer (PL) and gel layer (GL) of mucus, alveolar macrophages (M). Reproduced from Fröhlich & Meindl (2014).**

### 1.2.3. Non epithelial barriers: mucus, surfactants and alveolar macrophages

The airway epithelium is lined with two different types of fluids that characterise the two different areas of the respiratory system. A thick (up to 10 µm) mucus gel layer lines the epithelium of the upper airways. Its thickness is progressively reduced until mucus is replaced by a thin (0.07 µm on average) layer of alveolar surfactant in the alveolar region (Patton & Byron 2007).

Mucus is a complex fluid secreted by specialised serous and goblet cells, whose main components are water, glycoproteins (mucins), proteins, lipids and salts. Mucus represents the first barrier encountered by foreign materials upon entering the respiratory system. In fact, its thickness, composition and microstructure strongly affect the ability of deposited material (e.g. drug particles) to penetrate it and reach the underlying epithelium. In addition, mucus is constantly removed by the coordinated

beating of the cilia of ciliated cells, in the so called mucociliary escalator (Cone 2009; Haghi *et al*. 2014; Lansley 1993).

On the other hand, the alveoli are characterised by the presence of alveolar surfactant that is secreted by Clara and alveolar type II cells and is composed of a mixture of proteins and phospholipids. Additionally, macrophages can be found in the alveoli. These are specialised cells that represent the first line of defence in this area of the respiratory system, and exert their role by engulfing and digesting insoluble deposited inhaled material. They also produce a number of pro- and anti-inflammatory cytokines (Haghi *et al*. 2014).

## 1.3. Pulmonary delivery devices

The successful combination of new drugs and the technological advances of devices able to deliver defined doses to the respiratory tract produced significant improvements in the field. Drugs and formulations for inhalation therapy are delivered to the lungs after formation of an aerosol by means of three different types of devices: nebulisers, pressurized metered-dose inhalers (pMDI) and dry powder inhalers (DPI).

### 1.3.1. Nebulisers

Nebulisers exploit ultrasonic mechanisms or air jet to atomise aqueous based drug formulations and deliver large doses over multiple breaths. Depending on the manufacturer and the model, they are able to produce droplets between 1-5 µm in diameter. Since they do not require coordination between actuation and inhalation, they are easy to use and therefore they are mainly used for infants, elderly and critically ill patients. In addition, they also allow for the administration of higher doses of API although this often involves long exposure times (Ibrahim *et al*. 2015).

The first generation nebulisers were bulky and heavy, difficult to operate and expensive, but new portable and more convenient nebulisers are currently being developed (Daniher & Zhu 2008; Kleinstreuer *et al*. 2008; Ibrahim *et al*. 2015).

## 1.3.2. Pressurised metered-dose inhalers (pMDIs)

Pressurised metered-dose inhalers (pMDIs) are small compact devices designed for delivering multiple doses of droplet spray. Being reliable, user-friendly and low cost, they are the most widely used devices for the delivery of medications aimed at the treatment of COPD and asthma. Typically, a pMDI consists of a canister containing the formulation (therapeutic material and propellant), a metering valve, an actuator that allows the patient to operate the device and a mouth piece to direct the spray into the lungs. The propellant, typically hydrofluoroalkanes (HFA), is contained at high pressure into the canister in order to keep it in its liquid state. The metering valve is designed to deliver 20-100 μL of aerosol at each actuation. The spray angle and the droplet size distribution are controlled by the nozzle of the actuator. The effective delivery of the correct dose to the lungs is dependent on the patient's coordination between the actuation and the inhalation processes. The use of spacers between the mouthpiece and the patient's mouth is often recommended to overcome issues (e.g. administration of lower dose) due to the incorrect use of the device (Kleinstreuer *et al*. 2008; Ibrahim *et al*. 2015).

## 1.3.3. Dry powder inhalers (DPIs)

Dry powder inhalers (DPIs) are portable devices able to generate aerosols directly from dry powders. DPIs have received increased attention thank to their advantages in comparison to nebulisers and pMDIs: they produce the aerosol directly from dry powders, which are usually more stable than the suspensions used with pMDI, and do

not require the use of propellant gases therefore they are more environmentally friendly. In addition, they are easier to operate in comparison to pMDI, the coordination between breathing and actuation being minimum (Islam & Gladki 2008). There are different types of DPIs depending on the dose-type and the actuation mode. According to the dose-type, DPIs are classified into single-unit dose, multi-unit dose and multi-dose reservoir (Figure 1.3). The single-unit dose DPIs require the patient to load the device with a single unit capsule prior to each administration. The multi-unit ones can hold multiple doses in pre-sealed packages (strip blisters, replaceable disks or cartridges). The multi-dose reservoir devices have a built-in mechanism to dispense single doses from the powder in bulk.

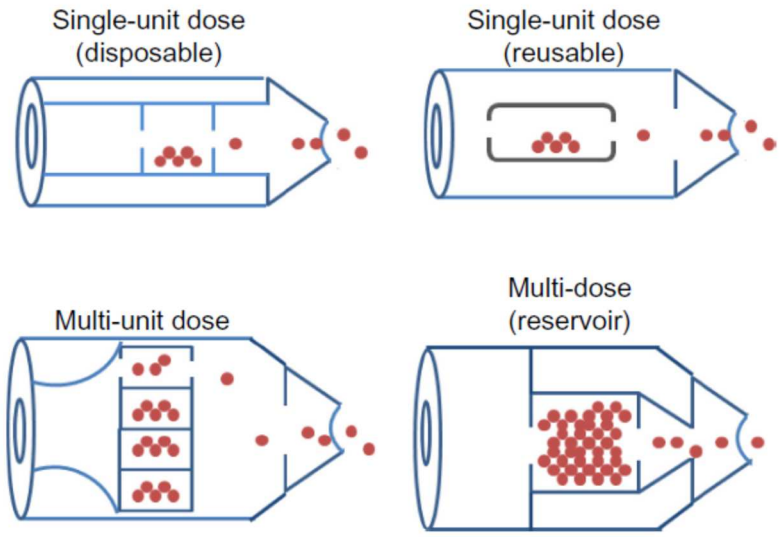


**Figure 1.3: DPIs classified according to the number of doses. Reproduced from Ibrahim *et al.* (2015)**

By the actuation mode, DPIs are divided into active and passive devices. While the active DPIs have an internal source of energy to aerosolise the powder, thus being independent from the patient's ability to inhale, the passive DPI are breath-actuated by the patient, resulting in a greater ease of use since there is no need to coordinate actuation with inspiration. However, they rely exclusively on patient's ability to provide sufficient air flow for the correct delivery of the formulation both in terms of

dose and particle size. In fact, the main issue associated with the first generation of passive DPIs was the lack of uniformity of the dose between patients of different age or affected by different conditions, but also between inspirations of the same patient. The new generation of passive DPIs are designed to reduce this variability. An example is Ellipta by GSK requiring low inspiration flow rates for its operation (Ibrahim *et al.* 2015).

The delivery of the formulation to the lungs from DPIs occurs in several steps: powder aerosolisation, deagglomeration, dispersion, transport and deposition (Figure 1.4).

Powder aerosolisation requires aerodynamic forces able to overcome the powder particle weight. This can be achieved by increasing the air velocity: either the patient inhales at a greater rate or the mechanism include a pressure drop by directing the flow through nozzles, venturis or contractions. Powder deagglomeration and dispersion are obtained by fluid dynamic shear that can be intensified by turbulences. Current DPIs employ various adornments to modify velocity and direction of the aerosol: cyclone and reverse-cyclone flow paths, turbulence/impaction grids, rotating impellers, as well as pressure drop devices such as nozzles, venturis, contractions or orifices (Figure 1.5) (Islam & Cleary 2012). Transport of the aerosolised particles in the respiratory system depends on the fluid mechanics in the lungs including convective gas transport (or bulk gas transport) and mixing (Golshahi & Finlay 2009).

Currently, more than 60 DPI designs can be found in the literature and on the internet, however, less than half are actually on the market, and most of them are breath-actuated (Hoppentocht *et al.* 2014).

The performance of DPIs does not only depend upon its design, the physical mechanisms exploited to aerosolise the drug powder and the patient's inhalation force,

but also on the physicochemical characteristics of the powder formulation (Weers & Miller 2015; Stegemann *et al*. 2013).

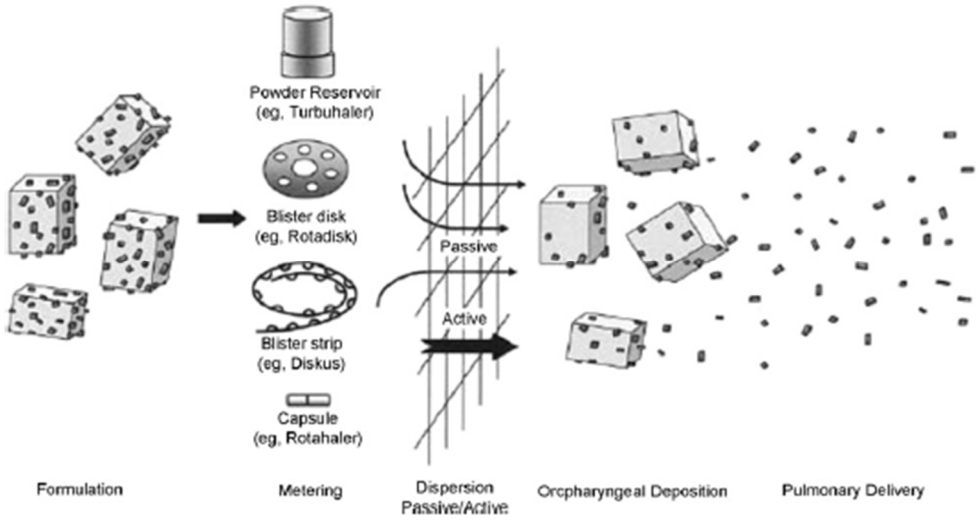


**Figure 1.4: principle of DPI design and functioning. Reproduced from Telko & Hickey (2005)**

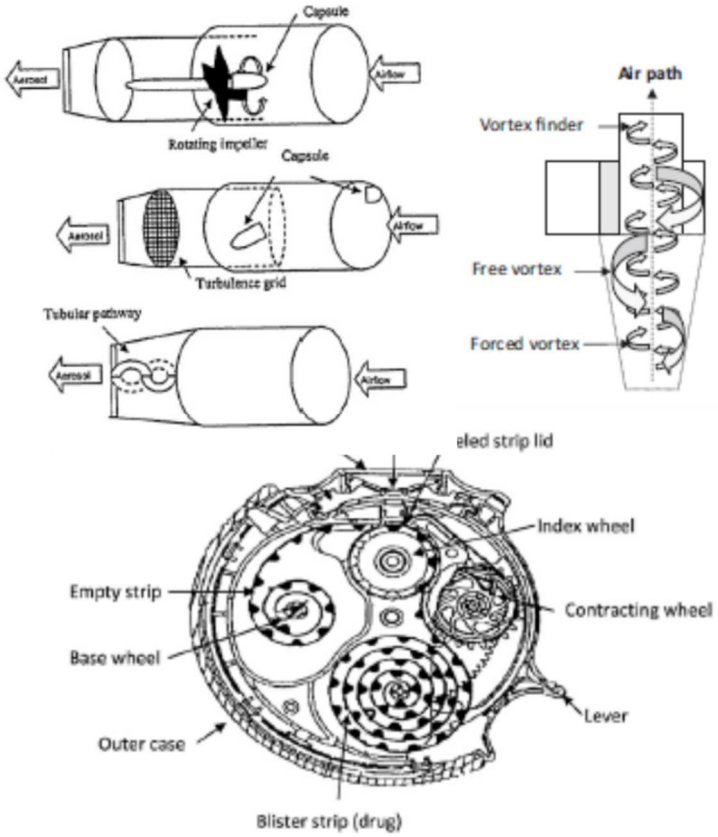


**Figure 1.5: DPI internal designs for drug deagglomeration and dispersion. Adapted from Islam & Cleary (2012)**

## 1.4. Formulations for pulmonary delivery

The formulations for pulmonary delivery are different depending on the physicochemical properties of the API as well as on the device selected for its delivery. Nebulisers and pMDIs require the formulation to be in solution or suspension, whereas DPIs formulations are prepared as a dry powder.

The respiratory solutions marketed for delivery by means of nebulisers usually contain the drug dissolved in aqueous isotonic systems. In order to improve the solubility of the API, surfactants can be used. The formulation often also contains preservatives (e.g. sodium bisulfite and ethylenediaminetetraacetic acid (EDTA)) to prevent bacterial growth; salts such as NaCl to adjust the osmolarity of the solution; and acids or bases (e.g. HCl, NaOH, phosphates) to buffer the solution at neutral pH.

In the case of pMDI the drug is dissolved or resuspended in the propellant (HFA), that serves as a vehicle for the drug and other excipients but also provides a source of energy for expelling the formulation from the metering valve as rapidly evaporating droplets. Also in this case, surfactants are used in order to stabilise the formulation (Pilcer & Amighi 2010).

As opposed to nebulisers and pMDIs, the formulations for DPIs consist of dry powder particles. As already highlighted, the performance of DPIs strongly depends on the physicochemical properties of the formulation, other than the DPI design. It is important that the powder formulation released from the inhaler at the inhalation flow rate at which it is operated by the patient, contains drug particles in the desired aerodynamic size range (1-5 μm) for deposition in the targeted region of the respiratory system. It is often the case that the characteristics of the emitted particles by the inhaler are not representative of the primary characteristics of the bulk dry powder (i.e. particle size distribution, PSD). It is therefore important that the formulation disperses

effectively, thus allowing for the dose compartment to be completely emptied, ensuring the delivery of the correct dose. (Hoppentocht *et al*. 2014).

The characteristics of the particles constituting the bulk powder (particle size, shape, morphology, density, charge, surface area) are crucial in determining the final properties of the bulk dry powder, and in order to meet the requirements, different types of formulations and specific particle engineering techniques can be applied.

DPIs formulations usually consist of micronised dry powder particles (1-5 μm), either of the API in its pure physical form or with carriers (Ibrahim *et al*. 2015).

The aerodynamic particle size is extremely important as it governs the regional deposition of the particles in the lungs (see paragraph 1.5.1). Size reduction is one of the most important steps during particle preparation. The aerodynamic diameter of the particles can be decreased by either reducing the geometric diameter or by reducing the particle density. Particle size is reduced by either top-down (e.g milling) or bottom-up (e.g. spray-drying, spray-freeze-drying, supercritical fluid drying) approaches. Top-down techniques are convenient as they permit an optimum control over the final PSD, but they often create flat surfaces with increased surface area, surface charging and distortion of the crystal lattice. On the other hand, bottom-up techniques allow to control the PSD as well as the particle shape and morphology (Pilcer & Amighi 2010; Hoppentocht *et al*. 2014).

Small particles are highly cohesive due to strong inter-particle forces that promote the formation of larger aggregates that modify the regional deposition in the lungs. In order to improve the flow properties of the final powder product, the pure particles can be blended together with larger carrier particles (50-200 μm), typically lactose but also glucose, mannitol, sorbitol, sucrose, trehalose (Daniher & Zhu 2008; Ibrahim *et al*. 2015; Pilcer & Amighi 2010). Alternatively, the use of larger porous particles as first

proposed by Edwards and colleagues (1997) has proven to be particularly effective. In fact, these are characterised by lower density thus maintaining the optimum aerodynamic diameter despite being larger and therefore less cohesive.

In order to improve the stability and the bioavailability of the API, such as in the case of poorly soluble drugs or peptides or proteins, other strategies have been explored more recently such as the employment of liposomes, polymeric nanoparticles as well as dendrimers, that are eventually agglomerated into micro sized particles (Mansour *et al*. 2009; Sung *et al*. 2007)

## 1.5. Fate of inhaled particles deposited on the lung epithelium

### 1.5.1. Intrapulmonary particle deposition

Particle deposition is the fundamental basis of inhalation therapy. It describes the phenomena occurring when particles are inhaled into the lung, in particular their capture through contact with the wet surface of the respiratory tract. The deposition sites and the amount of particles deposited depend on several factors related to both the physical properties of the inhaled particles, such as size, density and shape, and the specific features of the subject inhaling these particles, such as tidal volume, mode of breathing (oral or nasal) and respiratory flow rate (Schulz 1998).

The major mechanisms governing particle deposition in the lung are the three following (Schulz 1998):

1. **Impaction:** the probability of deposition by impaction depends on the mass of the single particle (defined by density and size), and on its velocity, determined by the flow rate in the airways.

2. **Sedimentation:** the probability of a particle to deposit by gravitational sedimentation depends on its settling distance in the airways, calculated as the product of the residence time and the settling velocity of a particle in the airways.
3. **Diffusion:** it is related to the Brownian motion of surrounding gas molecules. The diffusional displacement is effective for particles <0.5µm, so it only occurs for the smallest particles.

The region in which the particle deposits depends on its aerodynamic diameter ($d_a$). For a particle settling under gravity in air, it is defined as the diameter of a spherical particle having unitary density (1 g/cm$^3$) settling with the same velocity as the considered particle and is described by the following equation:

$$d_a = d_g \sqrt{\frac{\rho}{\rho_a}}$$

**Equation 1.1: definition of aerodynamic diameter**

Where $d_g$ is the geometric diameter, ρ is the mass density and $\rho_a$ is the unit density (1 g/cm$^3$) (Sung *et al.* 2007). The aerodynamic diameter is the key parameter in determining the deposition efficacy of the drug particles in the lung. To efficiently enter the lung it is necessary the particle aerodynamic diameter ranges between 1-5 µm (Patton *et al.* 2004; Patton & Byron 2007).

When discussing the particle deposition, it is common to divide the respiratory tract between the extra-thoracic region (nasopharyngeal and oropharyngeal spaces) and intra-thoracic region, divided into tracheobronchial and alveolar spaces.

When aerosols enter the respiratory tract, the particles deposit in different regions depending on their size (Figure 1.6): larger particles typically do not pass beyond the pharynx whereas the smaller drug particle fraction penetrates the lung where it deposits onto the bronchial and alveolar epithelium (Newman 1985). In particular, in the extra-

thoracic region, where the major deposition mechanism is inertial impaction and the flow rate is higher, 80% of 10 µm particles are captured; in the tracheobronchial region the dominant deposition mechanisms are inertial impaction and gravitational sedimentation, and particles <5µm are deposited. Finally, the most important deposition mechanism in the alveolar region is gravitational sedimentation and for particles < 0.5 µm diffusional displacement (Schulz 1998).

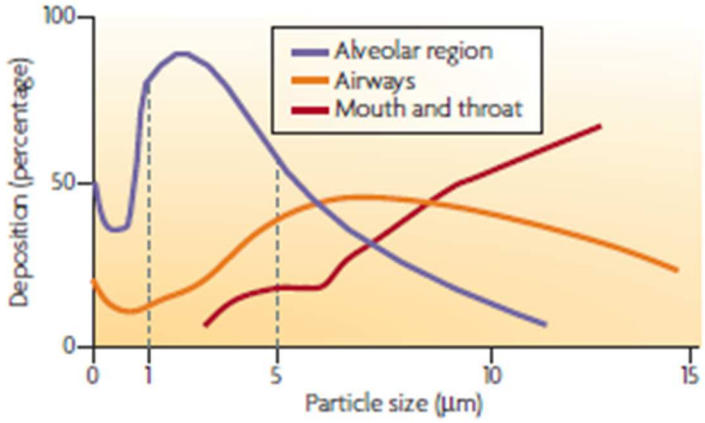


**Figure 1.6: regional deposition in the lung of inhaled particles as a function of the particle size. Reproduced from Patton & Byron (2007)**

Also the flow rate plays an important role in the regional deposition of the particle within the lungs. In fact, if the patient inhales too forcefully from a DPI, most of the particles emitted by the device will most likely deposit in mouth and throat, whereas the deposition in the deeper lungs will decrease (Patton & Byron 2007).

### 1.5.2. Mechanisms of particle dissolution and drug absorption and elimination in the lung

The fate of inhaled particles once deposited in the lung lining has not been yet fully understood. It has been often believed to be patient specific, thus influenced by the patient's physiological parameters of breathing (respiration rate, tidal volume and inhalation air flow), but also controllable by manipulating the physicochemical characteristics of the formulations such as PSD, tonicity and pH (Tolman & Williams 2010).

#### 1.5.2.1. Particle dissolution

One of the first barriers deposited particles come across is the lining fluid where they can be dissolved and drugs are released, and whose total volume is approximately 10-30 mL in humans (Patton *et al.* 2004). The thickness of the lining fluids distally varies from the conductive airways to the alveoli and particles will be immersed in the smallest volume of fluid the deepest they deposit in the lungs. As a consequence the dissolution rate is different in the various regions of the lung and the solid-liquid interface area between the lining fluid and the particle depends on the particle dimension in the conductive airways, whereas it is limited by the fluid thickness in the alveoli (Olsson, Bondesson, Katarina Gustavsson, *et al.* 2011).

If the drug particle dissolves, the free drug molecule, depending on its physicochemical properties (molecular weight, hydrophobicity, charge), could cross the mucus layer and reach the epithelium.

#### 1.5.2.2. Drug absorption

The route of absorption depends on the site of deposition and on the drug characteristics. In fact, the deposition of the drug in the appropriate site of absorption does not guarantee that it will be absorbed, as how it will be absorbed, the extent of absorption and disposition strongly depend on the physicochemical properties of the drug, including solubility and molecular weight (Ibrahim & Garcia-Contreras 2013). There are different routes through which the drug can be absorbed across the epithelium, including both active and passive transport mechanisms (Figure 1.7) (Olsson, Bondesson, Katarina Gustavsson, *et al.* 2011; Ibrahim & Garcia-Contreras 2013):

- **Paracellular transport**

  Paracellular transport is mainly mediated by tight-junctions, transmembrane and cytoskeleton proteins (claudins and occludins) occupying the apical side of intracellular area. They act as a barrier to the passive diffusion of ions and small uncharged solutes. The transepithelial electro resistance (TEER) provides a measurement of the tightness of the tight-junctions, and it has been reported to change along the pulmonary tract, with increasing values from the trachea to the distal regions (Alton *et al.,* 1991).

  Paracellular transport through the tight-junctions has been reported as the preferential route of absorption of small hydrophilic molecules, but also small peptides such as insulin. The mechanism is suggested to be the increase of the intercellular pores size due to stretching of the lung epithelium during the respiration movements (Mason *et al*. 2001). It is also possible to use absorption enhancers in the drug formulation that disrupt the tight junctions (Ibrahim & Garcia-Contreras 2013).

- **Transcellular transport**

  Drug absorption through the transcellular route is the major drug uptake mechanism. It is usually non-mediated (passive diffusion), however it includes also transport mechanisms mediated by transport proteins or non-coated vesicles (caveolae).

  *Passive diffusion* is the tendency of a compound to move from a point at higher concentration to a point at lower concentration. Inhaled drugs can diffuse through the epithelial cells upon a concentration gradient. Transcellular diffusion seems to be the route of absorption for lipophilic compounds (Olsson, Bondesson, Borgström, *et al*. 2011; Patton *et al*. 2010).

## 1. *Introduction*

*Transporters* have been recognised to play an important role in the absorption, distribution and disposition of drugs, together with passive diffusion (Sugano *et al.* 2010). Many transporters are expressed in the lungs, however their role in the pharmacodynamics and pharmacokinetics of inhaled drugs has not been completely clarified yet (Bosquillon 2010; Gumbleton *et al.* 2011). Transporters can enhance cellular uptake facilitating drug absorption through the cell membrane, especially for those drugs that cannot easily cross the cell membrane by passive diffusion. Transporters exploit different mechanisms including membrane potential and counter-transport of ions. This is the case of transporters of the solute carrier (SLC) family which comprises organic anion transporters and organic cation transporters (OAT and OCT). However, other types of transporters, such as ATP-binding cassette family (ABC transporters) efflux compounds out of the cell membrane *via* an ATP-dependent mechanism. Transporters are believed to work together with passive diffusion, influencing the drug absorption through the epithelial cell layer. They also seem to play a role in regulating the intracellular concentration of a drug, thus influencing its efficacy and toxicity (Ibrahim & Garcia-Contreras 2013).

The *vesicle-mediated* mechanism of absorption occurs by transfer of the drug into the cell cytoplasm by means of membrane vesicles called caveolae. These are small invaginations (10-100 nm) on the cell plasmalemma. The formation of vesicles is typical of alveolar epithelial type I and type II cells and has been suggested to be involved in the transport of macromolecules such as proteins (Kim & Malik 2003).

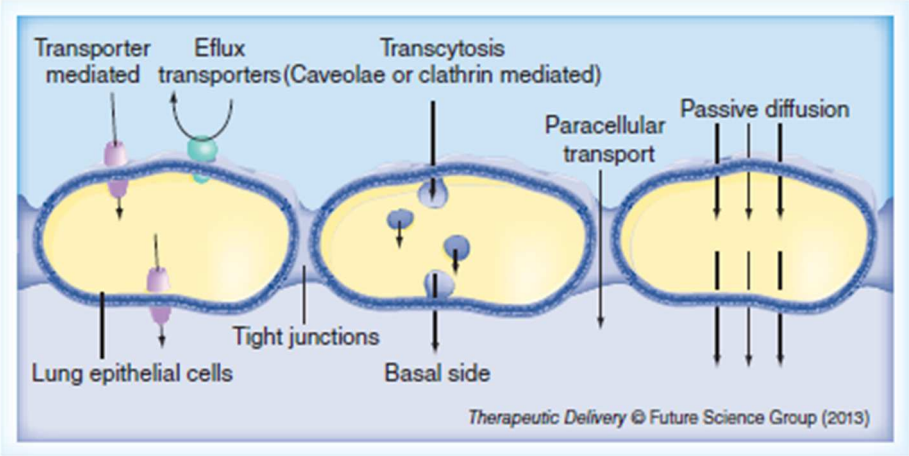


**Figure 1.7: possible absorption mechanisms of inhaled drugs through the lung epithelium. Reproduced from (Ibrahim & Garcia-Contreras 2013)**

### 1.5.2.3. Drug elimination

The lungs have particular mechanisms for the elimination of xenobiotics from their surface. Depending on the site of deposition, the particle/droplet size and the chemical composition, there are three possible mechanisms of clearance: mucociliary clearance, lymphatic circulation after macrophage uptake and enzymatic degradation.

Poorly soluble drug particles that deposit in the tracheobronchial area are disposed of by mucociliary clearance with significant reduction of the amount of drug absorbed. Mucociliary clearance is the first mechanism of defence of the lungs against foreign material deposited in the upper airways (trachea and bronchi), and, as already mentioned, it consists of the continuous removal of the mucus gel layer towards the mouth by the beating movement of the cilia (Ibrahim & Garcia-Contreras 2013; Cone 2009; Haghi *et al.* 2014; Lansley 1993). More detailed discussion about the role of mucus as a barrier is in Chapter 6 (page 179).

In the alveolar region, the elimination of unwanted materials is the macrophages' duty. As mentioned earlier, macrophages are specialised cells that clear the alveolar surface from foreign materials by phagocytosis (target size is 1.5-3 µm). They then transport the engulfed insoluble particle either to the mucociliary escalator or to the

tracheobronchial lymph (Olsson, Bondesson, Borgström, *et al.* 2011; Ibrahim & Garcia-Contreras 2013). It is possible to avoid elimination by macrophage uptake by accurately designing the drug formulation. For example, the use of larger porous particles (>10µm but with the appropriate aerodynamic diameter to deposit in the alveolar range) was showed to be particularly convenient, these particles being larger than the target size of the macrophages (Edwards *et al.* 1997). Also PEGylation was demonstrated to reduce macrophage uptake (Patton *et al.* 2010). In addition, macrophages themselves can be targeted in order to achieve specific effects in immune inflammatory therapy (Lee *et al.* 2015).

Xenobiotics can also undergo enzymatic degradation by metabolic cytochrome P450 enzymes found in the cytoplasm of the lung epithelial cells. However, the metabolic activity in the lungs is less than in the liver (Ibrahim & Garcia-Contreras 2013).

It is however noteworthy that the mechanisms of elimination and clearance of foreign materials, in particular insoluble particles, are necessary in the lungs as their long permanence on the lung epithelium may cause chronic lung inflammation. When excessive inflammatory mediators are secreted these can lead to severe lung injury (Oberdorster *et al.* 1992).

#### 1.5.2.4. Factors affecting drug absorption and elimination in the lungs

As already mentioned, the fate of the drug particles once deposited in the lung has not been fully understood.

It is well known that the physicochemical properties of the drug play an important role in its absorption in the gastrointestinal (GI) tract.

Lipophilic compounds are known to cross the epithelial barrier by passive diffusion, but it is not clear what happens to hydrophilic drugs (Kell *et al.* 2011). Small lipophilic

drugs are also quickly absorbed, and the absorption rate is directly proportional to the lipophilicity. However, if a drug is too lipophilic it may not dissolve in the lung lining fluids and it will eventually be eliminated by the mucociliary clearance, although intact particles may be able to cross the mucus blanket and being internalised by the epithelial cells without being dissolved (Patton *et al.* 2010). Also, Schanker *et al.* (1986) first demonstrated an inverse relationship between absorption rate in the lungs and molecular weight. This relationship was later confirmed by other researchers in the field (Patton *et al.* 2004). The same kind of relationship was found for macromolecule size and their absorption, for which it was found that small proteins ($M_w$ < 40 kDa) such as insulin are more rapidly absorbed than larger ones ($M_w$ > 40 kDa) (Labiris & Dolovich 2003).

Absorption of hydrophilic drugs is generally accepted to occur either *via* transporters or through tight junctions. However, in this last case the molecular weight is important, and it has been reported that molecules > 1000 Da could reside longer in the lungs thus being more susceptible to removal by the mucociliary clearance (Ibrahim & Garcia-Contreras 2013).

Also the acidic or alkaline nature of the drug can influence its absorption in the lungs. In particular, weakly acidic and basic drugs could be in both their ionised or un-ionised forms, with the latter being more lipophilic and therefore more susceptible to cross the membrane barrier through intracellular routes (Ibrahim & Garcia-Contreras 2013), although, as explained earlier, many anionic and cationic molecules are also transporter substrates.

It is then clear that a definitive explanation of the fate of inhaled particles in the lungs has not been given yet. Many questions remain to be answered regarding the fate of particles in the lung. In particular, it is not yet clear what happens after particle

deposition in the lungs, before the API is detected in the systemic circulation. Also the degradation pathways have not been fully explained yet.

Understanding these mechanisms would be extremely useful, especially during drug development.

## 1.6. Aims and objectives of the project

The rationale for this PhD project came from the hypothesis that the physicochemical properties of particles for inhalation have an impact on their dissolution, interaction with lung lining fluids and permeability across the lung epithelium. The main aim of the study was a better understanding of the relationship between drug particle physicochemical properties and their fate in lung tissue in terms of dissolution and drug absorption.

The primary objective was the development and validation of a simple and low cost deposition system to apply aerosolised dry powder particles in a narrow size range (3-5 µm) and a controlled dose to both epithelial and non-epithelial *in-vitro* lung models (Calu-3 cells grown at the air-liquid interface (ALI) and airway mucus).

Subsequently, we wanted to investigate the effect of the drug formulation (solution or dry powder) on absorption across the lung epithelium. The drugs used were salbutamol sulfate, a water soluble short-acting $\beta_2$-agonist of choice in the treatment of asthma, and indomethacin, a poorly water soluble non-steroidal anti-inflammatory drug (NSAID).

In the case of salbutamol sulfate, the attention was then focussed on a better understanding of the role of OCT transporters in drug absorption after delivery as a dry powder spray.

In the case of indomethacin, it was hypothesised that its poor solubility in water could limit the absorption rate of the drug across the lung epithelium. Novel indomethacin

dry powder formulations consisting of micro-agglomerates of nanoparticles were produced by UCL (University College London) colleagues in order to improve the bioavailability of poorly soluble drugs in the lung. Our aim was to assess their efficacy in improving indomethacin dissolution on lung lining fluid thus increasing drug bioavailability.

The final aim of this doctoral study was to provide a better understanding of the role of mucus on dry powder particle dissolution and drug absorption after deposition. In order to carry out this final study, there was a need for a system consisting of a thin mucus layer coating Transwell® inserts membranes to be developed. Successively, we wanted to look at the permeation of dry powder particles across the mucus layer, in comparison with the absorption across the Calu-3 cell layers taking into account the physicochemical properties of the drugs (solubility in water and acidic character).

## 1.7. References

Agu, R., Ugwoke, M. & Armand, M., 2001. The lung as a route for systemic delivery of therapeutic proteins and peptides. *Respiratory Research*, 2(4), pp.198–209.

Alton, E.W.F.W. *et al.* 1991. Effect of heart-lung transplantation on airway potential difference in patients with and without cystic fibrosis. European Respiratory Journal 4(1), pp.5–9.

Amrani, Y. & Panettieri, R.A., 2003. Airway smooth muscle: contraction and beyond. *The International Journal of Biochemistry & Cell Biology*, 35(3), pp.272–276.

Bérubé, K. *et al*., 2010. Human primary bronchial lung cell constructs: the new respiratory models. *Toxicology*, 278(3), pp.311–318.

Bosquillon, C., 2010. Drug transporters in the lung - Do they play a role in the biopharmaceutics of inhaled drugs? *Journal of Pharmaceutical Sciences*, 99(5), pp.2240–2255.

Boucher, R. C., Stutts, M. J. & Gatzy, J. T., 1981. Regional differences in bioelectric properties and ion flow in excised canine airways. *Journal of Applied Physiology*, 51(3), pp. 706-714

Cone, R.A., 2009. Barrier properties of mucus. *Advanced Drug Delivery Reviews*, 61(2), pp.75–85.

Crystal, R.G. *et al*., 2008. Airway epithelial cells. Current concepts and challenges. *Proceedings of the American Thoracic Society*, 5(7), pp.772–777.

Daniher, D.I. & Zhu, J., 2008. Dry powder platform for pulmonary drug delivery. *Particuology*, 6(4), pp.225–238.

Ducreux, J. & Vanbever, R., 2007. Crucial biopharmaceutica issues facing macromolecular candidates for inhalation: the rose of macrophages in pulmonary protein clearance. *Respiratory Drug Delivery Europe*, pp.31–41.

Edwards, D.A. *et al.*, 1997. Large porous particles for pulmonary drug delivery. *Science*, 276(5320), pp.1868–1872.

Forbes, B. *et al.*, 2011. Challenges in inhaled product development and opportunities for open innovation. *Advanced Drug Delivery Reviews*, 63(1), pp.69–87.

Fröhlich, E. & Meindl, C., 2014. In Vitro Assessment of Chronic Nanoparticle Effects on Respiratory Cells. In *Nanomaterials - Toxicity and Risk Assessment*. pp. 69–91.

Golshahi, L. & Finlay, W.H., 2009. Recent advances in understanding gas and aerosol transport in the lungs: application to predictions of regional deposition. *Advances in Transport Phenomena*, 1, pp.1–30.

Gonda, I., 2000. The ascent of pulmonary drug delivery. *Journal of Pharmaceutical Sciences*, 89(7), pp.940–945.

Gumbleton, M. *et al.*, 2011. Spatial expression and functionality of drug transporters in the intact lung: objectives for further research. *Advanced Drug Delivery Reviews*, 63(1), pp.110–118.

Haghi, M. *et al.*, 2014. Across the pulmonary epithelial barrier: Integration of physicochemical properties and human cell models to study pulmonary drug formulations. *Pharmacology & Therapeutics*, 144(3), pp.235–252.

Hoppentocht, M. *et al.*, 2014. Technological and practical challenges of dry powder inhalers and formulations. *Advanced Drug Delivery Reviews*, 75, pp.18–31.

Hou, S. *et al.*, 2015. Practical, regulatory and clinical considerations for development of inhalation drug products. *Asian Journal of Pharmaceutical Sciences*, 10(6), pp.490–500.

Hughes, J.M.B., 2010. *Physiology and practice of pulmonary function*, The association for respiratory technology and physiology (ARTP).

Ibrahim, M. & Garcia-Contreras, L., 2013. Mechanisms of absorption and elimination of drugs administered by inhalation. *Therapeutic Delivery*, 4(8), pp.1027–1045.

Ibrahim, M., Verma, R. & Garcia-Contreras, L., 2015. Inhalation drug delivery devices: technology update. *Medical devices (Auckland, N.Z.)*, 8, pp.131–139.

Islam, N. & Cleary, M.J., 2012. Developing an efficient and reliable dry powder inhaler for pulmonary drug delivery - A review for multidisciplinary researchers. *Medical Engineering & Physics*, 34(4), pp.409–427.

Islam, N. & Gladki, E., 2008. Dry powder inhalers (DPIs) - A review of device reliability and innovation. *International Journal of Pharmaceutics*, 360(1–2), pp.1–11.

Kell, D.B., Dobson, P.D. & Oliver, S.G., 2011. Pharmaceutical drug transport: the issues and the implications that it is essentially carrier-mediated only. *Drug Discovery Today*, 16(15), pp.704–714.

Kim, K.-J. & Malik, A.B., 2003. Protein transport across the lung epithelial barrier. *American Journal of Physiology. Lung Cellular and Molecular Physiology*, 284(2), pp.L247–L259.

Kleinstreuer, C., Zhang, Z. & Donohue, J.F., 2008. Targeted drug-aerosol delivery in the human respiratory system. *Annual Review of Biomedical Engineering*, 10, pp.195–220.

Labiris, N.R. & Dolovich, M.B., 2003. Pulmonary drug delivery. Part I: Physiological factors affecting therapeutic effectiveness of aerosolised medications. *British Journal of Clinical Pharmacology*, 56(6), pp.600–612.

Lansley, A.B., 1993. Mucociliary clearance and drug delivery via the respiratory tract. *Advanced Drug Delivery Reviews*, 11(3), pp.299–327.

Lee, W.-H. *et al.*, 2015. Nano- and micro-based inhaled drug delivery systems for

targeting alveolar macrophages. *Expert Opinion on Drug Delivery*, 5247(6), pp.1–18.

Mansour, H.M., Rhee, Y.-S. & Wu, X., 2009. Nanomedicine in pulmonary delivery. *International Journal of Nanomedicine*, 4, pp.299–319.

Mason, G. R., *et al*. 2001. Evaluation of pulmonary alveolar epithelial integrity by the detection of restriction to diffusion of hydrophilic solutes of different molecular sizes, *Clinical Science* 100, pp.231-236.

Mitchell, H.W., 2009. Airway smooth muscle contraction - perspectives on past, present and future. *Pulmonary Pharmacology & Therapeutics*, 22(5), pp.363–9.

Newman, S.P., 1985. Aerosol deposition in inhalation therapy. *Chest*, 88, p.152S–160S.

Oberdorster, G. *et al*., 1992. Role of the alveolar macrophage in lung injury: studies with ultrafine particles. *Environmental Health Perspectives*, 97, pp.193–199.

Olsson, B., Bondesson, E., Borgström, L., *et al*., 2011. Pulmonary drug methabolism, clearance and absorption. In H. D. C. Smyth & A. J. Hickey, eds. *Controlled Pulmonary Drug Delivery: Advances in Delivery Science and Technology*. Springer US, pp. 21–50.

Panettieri, R.A. *et al*., 2008. Airway smooth muscle in bronchial tone, inflammation, and remodeling: Basic knowledge to clinical relevance. *American Journal of Respiratory and Critical Care Medicine*, 177(3), pp.248–252.

Patton, J., 1996. Mechanism of macromolecule absorption by the lungs. *Advanced Drug Delivery Reviews*, 19(1), pp.3–36.

Patton, J.S. *et al*., 2010. The particle has landed - Characterizing the fate of inhaled pharmaceuticals. *Journal of Aerosol Medicine and Pulmonary Drug Delivery*, 23(S2), pp.S71–S87.

Patton, J.S. & Byron, P.R., 2007. Inhaling medicines: delivering drugs to the body through the lungs. *Nature Reviews, Drug Discovery*, 6(1), pp.67–74.

Patton, J.S., Fishburn, C.S. & Weers, J.G., 2004. The lungs as a portal of entry for systemic drug delivery. *Proceedings of the American Thoracic Society*, 1(4), pp.338–44.

Pilcer, G. & Amighi, K., 2010. Formulation strategy and use of excipients in pulmonary drug delivery. *International Journal of Pharmaceutics*, 392(1), pp.1–19. Available at: http://dx.doi.org/10.1016/j.ijpharm.2010.03.017.

Schanker, L.S., 1978. Drug absorption from the lung. *Biochemical Pharmacology*, 27(4), pp.381–385.

Schanker, L.S., Mitchell, E.W. & Brown, R.A., 1986. Species comparison of drug absorption from the lung after aerosol inhalation or intratracheal injection. *Pharmacology*, 14(1), pp.79–88.

Schulz, H., 1998. Mechanisms and factors affecting intrapulmonary particle deposition: implications for efficient inhalation therapies. *Pharmaceutical Science & Technology Today*, 1(8), pp.336–344.

Stegemann, S. *et al.*, 2013. Developing and advancing dry powder inhalation towards enhanced therapeutics. *European journal of pharmaceutical sciences : official journal of the European Federation for Pharmaceutical Sciences*, 48(1), pp.181–194.

Sugano, K. *et al.*, 2010. Coexistence of passive and carrier-mediated processes in drug transport. *Nature Reviews, Drug Discovery*, 9(8), pp.597–614.

Sung, J.C., Pulliam, B.L. & Edwards, D.A., 2007. Nanoparticles for drug delivery to the lungs. *Trends in Biotechnology*, 25(12), pp.563–570.

Telko, M.J. & Hickey, A.J., 2005. Dry powder inhaler formulation. *Respiratory*, 50(9),

pp.1209–1227.

Tolman, J.A. & Williams, R.O., 2010. Advances in the pulmonary delivery of poorly water-soluble drugs: influence of solubilization on pharmacokinetic properties. *Drug Development and Industrial Pharmacy*, 36(1), pp.1–30.

Weers, J.G. & Miller, D.P., 2015. Formulation design of dry powders for inhalation. *Journal of Pharmaceutical Sciences*, 104(10), pp.3259–3288.

Weibel, E.R. & Gomez, D.M., 1962. Architecture of the human lung. Use of quantitative methods establishes fundamental relations size and number of lung structures. *Science*, 137(3530), pp.577–585.

# Chapter 2
# General materials and methods

## 2.1. Materials

Micronised salbutamol sulfate and indomethacin dry powders ($DV_{50} \leq 3\mu m$) were kindly provided by GlaxoSmithKline (GSK; Ware, UK). Information about the particle size distribution was provided by GSK.

Calu-3 human adenocarcinoma cell line was purchased from the American Type Culture Collection (ATCC, Manassas, VA, USA).

Transwell® permeable supports (0.4 μm pore size, polyester membrane, 1.2 mm inserts, sterile), 12-well plates, 48-well plates and black 96-well plates were purchased from Corning Incorporated – Life Science (NY, USA).

HPLC grade methanol (MeOH) and acetonitrile (AcN), isopropanol (IPA) and industrial methylated spirits (IMS) came from Fisher Scientific (Loughborough, UK). HPLC grade water was produced with a Purelab Ultra ELGA system.

Salbutamol sulfate and indomethacin (99% pure) were purchased from Alfa Aesar (Heysham, UK).

Where not specified, chemicals were from Sigma Aldrich (St. Lewis, MO).

# 2.2. Methods

## 2.2.1. The deposition system

The deposition system developed and validated in this doctoral study consisted of a vacuum glass desiccator with the PennCentury™ Dry Powder Insufflator – Model DP-4 (Penn-Century. Inc. Wyndmoor, PA) secured in the desiccator vacuum port by means of a Fisherbrand™ rubber stopper (Ø=21 mm, Figure 2.1(A)).

The PennCentury™ device was fitted with a removable straight needle (length: 7.2 cm) and a PennCentury Air Pump™ – Model AP-1 (Penn-Century. Inc. Wyndmoor, PA).

Samples, namely microscopy slides, 12 Transwells® cell culture plates and individual Transwell® inserts, were placed on the internal support of the desiccator (Ø=18.4 cm). The distance between the port entrance of the desiccator and the deposition surface was 20.0 cm (Figure 2.1 (B)).

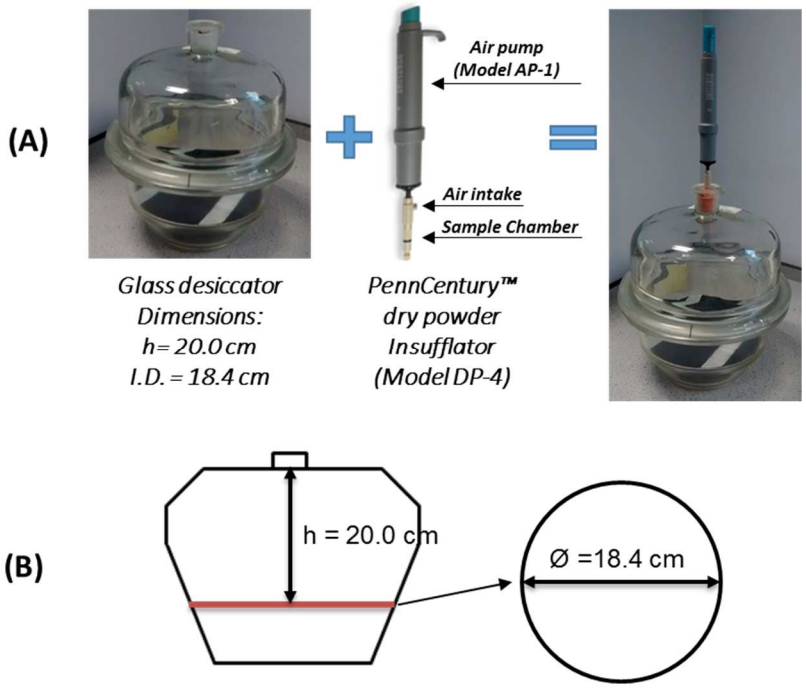


**Figure 2.1: deposition system representation. (A) elements composing the deposition system and their assembling; (B) dimensions of the desiccator chamber**

## 2.2.2. Cell culture

### 2.2.2.1. Calu-3 cell maintenance

Calu-3 cell line (passage 29-39) was cultured in 75 $cm^2$ culture flasks in Dulbecco's Modified Eagle's Medium: F-12 (DMEM:F-12) containing 10% (v/v) foetal bovine serum (FBS), 1% (v/v) non-essential amino acid, 1% (v/v) L-glutamine and 1% (v/v) penicillin-streptomycin solutions. Cells were maintained in a cell culture incubator (95% humidity, 5% $CO_2$, 37 °C) and were propagated and subcultured according to ATCC recommendations as follows.

### 2.2.2.2. Calu-3 cell revival

When necessary a new vial of Calu-3 cells was collected from the cell bank stored in liquid $N_2$ and thawed in the water bath at 37°C. The whole content (1 mL of cell suspension in DMEM-F12 – 10% (v/v) dimethyl sulfoxide (DMSO)) was transferred into a 75 $cm^2$ cell culture flask already containing 9 mL of fresh pre-warmed medium. Cells were left in the incubator (95% humidity, 37°C, 5% $CO_2$) overnight, and medium was changed the next day.

### 2.2.2.3. Changing medium

Medium was changed three times per week as follows: medium was removed from the cell culture flask and replaced with 10 mL of fresh pre-warmed (37°C) medium.

### 2.2.2.4. Passaging the cells

Cells were passaged once a week when a confluence of 80-90% was reached. Medium was removed and 10 mL of pre-warmed (37°C) sterile phosphate buffer saline solution (PBS) was used to wash the cells. PBS was removed and 5 mL of 1X trypsin- Ethylene-diamine-tetra-acetic acid (EDTA) solution, containing 0.5 g of porcine trypsin and 0.2 g EDTA-4Na per litre of Hank's Balanced Salt Solution (HBSS) with phenol red, was added to the flask. The flask was kept in the incubator (95% humidity, 37°C, 5% $CO_2$)

until cells were completely detached from the flask surface. Subsequently, 8 mL of prewarmed medium was added to the flask and the whole cell suspension was then transferred into a 15 mL centrifuge tube (Falcon™) for centrifugation (1,200 rpm, 5 minutes). The supernatant was removed and cells were re-suspended in 6 mL of fresh pre-warmed medium. One third (2 mL) of cell suspension was transferred to a new flask containing 8 mL of fresh pre-warmed medium.

#### 2.2.2.5. Cell culture well-plate seeding

Cells were seeded onto 12 well Transwell® polyester inserts supports on a weekly basis.

After centrifugation during the passaging process (see 2.2.2.4, page 33), the cell pellet was resuspended in 6 mL of fresh pre-warmed medium. Subsequently, 100 µL of the cell suspension was diluted 1:1 with Trypan-Blue solution and cells were counted using a haemocytometer (Figure 2.2).

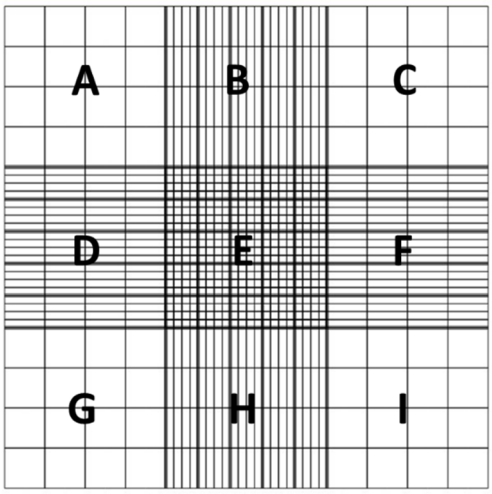


**Figure 2.2: haemocytometer grid schematic**

The average ($N_c$) between the number of cells counted in the four squares A, C, G and I was calculated and the number of cells per mL in the suspension was calculated as follows (Equation 2.1):

$$C_{cells} = N_c \times 2 \times 10^4$$

Cells were seeded onto 12 well Transwell® polyester inserts housed in 12-well plates at a seeding density of $1x10^5$ cells $mL^{-1}$ in 500 µL of apical medium and 1.5 mL of medium was added in the basolateral side. Plates were kept in the incubator (95% humidity, 37°C, 5% CO2) overnight. The culture was turned into the air-liquid interface (ALI) 24 hours after seeding by removing the medium from both the apical and the basolateral chambers and adding 500 µL of fresh pre-warmed medium in the basolateral chamber only.

Medium was changed every 2-3 days thereafter.

The Calu-3 monolayers were left to differentiate for 21 days allowing sufficient time for the development of tight junctions, expression of transporters and homogeneous mucus coverage (Haghi *et al.* 2010).

**2.2.2.6. Freezing cells for storage**

Cells (passage number 21-38) were frozen on a weekly basis.

After centrifugation during the passaging process (see 2.2.2.4, page 33), the cell pellet was resuspended in 3 mL of fresh pre-warmed medium containing 10% (v/v) DMSO. Aliquots of 1 mL were placed into cryo-vials (Thermo Fisher Scientific, Loughborough, UK) and immediately transferred to -80°C freezer into a freezing container (Mr. Frosty, Thermo Fisher Scientific, Loughborough, UK) overnight, and then transferred to a liquid nitrogen tank for long term storage.

**2.2.2.7. Transepithelial electrical resistance (TEER) measurement**

The transepithelial electrical resistance (TEER) of each cellular monolayer was monitored using a voltohmmeter (EVOM, equipped with STX-2 chopstick electrodes, World Precision Instruments, Sarasota, FL, USA).

The TEER was measured either in medium or in HBSS.

Briefly, 500 µL and 1.5 mL of pre-warmed medium or HBSS was added to the apical and basolateral side respectively. The cell monolayers were left to equilibrate for 30 minutes in the incubator (95% humidity, 5% $CO_2$, 37 °C). The chopstick electrodes were soaked in IMS for at least 15 minutes and rinsed in sterile PBS prior to TEER measurement.

To measure the TEER, the shorter chopstick was submerged in the apical medium, while the longer one was submerged in the basolateral medium, according to the configuration shown in Figure 2.3:

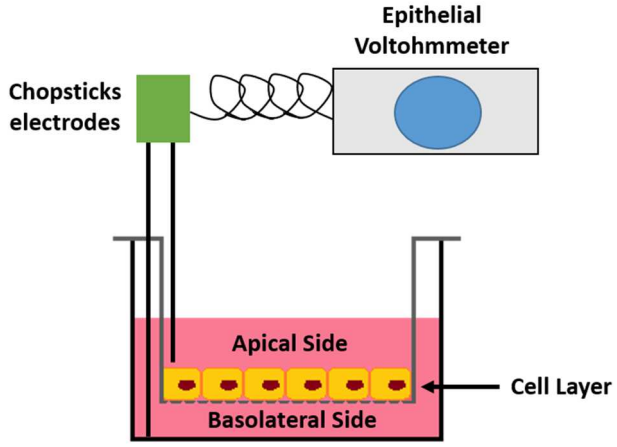


**Figure 2.3: schematic representation of the configuration of the epithelial voltohmmeter used to measure the TEER**

The TEER value expressed in [$\Omega \cdot cm^2$] for each monolayer was calculated by subtracting the resistance of the blank insert (estimated as being 100 $\Omega \cdot cm^2$) and correcting for the Transwell® insert growth area (1.12 $cm^2$).

### 2.2.2.8. Cell layer integrity assessment: lucifer yellow permeability assay

The integrity of the monolayer was assessed by monitoring the apical to basolateral (A→B) permeability of the paracellular marker lucifer yellow VS dilithium salt (LY) for one hour.

Briefly, 300 µL of 100 µM LY solution was placed in the apical chamber, and 900 µL of fresh pre-warmed HBSS was placed in the basolateral chamber. Samples (100 µL) were withdrawn from the basolateral chamber after 30 and 60 minutes and transferred

to a black 96 well plate (Nunc F96, Scientific Laboratory Supplies, Nottingham, UK). Samples (100 µL) were taken from the apical side at the beginning (time zero) and at the end of the experiment.

Samples were analysed for LY content using a Tecan (SPARK 10M) plate-reader and fluorescence was monitored at $\lambda_{em}$= 437 nm and $\lambda_{ex}$= 535 nm.

A flux<2.0% was accepted to indicate a tight and intact monolayer (Florea *et al.* 2002; Foster *et al.* 2000).

The apparent permeability ($P_{app}$) of LY was calculated as per Equation 2.2:

$$P_{app} = \left(\frac{dQ}{dt}\right) \cdot \frac{1}{A\ C_0}$$

**Equation 2.2: apparent permeability ($P_{app}$) calculation (Haghi *et al.* 2012)**

where $dQ/dt$ is the transport (or permeability) rate, $A$ is the surface area (1.12 $cm^2$) and $C_0$ is the concentration of the marker in the donor chamber at time zero.

## 2.2.3. *In-vitro* transepithelial transport studies

The transepithelial transport of salbutamol and indomethacin either in solution or delivered as dry powder was investigated.

For the solution transport experiment, 200 µL of 5.0 and 2.5 µg $mL^{-1}$ solutions (corresponding to doses of 1.0 and 0.5 µg) of drug in HBSS was placed in the apical chamber and 900 µL of fresh pre-warmed HBSS (37°C) was placed in the basolateral side. Due to the low water solubility of indomethacin, a 1 mg $mL^{-1}$ stock solution of indomethacin in 100 mM $Na_2CO_3$ was prepared and diluted accordingly in HBSS to obtain 5.0 and 2.5 µg $mL^{-1}$ solutions.

Drug dry powder deposition, dissolution and diffusion/transport across the bronchial epithelial barrier was investigated using the deposition system described above to deposit 1.0 and 0.5 µg of dry powder onto Calu-3 cellular layers. Four Transwell® inserts were transferred to positions B, C, E and F in the chamber (Figure 3.17(4), page

65). The PennCentury™ Dry Powder Insufflator was loaded with 1.0 and 2.0 mg of dry powder and 5.0 mL of ambient air was used to produce the spray. Before transferring the inserts to a clean 12 well plate, the inner and outer plastic surfaces of the Transwell® inserts were carefully wiped with Azowipes (Sinergyhealth, UK) to remove the drug particles that did not deposit on the cellular layer, paying extreme care not to touch the cell layers. Once the Transwell® inserts were transferred to a clean 12 well plate, 500 µL of fresh pre-warmed HBSS was placed in the basolateral chamber.

The plates containing the cell layers exposed to the dry powder spray or to the drug solution were kept in the incubator for the duration of the experiment.

Samples (200 µL) were withdrawn from the basolateral side after 5, 10, 15, 20, 30, 60, 120, 180 and 240 minutes, and 200 µL of fresh pre-warmed HBSS was used to restore the initial basolateral volume. After 4 hours the apical side was washed twice with 100 µL of fresh HBSS and samples were collected for analysis of the residual apical drug. Afterwards, cells were lysed with 500 µL of IPA:DMSO (1:1), harvested and centrifuged at 14,000 rpm for 5 minutes. The supernatant was collected and analysed for drug content. This allowed for the calculation of total drug deposited via sum of all samples.

In the case of the drug applied in solution to the Calu-3 cell layers, the $P_{app}$ [cm/sec] of the drug was calculated as per Equation 2.2 (page 37).

Experiments were performed in duplicate (N=2), using four Transwell® inserts per replicate (n=4).

## 2.2.4. PrestoBlue® cell viability assay

PrestoBlue® cell viability assay was employed to assess the cytotoxicity of various compounds in the appropriate concentration range, namely tetraethylammonium

(TEA), indomethacin, indomethacin formulations, individual excipients of indomethacin formulations under investigation and $Na_2CO_3$ (compounds are named in order of discussion in the following experimental chapters; the concentration range investigated for each compound is reported in the chapters of interest).

PrestoBlue® is a resazurin-based compound that undergoes chemical reduction by the mitochondrial enzymes of viable cells. The conversion of PrestoBlue® from the oxidised to the reduced form results in a change in colour and a shift in its fluorescence. It can be quantified by means of spectrophotometric or fluorometric methods (Boncler *et al*. 2014).

The assay was carried out on 48-well plates as these were the ones with growth area of the individual wells (0.95 $cm^2$) closest to that of Transwell® inserts (1.12 $cm^2$).

Calu-3 cells (passage 30-38) were seeded in 48-well plates at a density of $1x10^5$ cells $cm^{-2}$ per well and cultured until a confluence of 95-100% was reached (typically 7 days), changing the medium every 2-3 days.

The exposure time of the cell layers to PrestoBlue® reagent was evaluated first.

When ready, cell layers were washed twice with pre-warmed (37°C) PBS. Subsequently, 100 µL of PrestoBlue® solution (10% PrestoBlue® 10X in DMEM:F12 medium without supplements) was added to the cell layers, and the plates were kept in the incubator (95% humidity, 5% $CO_2$, 37°C) for the duration of the experiment. Samples of 50 µL were collected every 15 minutes for 1 hour, transferred to a black 96-well plate, and analysed by measuring fluorescence intensity ($\lambda_{ex}$= 560 nm, $\lambda_{em}$= 590 nm) using a TECAN plate reader.

As showed in Figure 2.4 the fluorescence intensity was linear in the time-span investigated. An exposure time of 30 minutes was judged to be appropriate to carry out the following experiments.

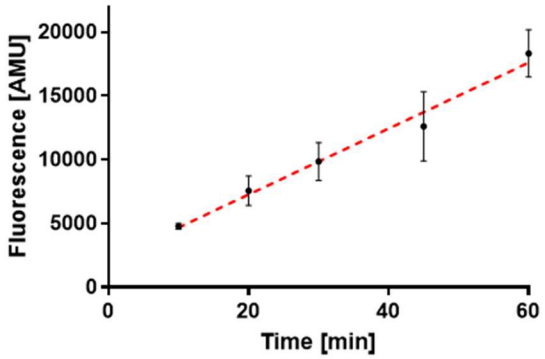


**Figure 2.4: optimisation of exposure time of Calu-3 cells to PrestoBlue® reagent.**

Once the appropriate exposure time of Calu-3 cells to PrestoBlue® reagent had been selected, the cytotoxicity of the compounds of interest was assessed.

On the day of the experiment, cells were washed twice with pre-warmed (37°C) PBS. Subsequently, 200 µL of the test solutions were applied to the cell layers. The test solutions were removed after a pre-determined exposure time (up to 4 hours in all cases; 10-20-30-60-120-180 and 240 minutes in the case of TEA). The cell layers were washed twice with pre-warmed (37°C) PBS and 100 µL of PrestoBlue® solution was added to each well. After 30 minutes, 50 µL samples were collected, transferred to a black 96-well plate, and analysed by measuring fluorescence intensity ($\lambda_{ex}$= 560 nm, $\lambda_{em}$= 590 nm) using a TECAN plate reader.

Cell culture plates were kept in the incubator (95% humidity, 5% $CO_2$, 37°C) for the duration of the experiments.

The positive control (100% viability) was represented by cells not exposed to any test compound and kept in normal medium. The negative control (0% viability) was represented by cells exposed to Triton® X-100 (2% in HBSS). Data were corrected for background noise by subtracting the fluorescence registered for fresh PrestoBlue® solution to the fluorescence of each sample.

The experiments were conducted once (N=1) using four wells per conditions (n=4).

## 2.2.5. HPLC-MS/MS drug analysis

Samples obtained from the drug (salbutamol sulfate and indomethacin) transport experiments described in chapters 4, 5 and 6, were analysed for drug content by HPLC-MS/MS.

The HPLC system consisted of an Agilent Hewlett Packard series 1100 coupled with a Micromass Quattro Ultima Pt mass spectrometer (Waters, Milford, USA) equipped with an electrospray ion source operated in positive mode for both salbutamol and indomethacin. An ACE3 C18 (3µm, 150 mm x i.d. 2.1 mm) column fitted with a C18 guard cartridge was used for all analysis.

Salbutamol sulfate in HBSS samples were diluted 1:1 with MeOH (HPLC grade) vortexed for 1 minute and centrifuged at 5,000 rpm for 5 minutes at 4°C. The supernatant was diluted 1:1 with phase A consisting of aqueous solution containing 0.1% v/v formic acid, ammonium formate 20 mM (pH 3.8), and 50 µL of the resulting solution was injected in the HPLC-MS/MS system for quantification.

Samples were run at 0.2 mL $min^{-1}$ isocratically using a mixture of phase A and MeOH (50:50) as mobile phase.

Salbutamol was detected in multi reaction monitoring (MRM) mode at m/z 240.1 → 148.1. MS parameters were as follows: capillary voltage, 3.5 kV; cone voltage, 35 V; source temperature, 125°C; desolvation temperature, 350°C; collision energy, 20 kV.

Indomethacin in HBSS samples were diluted 1:1 with the mobile phase (AcN:phase A, 50:50), vortexed for 1 minute and centrifuged at 5,000 rpm for 5 minutes at 4°C. The supernatant (40 µL) was injected in the HPLC-MS/MS system and run at 0.3 mL $min^{-1}$ isocratically using a mixture of phase A and acetonitrile (20:80) as mobile phase.

Indomethacin was detected in multi reaction monitoring (MRM) mode at m/z 359.03→139.11 and 359.03→111. MS parameters were as follows: capillary voltage,

3.5 kV; cone voltage, 37 V; source temperature, 125°C; desolvation temperature, 350°C; collision energy, 22 kV.

## 2.2.6. Statistical analysis

Statistical analysis of the data was performed using GraphPad Prism 6.02.

Unpaired t-test (multiple comparisons) and ANOVA one-way analysis (with Tukey's multiple comparison test) were carried out to compare between two or more than two groups respectively. Differences were considered significant when $p<0.05$.

## 2.3. References

Boncler, M. *et al.*, 2014. Comparison of PrestoBlue and MTT assays of cellular viability in the assessment of anti-proliferative effects of plant extracts on human endothelial cells. *Journal of Pharmacological and Toxicological Methods*, 69(1), pp.9–16.

Florea, B.I. *et al.*, 2002. Transfection efficiency and toxicity of polyethylenimine in differentiated Calu-3 and nondifferentiated COS-1 cell cultures. *AAPS PharmSci*, 4(3), pp.1–11.

Foster, K.A. *et al.*, 2000. Characterization of the Calu-3 cell line as a tool to screen pulmonary drug delivery. *International Journal of Pharmaceutics*, 208(1), pp.1–11.

Haghi, M. *et al.*, 2012. Deposition, diffusion and transport mechanism of dry powder microparticulate salbutamol, at the respiratory epithelia. *Molecular Pharmaceutics*, 9(6), pp.1717–1726.

Haghi, M. *et al.*, 2010. Time- and passage-dependent characteristics of a Calu-3 respiratory epithelial cell model. *Drug Development and Industrial Pharmacy*, 36(10), pp.1207–1214.

# Chapter 3
# Development of the dry powder deposition system

## 3.1. Introduction

Traditionally, the continuous development of new pharmaceutical products requires tests to be performed on animals prior to clinical evaluation in humans (Chapman *et al*. 2013).

In the case of inhaled medicines, these tests often involve forced inhalation or intra-tracheal administration, followed by blood or tissue analysis in order to obtain pharmacokinetic data. However, it is often very difficult to transfer the information obtained from animal tests to humans due to the inter-species differences in both aerosol administration and mechanisms of drug deposition, absorption and disposition (Hein *et al*. 2010).

In addition to that, ethical reasons and the "Three Rs principles" (Replacement, Reduction, Refinement) (Russel & Burch 1959) encourage the development of alternative systems (*in-vitro*) to investigate the effect of drugs after administration that would not involve the use of animals.

### 3.1.1. *In-vitro* models of the lung epithelium

As explained in Chapter 1 (paragraph 1.2, page 2), drugs for inhalation must overcome several barriers before reaching the targeted site, and the lung epithelium represents the primary obstacle (Patton *et al.* 2004).

The selection of a proper *in-vitro* model having the same characteristics of the lung epithelium is very important to study the mechanisms of deposition, absorption and elimination of drug particles delivered to the lungs.

The models used to mimic the lung epithelial barriers include isolated perfused organs, animal or human tissue explants and cell cultures. The first two models are very complex despite representing close imitations of the *in-vivo* situation. On the other hand, cell culture models are far less complicated systems (Steimer *et al.* 2005).

Cell cultures have proven to be very convenient in the development process of new pharmaceutical products in general. In fact, they are easier to use, less costly to maintain, allow for high-throughput screening, and do not present the ethical implications involved in the use of animals (Cabrera-Pérez *et al.* 2016). It must be remembered though, that their major limitations reside in the variability of the data obtained depending on the culture conditions used (cell passage number, growth media, and even the operator), the cell strain and the protocol selected, it is then difficult to make comparisons between laboratories.

*In-vitro* cell culture models can be either primary cells isolated from human or animal tissues, or continuously growing cell lines. Primary cells present some drawbacks, mainly due to the fact that the isolation procedure could be time-consuming. In addition, availability of the generating tissues could be limited and the resulting cells can only be used for a limited number of passages. Cell lines, on the other hand, are usually generated from tumour tissues, or by transformation of primary cell lines using

viral vectors. Moreover, they can be used for more passage numbers in comparison to primary cells and their culture is relatively straightforward and can follow standardised procedure that allow for increased reproducibility of data. However, cell lines often present different features compared to primary cell cultures (M. Haghi *et al*. 2014).

In the case of the lung, the cell cultures adopted should ideally reproduce the *in-vivo* composition and morphology of the specific region that is modelled. They should for example include the major cell types found in the region of interest (e.g. columnar cells for the upper airways and ATI cells for the alveolar region; see Chapter 1, (paragraph 1.2.2, page 4). In addition, these models should be human and form tight junctions indicating an effective barrier to solute permeability (Forbes & Ehrhardt 2005).

The growth conditions of the cell line are a crucial factor in determining the reliability of the system and its suitability to represent the lung epithelium. The classical methodologies consist in growing cell lines as liquid-covered cell cultures (LCC) where the medium layer is a few millimetres thick on top of the cell layer. This experimental design does not fully represent the real situation in the lungs where epithelial cells are covered by a mucus gel layer that separates them from the air. In this respect, Whitcutt *et al*. (1988) first developed a biphasic cell culture system (air-liquid interface culture, ALI) where the epithelial cells can be maintained between air (apical side) and liquid medium (basolateral side). The ALI culture technique is nowadays very well established and it usually performed in Transwell® inserts (Figure 3.1). This model better reproduces the situation *in-vivo* where the lung epithelium is exposed to air, also allowing to directly expose the cell layers to the test air flow when carrying out drug-cell interaction studies, drug permeation and active and passive drug transport studies.

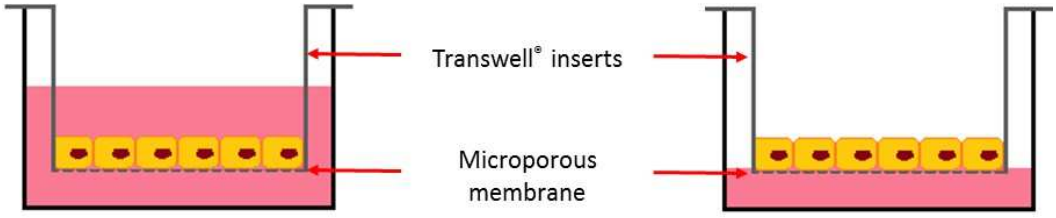


**Figure 3.1: representation of submerged (left) and air-liquid interface cell culture (right)**

The cell models available represent the alveolar or the bronchial epithelium.

#### 3.1.1.1. Alveolar cell lines

The most commonly used alveolar cell line is A549 that is derived from a human adenocarcinoma and presents morphology similar to alveolar type II cells. Studies have been conducted on drug absorption and drug metabolism using this cell line, however their use as a model for drug absorption is debatable as they are not able to polarise and form TJs (Forbes 2000; M. Haghi *et al.* 2014; Andrade *et al.* 2016). Alternative cell lines have been identified in the hAELVi (immortalized human alveolar type I-like cell line) and the TTI (immortalized human alveolar type I-like cell line). hAELVi cells present characteristics of ATI cells and barrier properties with the formation of TJs, whereas TTI cells do not form TJs despite showing ATI-like phenotype (Andrade *et al.* 2016).

#### 3.1.1.2. Bronchial cell lines

The bronchial cell lines available include BEAS-2B (pulmonary immortalised human epithelium bronchial cells), NCI-H441 (human bronchiolar epithelial cell line), Nuli-1, 16HBE14o- and Calu-3.

BEAS-2B do not form tight junctions and consequently they are not the system of choice to model drug absorption. On the other hand, NCI-H441 form polarised cell layers as well as tight junctions and are therefore better *in-vitro* model candidates. NuLi-1 is another cell line obtained from freshly isolated epithelial cells in primary culture that are able to form tight junctions with high TEER values registered (>600

$\Omega \cdot cm^2$). Despite its potential to be a good candidate for active and passive drug transport studies, it is still poorly used. Calu-3 and 16HBE14o- cell lines are the ones recognised to exhibit features that are more similar to the respiratory bronchial epithelium and therefore are the most commonly used (Acosta *et al.* 2016).

16HBE14o- was obtained with a SV40 large T antigen transformation of normal bronchial epithelial cells from a 1-year old heart lung transplant male patient (Cozens *et al.* 1994). They are cuboidal in shape, form polarised cell layers and form TJs, but the formation of functional layers is highly dependent upon the presence of apical fluids, which is not compatible with the ALI technique (Ehrhardt *et al.* 2002). For this reason, they are usually not the model of choice for drug/epithelial interactions and drug absorption studies although some examples can be found in the literature (Forbes *et al.* 2003; Manford *et al.* 2005).

Calu-3 cells come from bronchial adenocarcinoma of a 25-year-old Caucasian male (Shen *et al.* 1994; Fogh *et al.* 1977). They are mainly columnar in shape (Forbes & Ehrhardt 2005), and like 16HBE14o- exhibit suitable barrier properties in culture forming polarized cell layers and expressing proteins of the intercellular junctions (tight junctions, desmosomes and zonulae adherents). However, Calu-3 cells secrete mucin like substances more than 16HBE14o- cells, therefore they are more suitable for studies of drug absorption and transport (Grainger *et al.* 2006).

Calu-3 cells can be cultured under both conditions (LLC and ALI), but the two culture conditions result in cell layers with different morphological and permeability characteristics. In particular, it has been shown that when grown at the air-liquid interface, Calu-3 cells develop in a more morphologically representative model of the airway epithelium *in-vivo* forming a pseudostratified layer of columnar cells with enhanced ciliagenesis. Moreover, it has been found that they produce mucus secreted

on the apical side, and present good barrier properties with TEER value lower than when cultured according to the LLC model reflecting less restrictive tight-junctions (Grainger *et al*. 2006; Ong *et al*. 2013). However, it must be taken into account that although maintenance culture protocols are now very well established, variations in the TEER values of Calu-3 cells are registered between laboratories.

As reviewed by Ong *et al.* (2013) the Calu-3 cell line has also been extremely useful to investigate novel strategies to improve formulations for targeted lung delivery as well as to better understand the mechanisms of drug-cell interaction and drug absorption in the lung epithelium.

### 3.1.2. *In-vitro* exposure methods

The regional deposition of particles in the lungs can be simulated and predicted with a number of aerosol classification devices that reproduce the lung structure. These include the multistage liquid impinger (MSLI), the Andersen cascade impactor (ACI), the next generation impactor (NGI) and the glass twin stage impinger (TSI). These systems operate based on inertial impaction exclusively, and in addition they are not able to provide any information about dissolution and transport through the epithelium. Therefore, there has been a great attempt in the past years to modify these types of apparatuses in order to investigate particle dissolution and transport.

Test systems allowing both deposition and absorption studies are widely used in environmental toxicology (Aufderheide & Mohr 1999; Bitterle *et al.* 2006; Tang *et al.* 2012; Kim *et al*. 2013) and to study the effect of cigarette smoke (Phillips *et al*. 2005), however they reproduce long exposure and low-dose application of the test air or particles. These conditions are certainly not comparable to the short-time bolus (or puff) inhalation for therapeutic purposes. In addition, the aims and objectives of the

pharmaceutical science concerning inhaled particle-cell interaction are quite different from the environmental and toxicological ones.

The major problem of *in-vitro* devices is the proper design of the exposure system of the cell layer to the exogenous agent. Tarkington *et al.* (1994) first described an *in-vitro* system to expose cultured airway epithelial cells to ozone, where a vertical stream of the test air was directed over the cell layer cultured at the air-liquid interface.

Many researchers have modified the already existent devices in order to allocate cell layers into the system and expose them to the test air flow. An example is represented by the Astra-type liquid impinger (Figure 3.2) where the cells are placed under a nozzle conducting the test aerosol (Fiegel *et al*. 2003).

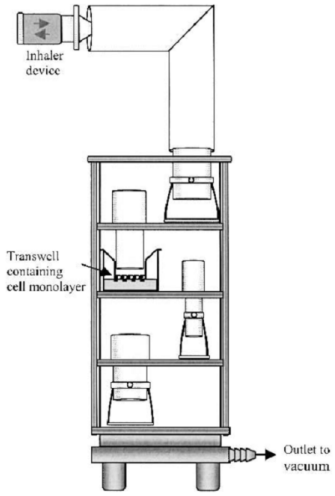


**Figure 3.2: schematic of the Astra-type liquid impinger (Fiegel *et al.* 2003)**

This setup causes turbulence that lead to a low deposition efficacy. Bur *et al.* (Bur *et al*. 2009) improved it cultivating the cells on the underside of Transwell® inserts and inserting these inserts through holes in the surface of the selected stage of the impinger. In this way, they managed to significantly reduce the turbulence and improve the deposition efficacy.

Sadler *et al.* (2011) adapted the cascade centripeter (CC), a commercial virtual impactor, to deposit microparticles onto cell layers (Figure 3.3). In this system,

particles are collected on a "virtual surface" at the entrance of the collection cone which is an area where the air flow is drastically reduced.

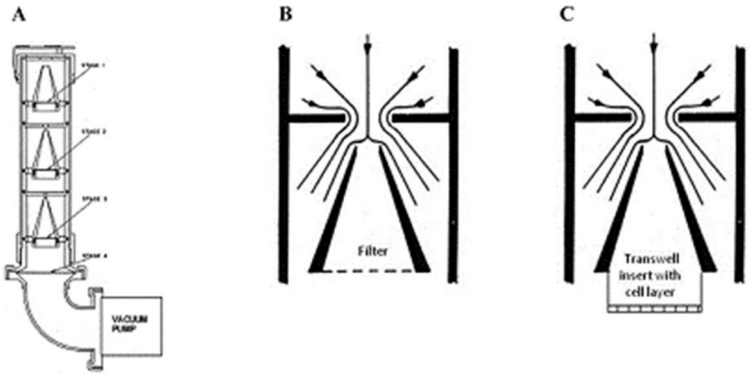


**Figure 3.3: Schematic of the cascade centripeter. A) the cascade centripeter; B) airflow around the impaction cone; C) application of a Transwell® insert (Sadler *et al.* 2011)**

The Andersen cascade impactor is another example of device that has been modified to perform dissolution and transport studies: Cooney *et al*. (2004) removed the impaction plate number 4 and placed Transwell® on the plate number 5, and deposited FITC-dextran on Calu-3 cell layers. However, this modification increases the distance between the jet and the plate as well as the flow through the system. A modification of the plate to allocate Snapwell® instead allows for a minimal change in the nozzle-plate distance that corresponds to a minimal change in the particles cut-off as showed in Figure 3.4 (Mehra Haghi *et al*. 2014).

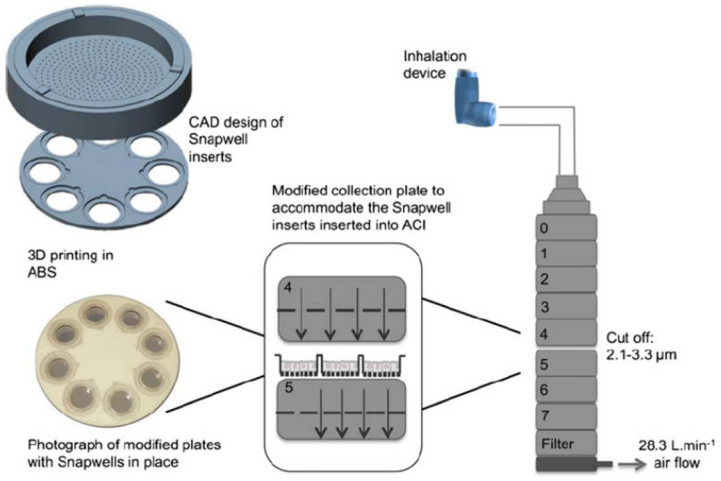


**Figure 3.4: Schematic of the modification of the Andersen cascade impactor (Mehra Haghi *et al.* 2014)**

Another interesting device is the twin-stage impinger (TSI, Figure 3.5) developed by GSK for the assessment of particles released from metered dose inhalers (MDIs) and dry powder inhalers (DPIs) (Saunders *et al.* 2008; Grainger *et al.* 2009). The particles emitted by the inhalers are separated into respirable and non-respirable fractions on the basis of the liquid impingement principle. Depending on the particle size range of interest, inserts are placed under the relevant jets.

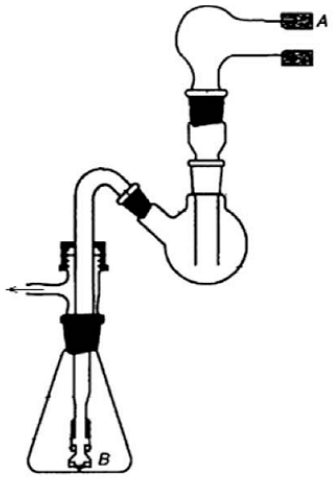


**Figure 3.5: schematic of twin-stage impinger (Grainger *et al.* 2009). A) Inhaler; B) Transwell® insert**

McDonnell *et al.* (2012) deposited budesonide on Calu-3 cell layers grown in Snapwell® fitted in a next generation impactor (NGI). However, they did not evaluate the cut-off diameter comparing the deposition with and without the modified stage of the impactor.

A different type of system called CULTEX was designed by Aufderheide *et al.* (Aufderheide & Mohr 1999) to expose the cells directly to airborne substances and investigate their toxicological effect. A later improvement brought the CULTEX Radial Flow System (RFS) where the test air stream is split into three radial tubes and directed onto the culture inserts which are separately supplemented with medium (Aufderheide *et al.* 2013). As showed in Figure 3.6, CULTEX-RFS consists of three modules: i) an inlet adapter to connect the aerosol generating unit to the ii) aerosol

guide which conducts the aerosol onto the cells, and iii) a sampling and socket module allocating three exposure chambers containing the cell layers (either petri dishes or Transwell® inserts).

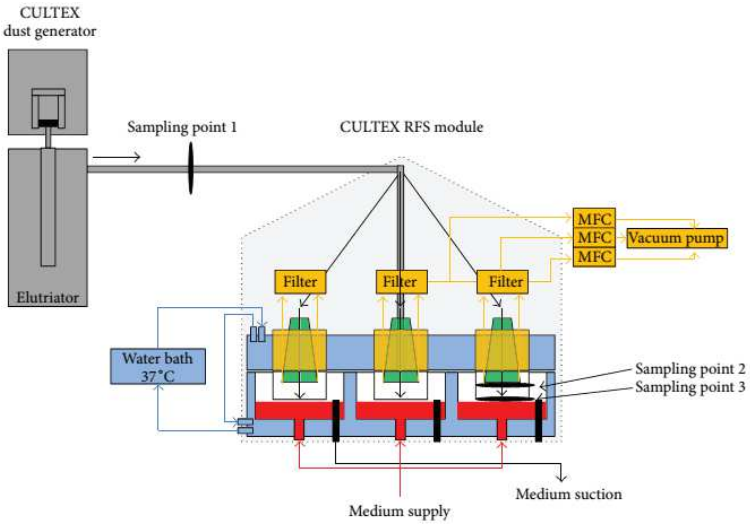


**Figure 3.6: schematic of CULTEX RFS (Aufderheide *et al.* 2013)**

The same system was further modified by Ritter *et al.* (2001) who added small openings in Teflon on top of the three inserts thus achieving a more balanced distribution of the gas flow over the cells.

Similar to the CULTEX is the VITROCELL (Figure 3.7) (Tang *et al.* 2012; Kim *et al.* 2013) mainly used to assess the toxicological effect of tobacco smoke, volatile organic compounds (VOC) and heavy metals (e.g. Cu). It consists of an aerosol distribution unit that drives the aerosol to the lung cells grown in ALI conditions. The chamber can accommodate up to three Transwell® inserts where the ALI growth conditions can be maintained throughout the exposure time since the system comprises also a container for cell culture medium.

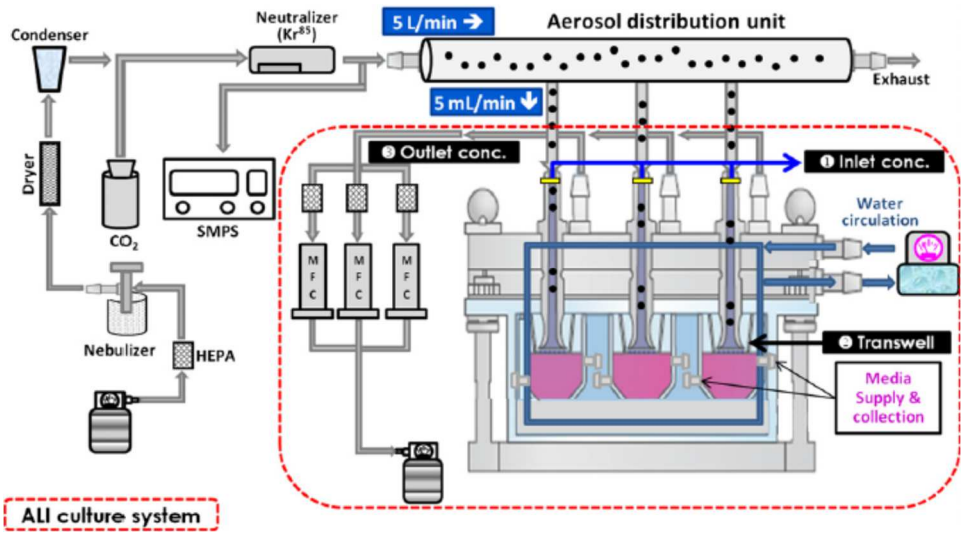


**Figure 3.7: schematic of VITROCELL system (Kim *et al.* 2013)**

Savi *et al.* (2008) developed a similar system to increase the deposition efficiency by charging particles and inducing an electrical field with opposite charge beneath the deposition surface (Figure 3.8).

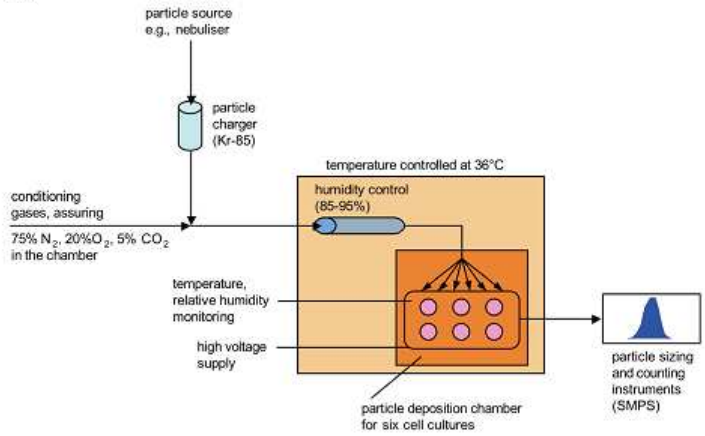


**Figure 3.8: Schematic of the experimental setup developed by Savi *et al.* (2008)**

It must be noted that the particle deposition in all the systems so far described occurs by impaction that is the prevalent mechanisms of deposition in the upper airways only. Devices allowing deposition based on sedimentation and diffusion processes better represent deposition in the deeper airways.

The sedimentation process of exogenous particles is predictable as the differentiation occurs according to the size, based on differential sedimentation velocities. On these

bases, Hein *et al.* (2010; 2011) developed their Pharmaceutical Aerosol Deposition Device on Cell Culture (PADDOCC) consisting of an air-flow control unit, an aerosolisation unit and a deposition unit (Figure 3.9).

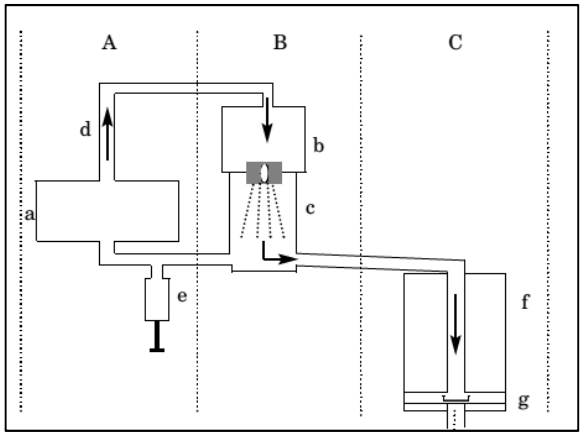


**Figure 3.9: schematic of PADDOCC (Hein *et al.* 2010). A) air-flow control unit; B) aerosolisation unit; C) deposition unit**

A modification of the commercially available MINUCELL (Figure 3.10) (Tippe *et al.* 2002; Bitterle *et al.* 2006), designed for exposure of cell cultures to fine and ultrafine ($0.1\ \mu m < d_a < 1.0\ \mu m$) airborne particles, is based on the deposition in a stagnation point of the aerosol fluid that provides a more spatially uniform deposition pattern in all the directions.

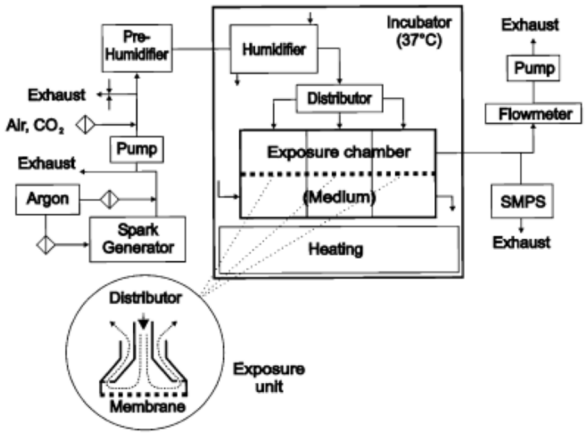


**Figure 3.10: Schematic of the experimental setup of MINUCELL (Bitterle *et al.* 2006)**

Another system is the air-liquid interface cell exposure (ALICE) system (Lenz *et al.* 2009) used to deliver controlled nanoparticle doses in liquids or solutions to cells. The

chamber consists of a nebuliser (droplet generator), a flow system, and a quartz crystal microbalance for real-time dose assessment (Figure 3.11). In this setup the deposition occurs by sedimentation exploiting the phenomenon of the "cloud settling" occurring when the droplet concentration in the aerosol is sufficiently high to provide enough resistance to the air that will not be able to go through the cloud droplets but will go around.

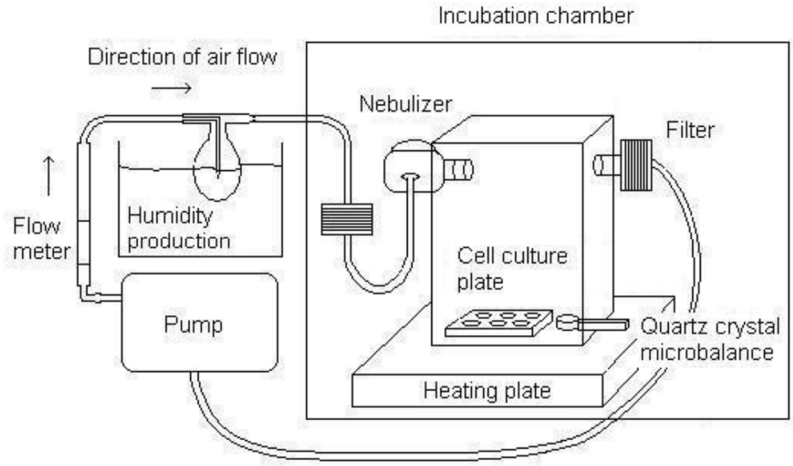


**Figure 3.11: Schematic of the experimental setup for the ALICE system (Lenz *et al.* 2009)**

More recent is the VITROCELL® Cloud system (Vitrocell systems) designed to deposit liquid aerosols on cells layers grown in ALI conditions in a spatially uniform and dose controlled manner (it is in fact provided with a micro-balance).

Alternative methodologies to expose cell cultures grown in ALI conditions to the test aerosol involve the use of microsprayers or insufflators. The most commonly used devices of this type are the PennCentury™ microsprayer or Dry Powder Insufflator (PennCentury, Philadelphia, PA, USA) that have been originally developed for administration of formulations for inhalation therapy to animals (rats and mice) for *in-vivo* studies (PennCentury Inc.). Nevertheless, examples of *in-vitro* studies where the PennCentury™ devices have been employed can also be found in the literature (Blank *et al.* 2006; Bur *et al.* 2010; Meindl *et al.* 2015).

### 3.1.3. Aim

The aim of the work reported in this chapter was to develop a system to deposit dry powder formulations for inhalation onto Calu-3 cell layers grown at the air-liquid interface, that was simpler and less costly in comparison to the systems already available in the market and described above.

We decided to use the PennCentury™ Dry Powder Insufflator – Model DP-4 (Penn-Century. Inc. Wyndmoor, PA) to aerosolise the dry powders of interest (salbutamol sulfate, indomethacin and indomethacin formulations). The device was fitted with the PennCentury Air Pump™ – Model AP-1 (Penn-Century. Inc. Wyndmoor, PA) to guarantee more reproducibility between repeated puffs.

Samples (e.g. Calu-3 cell layers cultured at the air-liquid interface) were contained in a glass desiccator chamber.

The system assembled was characterised in terms of reproducibility of the dose emitted by the PennCentury™ device, the spatial distribution of the particles on the deposition surface, the size distribution of the particles emitted by the insufflator as well as of the particles deposited on the surface, and the dose delivered to the cell layers. In particular, we aimed to achieve a reproducible emitted dose of dry powder that in combination with an even spatial distribution could guarantee consistency and reproducibility of the doses delivered to multiple cell layers within the same experiment but also between different experiments. Moreover, a size distribution of the particles reaching the cell layer surface in the inhalable range (3-5 µm) was desirable.

Ultimately, the viability and barrier properties of the cell layers exposed to the dry powder aerosol were assessed.

## 3.2. Materials and methods

The characterisation and validation of the deposition system developed was carried out by assessing first the performance of the PennCentury™ Dry Powder Insufflator in delivering consistent doses of dry powder. The deposition and dispersion of the spray on the surface of the deposition system was then investigated in order to choose the best positions to place the Transwell® inserts. Also, laser diffraction was used for the determination of the size distribution of the particles as released from the PennCentury™ device, while optical microscopy was used for the determination of the size distribution of the particles as deposited into Transwell® inserts. Finally, the dose of salbutamol sulfate delivered to the Transwell® inserts was determined as well as Calu-3 cell viability and cell layer integrity after exposure to the dry powder spray.

### 3.2.1. The deposition system

The deposition system developed and validated in this work consists of a vacuum glass desiccator with the PennCentury™ Dry Powder Insufflator – Model DP-4 (Penn-Century. Inc. Wyndmoor, PA) as described in Chapter 2 (Figure 2.1, paragraph 2.2.1, page 32).

A modification of the system involved the use of a Quickfit receiver with vented bend (RA2/33, socket size: 24/29, cone size: 24/29, SciLabware Limited, Staffordshire UK) as elutriation system (Figure 3.12):


**Figure 3.12: (a) Quickfit receiver with vented bend (RA2/33, socket size: 24/29, cone size: 24/29, SciLabware Limited, Staffordshire UK); (b) desiccator configuration with Quickfit glassware used as elutriation system.**

### 3.2.2. Dose released by the PennCentury™ Dry Powder Insufflator

Varied amounts of micronized salbutamol sulfate ranging between 1.0 and 5.0 mg were loaded into the PennCentury™ device without the needle and aerosolised three consecutive times using 5 mL of ambient air by means of the PennCentury Air Pump™. The cumulative doses delivered after the first, the second and the third puff were determined by difference, weighing the insufflator before and after each puff using a DENVER Instrument SI-234 balance. The experiment was performed in triplicate.

### 3.2.3. Particle shape and morphology

Shape and morphology of aerosolised salbutamol sulfate particles was assessed using a Jeol JSM-6060LV scanning electron microscope (SEM). The PennCentury™ device was loaded with 5.0 mg of micronised drug. Particles were sprayed using the PennCentury™ Dry Powder Insufflator without the needle onto SEM stubs coated with sticky carbon discs placed at the centre of the desiccator chamber below the spray, and covered in gold at 250 V for 5 minutes (Leica Sputter Coater SCD005).

### 3.2.4. Spray deposition and dispersion on the surface

The PennCentury™ device was loaded with either 5 mg of lactose (grade 3, particle size distribution, PSD, showed in Figure 3.13) or 1 mg of micronized salbutamol sulfate. The PennCentury™ device was used either with or without the needle.

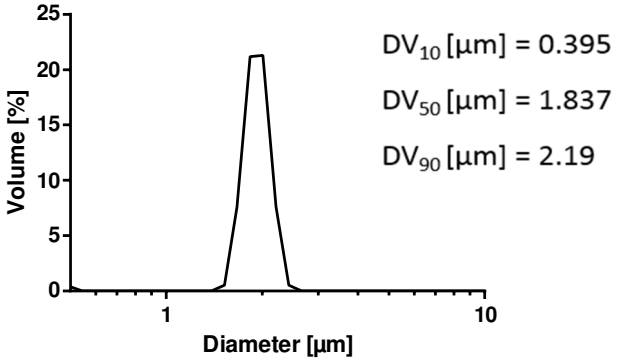


**Figure 3.13: Lactose grade 3 (GSK, Ware) particle size distribution measured by laser diffraction (dry powder module, Beckman coulter, series LS230)**

Powders were sprayed onto either 12 (slides A-L, Figure 3.14) or 4 (slides E-H, Figure 3.14) glass microscopy slides (78x26mm, ThermoScientific) arranged in such a way to cover the entire deposition surface inside the desiccator chamber. Some slides were modified by cutting off either one (slides B, C, J and K) or two corners (slides A and L) in order to fit them all into the chamber and guarantee as much coverage of the entire surface as possible:

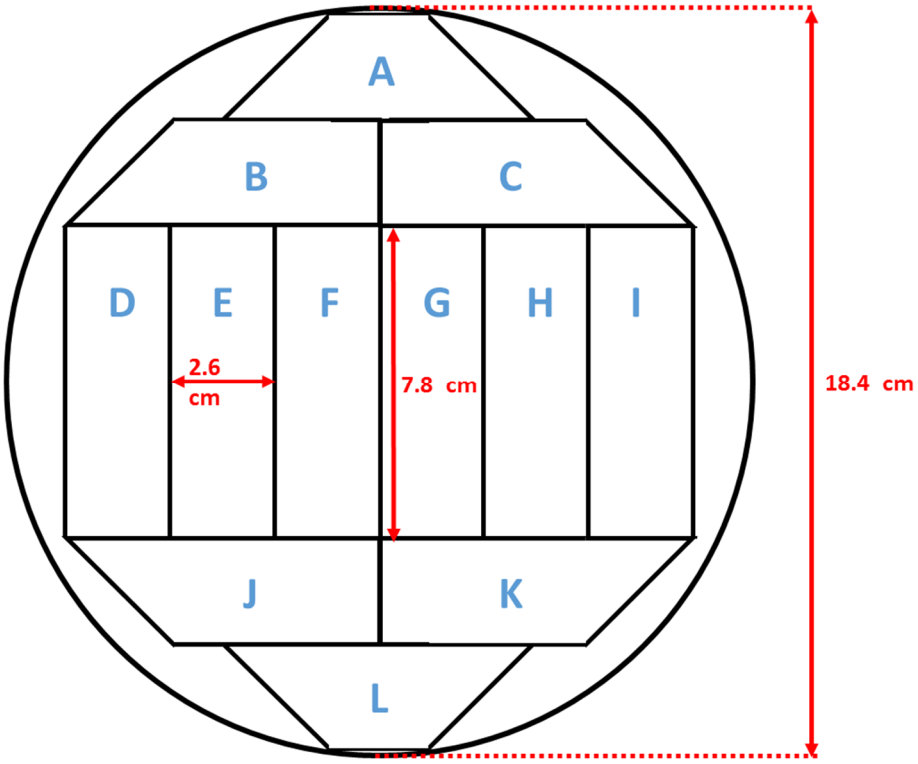


**Figure 3.14: Microscopy slides (78x26 mm) placement below the dry powder spray**

After particle deposition, the glass slides were scanned using the Imstar - smart imaging system for life optical microscope (Olympus Ix51) fitted with X10 objective, and equipped with an Olympus camera (th400). 30x78 images (897.6 x 673.3 µm) 1µm apart in both the vertical and the horizontal directions were acquired over the surface of each microscopy slide. The surface area covered by the particles was obtained processing the images with ImageJ free software (Abràmoff *et al.* 2004): a threshold of 0-91 was used to convert the images into binary masks, outliers of 2 pixels (1.32 µm) in diameter were removed. A macro was used in order to batch process the images in an automated way (Appendix I, paragraph I.1, page 225).

The surface coverage percentage (SC%) was calculated as following Equation 3.1:

$$SC\% = \frac{area\ covered\ by\ the\ particles}{total\ area\ of\ the\ image} \times 100$$

A colour-based map of the slides was reproduced to better visualise the results using Microsoft office Excel 2016 software. The colours red, yellow and white reflect 100%, 50% and 0% surface coverage respectively.

The spatial distribution over the central area of the desiccator chamber of lactose grade 3 was visualised using SEM. The PennCentury™ Dry Powder Insufflator fitted with the needle was loaded with 5.0 mg of material and 5.0 mL of ambient air was used to produce the spray. The aerosolised particles were collected onto a SEM stub coated with sticky carbon discs placed at the centre of the desiccator chamber below the spray. Samples were coated in gold at 250 V for 5 minutes (Leica Sputter Coater SCD005) prior to imaging with SEM.

## 3.2.5. Particle size distribution measurements

### 3.2.5.1 Size of particles released of particles released from the PennCentury™ Dry Powder Insufflator

Micronised lactose grade 3 ($DV_{50}$≤3μm) were measured for particle size distribution by laser diffraction using a Dry powder module (Beckman coulter, series LS230) fitted with a vacuum source (Nilfisk GM 80). The vibration was set at a value of 69. The sample was analysed in triplicate.

The particle size of salbutamol sulfate dry powder spray was determined using the Malvern Insitech Spray (Malvern Instruments Ltd, UK).

The PennCentury Dry Powder Insufflator™ was loaded with 1 and 2 mg of salbutamol sulfate. The measurement was conducted in different conditions: with and without the needle on the device, and using a bend between the nozzle and the laser as elutriation system (particle classificatory). Two different bends were used: 90° and 135°, as showed in Figure 3.15:

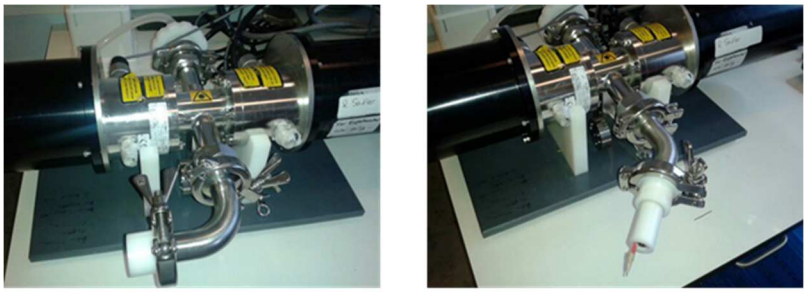


**Figure 3.15: Malvern Insitech Spray (Malvern Instruments Ltd, UK) fitted with (a) 90° and (b) 135° bend.**

The laser diffraction signal was acquired for 1000 ms and transmittance (T%) was set as 95%. The measurement in each condition was performed in triplicate.

### 3.2.5.2 Optical microscopy

The size distribution of salbutamol sulfate dry powder particles deposited into Transwell® insert housed in a 12-well cell culture plate (both the configurations with and without the Quickfit elutriation system were used) or arranged hexagonally in the desiccator chamber according to the geometry showed in Figure 3.16 (Quickfit elutriation system was not used), was determined by optical microscopy using an Imstar – smart imaging system for life (IMSTAR SA, Paris, France) optical microscope. In this second geometry six inserts were placed in the centre of petri dishes lids (Ø=3.5 cm) at a distance of 7.35 cm from the centre where another insert was located.

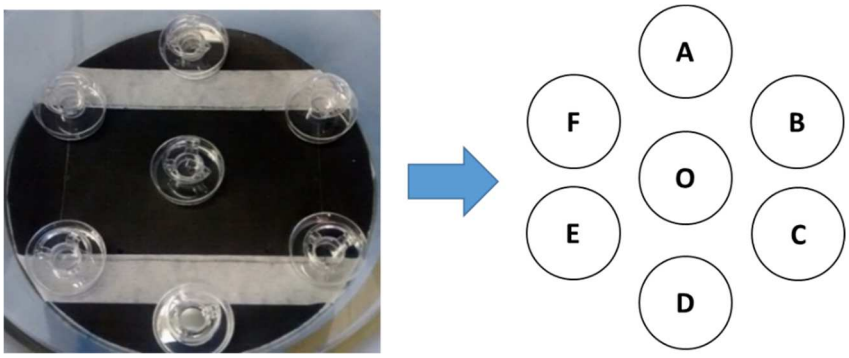


**Figure 3.16: arrangement of individual Transwell® inserts in the desiccator chamber. Distance between inserts and centre of the chamber was 7.35 cm.**

The combination of this two geometries would give us a good understanding of the particle size distribution across the deposition surface in the desiccator chamber.

The polyester membrane had been removed from all inserts and replaced with clean glass coverslips (1.2 cm in diameter, VWR (Germany)), and 1.0 mg of salbutamol sulfate was sprayed twice with the PennCentury™ insufflator without the needle and the inserts were transferred back to the 12-well plate. The surface of each coverslip was scanned under the Imstar – smart imaging system for life optical microscope fitted with a X20 objective, acquiring 20x20 images (448.8 x 332 µm) 1 µm apart in both the vertical and the horizontal directions over the surface of each coverslip.

The acquired images were batch processed using ImageJ free software (Abràmoff *et al*. 2004) as explained in paragraph 3.2.4 (page 60) using a macro (see Appendix I. paragraph I.2, page 226). The average between the major (M) and minor (m) diameters of the best ellipsis fitting the particle was used as the more representative dimension able to describe the particle size (diameter, D), and was calculated as per Equation 3.2:

$$D = \frac{M + m}{2}$$

A frequency distribution was drawn out of the set of diameters (D) by dividing the range of sizes from 0 µm to the maximum D calculated into bins (bin size: 0.4 µm). Each bin contained the number of diameters lying within the size range covered by the bin. The resulting distribution was normalised for number of particles in each bin (frequency %): 100% was associated with the bin containing the highest number of particle diameters, whereas 0% was associated with empty bins.

### 3.2.6. Dose delivered study

The PennCentury™ dry powder insufflator was loaded with 0.5, 1.0 and 2.0 mg of micronized salbutamol sulfate and 5 mL of air was used to aerosolize the dry powder onto Transwell® inserts placed 20 cm below the nozzle. The polyester membrane was

removed and replaced with clean glass coverslips (1.2 cm in diameter, VWR (Germany)) in all the inserts.

Both the configuration with a Quickfit receiver used as an elutriation system (Figure 3.12) and without (Figure 2.1 (A), paragraph 2.2.1, page 32) were employed.

The Transwell® inserts were arranged below the spray according to four different geometries: 12 Transwell® plate, triangle, small hexagon and large hexagon arrangements of individual wells (Figure 3.17):

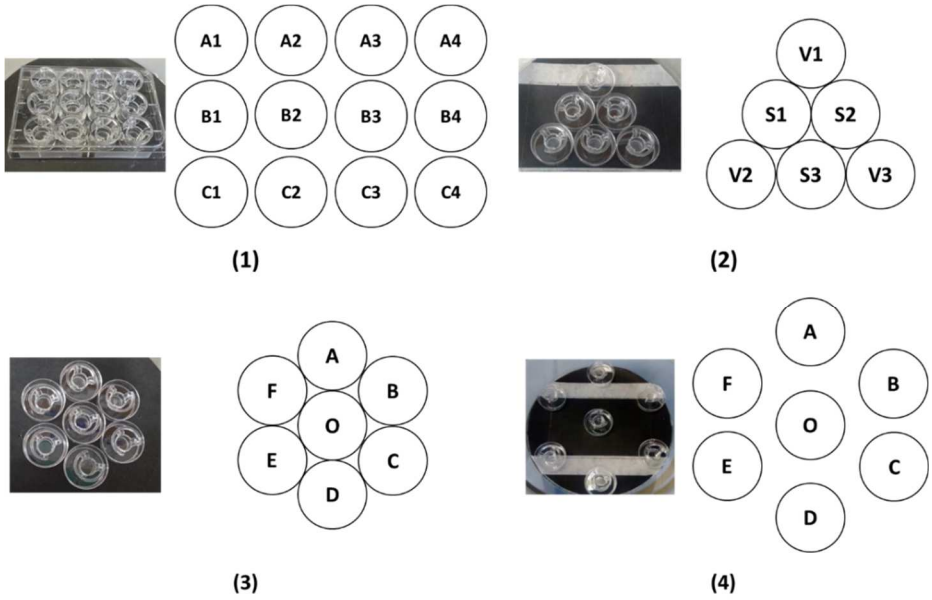


**Figure 3.17: position of the Transwell® inserts below the dry powder spray. (1) 12-well plate; (2) Triangle; (3) small hexagon; (4) large hexagon**

In the triangle and hexagon arrangements Transwell® inserts were placed in the centre of petri dish lids (Ø=3.5 cm).

Salbutamol sulfate deposited on each coverslip was recovered by washing the coverslip surface four times with 50 µL of MeOH (HPLC grade). MeOH was evaporated down using JOUAN centrifugal evaporator RCT90 for 20 minutes, and the sample was reconstituted with 1 mL of fresh MeOH (HPLC grade). The samples were analysed quantitatively by HPLC-UV.

Experiments were performed in triplicate.

### 3.2.6.1 *HPLC-UV*

For the determination of the best wavelength to use during the HPLC-UV analysis, a 1 mg/mL solution of salbutamol sulfate in MeOH was analysed by UV-Vis in scan mode from 800 nm to 200 nm using a DU®-800 Series UV-Vis spectrophotometer (Beckman Coulter Inc, UK). The maximum absorbance was found to be at 276 nm as shown in Figure 3.18:

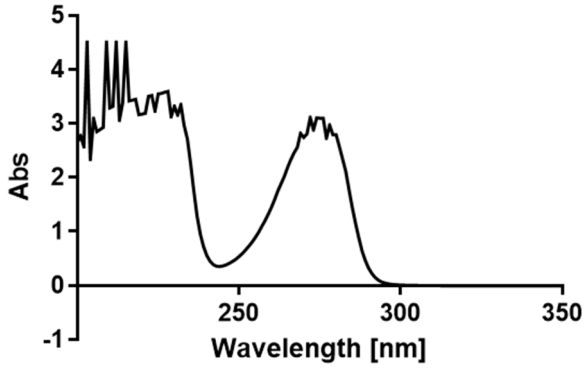


**Figure 3.18: UV-Vis spectrum of absorbance of salbutamol sulfate in MeOH.**

Salbutamol sulfate samples were analysed using a SUPELCOSIL™ LC-18-DB (5µm, 150 mm x 4.6 mm; Supelco™ analytical; Bellafonte, USA) column mounted on an Agilent Hewlett Packard series 1100 fitted with a UV microcell for UV-Vis detection. The injection volume was 100 µL, and the analysis was carried out at a flow rate of 1.0 mL $min^{-1}$ using 0.1% (w/v) sodium dodecyl sulfate (SDS) in water and MeOH (25:75) as mobile phases. The chromatographic runs were monitored at 276 nm (linear range: 0.01- 10 µg $mL^{-1}$).

The calibration curve was drawn from standard solutions of salbutamol sulfate in MeOH at various concentrations ranging from 0.01 to 10 µg $mL^{-1}$ prepared in triplicate ($y = 22.70x$; $R^2 = 0.9999$, Figure 3.19).

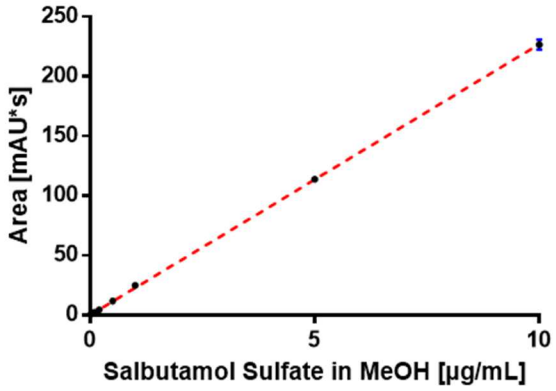


**Figure 3.19: calibration curve for salbutamol sulfate in MeOH, Range: 0.01 – 10 µg mL$^{-1}$. Y = 22.70 x; R$^2$= 0.9999**

### 3.2.7. Calu-3 cell viability and cell layer integrity after exposure to the dry powder spray

Calu-3 cell layers were seeded in 12 Transwell® well plates and grown in ALI conditions for 21 days as explained in Chapter 2 (paragraph 2.2.2.5, page 34).

On day 20, the transepithelial electrical resistance (TEER) of the Calu-3 cell layers was measured in HBSS following the protocol described in Chapter 2 (paragraph 2.2.2.7, page 35). At the end of the measurement, the HBSS solution was removed from both chambers and the cell culture was kept in ALI conditions with medium in the basolateral chamber only for the next 24 hours.

On day 21, three inserts were left in the incubator and used as reference, whereas medium was removed from the basolateral chamber in all other inserts. Three inserts at a time were transferred to the desiccator chamber and placed in positions B, C and E of the "large hexagon" geometry (see Figure 3.17(4), paragraph 3.2.6, page 64).

The cell layers were either transferred to the chamber for the time of a spray (about 30 seconds) but not exposed to any spray (blank), or exposed to a spray of only air or exposed to sprays of salbutamol sulfate after loading of 1.0 or 2.0 mg of the drug into the PennCentury™ device.

After the exposure, layers were moved to a clean 12-well plate, and prepared for the measurement of TEER (Chapter 2, paragraph 2.2.2.7, page 35) in order to assess the cell layer integrity immediately after exposure to the spray.

Following the TEER measurement, the transepithelial transport of lucifer yellow was monitored for 60 minutes as explained in Chapter 2 (paragraph 2.2.2.8, page 36).

At the end of the lucifer yellow assay, the cell layers were washed with fresh pre-warmed (37°C) HBSS, and prepared for the final measurement of the TEER (Chapter 2, paragraph 2.2.2.7, page 35).

## 3.3. Results and Discussion

### 3.3.1. Emitted dose consistency

A preliminary study on the performance of the PennCentury dry powder insufflator™ was carried out in order to investigate the amount of micronised powder delivered by the device as well as the reproducibility of the delivery between experiments.

Based on the information provided by the manufacturer, the PennCentury™ device was loaded with varied amounts of micronised salbutamol sulfate powder ranging from 1.0 to 5.0 mg. The powder was aerosolised three consecutive times using 5.0 mL of ambient air. This volume of air is the maximum allowed by the PennCentury Air Pump™ – Model AP-1. A recent characterisation of the PennCentury™ Dry Powder Insufflator (model DP-4) performances carried out by Hoppentocht *et al.* (2014) showed that the ability of the insufflator to disperse the dry powder into inhalable particles depends on the volume of air used for the aerosolisation. This parameter is particularly important for *in-vivo* applications of the PennCentury™ device where the tidal volume of the animal used in the test must be taken into account. However, in our application there is not such a limitation, but an optimum aerosolisation of the powder into single particles rather than aggregates was desirable, therefore the volume of air used for the insufflation was set at 5.0 mL.

The emitted dose expressed as percentage of the initial loading was determined by difference between the weight before and after each puff. Results are showed in Table 3.1:

**Table 3.1: cumulative percentages of initial loading of salbutamol sulfate emitted after three consecutive puffs by the PennCentury ™ device without the needle loaded with amounts of powder ranging between 1.0 and 5.0 mg.**

| Insufflation air [mL] | Initial loading [mg] | Emitted dose after 1st puff [%] | C.V.* [%] | Emitted dose after 2nd puff [%] | C.V. [%] | Emitted dose after 3rd puff [%] | C.V. [%] |
|---|---|---|---|---|---|---|---|
| 5.0 | 5.0 | 45.0 ± 18.4 | 40.9 | 59.0 ± 21.2 | 36.0 | 64.0 ± 22.6 | 35.4 |
| 5.0 | 4.0 | 40.0 ± 22.7 | 55.6 | 53.3 ± 26.7 | 50.1 | 59.2 ± 23.2 | 39.3 |
| 5.0 | 3.0 | 50.0 ± 33.0 | 66.0 | 63.3 ± 18.9 | 29.8 | 71.7 ± 16.5 | 23.0 |
| 5.0 | 2.0 | 57.5 ± 9.6 | 16.7 | 70.0 ± 14.1 | 20.2 | 77.5 ± 3.5 | 4.6 |
| 5.0 | 1.0 | 70.0 ± 18.7 | 26.7 | N.D.** | | N.D. | |

***C.V.= coefficient of variation; **N.D.= non detected**

For all loadings there is no significant difference ($p>0.05$) between the amount of drug released after the first, the second and the third puffs, suggesting that most of the material comes out with a single puff. When the PennCentury™ insufflator was loaded with 1.0 mg of dry powder, the amount of drug released after the second and the third puffs could not be detected due to the sensitivity of the balance.

Moreover, lower loadings (1.0 and 2.0 mg) allow for a more consistent amount of drug released from the PennCentury ™ device after the first puff. In fact, the variation in material released when the insufflator is loaded with 5.0, 4.0 and 3.0 mg is higher (CV>40%) than with lower loadings (CV<30%). Nevertheless, as reported in the literature with other drug formulations (Duret *et al.* 2012; Hoppentocht *et al.* 2014), the initial loading did not influence the percentage emitted dose.

These results reassured about the reproducibility of the dose delivered by the PennCentury Dry Powder Insufflator™ guaranteeing on the consistency between experiments.

## 3.3.2. Particle shape and morphology

Micronised salbutamol sulfate dry powder particles released by the PennCentury™ device were visualised using SEM for shape and morphology analysis. Salbutamol

sulfate particles look solid and of irregular shape with the presence of plate-like crystals (Figure 3.20).

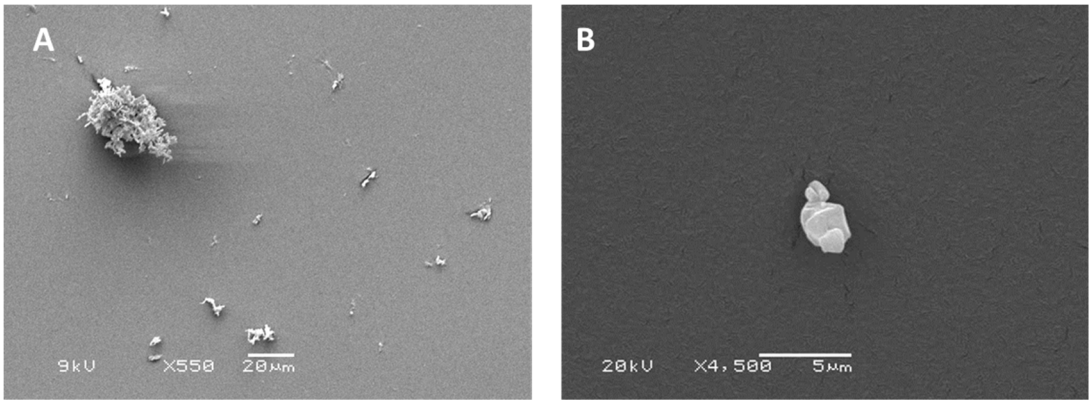


**Figure 3.20: SEM image of micronised salbutamol sulfate dry power particles after being sprayed from 20 cm without the needle. A) magnification X550, scale bar: 20 µm; B) magnification X4,500, scale bar: 5 µm**

## 3.3.3. Spray deposition and distribution on the surface

The deposition and surface distribution of the dry powder particles after aerosolisation was investigated *via* surface coverage percentage (SC%) calculation. This study was undertaken to define the best conditions for aerosolisation of the drug of interest as well as the geometrical arrangement of the cell layers within the desiccator for the following *in-vitro* studies. In particular, we were interested in achieving an even distribution of particles on the surface both within the same insert and between different inserts.

The desiccator used as deposition system allows for a maximum distance of 20 cm between the nozzle and the deposition surface (Figure 2.1 (B), paragraph 2.2.1, page 32).

The PennCentury$^{TM}$ device, either fitted with the needle (length: 7.2 cm) or not, was initially loaded with 5.0 mg of lactose grade 3, and the dry powder was aerosolised onto three microscopy glass slides placed one next to the other in the centre of the deposition surface.

The surface of the microscopy slides was scanned using the optical microscope and the images acquired were analysed for surface coverage (SC%) using ImageJ software. The results in Figure 3.21 and Figure 3.22 represent the centre of the spray as deposited on the surface of the microscopy slide. Each cell represents an image, and the number in it is the surface coverage (SC%) calculated as per Equation 3.1 (paragraph 3.2.4, page 61). Cells are coloured according to the SC% value (red: 100%; white: 0%).

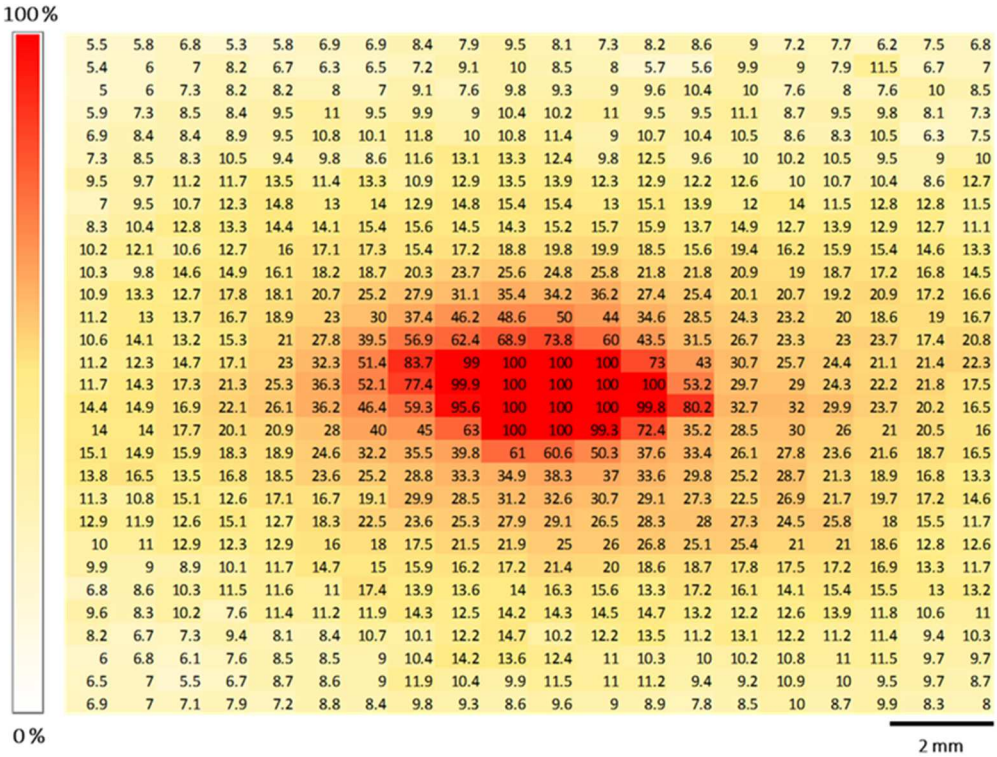


| | | | | | | | | | | | | | | | | | | |
|---|---|---|---|---|---|---|---|---|---|---|---|---|---|---|---|---|---|---|
| 5.5 | 5.8 | 6.8 | 5.3 | 5.8 | 6.9 | 6.9 | 8.4 | 7.9 | 9.5 | 8.1 | 7.3 | 8.2 | 8.6 | 9 | 7.2 | 7.7 | 6.2 | 7.5 | 6.8 |
| 5.4 | 6 | 7 | 8.2 | 6.7 | 6.3 | 6.5 | 7.2 | 9.1 | 10 | 8.5 | 8 | 5.7 | 5.6 | 9.9 | 9 | 7.9 | 11.5 | 6.7 | 7 |
| 5 | 6 | 7.3 | 8.2 | 8.2 | 8 | 7 | 9.1 | 7.6 | 9.8 | 9.3 | 9 | 9.6 | 10.4 | 10 | 7.6 | 8 | 7.6 | 10 | 8.5 |
| 5.9 | 7.3 | 8.5 | 8.4 | 9.5 | 11 | 9.5 | 9.9 | 9 | 10.4 | 10.2 | 11 | 9.5 | 9.5 | 11.1 | 8.7 | 9.5 | 9.8 | 8.1 | 7.3 |
| 6.9 | 8.4 | 8.4 | 8.9 | 9.5 | 10.8 | 10.1 | 11.8 | 10 | 10.8 | 11.4 | 9 | 10.7 | 10.4 | 10.5 | 8.6 | 8.3 | 10.5 | 6.3 | 7.5 |
| 7.3 | 8.5 | 8.3 | 10.5 | 9.4 | 9.8 | 8.6 | 11.6 | 13.1 | 13.3 | 12.4 | 9.8 | 12.5 | 9.6 | 10 | 10.2 | 10.5 | 9.5 | 9 | 10 |
| 9.5 | 9.7 | 11.2 | 11.7 | 13.5 | 11.4 | 13.3 | 10.9 | 12.9 | 13.5 | 13.9 | 12.3 | 12.9 | 12.2 | 12.6 | 10 | 10.7 | 10.4 | 8.6 | 12.7 |
| 7 | 9.5 | 10.7 | 12.3 | 14.8 | 13 | 14 | 12.9 | 14.8 | 15.4 | 15.4 | 13 | 15.1 | 13.9 | 12 | 14 | 11.5 | 12.8 | 12.8 | 11.5 |
| 8.3 | 10.4 | 12.8 | 13.3 | 14.4 | 14.1 | 15.4 | 15.6 | 14.5 | 14.3 | 15.2 | 15.7 | 15.9 | 13.7 | 14.9 | 12.7 | 13.9 | 12.9 | 12.7 | 11.1 |
| 10.2 | 12.1 | 10.6 | 12.7 | 16 | 17.1 | 17.3 | 15.4 | 17.2 | 18.8 | 19.8 | 19.9 | 18.5 | 15.6 | 19.4 | 16.2 | 15.9 | 15.4 | 14.6 | 13.3 |
| 10.3 | 9.8 | 14.6 | 14.9 | 16.1 | 18.2 | 18.7 | 20.3 | 23.7 | 25.6 | 24.8 | 25.8 | 21.8 | 21.8 | 20.9 | 19 | 18.7 | 17.2 | 16.8 | 14.5 |
| 10.9 | 13.3 | 12.7 | 17.8 | 18.1 | 20.7 | 25.2 | 27.9 | 31.1 | 35.4 | 34.2 | 36.2 | 27.4 | 25.4 | 20.1 | 20.7 | 19.2 | 20.9 | 17.2 | 16.6 |
| 11.2 | 13 | 13.7 | 16.7 | 18.9 | 23 | 30 | 37.4 | 46.2 | 48.6 | 50 | 44 | 34.6 | 28.5 | 24.3 | 23.2 | 20 | 18.6 | 19 | 16.7 |
| 10.6 | 14.1 | 13.2 | 15.3 | 21 | 27.8 | 39.5 | 56.9 | 62.4 | 68.9 | 73.8 | 60 | 43.5 | 31.5 | 26.7 | 23.3 | 23 | 23.7 | 17.4 | 20.8 |
| 11.2 | 12.3 | 14.7 | 17.1 | 23 | 32.3 | 51.4 | 83.7 | 99 | 100 | 100 | 100 | 73 | 43 | 30.7 | 25.7 | 24.4 | 21.1 | 21.4 | 22.3 |
| 11.7 | 14.3 | 17.3 | 21.3 | 25.3 | 36.3 | 52.1 | 77.4 | 99.9 | 100 | 100 | 100 | 100 | 53.2 | 29.7 | 29 | 24.3 | 22.2 | 21.8 | 17.5 |
| 14.4 | 14.9 | 16.9 | 22.1 | 26.1 | 36.2 | 46.4 | 59.3 | 95.6 | 100 | 100 | 100 | 99.8 | 80.2 | 32.7 | 32 | 29.9 | 23.7 | 20.2 | 16.5 |
| 14 | 14 | 17.7 | 20.1 | 20.9 | 28 | 40 | 45 | 63 | 100 | 100 | 99.3 | 72.4 | 35.2 | 28.5 | 30 | 26 | 21 | 20.5 | 16 |
| 15.1 | 14.9 | 15.9 | 18.3 | 18.9 | 24.6 | 32.2 | 35.5 | 39.8 | 61 | 60.6 | 50.3 | 37.6 | 33.4 | 26.1 | 27.8 | 23.6 | 21.6 | 18.7 | 16.5 |
| 13.8 | 16.5 | 13.5 | 16.8 | 18.5 | 23.6 | 25.2 | 28.8 | 33.3 | 34.9 | 38.3 | 37 | 33.6 | 29.8 | 25.2 | 28.7 | 21.3 | 18.9 | 16.8 | 13.3 |
| 11.3 | 10.8 | 15.1 | 12.6 | 17.1 | 16.7 | 19.1 | 29.9 | 28.5 | 31.2 | 32.6 | 30.7 | 29.1 | 27.3 | 22.5 | 26.9 | 21.7 | 19.7 | 17.2 | 14.6 |
| 12.9 | 11.9 | 12.6 | 15.1 | 12.7 | 18.3 | 22.5 | 23.6 | 25.3 | 27.9 | 29.1 | 26.5 | 28.3 | 28 | 27.3 | 24.5 | 25.8 | 18 | 15.5 | 11.7 |
| 10 | 11 | 12.9 | 12.3 | 12.9 | 16 | 18 | 17.5 | 21.5 | 21.9 | 25 | 26 | 26.8 | 25.1 | 25.4 | 21 | 21 | 18.6 | 12.8 | 12.6 |
| 9.9 | 9 | 8.9 | 10.1 | 11.7 | 14.7 | 15 | 15.9 | 16.2 | 17.2 | 21.4 | 20 | 18.6 | 18.7 | 17.8 | 17.5 | 17.2 | 16.9 | 13.3 | 11.7 |
| 6.8 | 8.6 | 10.3 | 11.5 | 11.6 | 11 | 17.4 | 13.9 | 13.6 | 14 | 16.3 | 15.6 | 13.3 | 17.2 | 16.1 | 14.1 | 15.4 | 15.5 | 13 | 13.2 |
| 9.6 | 8.3 | 10.2 | 7.6 | 11.4 | 11.2 | 11.9 | 14.3 | 12.5 | 14.2 | 14.3 | 14.5 | 14.7 | 13.2 | 12.2 | 12.6 | 13.9 | 11.8 | 10.6 | 11 |
| 8.2 | 6.7 | 7.3 | 9.4 | 8.1 | 8.4 | 10.7 | 10.1 | 12.2 | 14.7 | 10.2 | 12.2 | 13.5 | 11.2 | 13.1 | 12.2 | 11.2 | 11.4 | 9.4 | 10.3 |
| 6 | 6.8 | 6.1 | 7.6 | 8.5 | 8.5 | 9 | 10.4 | 14.2 | 13.6 | 12.4 | 11 | 10.3 | 10 | 10.2 | 10.8 | 11 | 11.5 | 9.7 | 9.7 |
| 6.5 | 7 | 5.5 | 6.7 | 8.7 | 8.6 | 9 | 11.9 | 10.4 | 9.9 | 11.5 | 11 | 11.2 | 9.4 | 9.2 | 10.9 | 10 | 9.5 | 9.7 | 8.7 |
| 6.9 | 7 | 7.1 | 7.9 | 7.2 | 8.8 | 8.4 | 9.8 | 9.3 | 8.6 | 9.6 | 9 | 8.9 | 7.8 | 8.5 | 10 | 8.7 | 9.9 | 8.3 | 8 |

**Figure 3.21: surface coverage (SC%) of the portion of the microscopy glass slides where the spray deposited when 5.0 mg of lactose was aerosolised using the PennCentury™ insufflator fitted with the needle. Each cell represents an image, and the number in it is the SC% calculated. Cells are coloured according to the SC% value (red: 100%; white: 0%).**

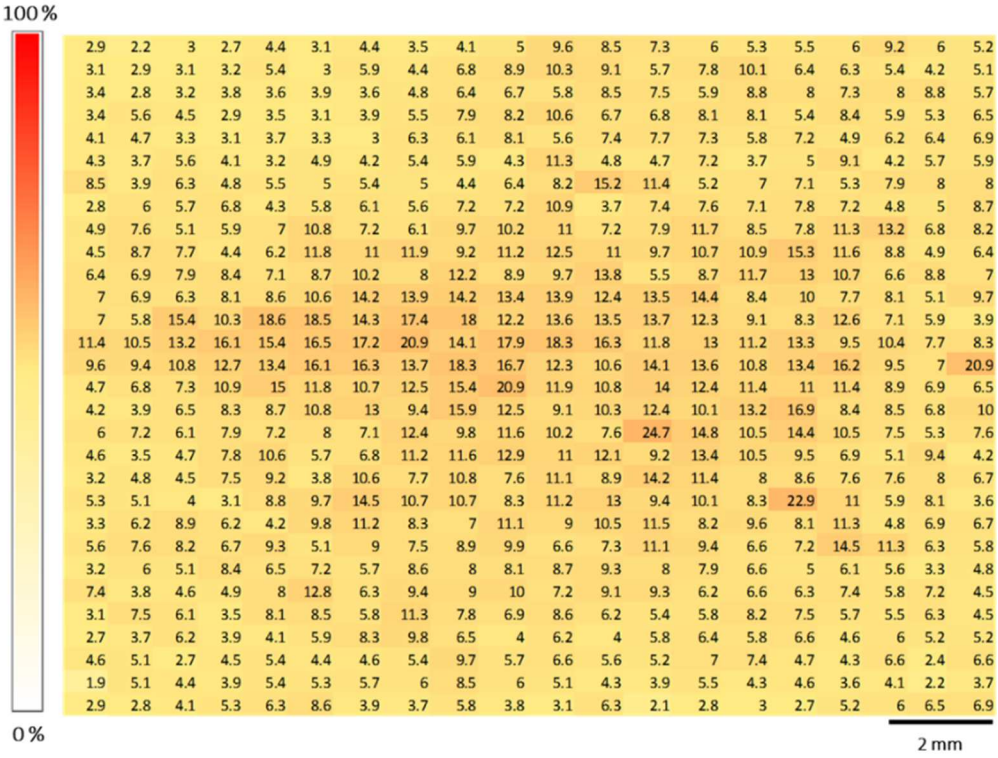


| | | | | | | | | | | | | | | | | | | | |
|---|---|---|---|---|---|---|---|---|---|---|---|---|---|---|---|---|---|---|---|
| 2.9 | 2.2 | 3 | 2.7 | 4.4 | 3.1 | 4.4 | 3.5 | 4.1 | 5 | 9.6 | 8.5 | 7.3 | 6 | 5.3 | 5.5 | 6 | 9.2 | 6 | 5.2 |
| 3.1 | 2.9 | 3.1 | 3.2 | 5.4 | 3 | 5.9 | 4.4 | 6.8 | 8.9 | 10.3 | 9.1 | 5.7 | 7.8 | 10.1 | 6.4 | 6.3 | 5.4 | 4.2 | 5.1 |
| 3.4 | 2.8 | 3.2 | 3.8 | 3.6 | 3.9 | 3.6 | 4.8 | 6.4 | 6.7 | 5.8 | 8.5 | 7.5 | 5.9 | 8.8 | 8 | 7.3 | 8 | 8.8 | 5.7 |
| 3.4 | 5.6 | 4.5 | 2.9 | 3.5 | 3.1 | 3.9 | 5.5 | 7.9 | 8.2 | 10.6 | 6.7 | 6.8 | 8.1 | 8.1 | 5.4 | 8.4 | 5.9 | 5.3 | 6.5 |
| 4.1 | 4.7 | 3.3 | 3.1 | 3.7 | 3.3 | 3 | 6.3 | 6.1 | 8.1 | 5.6 | 7.4 | 7.7 | 7.3 | 5.8 | 7.2 | 4.9 | 6.2 | 6.4 | 6.9 |
| 4.3 | 3.7 | 5.6 | 4.1 | 3.2 | 4.9 | 4.2 | 5.4 | 5.9 | 4.3 | 11.3 | 4.8 | 4.7 | 7.2 | 3.7 | 5 | 9.1 | 4.2 | 5.7 | 5.9 |
| 8.5 | 3.9 | 6.3 | 4.8 | 5.5 | 5 | 5.4 | 5 | 4.4 | 6.4 | 8.2 | 15.2 | 11.4 | 5.2 | 7 | 7.1 | 5.3 | 7.9 | 8 | 8 |
| 2.8 | 6 | 5.7 | 6.8 | 4.3 | 5.8 | 6.1 | 5.6 | 7.2 | 7.2 | 10.9 | 3.7 | 7.4 | 7.6 | 7.1 | 7.8 | 7.2 | 4.8 | 5 | 8.7 |
| 4.9 | 7.6 | 5.1 | 5.9 | 7 | 10.8 | 7.2 | 6.1 | 9.7 | 10.2 | 11 | 7.2 | 7.9 | 11.7 | 8.5 | 7.8 | 11.3 | 13.2 | 6.8 | 8.2 |
| 4.5 | 8.7 | 7.7 | 4.4 | 6.2 | 11.8 | 11 | 11.9 | 9.2 | 11.2 | 12.5 | 11 | 9.7 | 10.7 | 10.9 | 15.3 | 11.6 | 8.8 | 4.9 | 6.4 |
| 6.4 | 6.9 | 7.9 | 8.4 | 7.1 | 8.7 | 10.2 | 8 | 12.2 | 8.9 | 9.7 | 13.8 | 5.5 | 8.7 | 11.7 | 13 | 10.7 | 6.6 | 8.8 | 7 |
| 7 | 6.9 | 6.3 | 8.1 | 8.6 | 10.6 | 14.2 | 13.9 | 14.2 | 13.4 | 13.9 | 12.4 | 13.5 | 14.4 | 8.4 | 10 | 7.7 | 8.1 | 5.1 | 9.7 |
| 7 | 5.8 | 15.4 | 10.3 | 18.6 | 18.5 | 14.3 | 17.4 | 18 | 12.2 | 13.6 | 13.5 | 13.7 | 12.3 | 9.1 | 8.3 | 12.6 | 7.1 | 5.9 | 3.9 |
| 11.4 | 10.5 | 13.2 | 16.1 | 15.4 | 16.5 | 17.2 | 20.9 | 14.1 | 17.9 | 18.3 | 16.3 | 11.8 | 13 | 11.2 | 13.3 | 9.5 | 10.4 | 7.7 | 8.3 |
| 9.6 | 9.4 | 10.8 | 12.7 | 13.4 | 16.1 | 16.3 | 13.7 | 18.3 | 16.7 | 12.3 | 10.6 | 14.1 | 13.6 | 10.8 | 13.4 | 16.2 | 9.5 | 7 | 20.9 |
| 4.7 | 6.8 | 7.3 | 10.9 | 15 | 11.8 | 10.7 | 12.5 | 15.4 | 20.9 | 11.9 | 10.8 | 14 | 12.4 | 11.4 | 11 | 11.4 | 8.9 | 6.9 | 6.5 |
| 4.2 | 3.9 | 6.5 | 8.3 | 8.7 | 10.8 | 13 | 9.4 | 15.9 | 12.5 | 9.1 | 10.3 | 12.4 | 10.1 | 13.2 | 16.9 | 8.4 | 8.5 | 6.8 | 10 |
| 6 | 7.2 | 6.1 | 7.9 | 7.2 | 8 | 7.1 | 12.4 | 9.8 | 11.6 | 10.2 | 7.6 | 24.7 | 14.8 | 10.5 | 14.4 | 10.5 | 7.5 | 5.3 | 7.6 |
| 4.6 | 3.5 | 4.7 | 7.8 | 10.6 | 5.7 | 6.8 | 11.2 | 11.6 | 12.9 | 11 | 12.1 | 9.2 | 13.4 | 10.5 | 9.5 | 6.9 | 5.1 | 9.4 | 4.2 |
| 3.2 | 4.8 | 4.5 | 7.5 | 9.2 | 3.8 | 10.6 | 7.7 | 10.8 | 7.6 | 11.1 | 8.9 | 14.2 | 11.4 | 8 | 8.6 | 7.6 | 7.6 | 8 | 6.7 |
| 5.3 | 5.1 | 4 | 3.1 | 8.8 | 9.7 | 14.5 | 10.7 | 10.7 | 8.3 | 11.2 | 13 | 9.4 | 10.1 | 8.3 | 22.9 | 11 | 5.9 | 8.1 | 3.6 |
| 3.3 | 6.2 | 8.9 | 6.2 | 4.2 | 9.8 | 11.2 | 8.3 | 7 | 11.1 | 9 | 10.5 | 11.5 | 8.2 | 9.6 | 8.1 | 11.3 | 4.8 | 6.9 | 6.7 |
| 5.6 | 7.6 | 8.2 | 6.7 | 9.3 | 5.1 | 9 | 7.5 | 8.9 | 9.9 | 6.6 | 7.3 | 11.1 | 9.4 | 6.6 | 7.2 | 14.5 | 11.3 | 6.3 | 5.8 |
| 3.2 | 6 | 5.1 | 8.4 | 6.5 | 7.2 | 5.7 | 8.6 | 8 | 8.1 | 8.7 | 9.3 | 8 | 7.9 | 6.6 | 5 | 6.1 | 5.6 | 3.3 | 4.8 |
| 7.4 | 3.8 | 4.6 | 4.9 | 8 | 12.8 | 6.3 | 9.4 | 9 | 10 | 7.2 | 9.1 | 9.3 | 6.2 | 6.6 | 6.3 | 7.4 | 5.8 | 7.2 | 4.5 |
| 3.1 | 7.5 | 6.1 | 3.5 | 8.1 | 8.5 | 5.8 | 11.3 | 7.8 | 6.9 | 8.6 | 6.2 | 5.4 | 5.8 | 8.2 | 7.5 | 5.7 | 5.5 | 6.3 | 4.5 |
| 2.7 | 3.7 | 6.2 | 3.9 | 4.1 | 5.9 | 8.3 | 9.8 | 6.5 | 4 | 6.2 | 4 | 5.8 | 6.4 | 5.8 | 6.6 | 4.6 | 6 | 5.2 | 5.2 |
| 4.6 | 5.1 | 2.7 | 4.5 | 5.4 | 4.4 | 4.6 | 5.4 | 9.7 | 5.7 | 6.6 | 5.6 | 5.2 | 7 | 7.4 | 4.7 | 4.3 | 6.6 | 2.4 | 6.6 |
| 1.9 | 5.1 | 4.4 | 3.9 | 5.4 | 5.3 | 5.7 | 6 | 8.5 | 6 | 5.1 | 4.3 | 3.9 | 5.5 | 4.3 | 4.6 | 3.6 | 4.1 | 2.2 | 3.7 |
| 2.9 | 2.8 | 4.1 | 5.3 | 6.3 | 8.6 | 3.9 | 3.7 | 5.8 | 3.8 | 3.1 | 6.3 | 2.1 | 2.8 | 3 | 2.7 | 5.2 | 6 | 6.5 | 6.9 |

**Figure 3.22: surface coverage (SC%) of the portion of the microscopy glass slides where the spray deposited when 5.0 mg of lactose was aerosolised using the PennCentury™ insufflator without the needle. Each cell represents an image, and the number in it is the SC% calculated. Cells are coloured according to the SC% value (red: 100%; white: 0%).**

As expected, the removal of the needle allows for a more even distribution of the powder on the surface. The SC% after spraying without the needle spans from 1.9 and 24.7% (Figure 3.22), on the other hand it reaches 100% when the same amount of powder is sprayed through the needle (red area in Figure 3.21).

In fact, the PennCentury™ Dry Powder Insufflator is mainly designed for intra-tracheal administration of dry powder formulations to guinea pigs and rats (PennCentury Inc. n.d.), and the needle serves to precisely drive the powder into the animal's pulmonary system, helping focussing it on a narrow area. In this work, we are exploring the use of the PennCentury™ Dry Powder Insufflator for *in-vitro* applications, aiming to apply aerosolised dry powder particles in a narrow size range and a controlled dose to cell layers. The more even distribution of the powder on a wider area achievable by removing the needle could result in a more even deposition

of particles both in the same Transwell® insert and between different inserts arranged below the spray. In fact, it has to be noted that the area with SC%=100% is about 4 $mm^2$ (2 x 2 mm), thus smaller than the surface area of the Transwell® inserts (1.12 $cm^2$ (Corning Inc. n.d.)]. This was confirmed by SEM analysis (Figure 3.23) revealing how most of the particles were concentrated in a very small area. It can be speculated that the use of the needle could create dose gradients also within the same insert.

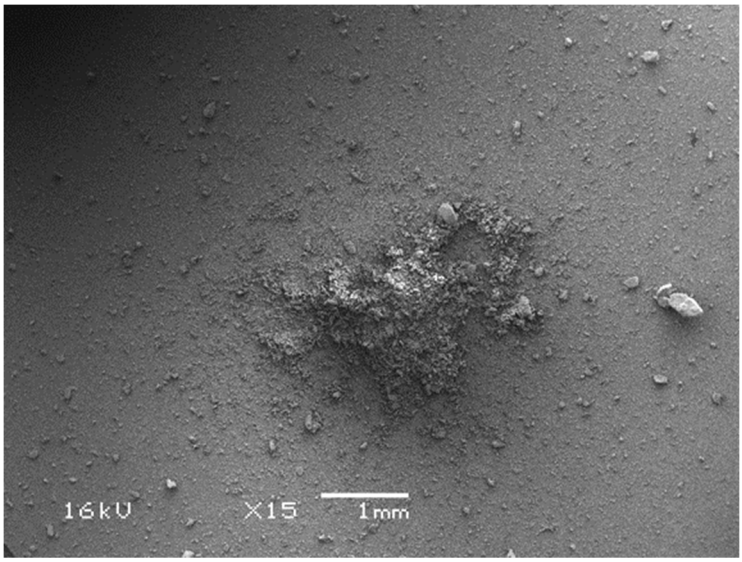


**Figure 3.23: SEM image of lactose grade 3 particles deposited at the centre of the spray after being aerosolised using the PennCentury™ dry powder insufflator fitted with the needle.**

The same experiment was also performed loading the PennCentury™ with 1 mg of micronized salbutamol sulfate dry powder ($DV_{50}$<3 μm, data provided by GSK) on 12 glass slides arranged as showed in Figure 3.14 (paragraph 3.2.4, page 61).

The results are presented in Figure 3.24 and Figure 3.25 and show that loading the PennCentury™ device with a lower dose (1.0 mg instead of 5.0 mg) allows for an evenly distributed spray on the surface even in the presence of the needle that, in this case, did not have an effect as obvious as seen for lactose with the higher loading. However, at a closer look, the SC% at the more peripheral areas looks more even when the powder is aerosolised without the needle as fewer areas with different colours can be noticed. In particular, we found that the SC% of 1.0 mg salbutamol sulfate sprayed with the needle spanned between 0.20% and 31.60%, with an average of 1.27% ±

1.15% (variance=1.27) across the whole surface, but when the needle was removed, SC% averaged across the surface is 1.06% ± 0.72% (variance=0.52), with minimum and maximum values of 0.10% and 21.10% respectively.

These data demonstrated that removing the needle from the PennCentury™ Dry Powder Insufflator improved the spatial distribution of the particles on the surface.

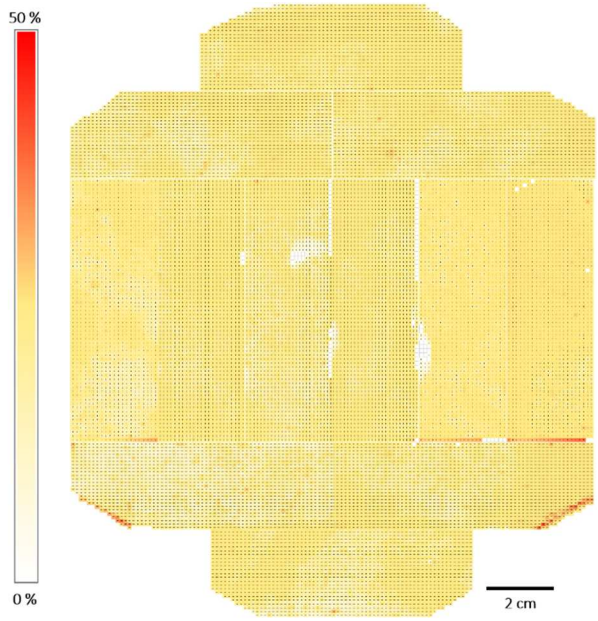


**Figure 3.24: SC% of 1.0 mg salbutamol sulfate sprayed onto 12 microscopy glass slides fitting the PennCentury ™ device with the needle. Each cell represents an image, and the number in it is the SC% calculated. Cells are coloured according to the SC% value (red: 50%; white: 0%).**

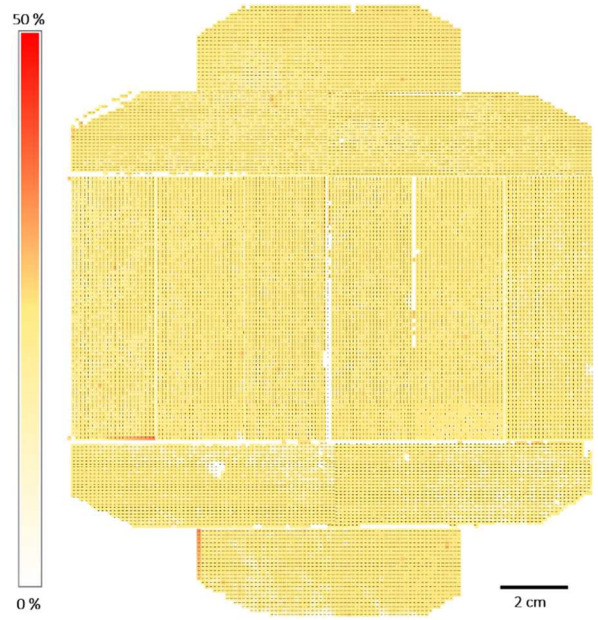


**Figure 3.25: SC% of 1.0 mg salbutamol sulfate sprayed onto 12 microscopy glass slides using the PennCentury ™ device without the needle. Each cell represents an image, and the number in it is the SC% calculated. Cells are coloured according to the SC% value (red: 50%; white: 0%).**

## 3.3.4. Spray particle size distribution

### 3.3.4.1 *Laser Diffraction*

The particle size distribution of the spray as it is produced by the PennCentury$^{TM}$ Dry Powder Insufflator was determined by laser diffraction. The importance of this evaluation has been highlighted by Hoppentocht *et al.* (2014) who questioned the efficacy of the PennCentury$^{TM}$ device in re-dispersing the powder as well as an inhaler, which could increase the proportion of the non-inhalable particle fraction released from the device

Different operative conditions were investigated in order to determine the effect of the presence of the needle and a bend as elutriation system on the particle size distribution. The results (Table 3.2) are expressed as percentiles: $DV_{10}$, $DV_{50}$ and $DV_{90}$, which represent the volume weighted maximum particle size (expressed as diameter [µm]) for a given percentage volume of the sample, in this case 10%, 50% and 90% respectively.

**Table 3.2: Particle size (expressed as $DV_{10}$, $DV_{50}$ and $DV_{90}$) of salbutamol sulfate spray as it is produced by the PennCentury$^{TM}$ Dry Powder Insufflator.**

| | Operative conditions | | | $DV_{10}$ [µm] | $DV_{50}$ [µm] | $DV_{90}$ [µm] |
|---|---|---|---|---|---|---|
| | Needle | Bend | Loading [mg] | | | |
| 1 | Yes | No | 1.0 | 0.77 ± 0.04 | 3.75 ± 0.23 | 18.50 ± 2.85 |
| 2 | Yes | No | 2.0 | 0.93 ± 0.07 | 5.23 ± 0.75 | 39.66 ± 19.80 |
| 3 | Yes | Yes (135°) | 1.0 | 1.00 ± 0.05 | 5.42 ± 0.41 | 18.75 ± 0.70 |
| 4 | No | No | 1.0 | 0.74 ± 0.02 | 3.55 ± 0.20 | 15.65 ± 1.20 |
| 5 | No | Yes (135°) | 1.0 | 0.80 ± 0.04 | 3.89 ± 0.31 | 14.84 ± 1.12 |
| 6 | No | Yes (90°) | 1.0 | 0.80 ± 0.06 | 3.95 ± 0.50 | 15.68 ± 2.65 |

As we can see from Table 3.2, the $DV_{50}$ is between 3.55 and 5.42 µm for all 1 mg loadings.

Lines 1 and 2 show the effect of the loading on the particle size distribution. We observe a statistically significant ($p<0.05$) higher particle size of 5.23 μm and increased $DV_{90}$ with 2 mg loading, indicating higher aggregation of powder particles. Previous studies have demonstrated how particle size measurements are affected by the amount of drug used to perform the measurements, as well as the number of puffs and the sampling techniques. Nasr and colleagues (Nasr & Allgire 1995) found that the mass median aerodynamic diameter (MMAD) measured on a cascade impactor increases as the amount of salbutamol per puff or the number of puffs is increased. They later hypothesize electrostatic forces between particles could cause this effect (EL-Araud *et al*. 1998). Electrostatic forces in fact represent one of the causes of the typical aggregation of inhalation drug powders: friction between particles leads to the so-called "tribo-electric charging" resulting in cohesion of the powder by Coulomb attraction between the particles (Daniher & Zhu 2008).

On the other hand, the presence of the needle does not affect the particle size distribution, in fact looking at lines 1 and 4 there is no statistical variation in $DV_{10}$, $DV_{50}$ and $DV_{90}$ ($p<0.05$). This suggests that the needle of the PennCentury™ insufflator only serves to drive the powder into the animal's pulmonary system in *in-vivo* studies, but it does not create any shear effect able to break the aggregates.

The same can be said on the presence of the bend (Lines 1-3 and 4-5). Also, there is no statistically significant difference between the distributions obtained using two different bends (Lines 5 and 6).

With this set of experiments, we have demonstrated that the presence of the needle on the PennCentury™ device does not affect the particle size distribution of the spray, and if removed the particle spatial distribution on the deposition surface is improved.

In addition to this, it has to be noted that in the presence of the needle the distance between the nozzle and the deposition surface is significantly reduced (by 7.2 cm). This could affect the mechanism of deposition of the particles on the surface in addition to their spatial distribution. In fact, when the powder is aerosolised with the PennCentury Air Pump™, particles are released at a high velocity as suggested in the literature (Duret *et al.* 2012; Tonnis *et al.* 2014; Hoppentocht *et al.* 2014). It can be argued that the presence of the needle may not allow for enough travel distance for the particles to lose some of the initial acceleration applied by the PennCentury™ device. They may thus impact on the cell layers with a too high energy that may compromise their viability and integrity.

For these reasons we decided to complete the characterisation and the validation of our deposition system aerosolising the powders of interest using the PennCentury™ Dry Powder Insufflator without the needle.

#### 3.3.4.2 *Optical Microscopy*

Since the aim of this project was to develop a system able to deliver dry powder drug particles for inhalation onto cell layers grown on Transwell® inserts for *in-vitro* studies, the determination of the size distribution of the particles that reach the Transwell® inserts was of fundamental importance.

In order to assess the size distribution of the particles deposited in each insert, 1.0 mg of salbutamol sulfate was sprayed twice onto glass coverslips placed in Transwell® inserts housed either in a 12-well plate (both the configurations with and without the Quickfit elutriation system were used) or hexagonally in the desiccator chamber (Figure 3.16, paragraph 3.2.5, page 63; Quickfit elutriation system was not used).

The combination of this two geometries would give us a good understanding of the particle size distribution across the deposition surface in the desiccator chamber. Also,

aerosolising 1.0 mg of dry powder twice was found to be the best experimental condition in order to have a sufficient number of particles in each insert and thus be able to focus on the upper surface of the coverslips.

The size distributions and relative statistics of drug particles deposited on each Transwell® of the 12-well plate (refer to Figure 3.17(1) for position names) are showed in Figure 3.26 (without elutriation system) and Figure 3.27 (with elutriation system) and Table 3.3 (without elutriation system) and Table 3.4 (with elutriation system) respectively.

Analysis of the size distribution of the drug particles deposited in the Transwell® inserts when the Quickfit receiver is not used shows the particle diameters span between 1 and 100 μm, with 90% of the analysed particles below 5 μm and maximum number of particles between 2 and 3 μm. In addition, the size distribution is very similar between the different Transwell®.

When the Quickfit receiver is inserted in the deposition system, the drug particles deposited are between 1 and 137 μm, with 90% of the analysed particles below 21 μm, and maximum number of particles between 5 and 10 μm.

The positions around the centre of the surface (A2, A3 and B3) present a mean particle size higher than any other position in the plate (7.71, 9.60 and 7.04 μm respectively).

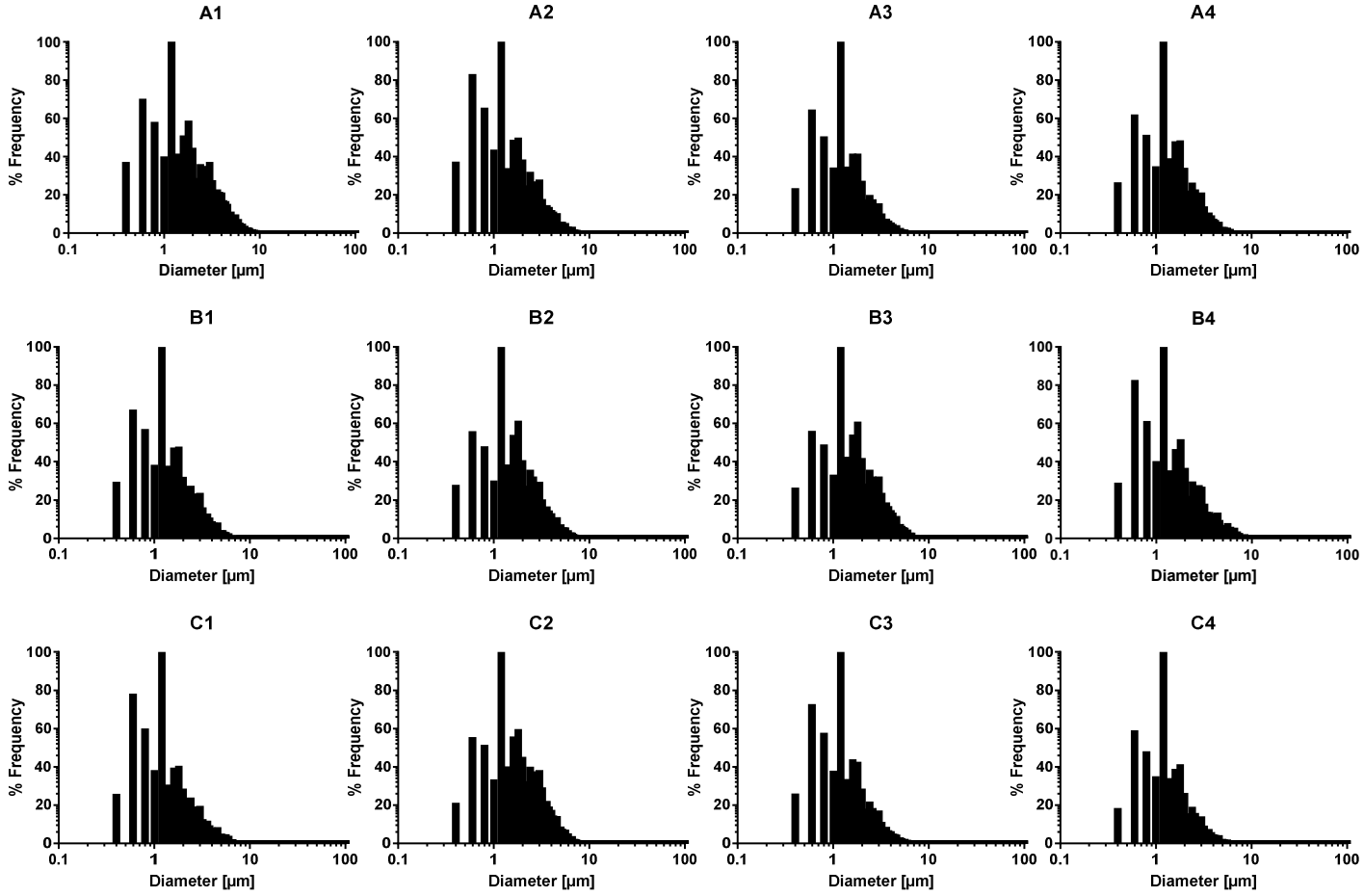


**Figure 3.26: particle size distributions of salbutamol sulfate dry powder deposited onto Transwell® inserts housed in a 12-well plate after being sprayed from 20 cm without use of the elutriation system.**

**Table 3.3: Descriptive statistics of the particle size distributions of salbutamol sulfate dry powder deposited onto Transwell® inserts housed in a 12-well plate after being sprayed from 20 cm without use of the elutriation system.**

| Position | A1 | A2 | A3 | A4 | B1 | B2 | B3 | B4 | C1 | C2 | C3 | C4 |
|---|---|---|---|---|---|---|---|---|---|---|---|---|
| Min [µm] | 0.40 | 0.40 | 0.40 | 0.40 | 0.40 | 0.40 | 0.40 | 0.40 | 0.40 | 0.40 | 0.40 | 0.40 |
| Max [µm] | 44.00 | 65.30 | 101.20 | 66.85 | 51.70 | 86.90 | 83.65 | 31.85 | 47.65 | 94.85 | 63.15 | 32.20 |
| $DV_{10}$ [µm] | 0.70 | 0.65 | 0.65 | 0.70 | 0.65 | 0.70 | 0.70 | 0.65 | 0.65 | 0.80 | 0.65 | 0.70 |
| $DV_{90}$ [µm] | 5.30 | 4.45 | 3.45 | 3.75 | 3.90 | 4.60 | 4.40 | 4.95 | 4.40 | 4.75 | 3.65 | 3.45 |
| Mean [µm] | 2.68 | 2.30 | 1.83 | 1.98 | 2.02 | 2.46 | 2.33 | 2.49 | 2.17 | 2.52 | 1.91 | 1.85 |
| St. Dev [µm] | 2.36 | 2.43 | 1.49 | 1.57 | 1.57 | 2.47 | 1.73 | 2.62 | 2.11 | 2.06 | 1.71 | 1.51 |

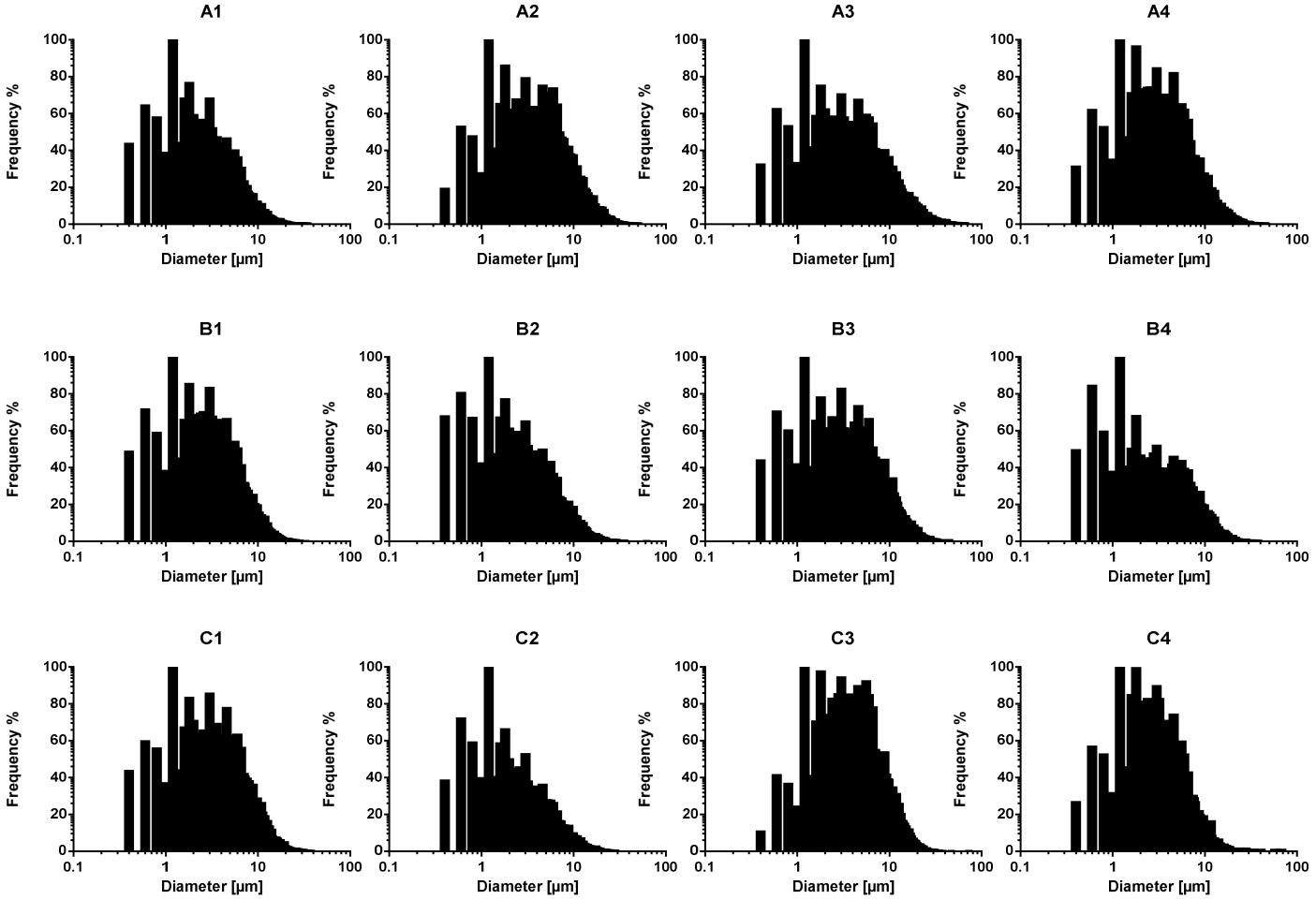


**Figure 3.27: particle size distributions of salbutamol sulfate dry powder deposited onto Transwell® housed in a 12-well plate inserts after being sprayed from 20 cm using the Quickfit receiver as elutriation system.**

**Table 3.4: Descriptive statistics of the particle size distributions of salbutamol sulfate dry powder deposited onto Transwell® inserts housed in a 12-well plate after being sprayed from 20 cm using the Quickfit receiver as elutriation system.**

| Position | A1 | A2 | A3 | A4 | B1 | B2 | B3 | B4 | C1 | C2 | C3 | C4 |
|---|---|---|---|---|---|---|---|---|---|---|---|---|
| Min [µm] | 0.40 | 0.40 | 0.40 | 0.40 | 0.40 | 0.40 | 0.40 | 0.40 | 0.40 | 0.40 | 0.40 | 0.40 |
| Max [µm] | 45.45 | 60.75 | 131.80 | 62.65 | 60.65 | 137.50 | 77.05 | 56.95 | 80.30 | 56.35 | 78.20 | 67.65 |
| $DV_{10}$ [µm] | 1.00 | 1.65 | 1.55 | 1.40 | 1.15 | 0.95 | 1.35 | 1.00 | 1.30 | 0.90 | 1.80 | 1.30 |
| $DV_{90}$ [µm] | 10.05 | 15.90 | 21.05 | 13.70 | 10.45 | 11.60 | 14.55 | 12.15 | 12.20 | 10.20 | 13.10 | 9.63 |
| Mean [µm] | 4.81 | 7.71 | 9.60 | 6.55 | 5.16 | 5.38 | 7.04 | 5.82 | 6.10 | 4.70 | 6.74 | 4.90 |
| St. Dev [µm] | 4.03 | 6.18 | 9.09 | 5.46 | 4.04 | 4.93 | 5.63 | 4.90 | 4.72 | 4.25 | 4.82 | 4.05 |

The size distributions and relative statistics of drug particles deposited on each Transwell® in the hexagonal geometry are showed in Figure 3.28 and Table 3.5 respectively.

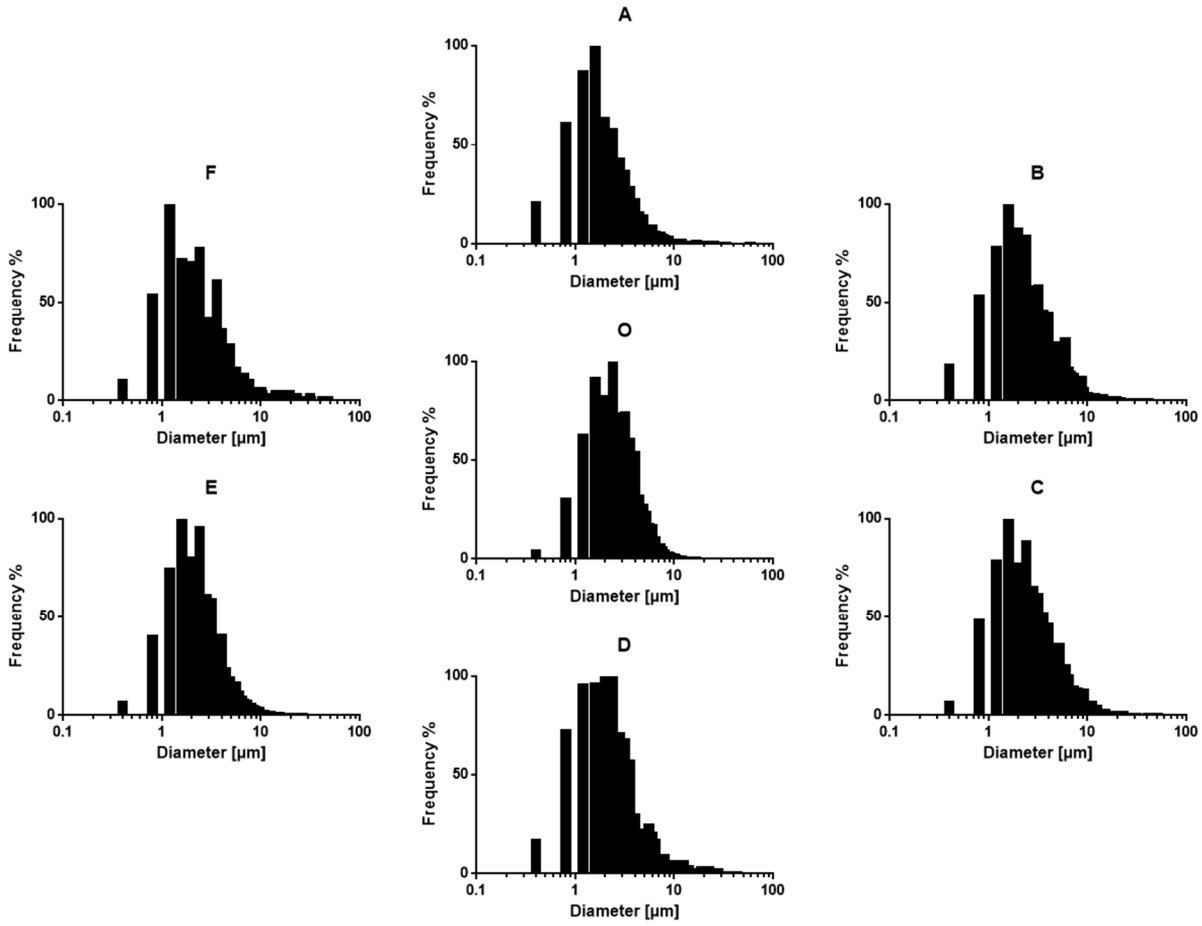


**Figure 3.28: particle size distributions of salbutamol sulfate dry powder deposited onto six Transwell® arranged hexagonally below the spray at a distance of 7.5 cm from the centre of the desiccator chamber where a seventh insert is located.**

**Table 3.5: descriptive statistics of the particle size distributions of salbutamol sulfate dry powder deposited onto seven Transwell® arranged as described above.**

| Position | A | B | C | D | E | F | O |
|---|---|---|---|---|---|---|---|
| Min [µm] | 0.40 | 0.40 | 0.40 | 0.40 | 0.40 | 0.40 | 0.40 |
| Max [µm] | 79.15 | 41.55 | 51.75 | 43.10 | 84.55 | 47.60 | 106.6 |
| $DV_{10}$ [µm] | 1.30 | 1.20 | 1.15 | 1.00 | 1.30 | 1.20 | 1.00 |
| $DV_{90}$ [µm] | 5.75 | 8.80 | 6.30 | 8.46 | 5.75 | 8.80 | 9.02 |
| Mean [µm] | 3.45 | 4.39 | 3.55 | 4.34 | 3.45 | 4.39 | 4.29 |
| St. Dev [µm] | 3.54 | 4.34 | 4.18 | 5.40 | 3.54 | 4.36 | 5.16 |

Analysis of the size distribution of the drug particles deposited in the Transwell® inserts arranged hexagonally below the spray shows the particle diameters span between 1 and 106 µm, with 90% of the analysed particles below 10 µm in all inserts and maximum number of particles between 2 and 3 µm. It is noteworthy that the insert positioned in the centre of the chamber (position O) received the largest particles (maximum diameter=106.6 µm; $DV_{90}$=9.02 µm). This suggests that larger particles are more likely to fall perpendicularly depositing by inertial impaction thus reaching the positions closer to the centre. In contrast, smaller particles are more free to follow the airflow before depositing by sedimentation, thus having the possibility to reach peripheral areas.

It is important to note that no significant change was observed in the characteristics of the powder before and after the aerosolisation in terms of particle size distribution, with the $DV_{50}$ remaining ≈ 3-4 µm.

The reason why large salbutamol sulfate particles (in the range of 20-40 µm) deposit on the Transwell® inserts is that small particles tend to aggregate together and, as previously explained, the PennCentury™ device is not able to create shear forces strong enough to disaggregate them. In fact, the sample chamber of the PennCentury dry powder insufflator™ (Figure 3.29) simply consists in a cavity where there is no system similar to those typically found in the DPIs (e.g. grids, venturi or impellers) to disaggregate the aggregates.

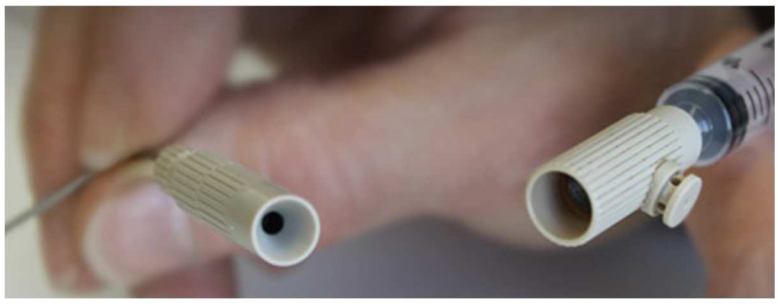

**Figure 3.29: sample chamber of the PennCentury Dry powder insufflator™ (PennCentury Inc. n.d.)**

The use of the Quickfit receiver was added as an elutriation system in the hope to remove the larger particles and aggregates released from the PennCentury™ insufflator, mimicking the throat in real life. Similar systems have been employed by other researchers who adapted artificial throats to impactors (Marple & Willeke 1976; Nasr & Allgire 1995; EL-Araud *et al.* 1998; Aufderheide & Mohr 1999). However, their systems involved high flow rates (about 60 L/min) to drive the aerosol coming out of inhalers into the impactors. These conditions, as well as a proper design of the artificial throat in terms of length, hydraulic diameter and nozzle-plate distance, help in cutting-off the non-inhalable fraction letting through only the particles in the right size range. In our system, the flow rate provided by the PennCentury Air Pump™ to aerosolise the powder did not seem to be high enough for the large particles to accelerate and gain enough kinetic energy to impact at the end of the Quickfit. As a result, the whole population managed to enter the chamber, including large particles and aggregates. However, these were mainly concentrated on the central deposition area suggesting that the larger particles fell perpendicularly on the surface by gravity after hitting the bend's inner wall.

## 3.3.5. Dose control studies

Knowing the dose delivered to the targeted cells is also very important in order to be able to correctly analyse and interpret the data from the *in-vitro* studies.

Our aim was to develop a deposition system that could deliver dry powder particles in the respirable size range (3-5μm) but also a controlled and reproducible dose.

A series of experiments were performed to determine the amount of salbutamol sulfate deposited in the Transwell® inserts after aerosolisation, in order to be able to predict the dose that will be delivered to the cells in future *in-vitro* experiments.

The Transwell® inserts were arranged below the spray according to four different geometries: 12-well plate, triangle, small hexagon and large hexagon, as showed in Figure 3.17 (paragraph 3.2.6, page 65).

The PennCentury™ device was loaded with 0.5, 1.0 and 2.0 mg of micronised drug which was sprayed with 5.0 mL of ambient air until the device was emptied (typically once or twice). The experiment was carried out both with and without the Quickfit receiver used as elutriation system for all geometries but the large hexagon. The doses recovered from each insert are reported in Figure 3.31 and Figure 3.32, and in Table I. 1 and Table I.2 (Appendix II, page 227).

To better visualise and understand the data, the distance between the centre of the spray and each Transwell® insert was measured (Figure 3.30)

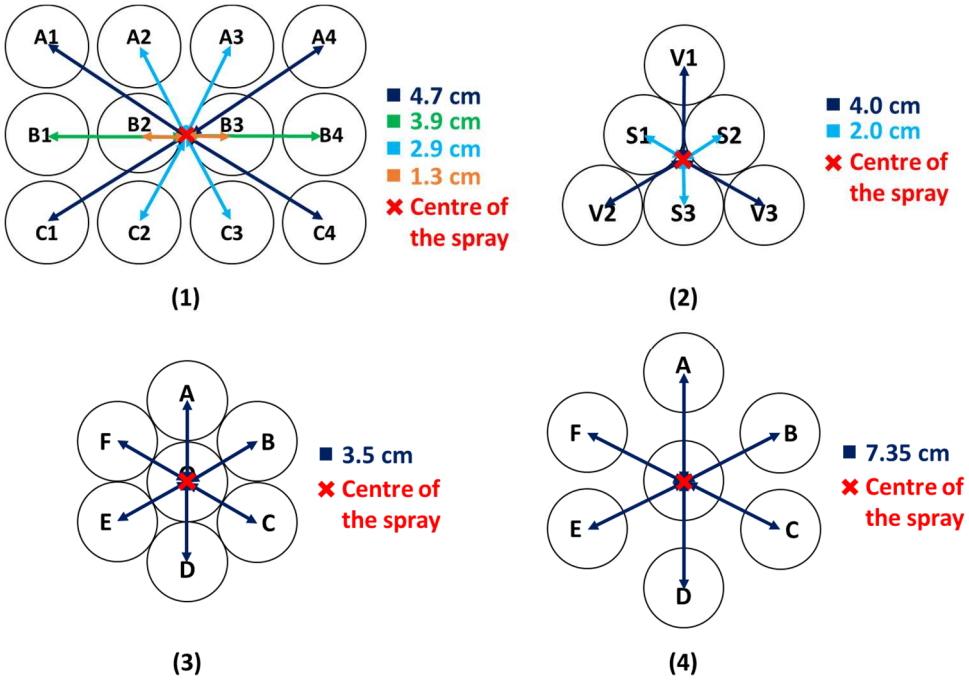


**Figure 3.30: distances between Transwell® inserts and centre of the spray in the different geometries used. (1) 12-well plate; (2) Triangle; (3) Small hexagon; (4) Large hexagon**

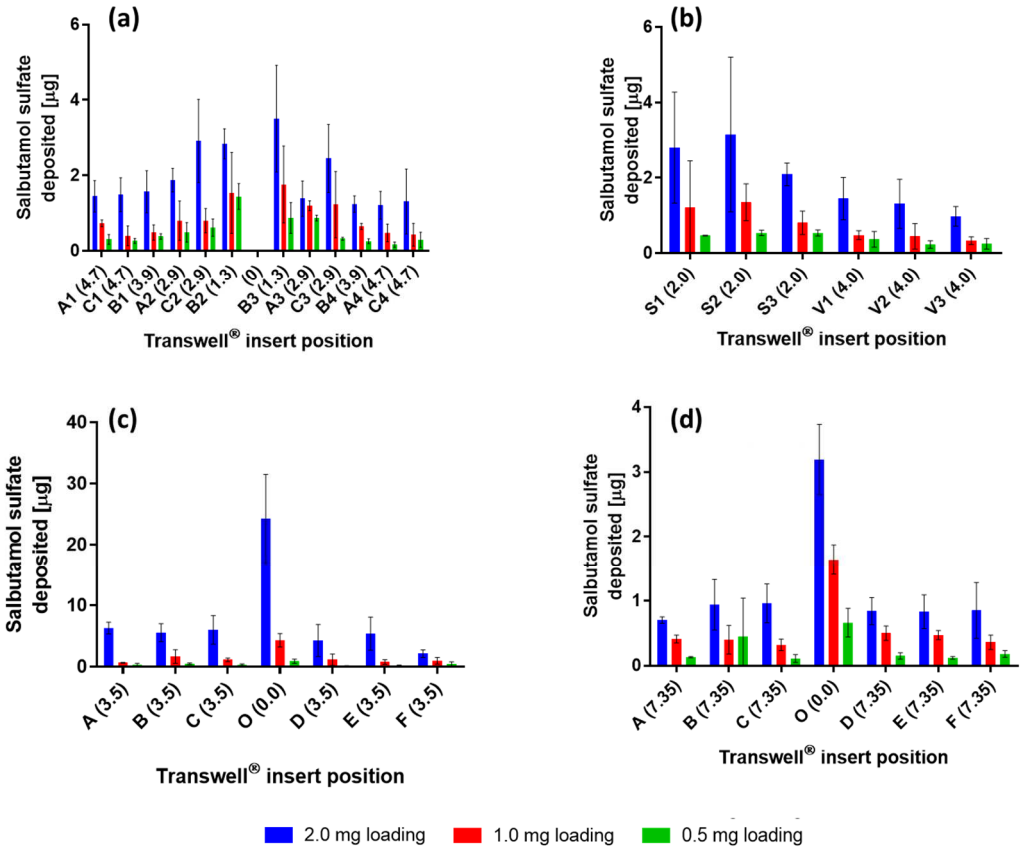


**Figure 3.31: doses of salbutamol sulfate deposited in each Transwell® inserts. In brackets is the distance between the centre of the spray (O) and the centre of the Transwell® insert. The PennCentury™ insufflator was loaded with 2.0, 1.0 and 0.5 mg of dry powder. The drug was sprayed from 20 cm without Quickfit elutriation system. (a) 12-well plate; (b) Triangle; (c) Small hexagon; (d) Large hexagon.**

As expected, by increasing the PennCentury™ device loading from 0.5 mg to 2.0 mg, the amount of drug received by each insert was also increased.

Similarly, we expected the inserts positioned at the centre of the spray to receive higher doses of salbutamol sulfate compared to the others. In fact, in the 12-well plate, positions B2 and B3 (1.3 cm away from the centre) received the highest doses, whereas the inserts further away from the centre (A1, C1, A4 and C4, 4.7 cm) gained the lower doses (Figure 3.31(a)).

The same can be noticed in the triangle geometry where positions S1, S2 and S3 received similar doses between each other ($p>0.05$) being at the same distance of 2.0 cm from the centre, and higher doses compared to V1, V2 and V3 positions ($p<0.05$) located 4.0 cm away from the centre (Figure 3.31(b)), as well as in both the hexagonal geometries where positions Os always received a higher dose of drug ($p<0.05$, Figure 3.31(c-d)).

In general, the further away the Transwell® inserts were placed from the centre of the spray the lower dose they received.

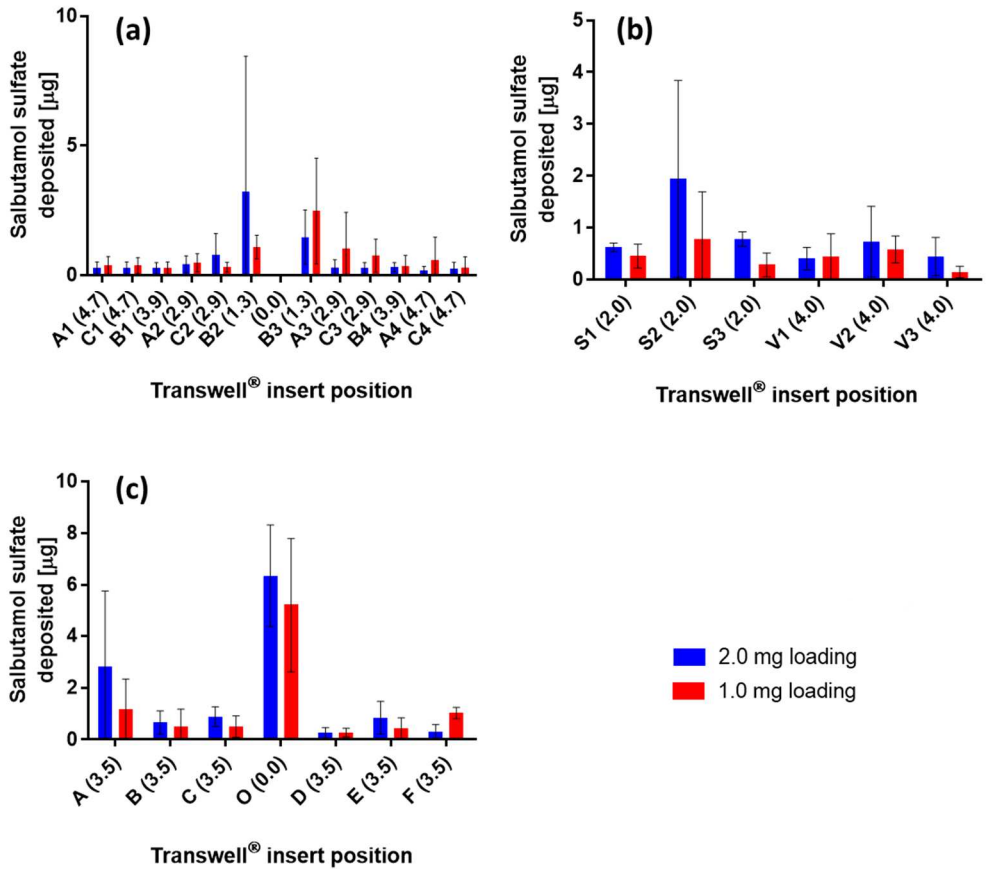


**Figure 3.32: doses of salbutamol sulfate deposited on Transwell® inserts against the distance of the insert from the centre of the spray. In brackets is the distance between the centre of the spray (O) and the centre of the Transwell® insert. The PennCentury™ insufflator was loaded with 2.0, 1.0 and 0.5 mg of dry powder. The drug was sprayed from 20 cm using the Quickfit elutriation system. (a) 12-well plate; (b) Triangle; (c) Small hexagon.**

On the other hand, when the Quickfit elutriation system was inserted in the desiccator the amount of drug powder reaching the surface was much lower. In fact, a lot of material remained in the glass tube (it was found to be 1.5 and 0.5 mg with 2.0 and 1.0 mg loading respectively) and could not therefore reach the surface.

Also in this case some Transwell® inserts always received more dose than the others such as positions B2 and B3 in the 12-well plate and position C in the hexagon arrangement ($p<0.05$, Figure 3.32).

Transwell® inserts at the same distance from the centre (O) were expected to receive similar amounts of drug, but experimentally this was not always the case. In fact, for example positions B2 and B3 in the 12-well plate received respectively 7.25 ± 1.67 µg

and 5.61 ± 3.20 μg with 2.0 mg loading and without Quickfit. Similarly, the position S2 received more dose (1.94 ± 1.90 μg) than S1 and S3 (0.62 ± 0.08 and 0.78 ± 0.14 μg respectively) in the triangle geometry with 2.0 mg loading and the Quickfit inserted. These results suggest that probably the PennCentury$^{TM}$ device was not positioned perfectly vertically to the surface underneath, thus spraying the particles slightly off-centre in real life.

When the doses deposited on the inserts positioned at the same distance from the centre were averaged, the variability (CV) was quite high (CV>20% with maximum value of 69.11%) in several cases when the Quickfit receiver was not fitted to the chamber as elutriation system (Table 3.6). However, examples for which CV<20% could be found: the inserts positioned 3.9 and 1.3 cm away from the centre (B1-B4 and B2-B3) for 1.0 mg loading and 1.0 and 2.0 mg loading respectively in the 12-well plate; the inserts positioned 4.0 and 2.0 cm away from the centre (V1-V2-V3, and S1-S2-S3) for 1.0 and 2.0 mg loading and 0.5 mg loading respectively in the triangle geometry; the inserts 7.35 cm away from the centre (A-B-C-D-E-F) for 1.0 and 2.0 mg loading in the large hexagon.

On the other hand, the variability increased for all geometries when the Quickfit receiver was inserted in the system (Table 3.7) in comparison to the configuration without this elutriation system (Table 3.6).

Overall all the arrangements taken into account present advantages and disadvantages. For example, the triangle and the hexagons configurations provide more replicates of the same experiment since at least three inserts always received similar doses in the same experimental conditions. On the other hand, in the case of the 12-well plate only couples of inserts receive similar doses (B2 and B3; A2 and C2; A3 and C3; A1, B1

and C1; A4, B4 and C4). However, as highlighted before, a good reproducibility between equivalent inserts could not always be achieved.

The geometry providing the best results for both reproducibility and statistical relevance was the large hexagon when the elutriation system was not used. However, position O in this geometry could be critical in terms of cell viability. In fact, being at the centre of the spray this insert could be exposed to a stronger spray that could disrupt the cell layer. In addition, it is the position receiving the highest dose (up to 24.27 µg of salbutamol) which seems to be a very high dose for 1.12 $cm^2$ cell layer, although Haghi *et al*. (2012) deposited up to 230 µg of salbutamol on Calu-3 cell layers.

Considering only the six inserts positioned at the edges of the desiccator chamber (A, B, C, D, E and F), we could deliver 0.41 ± 0.07 µg and 0.85 ± 0.09 µg of salbutamol sulfate with 1.0 and 2.0 mg loadings respectively (Table 3.6).

**Table 3.6: averaged doses of salbutamol sulfate between positions at the same distance from the centre of the spray for the four geometries investigated when no elutriation system was used.**

| Geometry | Position (distance from centre [cm]) | Loading [mg] | Dose averaged between positions [µg] | CV [%] |
|---|---|---|---|---|
| *12 well plate* | A1, A4, C1, C4 (4.7) | 0.5 | 0.26 ± 0.06 | 24.38 |
| | | 1.0 | 0.51 ± 0.15 | 29.77 |
| | | 2.0 | 1.75 ± 1.02 | 57.99 |
| | B1, B4 (3.9) | 0.5 | 0.32 ± 0.09 | 28.09 |
| | | 1.0 | 0.57 ± 0.11 | 19.66 |
| | | 2.0 | 2.21 ± 1.29 | 58.40 |
| | A2, A3, C2, C3 (2.9) | 0.5 | 0.58 ± 0.23 | 39.86 |
| | | 1.0 | 1.01 ± 0.24 | 23.92 |
| | | 2.0 | 3.94 ± 1.02 | 25.94 |
| | B2, B3 (1.3) | 0.5 | 1.16 ± 0.40 | 34.63 |
| | | 1.0 | 1.65 ± 0.16 | 9.53 |
| | | 2.0 | 6.43 ± 1.16 | 18.05 |
| *Triangle* | V1, V2, V3 (4.0) | 0.5 | 0.29 ± 0.08 | 27.36 |
| | | 1.0 | 0.42 ± 0.08 | 18.58 |
| | | 2.0 | 1.24 ± 0.24 | 19.56 |
| | S1, S2, S3 (2.0) | 0.5 | 0.52 ± 0.04 | 7.28 |
| | | 1.0 | 1.12 ± 0.28 | 24.98 |
| | | 2.0 | 2.68 ± 0.54 | 20.27 |
| *Small hexagon* | A, B, C, D, E, F (3.5) | 0.5 | 0.32 ± 0.13 | 41.07 |
| | | 1.0 | 1.06 ± 0.36 | 33.61 |
| | | 2.0 | 4.94 ± 1.54 | 31.13 |
| *Large hexagon* | A, B, C, D, E, F (7.35) | 0.5 | 0.19 ± 0.13 | 69.11 |
| | | 1.0 | 0.41 ± 0.07 | 16.55 |
| | | 2.0 | 0.85 ± 0.09 | 10.79 |

**Table 3.7: averaged doses of salbutamol sulfate between positions at the same distance from the centre of the spray for the three geometries investigated when the elutriation system was used.**

| Geometry | Position (distance from centre [cm]) | Loading [mg] | Dose averaged between positions [µg] | CV [%] |
|---|---|---|---|---|
| *12 well plate* | A1, A4, C1, C4 (4.7) | 1.0 | 0.39 ± 0.12 | 29.79 |
| | | 2.0 | 0.23 ± 0.05 | 19.30 |
| | B1, B4 (3.9) | 1.0 | 0.30 ± 0.06 | 18.97 |
| | | 2.0 | 0.28 ± 0.03 | 10.01 |
| | A2, A3, C2, C3 (2.9) | 1.0 | 0.71 ± 0.32 | 44.76 |
| | | 2.0 | 0.41 ± 0.23 | 56.64 |
| | B2, B3 (1.3) | 1.0 | 1.77 ± 0.98 | 55.53 |
| | | 2.0 | 2.33 ± 1.23 | 52.93 |
| *Triangle* | V1, V2, V3 (4.0) | 1.0 | 0.39 ± 0.22 | 58.00 |
| | | 2.0 | 0.52 ± 0.18 | 34.25 |
| | S1, S2, S3 (2.0) | 1.0 | 0.50 ± 0.26 | 51.09 |
| | | 2.0 | 1.11 ± 0.72 | 64.63 |
| *Small hexagon* | A, B, C, D, E, F (3.5) | 1.0 | 0.64 ± 0.36 | 55.53 |
| | | 2.0 | 0.96 ± 0.95 | 98.73 |

Given the results showed, we decided that the best conditions for carrying out the future *in-vitro* experiments discussed in this PhD thesis consisted in loading the PennCentury™ Dry Powder Insufflator with either 1.0 or 2.0 mg of micronised salbutamol sulfate dry powder without use of the needle nor the Quickfit vented receiver as elutriation system as none of them provide any improvement to the performance of the deposition system. The dry powder was deposited onto Transwell® inserts arranged according to the "large hexagon" geometry. In particular, four of the seven possible positions were employed: B, C, E and F, as to have a symmetrical arrangement of inserts around the centre of the spray. The system could allow for the exposure of a higher number of layers to the dry powder aerosol, however the use of four inserts was judged to be the optimum compromise between the need of having statistical relevant data and cost of individual experiment.

### 3.3.6. Calu-3 cell viability and cell layer integrity after exposure to the dry powder spray

The effect of the exposure of Calu-3 cell layers grown at the air liquid interface (ALI) to the micronised dry powder spray produced by the PennCentury™ Dry Powder Insufflator on cell viability and cell layer integrity was assessed by monitoring the transepithelial electrical resistance (TEER) of the cell layers and the apical to basolateral (A→B) transepithelial flux of the paracellular marker lucifer yellow (LY). The TEER is a unanimously accepted non-invasive quantitative measure of the resistance to ion movement across the cell layer and reflects the barrier integrity (Srinivasan *et al.* 2015). For Calu-3 cells grown at the air-liquid interface the values of TEER reported in the literature vary depending on the culture conditions (e.g. growth medium used, nature of the growth membrane, etc). Here, we consider a Calu-3 cell layer tight and intact when TEER>400 $\Omega \cdot cm^2$ (Foster *et al.* 2000).

In Figure 3.33 is reported the TEER measured before (day 20) and after (day 21) treatment of the 21-days old Calu-3 cell layers grown in ALI conditions. The TEER "before exposure" refers to the value measured 20 days post seeding rather than on the experimental day. This was done in order to avoid the removal of the mucus layer produced by the Calu-3 cells when grown in ALI conditions (Grainger *et al.* 2006) when removing the volume of HBSS added on the apical side for the TEER measurement. Also, this could have caused an increase in the apical surface volumes if the HBSS was not completely removed.

The TEER value dropped in all conditions after exposure to a spray, however its value always remained above 500 $\Omega cm^2$ (Figure 3.33).

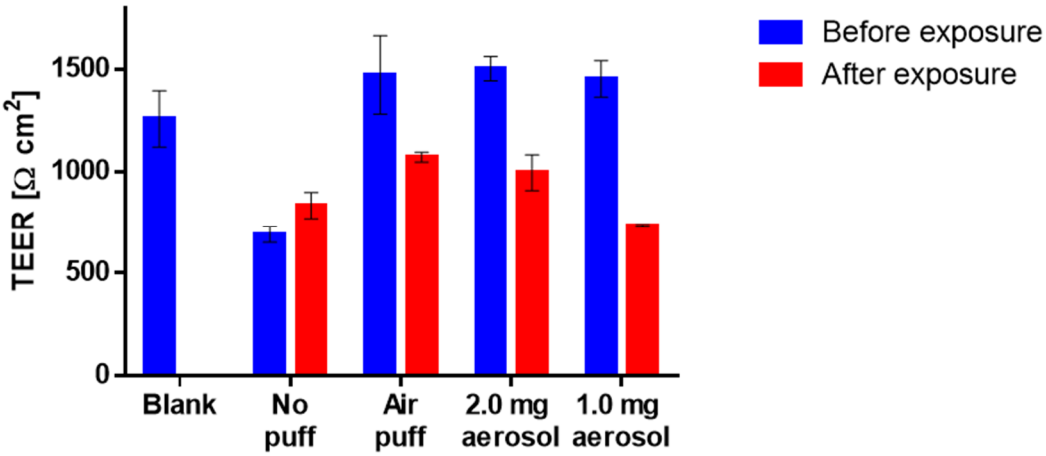


**Figure 3.33: transepithelial electrical resistance (TEER) before and after exposure of Calu-3 cell layers grown in ALI conditions to 1) Blank: layers kept in the incubator; 2) No puff: layers moved to and kept in the desiccator chamber for the time of a spray (30 s) but not exposed to the spray; 3) Air puff: layers moved to the desiccator chamber and exposed to 5.0 mL of ambient air puff; 4) 2.0 mg aerosol: layers moved to the desiccator chamber and exposed to salbutamol aerosol produced with the PennCentury™ device loaded with 2.0 mg of dry powder; 5) 1.0 mg aerosol: layers moved to the desiccator chamber and exposed to salbutamol aerosol produced with the PennCentury™ device loaded with 1.0 mg of dry powder**

On the other hand, lucifer yellow is a small hydrophilic molecule (lucifer yellow VS dilithium salt $M_w$=457.25 Da) used as a paracellular marker. In fact, it has been demonstrated that it is not internalised in Calu-3 cells and is able to cross the cellular barrier mainly through the paracellular route (Foster *et al.* 2000). The use of a paracellular marker is another way of assessing the barrier integrity. This assay measures the transfer of a small molecule through the intercellular spaces and gives an indication of the tight junctions pore size (Srinivasan *et al.* 2015).

The results obtained for the LY assay are showed in Figure 3.34.

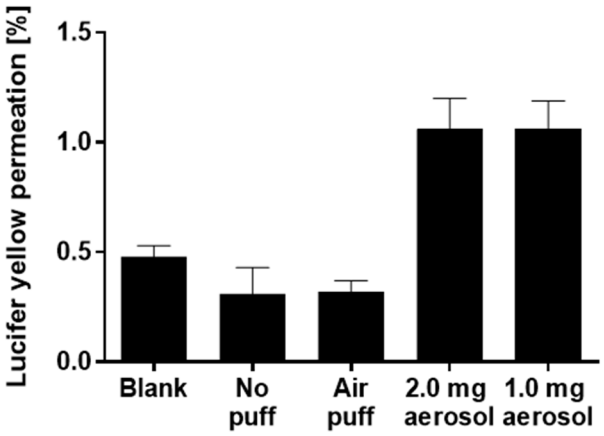


**Figure 3.34: lucifer yellow transepithelial transport [%] across Calu-3 cell layers 60 minutes after exposure of the cell layers grown in ALI conditions to 1) Blank: layers kept in the incubator; 2) No puff: layers moved to and kept in the desiccator chamber for the time of a spray (30 s) but not exposed to the spray; 3) Air puff: layers moved to the desiccator chamber and exposed to 5.0 mL of ambient air puff; 4) 2.0 mg aerosol: layers moved to the desiccator chamber and exposed to salbutamol aerosol produced with the PennCentury™ device loaded with 2.0 mg of dry powder; 5) 1.0 mg aerosol: layers moved to the desiccator chamber and exposed to salbutamol aerosol produced with the PennCentury™ device loaded with 1.0 mg of dry powder**

The transport of LY was higher when the cell layers were exposed to 1.0 and 2.0 mg sprays of drug. However, it was lower than 2% that in this work was accepted as a threshold between a tight and intact cellular layer and a damaged or not formed yet cellular layer. The $P_{app}$ calculated according to Equation 2.2 (Chapter 2, page 37) was 3.4 x $10^{-7}$ cm $s^{-1}$, and values of $P_{app}$ of similar magnitude $10^{-7}$ cm $s^{-1}$ have been reported in the literature (Florea *et al.* 2003).

Combined together, the data obtained from the TEER measurement and the lucifer yellow assay, confirmed that the cell layers survived and maintained their barrier properties after exposure to the spray. This guaranteed that the system developed in this project was suitable for applying dry powder particles onto cell cultures and being used for the investigation of the fate of dry powder particles for inhalation in the lungs.

## 3.4. Conclusions

The aim of the work described in this chapter was the development and validation of a simple and low cost *in-vitro* system to apply dry powder particles for inhalation onto multiple Calu-3 cell layers grown at the air-liquid interface used to model the lung epithelium *in-vitro*. The system would later be used to investigate the factors that affect the particles' fate in the lung.

A very simple and low cost system to apply dry powder particles onto Calu-3 cell layers was successfully developed and validated.

Salbutamol sulfate dry powder could be homogenously dispersed in the chamber. Provided that the bulk dry powder PSD was in the respirable range (3-5 μm), a good control over the particle size distribution could be achieved,

The arrangement of the Transwell® inserts in a "large hexagon" geometry allowed a consistent dose to be delivered to at least four inserts and thus offered a compromise between the need of having statistical relevant data and cost of individual experiment.

Finally, it was also demonstrated that Calu-3 cell layers cultured in ALI conditions were maintained intact and tight after transfer to the desiccator chamber and exposure to the aerosol.

## 3.5. References

Abràmoff, M.D., Magalhães, P.J. & Ram, S.J., 2004. Image processing with imageJ. *Biophotonics International*, 11(7), pp.36–41.

Acosta, M.F. *et al.*, 2016. In vitro pulmonary cell culture in pharmaceutical inhalation aerosol delivery: 2-D, 3-D, and in situ bioimpactor models. *Current Pharmaceutical Design*, 22(17), pp.2522–2531.

Andrade, F., Albuquerque, J. & Nascimento, A.V., 2016. Cell-based in vitro models for pulmonary permeability studies. In *Concepts and Models for Drug Permeability Studies*. Elsevier, pp. 373–385.

Aufderheide, M. *et al.*, 2013. The CULTEX RFS: a comprehensive technical approach for the in vitro exposure of airway epithelial cells to the particulate matter at the air-liquid interface. *BioMed Research International*, 2013(Article ID 734137), pp.1–15.

Aufderheide, M. & Mohr, U., 1999. CULTEX - A new system and technique for the cultivation and exposure of cells at the air/liquid interface. *Experimental and Toxicologic Pathology*, 51(6), pp.489–490.

Bitterle, E. *et al.*, 2006. Dose-controlled exposure of A549 epithelial cells at the air-liquid interface to airborne ultrafine carbonaceous particles. *Chemosphere*, 65(10), pp.1784–1790.

Blank, F. *et al.*, 2006. An optimized in vitro model of the respiratory tract wall to study particle cell interactions. *Journal of Aerosol Medicine*, 19(3), pp.392–405.

Bur, M. *et al.*, 2009. A novel cell compatible impingement system to study in vitro drug absorption from dry powder aerosol formulations. *European Journal of Pharmaceutics and Biopharmaceutics*, 72(2), pp.350–357.

Bur, M. *et al.*, 2010. Drug transport across pulmonary epithelial cell monolayers: effect

of particle size, apical liquid volume and deposition technique. *Journal of Aerosol Medicine and Pulmonary Drug Delivery*, 23(3), pp.119–127.

Cabrera-Pérez, M.Á. *et al.*, 2016. Importance and applications of cell- and tissue-based in vitro models for drug permeability screening in early stages of drug development. In *Concepts and Models for Drug Permeability Studies*. Elsevier, pp. 3–29.

Chapman, K.L. *et al.*, 2013. Pharmaceutical toxicology: designing studies to reduce animal use, while maximizing human translation. *Regulatory Toxicology and Pharmacology*, 66(1), pp.88–103.

Cooney, D., Kazantseva, M. & Hickey, A.J., 2004. Development of size- dependent aerosol deposition model utilizing human airway epithelial cells for evaluating aerosol Drug Delivery. *ALTA*, 32(6), pp.581–590.

Corning Inc., Transwell® permeable inserts selection and user guide, Corning Incorporated (NY, USA). Available at: http://www.corning.com/lifesciences/surfaces/en/transwell.aspx.

Cozens, A.L. *et al.*, 1994. CFTR expression and chloride secretion in polarized immortal human bronchial epithelial cells. *American Journal of Respiratory Cell and Molecular Biology*, 10(1), pp.38–47.

Daniher, D.I. & Zhu, J., 2008. Dry powder platform for pulmonary drug delivery. *Particuology*, 6(4), pp.225–238.

Duret, C. *et al.*, 2012. In vitro and in vivo evaluation of a dry powder endotracheal insufflator device for use in dose-dependent preclinical studies in mice. *European Journal of Pharmaceutics and Biopharmaceutics*, 81(3), pp.627–634.

Ehrhardt, C. *et al.*, 2002. Influence of apical fluid volume on the development of functional intercellular junctions in the human epithelial cell line 16HBE14o-:

Implications for the use of this cell line as an in vitro model for bronchial drug absorption studies. *Cell and Tissue Research*, 308(3), pp.391–400.

EL-Araud, K.A. *et al.*, 1998. The effect of dose on the characterization of aerodynamic particle-size distributions of beclomethasone dipropionate metered-dose inhalers. *The Journal of Pharmacy and Pharmacology*, 50(10), pp.1081–1085. Available at: http://www.ncbi.nlm.nih.gov/pubmed/9821652.

Fiegel, J. *et al.*, 2003. Large porous particle impingement on lung epithelial cell monolayers - Toward improved particle characterization in the lung. *Pharmaceutical research*, 20(5), pp.788–796.

Florea, B.I. *et al.*, 2003. Drug transport and metabolism characteristics of the human airway epithelial cell line Calu-3. *Journal of Controlled Release*, 87(1), pp.131–138.

Fogh, J., Fogh, J.M. & Orfeo, T., 1977. One hundred and twenty-seven cultured human tumor cell lines producing tumors in nude mice. *Journal of the National Cancer Institute*, 59(1), pp.221–226.

Forbes, B. *et al.*, 2003. The human bronchial epithelial cell line 16HBE14o- as a model system of the airways for studying drug transport. *International Journal of Pharmaceutics*, 257(1), pp.161–167.

Forbes, B. & Ehrhardt, C., 2005. Human respiratory epithelial cell culture for drug delivery applications. *European Journal of Pharmaceutics and Biopharmaceutics*, 60(2), pp.193–205.

Forbes, I., 2000. Human airway epithelial cell lines for in vitro drug transport and metabolism studies. *Pharmaceutical science & technology today*, 3(1), pp.18–27.

Foster, K.A. *et al.*, 2000. Characterization of the Calu-3 cell line as a tool to screen pulmonary drug delivery. *International Journal of Pharmaceutics*, 208(1), pp.1–

11.

Grainger, C.I. *et al.*, 2006. Culture of Calu-3 cells at the air interface provides a representative model of the airway epithelial barrier. *Pharmaceutical Research*, 23(7), pp.1482–1490.

Grainger, C.I. *et al.*, 2009. The permeability of large molecular weight solutes following particle delivery to air-interfaced cells that model the respiratory mucosa. *European Journal of Pharmaceutics and Biopharmaceutics*, 71(2), pp.318–324.

Haghi, M. *et al.*, 2014. Across the pulmonary epithelial barrier: Integration of physicochemical properties and human cell models to study pulmonary drug formulations. *Pharmacology & Therapeutics*, 144(3), pp.235–252.

Haghi, M. *et al.*, 2012. Deposition, diffusion and transport mechanism of dry powder microparticulate salbutamol, at the respiratory epithelia. *Molecular Pharmaceutics*, 9(6), pp.1717–1726.

Haghi, M., Traini, D. & Young, P., 2014. In vitro cell integrated impactor deposition methodology for the study of aerodynamically relevant size fractions from commercial pressurised metered dose inhalers. *Pharmaceutical Research*, 31(7), pp.1779–1787.

Hein, S. *et al.*, 2011. A new Pharmaceutical Aerosol Deposition Device on Cell Cultures (PADDOCC) to evaluate pulmonary drug absorption for metered dose dry powder formulations. *European journal of pharmaceutics and biopharmaceutics*, 77(1), pp.132–138.

Hein, S. *et al.*, 2010. The Pharmaceutical Aerosol Deposition Device on Cell Cultures (PADDOCC) in vitro system: design and experimental protocol. *Alternatives to Laboratory Animals: ATLA*, 38(4), pp.285–295.

Hoppentocht, M. *et al.*, 2014. In vitro evaluation of the DP-4M PennCentury™ insufflator. *European Journal of Pharmaceutics and Biopharmaceutics*, 88(1), pp.153–159.

Kim, J.S. *et al.*, 2013. Validation of an in vitro exposure system for toxicity assessment of air-delivered nanomaterials. *Toxicology In Vitro*, 27(1), pp.164–173.

Lenz, A.G. *et al.*, 2009. A dose-controlled system for air-liquid interface cell exposure and application to zinc oxide nanoparticles. *Particle and Fibre Toxicology*, 32(6).

Manford, F. *et al.*, 2005. Drug permeability in 16HBE14o- airway cell layers correlates with absorption from the isolated perfused rat lung. *European Journal of Pharmaceutical Sciences*, 26(5), pp.414–420.

Marple, V. a. & Willeke, K., 1976. Impactor design. *Atmospheric Environment*, 10(10), pp.891–896.

McDonnell, C. *et al.*, 2012. Investigation deposition and drug absorption of budesonide microparticles using a cell compatible next generation impactor. *Respiratory Drug Delivery Proc*, 3, pp.785–788.

Meindl, C. *et al.*, 2015. Permeation of therapeutic drugs in different formulations across the airway epithelium in vitro. *PLoS ONE*, 10(8), pp.1–19.

Nasr, M.M. & Allgire, J.F., 1995. Loading effect on particle size measurements by inertial sampling of albuterol metered dose inhalers. *Pharmaceutical research*, 12(11), pp.1677–1681.

Ong, H.X., Traini, D. & Young, P.M., 2013. Pharmaceutical applications of the Calu-3 lung epithelia cell line. *Expert Opinion on Drug Delivery*, 10(9), pp.1287–1302.

Patton, J.S., Fishburn, C.S. & Weers, J.G., 2004. The lungs as a portal of entry for systemic drug delivery. *Proceedings of the American Thoracic Society*, 1(4), pp.338–44.

PennCentury Inc., PennCentury™ official web page. Available at: http://penncentury.com/products/dry-powder-devices/dry-powder-insufflator-dp-4/.

Ritter, D., Knebel, J.W. & Aufderheide, M., 2001. In vitro exposure of isolated cells to native gaseous compounds - Development and validation of an optimized system for human lung cells. *Experimental and Toxicologic Pathology*, 53(5), pp.373–386.

Russel, W.M.S. & Burch, R.L., 1959. *The principles of humane experimental technique*, Methuen & Co., Ltd, London.

Sadler, R.C. *et al*., 2011. Integrated in vitro experimental modelling of inhaled drug delivery: deposition, dissolution and absorption. *Journal of Drug Delivery Science and Technology*, 21(4), pp.331–338.

Saunders, M. *et al*., 2008. Characterization of particles emitted from beclomethasone doproprionate solution metered dose inhalers. In *Aerosols Conference - Drug Delivery to the Lungs - DDL19*. pp. P89–P92.

Savi, M. *et al*., 2008. A novel exposure system for the efficient and controlled deposition of aerosol particles onto cell cultures. *Environmental Science & T Technology*, 42(15), pp.5667–5674.

Shen, B.Q. *et al*., 1994. Calu-3: a human airway epithelial cell line that shows cAMP-dependent Cl-secretion. *American Journal of Physiology*, 266(5), pp.L493–L501.

Srinivasan, B. *et al*., 2015. TEER Measurement Techniques for In Vitro Barrier Model Systems. *Journal of Laboratory Automation*, 20(2), pp.107–126.

Steimer, A., Haltner, E. & Lehr, C.-M., 2005. Cell culture models of the respiratory tract relevant to pulmonary drug delivery. *Journal of Aerosol Medicine*, 18(2), pp.137–182.

Tang, T. *et al*., 2012. Investigations on cytotoxic and genotoxic effects of laser printer emissions in human epithelial A549 lung cells using an air/liquid exposure system. *Environmental and Molecular Mutagenesis*, 135(2), pp.125–135.

Tarkington, B.K. *et al*., 1994. In vitro exposure of tracheobronchial epithelial cells and of tracheal explants to ozone. *Toxicology*, 88(17), pp.51–68.

Tippe, A., Heinzmann, U. & Roth, C., 2002. Deposition of fine and ultrafine aerosol particles during exposure at the air/cell interface. *Aerosol Scicence*, 33(2), pp.207–218.

Tonnis, W.F. *et al*., 2014. A novel aerosol generator for homogenous distribution of powder over the lungs after pulmonary administration to small laboratory animals. *European Journal of Pharmaceutics and Biopharmaceutics*, 88(3), pp.1056–1063.

Vitrocell systems, Vitrocell systems webpage. Available at: http://www.vitrocell.com/inhalation-toxicology/exposure-systems/vitrocell-cloud-system [Accessed June 26, 2016].

Whitcutt, M.J., Adler, K.B. & Wu, R., 1988. A biphasic chamber system for maintaining polarity of differentiation of cultured respiratory tract epithelial cells. *In Vitro Cellular & Developmental Biology*, 24(5), pp.420–428.

# Chapter 4
# Salbutamol sulfate absorption across Calu-3 layers after delivery as a dry powder for inhalation

## 4.1. Introduction

### 4.1.1. Salbutamol sulfate: therapeutic use and mechanism of action

Salbutamol (in Europe) or albuterol (in the USA) (Figure 4.1b) is a selective short acting $\beta_2$-adrenoreceptor (AR) agonist (Figure 4.1a) discovered by Sir David Jack and colleagues in 1966 (Jack 1991).

Since its discovery, salbutamol has been used for the treatment of mild to severe bronchospasm associated to clinical conditions such as asthma. In fact it is able to relax the airway smooth muscle (ASM) by binding to the active site of $\beta_2$-ARs, that are very densely present in the ASM (Mamlouk *et al*. 2013).

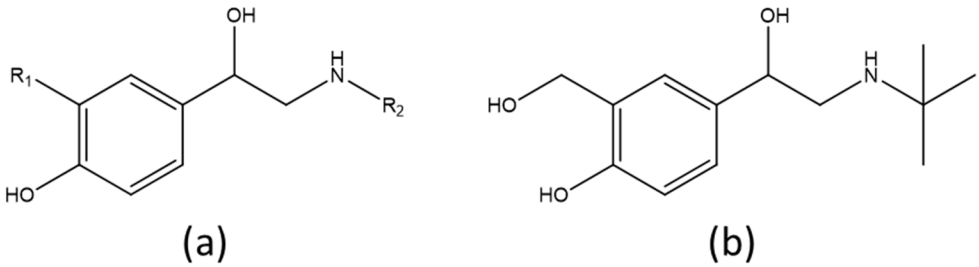


**Figure 4.1: chemical structure of (a) $\beta_2$-adrenoreceptor agonists and (b) salbutamol**

Salbutamol is highly selective for $\beta_2$-ARs and its effect after inhalation is observed within a very short time (15 minutes). Its duration of action is reported to be between 4 and 6 hours (Sears & Lotvall 2005) due to the weak binding with the receptor. Due

to its fast onset it is the drug of choice for the immediate relief of obstructive lung diseases in doses varying between 200 and 400 µg. However, its short half-life limits its use in a prolonged therapy (Cazzola *et al*. 2013).

Salbutamol is most commonly manufactured and administered as the sulfate salt. Salbutamol sulfate has been formulated for more than 30 years in various forms including suspensions for nebulisers or pMDI and dry powders for DPI, but it may be delivered intravenously if the patient's breathing capability is compromised (Cazzola *et al*. 2012).

## 4.1.2. Mechanisms of pulmonary absorption of salbutamol sulfate

In order to reach the $\beta_2$-ARs located in the smooth muscle and exert its therapeutic action, salbutamol sulfate must pass across the lung epithelium.

Salbutamol sulfate has two $pK_a$ values (Figure 4.2): 9.3 for the amino group and 10.3 for the phenolic group (Mamlouk *et al*. 2013). This means that this molecule carries a net positive charge at physiological pH (pH=7.4).

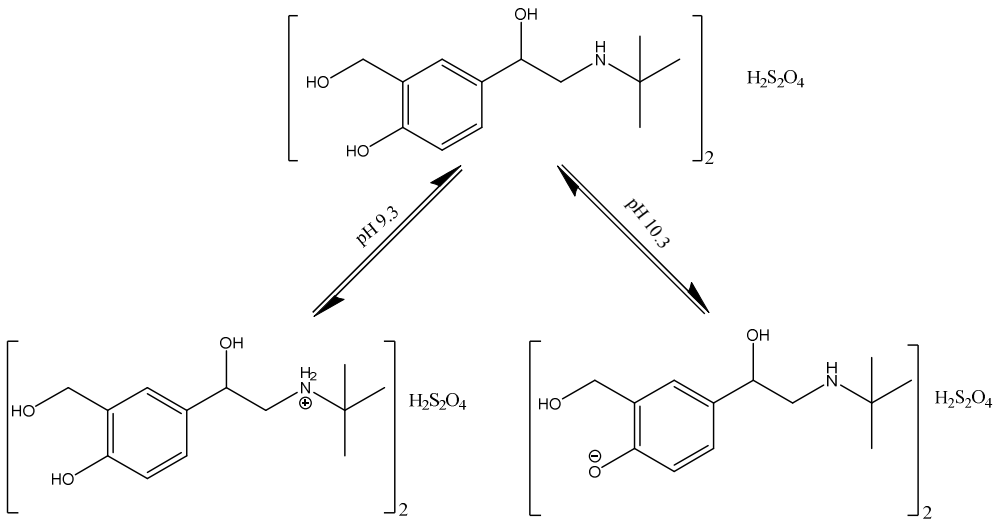


**Figure 4.2: $pK_a$ of salbutamol sulfate**

As a cation, it may not easily reach its receptor in the smooth muscle by freely diffusing across the lipid bilayer of the cellular membrane of the lung epithelium, as opposed to

the non-ionised drug. The lung epithelium then represents the main physicochemical barrier to salbutamol sulfate absorption.

Several researchers in the field hypothesized that transporters, in particular those associated with cation translocation (organic cation transporters, OCTs and OCTNs; solute link carriers, SLC22A1-A5), might be involved in the absorption and clearance mechanisms of bronchodilators, modulating their access to the submucosal lung tissues.

As mentioned in Chapter 1 (paragraph 1.5.2.2, page 17), many uptake and efflux transporters are found to be expressed at high levels in various tissues including the lungs *in-vivo* (Gumbleton *et al.* 2011). Also, both primary and immortalised cell lines used as models of the lung epithelium *in-vivo* have shown different levels of these transporters (Endter *et al.* 2009; Mukherjee *et al.* 2012; Sakamoto *et al.* 2013; Salomon *et al.* 2014; Sakamoto *et al.* 2015; Nickel *et al.* 2016). In particular, Mukherjee *et al.* (2012) demonstrated that Calu-3 cells grown in ALI conditions express a OCT1, OCT3, OCTN1 and OCTN2 transporters on their apical side. However, their role in the biopharmaceutics of inhaled drugs has not been completely clarified yet (Bosquillon 2010; Salomon & Ehrhardt 2012).

The interaction between salbutamol and cation transporters in the lung has been reported in a number of studies (Ehrhardt *et al.* 2005; Horvath, Schmid, *et al.* 2007; Haghi *et al.* 2012; Mukherjee *et al*. 2012; Mamlouk *et al*. 2013; Salomon *et al*. 2015). Ehrhardt and colleagues (2005) first reported that salbutamol was absorbed across Calu-3 and 16HBE14o- cell lines in a concentration and temperature-dependent manner and so hypothesized the involvement of transporter, specifically OCT-type. Other studies provided evidence of $\beta_2$-AR agonists acting as inhibitors of OCT-mediated pathways in both epithelial and smooth muscle cell lines *in-vitro* (Horvath,

Mendes, *et al*. 2007; Horvath, Schmid, *et al*. 2007). Data published by Mamlouk *et al.* (2013) also suggested that OCT transporters might be involved in salbutamol absorption mechanism in Calu-3 cultured in LLC, but this was also described in the case of Calu-3 cells grown at the air-liquid interface (Haghi *et al*. 2012; Salomon *et al*. 2015). The interaction between β2-agonists and cation transporters was also reported using a human lung reperfusion *ex-vivo* model (Gnadt *et al*. 2012).

However, data in the literature is not always in agreement as also evidence of a transporter-independent absorption of cations, including salbutamol, has been reported (Mathias *et al*. 2002; Unwalla *et al*. 2012).

Although the interaction between β2-agonists (in particular salbutamol) and OCT transporters has been investigated to some extent, a definitive proof of either the active or passive transport of these drugs across the lung epithelium by means of OCT-type transporters has not been provided yet and therefore the mechanism of absorption is still not completely and definitely understood (Salomon & Ehrhardt 2012). The possible mechanism of β2-agonists absorption is showed in Figure 4.3:

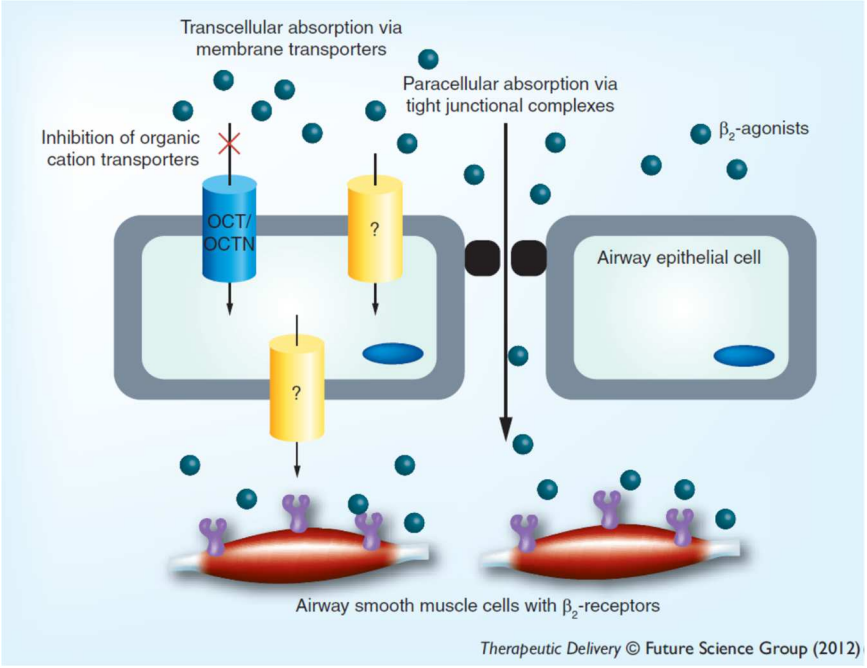


**Figure 4.3: schematic of the possible absorption pathway of β2-agonists across the lung epithelial barrier reproduced from Salomon & Ehrhardt (2012). OCT: Organic Cationic Transporter; OCTN: Organic Carnitine Transporter**

### *4. Salbutamol sulfate absorption across Calu-3 layers after delivery as a dry powder for inhalation*

Another important parameter that seems to affect the absorption of drugs, including salbutamol, is the physical form of the formulation used. In particular, significant differences in transport profile and rate have been highlighted when the drug was applied to the apical surface of Calu-3 cell layers in solution or as a dry powder, with the dry powder being always more rapidly absorbed than the solution (Haghi *et al.* 2012; Bur *et al.* 2010; Meindl *et al.* 2015). Researchers have attributed this different behaviour to the higher concentration gradient created between the apical and the basolateral side of the cell layers by the dry powder in comparison to the solution. These differences have important clinical implications, as they pose questions for the choice of different types of formulation depending on the severity and the urgency of the clinical condition to be addressed.

## 4.1.3. Aim

The aim of the work illustrated in this chapter was to complete the validation of the dry powder deposition system described in Chapter 3 by looking at the transepithelial transport characteristics of salbutamol sulfate delivered to the Calu-3 cell layers grown at the air-liquid interface either as a dry powder or applied as a solution. The validation was finalised by comparing the data collected using our *in-vitro* system with that already available from the literature (Bur *et al*. 2010; Haghi *et al*. 2012) where more complex systems approved by the British Pharmacopoeia (BP), such as TSI and Andersen cascade impactor, had been used.

Once it was confirmed the system was able to provide information about drug permeation across the cell layer comparable with that already published, we focussed on a better understanding of the mechanisms of absorption of salbutamol sulfate when administered as a dry powder for inhalation. In particular, following up from a previous study carried out in our research group by a former PhD student (Dr. Manali Mukherjee) where a significantly increased expression of OCT transporters (OCT1, OCT3, OCTN1, OCTN2) in Calu-3 cell layers grown in ALI conditions was observed as a consequence of 48h exposure to the LPS from *E. Coli.* (Mukherjee 2012), we aimed at designing a transepithelial transport experiment to investigate how the role of OCT transporters (if involved) is affected when salbutamol is delivered as a dry powder.

To our knowledge, this was the first attempt to study the role of transporters in drug absorption, if any, entirely at the air-liquid interface.

## 4.2. Materials and methods

For the origin of the material used refer to Chapter 2.

For the Calu-3 cell culture protocols (maintenance and propagation of the cell line and 12-Transwell® and 24-well culture plates seeding) refer to Chapter 2 (paragraph 2.2.2, page 33).

For the apical to basolateral (A→B) transepithelial transport of salbutamol sulfate protocol, refer to Chapter 2 (paragraph 2.2.3, page 37).

Samples were processed and analysed by LC-MS/MS according to protocol and conditions described in Chapter 2 (paragraph 2.2.5, page 41).

### 4.2.1. Transepithelial transport of salbutamol sulfate after lipopolysaccharide (LPS) exposure

Lipopolysaccharide (LPS) from *E. Coli* (0:111B4, 127K4037; Sigma: #L4391) was reconstituted with serum-free DMEM:F12 medium at 1.0 mg/mL and kept at -20°C until further use, according to the manufacturer's recommendations. The suitable concentration of LPS and exposure time-span had been optimised by a former PhD student (Dr. Manali Mukherjee) working in the same laboratory.

On day 19 (48 hours before the A→B transepithelial transport experiment), medium was removed from the basolateral side of individual Calu-3 cell culture layers. A solution 10 µg/mL of LPS in serum-free medium was freshly prepared and 500 µL of it was placed in the apical side, while 1.5 mL of fresh pre-warmed regular medium was placed in the basolateral chamber according to the LLC cell culture model.

Individual Calu-3 cell layers kept in LLC from day 19 in regular DMEM:F12 medium were used as reference (Calu-3 cell layers not exposed to LPS insult).

***4. Salbutamol sulfate absorption across Calu-3 layers after delivery as a dry powder for inhalation***

On day 21, medium was removed from both the apical and basolateral sides and all Calu-3 cell layers were washed once with 0.5 mL of fresh pre-warmed PBS, and the cell layers were moved to clean 12-well plates.

The effect of LPS on the transepithelial transport of salbutamol sulfate was investigated for the drug delivered either in solution or as a micronised dry powder.

In the case of salbutamol sulfate in solution, the drug transport was observed either in the presence on both sides of an OCT inhibitor, tetraethylammonium (TEA, >99% purity), or not.

The experimental conditions adopted for the A→B transepithelial transport experiment of salbutamol sulfate applied as a solution are reported in Table 4.1:

**Table 4.1: experimental conditions adopted for the A→B transepithelial transport experiment of salbutamol sulfate applied as a solution (5.0 µg/mL in HBSS, corresponding to 1.0 µg dose) to Calu-3 cell layers grown in ALI conditions after LPS insult**

| Condition | Apical chamber (0.2 mL) | Basolateral Chamber (0.9 mL) |
|---|---|---|
| NO LPS insult | 5.0 µg/mL salbutamol sulfate (in HBSS) | HBSS |
| NO LPS insult – TEA | 5.0 µg/mL salbutamol sulfate + 5mM TEA (in HBSS) | 5mM TEA in HBSS |
| LPS insult | 5.0 µg/mL salbutamol sulfate (in HBSS) | HBSS |
| LPS insult – TEA | 5.0 µg/mL salbutamol sulfate + 5mM TEA (in HBSS) | 5mM TEA in HBSS |

In the case of salbutamol sulfate dry powder, the inserts were transferred to the dry powder deposition system and exposed to a spray produced loading the PennCentury™ Dry Powder Insufflator with 2.0 mg of micronised dry powder, corresponding to 1.0 µg dose (Chapter 3, paragraph 3.3.5, page 85), according to the protocol reported in Chapter 2 (paragraph 2.2.3, page 37). In this case, the drug transport was observed only across Calu-3 cell layers either exposed or not to LPS insult, without use of TEA in either case.

***4. Salbutamol sulfate absorption across Calu-3 layers after delivery as a dry powder for inhalation***

Samples were collected at determined time points over a period of four hours as explained in Chapter 2 (paragraph 2.2.3, page 37).

The cell layer integrity was assessed before and after the experiment by measuring the TEER and at the end of the experiment and by monitoring the A→B flux of lucifer yellow, according to the protocols reported in Chapter 2 (paragraphs 2.2.2.7 and 2.2.2.8, pages 35-36).

Samples were processed and analysed by LC-MS/MS according to protocol and conditions described in Chapter 2 (paragraph 2.2.5, page 41).

Experiments were performed in duplicate (N=2), using four Transwell® inserts per condition per replicate (n=4).

## 4.2.2. TEA cytotoxicity: PrestoBlue® cell viability assay

The cytotoxicity of a solution 5mM of TEA was assessed by performing the PrestoBlue® cell viability assay as explained in Chapter 2 (paragraph 2.2.4, page 38).

TEA cytotoxicity was investigated for different exposure times up to four hours: 10, 20, 30, 60, 120, 180 and 240 minutes.

## 4.3. Results and discussion

### 4.3.1. Transepithelial transport of salbutamol delivered in solution or as a dry powder

A further validation of the deposition system was conducted by looking at the apical to basolateral (A→B) transepithelial transport of salbutamol sulfate delivered as a micronised dry powder or in solution, and comparing the results obtained using our system with the data published by other researchers that used systems approved by the BP.

The salbutamol sulfate doses applied to Calu-3 cell layers cultured in ALI conditions were 0.5 and 1.0 μg. In the case of the dry powder these doses corresponded to 1.0 and 2.0 mg PennCentury™ device loadings respectively (Chapter 3, paragraph 3.3.5, page 85).

The TEER and lucifer yellow permeation values registered at the end of the transport experiments were within the acceptable ranges as showed in Table 4.2:

**Table 4.2: TEER and lucifer yellow values registered at the end of the transport experiment after application of salbutamol sulfate either in solution or as a dry powder. Data are presented as mean ± sem (N=2, n=4).**

| Dosage form | Dose [μg] | TEER [Ω·cm²] | Lucifer yellow permeation [%] |
|---|---|---|---|
| Solution | 0.5 | 844 ± 141 | 0.26 ± 0.06 |
| | 1.0 | 977 ± 203 | 0.24 ± 0.11 |
| Dry powder | 0.5 (1.0 mg loading) | 795 ± 75 | 0.79 ± 0.14 |
| | 1.0 (2.0 mg loading) | 872 ± 124 | 0.80 ± 0.17 |

***4. Salbutamol sulfate absorption across Calu-3 layers after delivery as a dry powder for inhalation***

The A→B transepithelial transport profile of salbutamol sulfate applied in solution or delivered as dry powder across the Calu-3 cell layer is shown in Figure 4.4 and Figure 4.5 respectively.

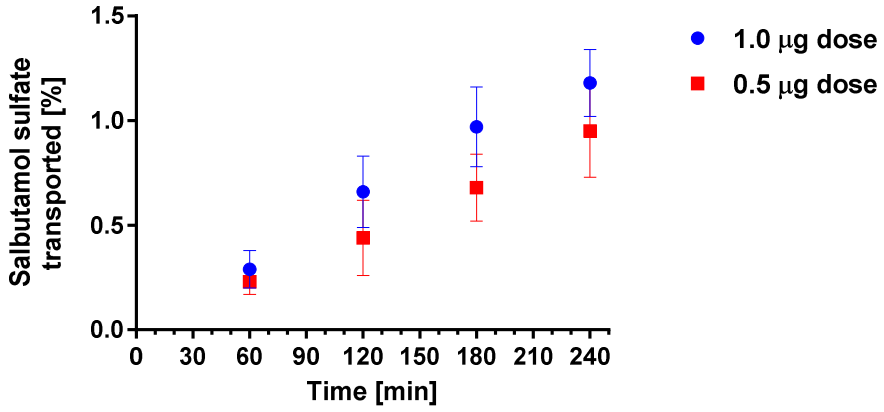


**Figure 4.4: apical to basolateral (A→B) transport profile of salbutamol sulfate applied in solution (200 µL of 5.0 and 2.5 µg mL$^{-1}$, corresponding to 1.0 and 0.5 µg doses respectively). Data are presented as mean ± sem (N=2, n=4).**

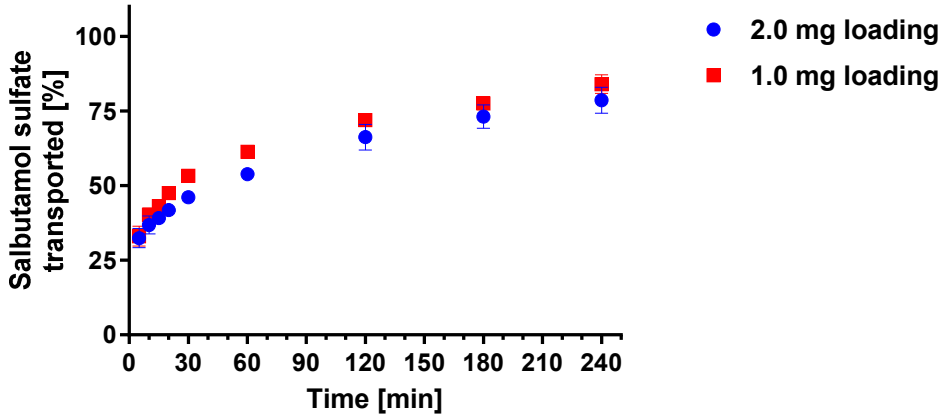


**Figure 4.5: apical to basolateral (A→B) transport profile of salbutamol sulfate delivered as a dry powder (2.0 and 1.0 mg PennCentury$^{TM}$ insufflator loading, corresponding to 1.0 and 0.5 µg doses respectively (Chapter 3, paragraph 3.3.5, page 85). Data are presented as mean ± sem (N=2, n=4).**

When salbutamol was applied in solution, the percentage of salbutamol transported followed a linear trend reaching ≈1% in four hours. The percentage of drug transported was not dependent on the initial dose applied for all time-points, but t=180 mins (multiple t-test, p>0.05), however the flux were found to be statistically different and equal to 5.0 ± 0.2 x10$^{-3}$ and 3.9 ± 0.1 x10$^{-3}$ % units/min for 1.0 and 0.5 µg dose

respectively. Salbutamol sulfate was quicker at crossing the cell layer when the donor solution was more concentrated as demonstrated also by the $P_{app}$ values calculated and reported in Table 4.3:

**Table 4.3: $P_{app}$ values calculated for salbutamol sulfate applied in solution on Calu-3 cell layers for the two doses under investigation (0.5 and 1.0 µg)**

| Dose [µg] | $P_{app}$ ($x10^{-7}$ cm/s) |
|---|---|
| 0.5 | 1.35 ± 0.10 |
| 1.0 | 10.76 ± 1.34 |

These $P_{app}$ values are in agreement with what is reported in the literature. Haghi *et al.* (2012) for example report a $P_{app}$ of about $2x10^{-6}$ cm/sec after application of a solution 0.01 mM salbutamol sulfate (equivalent to ≈5 µg $mL^{-1}$, corresponding to our 1µg dose (Chapter 2, paragraph 2.2.3, page 37)).

The observed trend is partially in agreement with Fick's first law used to describe the transepithelial passive diffusion of drugs, where the concentration gradient represents one of the most important forces regulating the drug transport across cellular barriers. In particular, a steeper concentration gradient between the apical and the basolateral side results in a faster transport rate of the drug across the cell surface. However, neither the flux or the $P_{app}$ values are exactly proportional to the dose applied (i.e. they are not doubled when the dose is increased from 0.5 µg to 1.0 µg), and this could suggest the possible involvement of OCT transporters as well. OCT transporters are "assisted diffusion" transporters, so are more active as the concentration increases, until they become saturated (Koepsell 2004).

In the case of the dry powder, the transport profile showed an initial burst with 25% of drug transported in the first 5 minutes. It then followed a linear trend for the first 30 minutes to finally slowly plateau out at ≈80% transport within four hours.

### *4. Salbutamol sulfate absorption across Calu-3 layers after delivery as a dry powder for inhalation*

Although both the TEER and lucifer yellow permeability values demonstrated that the Calu-3 cell layers were intact at the end of the transport experiment (Table 4.2), the high percentage of drug transported in the first 5 minutes suggests a temporary disruption of the cell layer soon after the particle deposition. This was in contrast with the literature where no initial burst of drug transport has been reported, but different deposition systems have been used (Bur *et al.* 2009; Haghi *et al.* 2012).

Also in the case of the dry powder, the percentage of drug transported did not depend on the initial dose applied at all time points (multiple t-test, $p>0.05$). Nevertheless, after the 5 minutes' transport burst, two distinct regions can be distinguished for both doses that are characterised by different transport rates. In particular, between 5 and 30 minutes the flux were found to be statistically different for the two doses applied and equal to 0.53 ± 0.04 and 0.78 ± 0.08 % units/min for 2.0 and 1.0 mg loading respectively, whereas between 30 and 240 minutes there was no statistical difference between the flux and the pooled flux calculated was 0.14 % units/min. As the concentration of salbutamol sulfate on the cell surface was decreasing during the experiment, the flux calculated was also decreasing. Moreover, as opposed to what was found by Haghi *et al.* (2012), when a higher dose was sprayed onto the cell layers, the $t_{50}$ was also increased (doubled) from ≈25 minutes to ≈47 minutes.

The flux of salbutamol across the Calu-3 cell layers was increased as well as the percentage of drug transported when it was delivered as a dry powder (≈80% after 4 hours) compared to when it was applied as a solution (≈1% after 4 hours).

The $P_{app}$ values calculated for salbutamol sulfate applied as a dry powder for the different regions of the curves are reported in Table 4.4. The $P_{app}$ values were not significantly different between the two doses applied (t-test, $p>0.05$). but a significant difference was found between the $P_{app}$ calculated for the first two parts of the curve

(i.e. between 0 and 5 and between 5 and 30 minutes), but not between 5 to 30 minutes and 30 to 240 minutes (2-WAY ANOVA/Tukey's test, $p<0.05$), confirming the hypothesis of a temporary disruption of the cell layers soon after the particle deposition.

**Table 4.4: $P_{app}$ values calculated for salbutamol sulfate applied as a dry powder on Calu-3 cell layers for the two doses under investigation (0.5 and 1.0 µg, corresponding to 1.0 and 2.0 mg loading respectively) in the three different regions of the transport curves.**

| Time range | $P_{app}$* ($x10^{-6}$ cm/s) |
|---|---|
| Between 0 and 5 minutes | 11.69 ± 0.16 |
| Between 5 and 30 minutes° | 4.62 ± 0.28 |
| Between 30 and 240 minutes°° | 1.27 ± 0.13 |

***$P_{app}$ calculated assuming the volume of fluid coating the cell layer to be 12 µL (volume calculated for 1.12 $cm^2$ inserts from data published by Grainger *et al.* (2009) for 0.33 $cm^2$ insert)**
**°$C_0$ was calculated subtracting the amount of drug transported after 5 minutes from the total dose deposited.**
**°°$C_0$ was calculated subtracting the amount of drug transported after 30 minutes from the total dose deposited.**

Being these $P_{app}$ values in the same range as for salbutamol applied in solution, the difference in the flux observed between the two dosage forms can be attributed to the difference in concentration of the drug at the cell surface between the two experimental setups. In fact, in the case of the solutions experiments, 0.5 or 1.0 µg of salbutamol was dissolved in 200 µL of HBSS prior to being applied to the cell layers. On the other hand, in the case of the dry powder the same drug doses had to dissolve in the much lower volume of the mucus layer covering the cell layer. In this case the permeation process can be assumed to happen in two separate steps: dissolution of the dry powder particles in the mucus layer followed by absorption that was hypothesised to be transporter-mediated (Bur *et al.* 2010; Haghi *et al.* 2012).

The volume of the mucus layer covering the cells amounts to ≈12 µL in a 1.12 $cm^2$ insert (volume calculated for 1.12 $cm^2$ inserts from data published by Grainger *et al.* (2009) for 0.33 $cm^2$ insert), leading to a situation of local high drug concentration when

the dry powder particles dissolve. Haghi and colleagues (2012) assumed this high concentration to approach saturation (solubility of salbutamol sulfate in simulated lung fluid was reported to be 88.59 ± 7.52 mg $mL^{-1}$ (Haghi *et al.* 2012)). The doses of salbutamol sulfate they applied was 230 µg, corresponding to ≈19 mg $mL^{-1}$ in 12 µL, whereas in our case the doses were 0.5 and 1.0 µg, corresponding to ≈0.04 and 0.08 mg $mL^{-1}$ in 12 µL respectively, therefore far from the solubility limit.

As observed by Haghi *et al.* (2012), the percentage of salbutamol transported across the cell layer was independent from the initial dose applied in the case of the dry powder (multiple t-test, $p>0.05$), suggesting that the rate-limiting step is not the drug solubility. In addition, when a dry powder particle lands on the cell surface, it creates a local concentration gradient between the apical and the basolateral side confined to the spot where it deposited. Similar concentration gradients would occur on every spot where particles have landed. And this would not depend on the number of particles deposited (dose).

Our observation of the percentage of drug dry powder transported is overall comparable with what has been reported in the literature (Bur *et al.* 2009; Haghi *et al.* 2012; Haghi *et al.* 2014) where similar transport experiments of salbutamol sulfate were carried out employing more sophisticated devices such as the twin stage impinger and a modified version of the Anderson cascade impactor, that are approved by the BP for the prediction of inhalable particle regional deposition.

These results are very important in the context of this doctorate work as they demonstrate that our deposition system is able to provide reliable data about the drug permeability across Calu-3 cell layers *in-vitro*, despite being much simpler in comparison to the abovementioned devices.

### 4.3.2. Effect of dry powder deposition on salbutamol transport mechanism

As explained in paragraph 4.1.2 (page 104), there is still debate on whether $\beta_2$-agonists, in particular salbutamol sulfate, are absorbed through the lung epithelium by simple passive diffusion or if transmembrane transporters (particularly OCT-type) have a role in this mechanism. Despite a lot of effort into finding an answer to this question, no definitive proof of either active transport or passive diffusion has been provided yet.

The standard methods to investigate drug transport *in-vitro* in vectorial transport systems such as Transwell® inserts involve the measurement of the flux in two directions (apical-to-basolateral (A→B) and basolateral-to-apical (B→A)) across polarised cell lines, allowing for the differentiation between passive diffusion and transporter-mediated transport. (Giacomini *et al*. 2012; Lai 2013). In addition, the study has to be carried out under very well-controlled conditions, typically under sink conditions adopting the LLC model as recommended by the European Medicine Agency in their guidelines (European Medicines Agency 2012). It is clear that this experimental setup represents a limitation when studying the role of transporters in drug absorption through the lung epithelium. As explained in Chapter 3 (paragraph 3.1.1, page 45), the LLC conditions do not represent the real situation *in-vivo* where the epithelium is at the air-liquid interface. However, as highlighted by Haghi *et al*. (2012), this is the only way of exposing the cell layers to a fixed concentration of the inhibitor.

An alternative methodology is represented by the manipulation of the expression of transporters. For example, it is possible to inhibit the transporter expression by knocking-out the gene responsible for it by using chemically synthesised RNA interference molecules. Alternatively, it is possible to transfect the cell line of interest

in order to induce the expression of one or more recombinant transporters (Giacomini *et al.* 2012). However, differentiated Calu-3 cells revealed to be resistant to transfection, possibly because of the mucus secretions that constitutes a barrier (Florea *et al.* 2002), so this may not be the most appropriate method to prepare the cell layer to the investigation of the role of transporters in drug absorption.

Data previously obtained in our research group revealed an overexpression of OCT transporters (OCT1, OCT3, OCTN1, OCTN2) in Calu-3 cell layer as a consequence of 48-hours exposure to LPS from *E. Coli* (0:111B4, 127K4037; Sigma: #L4391) (Mukherjee 2012).

Based on this data we designed a transport experiment for salbutamol sulfate carried out at the air-liquid interface, aimed at the investigation of the role of OCT transporters, if involved, in salbutamol sulfate absorption after dry powder deposition.

We first collected preliminary data from the transport experiment of salbutamol sulfate applied in solution on the apical side of Calu-3 cell layers either exposed to LPS or not. In both cases, the drug transport was observed either in the presence or not of TEA on both sides. The data from these preliminary experiments in LLC conditions would give us basis to correctly interpret the results from the following investigation conducted in ALI conditions delivering salbutamol as a micronised dry powder.

The effect of TEA on the cell layers for the duration of the experiment was assessed using the PrestoBlue assay (4 hours). As showed in Figure 4.6 there is no significant difference in the cell viability throughout the time-span observed (ANOVA, $p>0.05$).

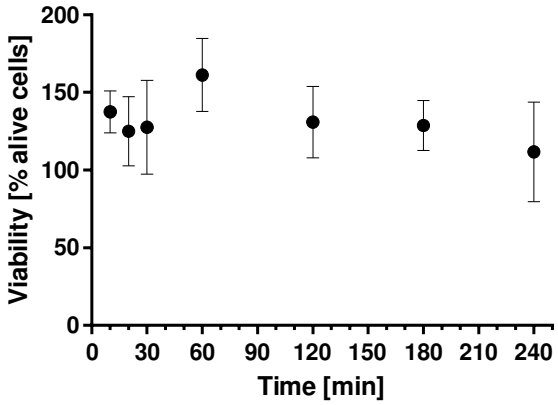


**Figure 4.6: effect of 5mM TEA on cell viability assessed by means of PrestoBlue® assay carried out on Calu-3 cells grown on 24-well plates (growth area: 0.95 $cm^2$).**

The TEER and lucifer yellow permeation values registered at the end of the transport experiments were within the acceptable ranges in all conditions as showed in Table 4.5:

**Table 4.5: TEER and lucifer yellow values registered at the end of the transport experiment after application of salbutamol sulfate in solution (5.0 µg $mL^{-1}$, corresponding to 1.0 µg dose) for all the conditions investigated: either after LPS insult or not, either in the presence of 5mM TEA or not. Data are presented as mean ± sem (N=2, n=between 4 and 6).**

| Condition | TEER [Ω·$cm^2$] | Lucifer yellow permeation [%] |
|---|---|---|
| NO LPS insult | 644 ± 144 | 0.37 ± 0.13 |
| NO LPS insult – TEA | 642 ± 168 | 0.57 ± 0.19 |
| LPS insult | 562 ± 162 | 0.81 ± 0.28 |
| LPS insult – TEA | 602 ± 51 | 0.68 ± 0.14 |

***4. Salbutamol sulfate absorption across Calu-3 layers after delivery as a dry powder for inhalation***

As showed in Figure 4.7, the A→B transepithelial transport of salbutamol sulfate across cell layers that had not been challenged with LPS was reduced in the presence of TEA. The same was observed with the calculated flux that was reduced from 1.43 ± 0.03 $x10^{-2}$ to 0.68 ± 0.08 $x10^{-2}$ % units/min in the presence of TEA. The difference between the percentage of drug transported was found to be significantly different from 1 hour onwards (t-test, $p<0.05$). TEA being a substrate of OCT transporters (Roth *et al.* 2012) and also acting as an inhibitor for all five OCT subtypes at the concentration used in this study (5mM) (Koepsell *et al.* 2007), this data suggests that one or more OCT subtypes are involved in salbutamol sulfate absorption. This is in agreement with some of the evidence reported in the literature of salbutamol being actively transported across the Calu-3 cell layers (Ehrhardt *et al.* 2005; Haghi *et al.* 2012; Mamlouk *et al.* 2013; Salomon *et al.* 2015). More specifically, Salomon *et al.* (2015) reported data suggesting that $\beta_2$-agonists act as substrates/inhibitors of OCT1 in human respiratory epithelial cells.

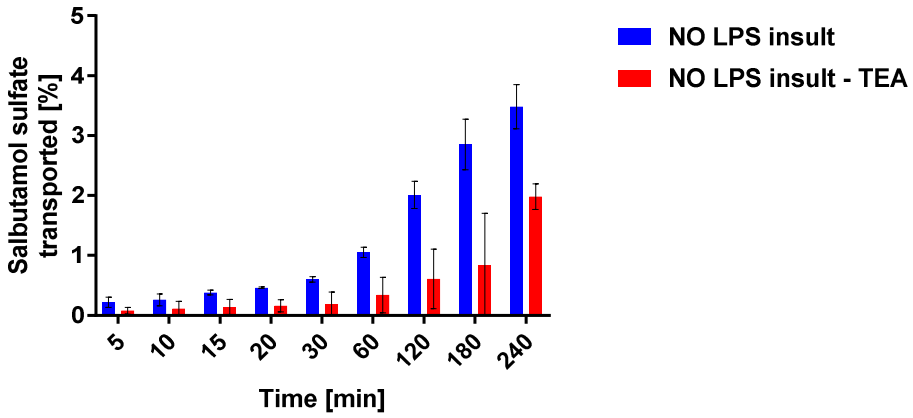


**Figure 4.7: apical to basolateral (A→B) transport profile across Calu-3 cell layers of salbutamol sulfate applied as a solution (5.0 µg $mL^{-1}$, corresponding to 1.0 µg dose) either in the presence or not of 5mM TEA (mean ± sem; N=2, n=6-4).**

This data agrees with what was found by other researchers in the field who hypothesised the interaction between salbutamol and OCT transporters.

To confirm this hypothesis, we looked at the effect of LPS insult on the transport of salbutamol sulfate comparing the percentage of drug transported between the cell layers not exposed to LPS (NO LPS insult) and those exposed to LPS (LPS insult). The results obtained are showed in Figure 4.8 and revealed that the permeation of salbutamol sulfate after LPS insult was significantly higher than in normal conditions after 60 minutes (t-test, $p<0.05$), and the flux was increased from $1.43 \pm 0.03 \times 10^{-2}$ to $3.37 \pm 0.29 \times 10^{-2}$ % units/min.

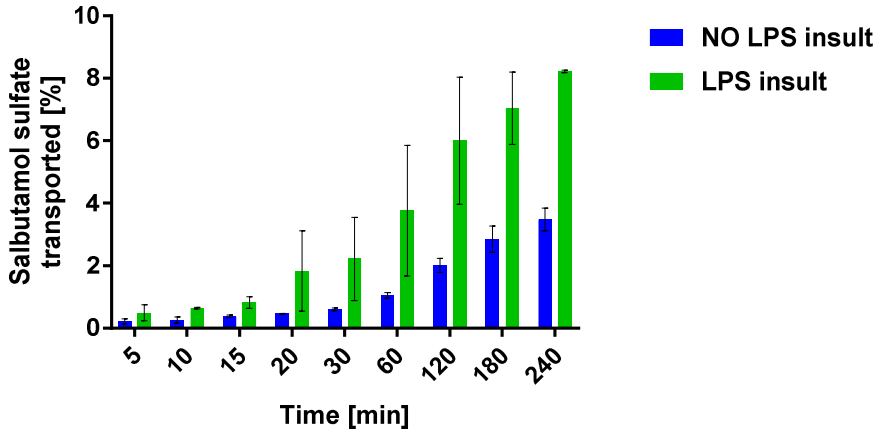


**Figure 4.8: apical to basolateral (A→B) transport profile across Calu-3 cell layers of salbutamol sulfate applied as a solution (5.0 µg mL$^{-1}$, corresponding to 1.0 µg dose) either after LPS insult or not (mean ± sem; N=2, n=5-6).**

This data confirmed that the exposure to LPS insult had an effect on the transport of salbutamol sulfate. As already explained, previous data obtained in our research group demonstrated that LPS insult induced an overexpression of OCT transporters (OCT1, OCT3, OCTN1, OCTN2) in Calu-3 cells. These results, in combination with the previous observation of a decreased salbutamol transport in the presence of TEA in un-challenged Calu-3 cell layers, would lead to conclude that the absorption of salbutamol could also be OCT transporter-mediated. However, there is also another possible scenario that could have occurred: LPS insult induced an inflammatory reaction too. In fact, LPS represents the pure chemical form of endotoxin and can be found in the outer leaflet of the outer membrane of Gram-negative bacteria, while the

inner leaflet is composed of phospholipids (Okuda *et al.* 2016). Mammalian monocytes and macrophages are responsible for the recognition of LPS during a Gram-negative infection. This normally leads to a cascade reaction with the release of inflammatory mediators (such as TNF-α, IL-6 and IL1β) that promote inflammation and prime the immune system to the elimination of the extraneous organism. However, if the body is in contact with LPS for a prolonged period of time, a systemic inflammatory reaction can occur that could lead to multiple organ failure and ultimately to the host's death (Erridge *et al.* 2002). LPS has been widely used as a model insult to investigate epithelial barrier dysfunction (Liu *et al.* 2015). For example, a loss in the E-cadherin and tight junction proteins (ZO-1 and occludin) localisation was reported after *E. Coli* LPS challenge in mouse lungs (Evans *et al.* 2002), possibly causing an enhanced permeability of the lung epithelium.

However, it must be noted that the TEER measurement and the lucifer yellow permeability of the cell layers included in the analysis were within the accepted threshold.

In order to better understand which scenario was more likely to have happened, or if a combination of the two was the real situation occurring, the transport of salbutamol after LPS insult was monitored in the presence of TEA.

The results obtained are showed in Figure 4.9. The A→B transport of salbutamol after exposure to LPS was significantly lower in the presence of TEA after 180 minutes and the flux was decreased from $3.37 \pm 0.29 \times 10^{-2}$ to $1.03 \pm 0.09 \times 10^{-2}$ % units/min, suggesting that TEA was interfering with the process, most likely by competing for the same binding site of OCT transporters.

*4. Salbutamol sulfate absorption across Calu-3 layers after delivery as a dry powder for inhalation*

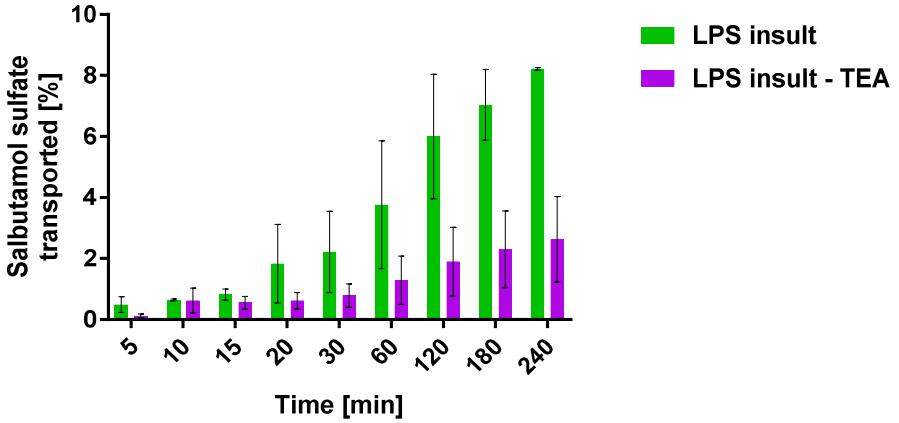


**Figure 4.9: apical to basolateral (A→B) transport profile across Calu-3 cell layers of salbutamol sulfate applied as a solution (5.0 µg mL$^{-1}$, corresponding to 1.0 µg dose) after LPS insult either in the presence of 5mM TEA or not (mean ± sem; N=2, n=6-5).**

This data suggested that the mechanism of absorption of salbutamol sulfate was prevalently mediated by OCT transporters, although it was not possible to establish which transporter of the family was involved in particular.

The information gathered with this set of experiments conducted in LLC conditions could help in the interpretation of the data obtained performing the transport experiment in ALI conditions.

***4. Salbutamol sulfate absorption across Calu-3 layers after delivery as a dry powder for inhalation***

The transport of salbutamol sulfate after dry powder deposition was monitored across Calu-3 cell layers either exposed to LPS insult or not. In this case, it was not possible to use any transporter inhibitor, as this would have had to be applied in the basolateral chamber only, but as mentioned in paragraph 4.1.2 (page 104) OCT transporters a located at the apical side of Calu-3 grown in ALI conditions.

The results obtained from this experiment are showed in Figure 4.10:

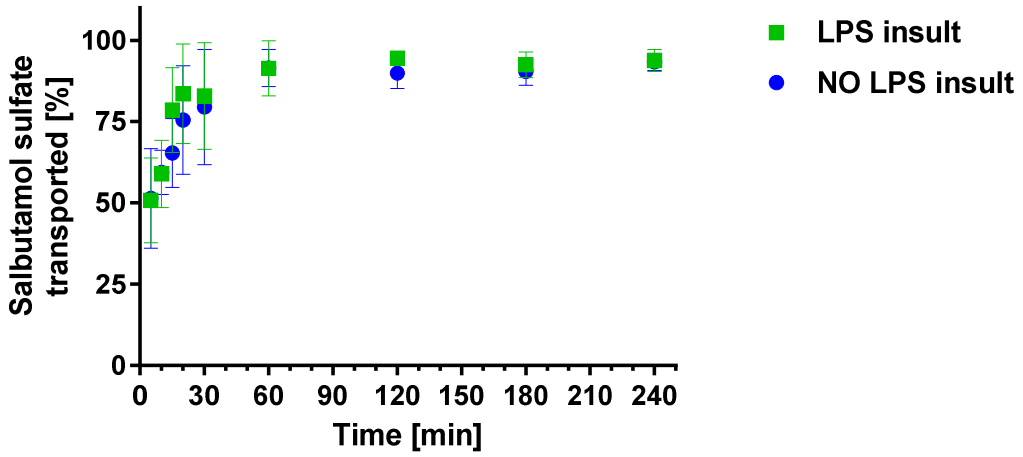


**Figure 4.10: apical to basolateral (A→B) transport profile across Calu-3 cell layers of salbutamol sulfate delivered as dry powder (2.0 mg loading of PennCentury™ Dry Powder Insufflator, corresponding to 1.0 µg dose (Chapter 3, paragraph 3.3.5, page 85)) either after LPS insult or not. Data are presented as mean ± SD (N=2, n=4).**

In this case, non-significant difference between the A→B transepithelial transport of salbutamol sulfate either after LPS insult or not was registered.

It must be noted that in this case the cell layers failed to pass both the TEER measurement and the LY permeability assay in both conditions. This meant that the cell layers were completely disrupted at the end of the experiment, although at the start of the experiment the TEER values were above 400 $\Omega \cdot cm^2$ for all cell layers. This suggested that it was only after the exposure to the spray that the cell layers were damaged.

It must also be observed that the permeation of salbutamol across the cell layers not insulted by LPS but kept in LLC for 48 hours reached ≈90% and was significantly

higher in comparison to the transport percentage observed across Calu-3 cell layers kept in ALI condition at all times (Figure 4.5). This was probably due to the complete removal of mucus that detached from the cell layers kept in LLC for the last 48 hours of the culture. As hypothesised by Fiegel *et al*. (2003) and Bur *et al*. (2010), the mucus layer produced by Calu-3 when cultured in ALI conditions provides a protection to the cell layers from the bombardment of particles released by the PennCentury™ Dry Powder Insufflator, cushioning their landing on the cell layer surface. The moment this protective barrier was removed; the cell layers were found more vulnerable to the impaction forces.

## 4.4. Conclusions

The first aim of the work presented in this chapter was to complete the validation of the system described in Chapter 3. The transepithelial transport characteristics of salbutamol sulfate sprayed as a micronised dry powder onto multiple Calu-3 cell layers grown at the air-liquid interface were comparable to those reported in the literature using systems approved by the BP, proving the system as a reliable tool for the investigation of the fate of particles at the air-epithelium interface in the lung.

The second aim was to gain a better understanding of the mechanism of absorption of salbutamol sulfate through the lung epithelium, especially when the drug was delivered as a dry powder. The data obtained when salbutamol was applied in solution suggested that OCT transporters are likely to be involved in salbutamol absorption. On the other hand, it was not possible to draw valid conclusions when salbutamol was delivered as a dry powder, due to the fact that the cell layers failed to pass both the TEER measurement and the LY permeability assay.

## 4.5. References

Bosquillon, C., 2010. Drug transporters in the lung - Do they play a role in the biopharmaceutics of inhaled drugs? *Journal of Pharmaceutical Sciences*, 99(5), pp.2240–2255.

Bur, M. *et al*., 2009. A novel cell compatible impingement system to study in vitro drug absorption from dry powder aerosol formulations. *European Journal of Pharmaceutics and Biopharmaceutics*, 72(2), pp.350–357.

Bur, M. *et al*., 2010. Drug transport across pulmonary epithelial cell monolayers: effect of particle size, apical liquid volume and deposition technique. *Journal of Aerosol Medicine and Pulmonary Drug Delivery*, 23(3), pp.119–127.

Cazzola, M. *et al*., 2012. Pharmacology and therapeutics of bronchodilators. *Pharmacological Reviews*, 64(3), pp.450–504.

Cazzola, M. *et al*., 2013. B2-Agonist therapy in lung disease. *American Journal of Respiratory and Critical Care Medicine*, 187(7), pp.690–696.

Ehrhardt, C. *et al*., 2005. Salbutamol is actively absorbed across human bronchial epithelial cell layers. *Pulmonary Pharmacology & Therapeutics*, 18(3), pp.165–170.

Endter, S. *et al*., 2009. RT-PCR analysis of ABC, SLC and SLCO drug transporters in human lung epithelial cell models. *Journal of Pharmacy and Pharmacology,* 61(5), pp. 583-591

Erridge, C., Bennett-Guerrero, E. & Poxton, I.R., 2002. Structure and function of lipopolysaccharide. *Microbes and Infections*, 4(8), pp.837–851.

European Medicines Agency, 2012. *Guideline on the investigation of drug interactions*,

Evans, S.M. *et al*., 2002. Decreased distribution of lung epithelial junction proteins

after intratracheal antigen or lipopolysaccharide challenge: Correlation with neutrophil influx and levels of BALF sE-cadherin. *American Journal of Respiratory Cell and Molecular Biology*, 27(4), pp.446–454.

Fiegel, J. *et al.*, 2003. Large porous particle impingement on lung epithelial cell monolayers - Toward improved particle characterization in the lung. *Pharmaceutical research*, 20(5), pp.788–796.

Florea, B.I. *et al.*, 2002. Transfection efficiency and toxicity of polyethylenimine in differentiated Calu-3 and nondifferentiated COS-1 cell cultures. *AAPS PharmSci*, 4(3), pp.1–11.

Giacomini, K.M. *et al.*, 2012. Membrane transporters in drug development. *Nature*, 9(3), pp.215–236.

Gnadt, M. *et al.*, 2012. Methacholine delays pulmonary absorption of inhaled β2-agonists due to competition for organic cation/carnitine transporters. *Pulmonary Pharmacology and Therapeutics*, 25(1), pp.124–134.

Grainger, C.I. *et al.*, 2009. The permeability of large molecular weight solutes following particle delivery to air-interfaced cells that model the respiratory mucosa. *European Journal of Pharmaceutics and Biopharmaceutics*, 71(2), pp.318–324.

Haghi, M. *et al.*, 2012. Deposition, diffusion and transport mechanism of dry powder microparticulate salbutamol, at the respiratory epithelia. *Molecular Pharmaceutics*, 9(6), pp.1717–1726.

Haghi, M., Traini, D. & Young, P., 2014. In vitro cell integrated impactor deposition methodology for the study of aerodynamically relevant size fractions from commercial pressurised metered dose inhalers. *Pharmaceutical Research*, 31(7), pp.1779–1787.

Horvath, G., Schmid, N., *et al*., 2007. Epithelial organic cation transporters ensure pH-dependent drug absorption in the airway. *American Journal of Respiratory Cell and Molecular Biology*, 36(1), pp.53–60.

Horvath, G., Mendes, E.S., *et al*., 2007. The effect of corticosteroids on the disposal of long-acting beta2-agonists by airway smooth muscle cells. *The Journal of Allergy and Clinical Immunology*, 120(5), pp.1103–1109.

Jack, D., 1991. THE 1990 LILLY PRIZE LECTURE. A way of looking at agonism and antagonism: lessons from salbutamol, salmeterol and other beta-adrenoceptor agonists. *British Journal of Clinical Pharmacology*, 31(5), pp.501–514.

Koepsell, H., 2004. Polyspecific organic cation transporters: Their functions and interactions with drugs. *Trends in Pharmacological Sciences*, 25(7), pp.375–381.

Koepsell, H., Lips, K. & Volk, C., 2007. Polyspecific organic cation transporters: Structure, function, physiological roles, and biopharmaceutical implications. *Pharmaceutical Research*, 24(7), pp.1227–1251.

Lai, Y., 2013. Transporter study methodologies. In *Transporters in Drug Discovery and Development*. Elsevier, pp. 675–718.

Liu, H. *et al*., 2015. Molecular mechanisms in lipopolysaccharide-induced pulmonary endothelial barrier dysfunction. *International Immunopharmacology*, 29(2), pp.937–946.

Mamlouk, M. *et al*., 2013. Salbutamol sulfate absorption across Calu-3 bronchial epithelia cell monolayer is inhibited in the presence of common anionic NSAIDs. *Journal of Asthma*, 50(4), pp.334–341.

Mathias, N.R. *et al*., 2002. Permeability characteristics of calu-3 human bronchial epithelial cells: in vitro-in vivo correlation to predict lung absorption in rats. *Journal of Drug Targeting*, 10(1), pp.31–40.

Meindl, C. *et al.*, 2015. Permeation of therapeutic drugs in different formulations across the airway epithelium in vitro. *PLoS ONE*, 10(8), pp.1–19.

Mukherjee, M., 2012. *An in-vitro analysis of the expression and function of bronchial Organic Cation Transporters,* PhD thesis submitted to The University of Nottingham.

Mukherjee, M., Pritchard, D.I. & Bosquillon, C., 2012. Evaluation of air-interfaced Calu-3 cell layers for investigation of inhaled drug interactions with organic cation transporters in vitro. *International Journal of Pharmaceutics*, 426(1–2), pp.7–14.

Nickel, S *et al.*, 2016. Transport mechanisms at the pulmonary mucosa: implications for drug delivery, *Expert Opinion on Drug Delivery*, 13(5), pp. 667-690

Okuda, S. *et al.*, 2016. Lipopolysaccharide transport and assembly at the outer membrane: the PEZ model. *Nature reviews. Microbiology*, 14(6), pp.337–345.

Roth, M., Obaidat, A. & Hagenbuch, B., 2012. OATPs, OATs and OCTs: The organic anion and cation transporters of the SLCO and SLC22A gene superfamilies. *British Journal of Pharmacology*, 165(5), pp.1260–1287.

Sakamoto, A *et al.*, 2013. Quantitative expression of human drug transporter proteins in lung tissues: analysis of regional, gender, and interindividual differences by liquid chromatography–tandem mass spectrometry. *Journal of Pharmaceutical Sciences*. 102(9), pp. 3395–3406.

Sakamoto, A *et al.*, 2015. Drug transporter protein quantification of immortalized human lung cell lines derived from tracheobronchial epithelial cells (Calu-3 and BEAS2-B), bronchiolar–alveolar cells (NCI-H292 and NCI-H441), and alveolar type II-like Cells (A549) by Liquid Chromatography–Tandem Mass Spectrometry. *Journal of Pharmaceutical Sciences*. 104(9), pp. 3029–3038.

Salomon, J.J. *et al*., 2014. The cell line NCl-H441 is a useful *in vitro* model for transport studies of human distal lung epithelial barrier. *Molecular Pharmaceutics*, 11(2), pp. 995-1006

Salomon, J.J. *et al*., 2015. Beta-2 adrenergic agonists are substrates and inhibitors of human organic cation transporter 1. *Molecular Pharmaceutics*, 12(8), pp.2633–2641.

Salomon, J.J. & Ehrhardt, C., 2012. Organic cation transporters in the blood–air barrier: expression and implications for pulmonary drug delivery. *Therapeutic Delivery*, 3(6), pp.735–747.

Sears, M.R. & Lotvall, J., 2005. Past, present and future: Beta2-adrenoceptor agonists in asthma management. *Respiratory Medicine*, 99(2), pp.152–170.

Unwalla, H.J. *et al*., 2012. Albuterol modulates its own transepithelial flux via changes in paracellular permeability. *American Journal of Respiratory Cell and Molecular Biology*, 46(4), pp.551–558.

# Chapter 5
# Pulmonary delivery of poorly soluble drugs. Case study: Indomethacin

## 5.1. Introduction

### 5.1.1. The Biopharmaceutical Classification System (BCS): relevance for pulmonary delivery

Solubility is an intrinsic property of a defined molecule. The International Union Of Pure and Applied Chemistry (IUPAC) defines solubility as "the proportion of the designated component in the designated mixture or solution (solvent)" (Gamsjäger *et al*. 2008).

APIs must be soluble in the various physiological fluids in order to achieve a pharmacological activity. Solubility in water is the main parameter used to predict the bioavailability and pharmacokinetics of an API (Stegemann *et al*. 2007). The British Pharmacopoeia (BP) uses seven expressions to define the solubility of a compound (Table 5.1), without specifying the solvent but only in terms of number of parts of solvent required to completely solubilise one part of compound (British Pharmacopoeia Commission 2016):

**Table 5.1: solubility ranges in the British Pharmacopoeia (British Pharmacopoeia Commission 2016)**

| Descriptive Term | Parts of solvent required for one part of solute |
|---|---|
| Very soluble | < 1 |
| Freely soluble | From 1 to 10 |
| Soluble | From 10 to 30 |
| Sparingly soluble | From 30 to 100 |
| Slightly soluble | From 100 to 1,000 |
| Very slightly soluble | From 1,000 to 10,000 |
| Practically insoluble | > 10,000 |

If solubility is extremely important to the definition of the bioavailability of a drug, permeability is another key characteristic.

Amidon and colleagues (1995) established the basis of the Biopharmaceutical Classification System (BCS) to classify drugs into four types according to their solubility in water and intestinal permeability.

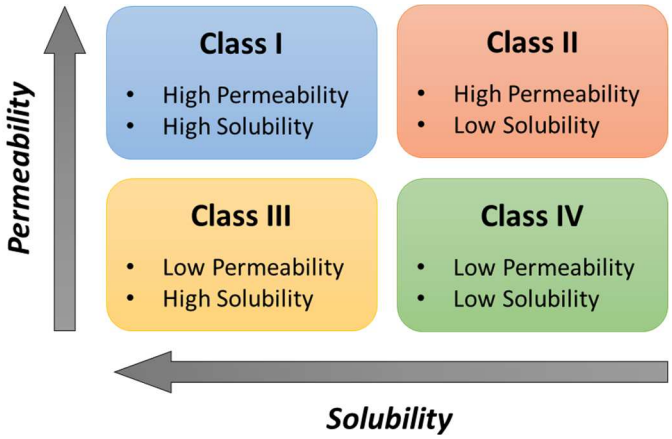


**Figure 5.1: classes of drugs in the Biopharmaceutical Classification Systems (BCS)**

The BCS represents a very useful guide to improve structure and physicochemical properties of lead candidates and predict the *in-vivo* pharmacokinetic of a drug during drug development. It has also been used by the Food and Drug Administration (FDA) in several guidelines (Eixarch *et al*. 2010).

In the BCS a drug is considered highly soluble when the highest-dose strength is soluble in 250 mL of aqueous media with a pH in the range 1-7.5. The volume of 250 mL is derived from the standard protocol of delivery with a glass of water in the fasted state (Savjani *et al.* 2012). These conditions are far from the situation in the lungs, where the volume of the lining fluid is 10-30 mL (Patton *et al.* 2010) and its thickness varies between 10-30 µm in the trachea and 2-5 µm in the bronchi (Kaialy & Nokhodchi 2015). In addition to this, the pulmonary route adds some other variables that strongly affect the entire absorption process. These are the inhalation device, the aerodynamic particle size distribution, the distribution of the dispersed product within the different regions of the lungs and the physicochemical properties of the drug (Hastedt *et al.* 2016). For these reasons, the need to establish a Pulmonary Biopharmaceutical Classification System (pBCS) was recognised and an attempt to define some basis for it was first done by Eixarch *et al.* (2010). In contrast to the BCS, it was recognised that in the pBCS the rate of solubility is a more representative measure of drug availability than solubility. In the case of local therapy, permeability or rate of absorption could be used to predict the residence time that can be correlated to the duration of effect before the drug is removed from its site of action. Slow dissolution/absorption are, in this case, more favourable properties as they would reflect a longer residence time. This is in opposition to the oral BCS model, and demonstrate how a more accurate and appropriate model would require the consideration of other factors, including the deposition site and its specific clearance mechanisms, the presentation of the drug to the targeted site or the therapeutic effect desired (local or systemic) (Hastedt *et al.* 2016)

## 5.1.2. Poorly soluble drugs: a challenge for pulmonary drug delivery

Poorly soluble APIs (e.g. corticosteroids, anti-infective agents, oligopeptides, chemotherapeutic agents) have become very common, representing about 40% of the marketed drugs and 70-90% of the new drug candidates (Tolman & Williams 2010; Chen *et al.* 2016). Independently from the administration route, it is essential that the drug dissolves in order to be absorbed, therefore drugs that are poorly soluble in water represent a challenge for the formulation scientist (Kaialy & Nokhodchi 2015).

This is particularly important for inhalation therapy with DPIs. In fact, as discussed in Chapter 1 (paragraph 1.5.2, page 16), after the inhaled particles have landed on the lung surface at the air-liquid interface, the absorption of poorly soluble drugs is dependent upon dissolution in the lung lining fluids. It is essential that the dissolution occurs more quickly than the major mechanisms of clearance, that are the mucociliary clearance in the upper airways and macrophage uptake in the bronchial region, otherwise the drug bioavailability can be significantly reduced (Forbes *et al.* 2015).

Focussing on the bronchial region, if the particles dissolve slowly, the mucociliary clearance will be the overriding mechanism and the particles will be swept away towards the throat, and eventually swallowed (Forbes *et al.* 2015). But if the particles persist for too long in the lungs they may cause inflammatory reactions (Chen *et al.* 2016).

It is then clear that the API solubility can influence its activity, side effects and dosing, thus representing a challenge and limitation for formulation development.

### 5.1.3. Possible strategies to improve solubility of drugs for pulmonary delivery

The strategies adopted for the formulation of poorly soluble drugs for pulmonary delivery are derived from those used to formulate drugs destined for other administration routes, such as oral or intravenous (Kaialy & Nokhodchi 2015) .

The most commonly used approach is size reduction, usually adopting top-down methods such as high-pressure homogenisation (HPH) or milling or bottom-up methods such as precipitation/crystallisation (Stegemann *et al.* 2007). Size reduction results in a significant increase of the surface area which in turn improves solubility, especially if the size is reduced to the nanometre scale (<1 μm). Nowadays, the DPI formulations are based on micronised API dry powders blended with larger carrier particles (typically lactose, 50-100 μm) (Kaialy & Nokhodchi 2015). As explained in Chapter 1 (paragraph 1.5.1, page 14), the limit size for successful pulmonary delivery is 1 μm, but it is possible to deliver nanoparticles as well, either in suspension using a nebuliser that produces droplets between 2 and 5 μm in size, or agglomerated into micro particles (nanoclusters) using appropriate surfactants or flocculating agents in the case of DPI formulations. DPI formulations based on nanoclusters are obtained by drying techniques that are usually lyophilisation (freeze drying) or spray drying.

Hydrophilic excipients such as mannitol or tocopherol polyethylene glycol 1000 succinate (TPGS) are often found to be key components of spray dried nanoparticle-based formulations for DPI. The role of these excipients is to create a hydrophilic microenvironment around the nanoparticles that improves solubility.

Another possible strategy to improve solubility of poorly aqueous soluble drugs is the use of solid dispersions (SDs) of the poorly soluble API (either crystalline or

amorphous) in highly hydrophilic carrier. Different classes of SD can be distinguished depending on how the drug is dispersed in the matrix, but the most common in the pharmaceutical field is the glass solution/suspension, where the amorphous drug could be molecularly dispersed or form a precipitate in the glassy carrier.

The use of higher energy states of APIs like the amorphous state enhances solubility as the energy required to break the interactions between molecules is lower than in the crystalline state. However, care must be used during manufacturing, transport and storage, as amorphous forms are usually less stable than the crystalline counterpart (Chen *et al*. 2016).

## 5.1.4. Indomethacin: therapeutic use and administration routes

Indomethacin is an example of poorly aqueous soluble drug. It is a non-steroidal anti-inflammatory drug (NSAID). From a chemical point of view, it is an indole-acetic acid derivative (Lucas 2016). Like all the NSAIDs, indomethacin has analgesic, antipyretic and anti-inflammatory properties, therefore it can be used for the treatment of numerous conditions, including swelling, fever and pain (Lucas 2016).

Indomethacin has a $pk_a$ = 4.5 (Budavari *et al*. 1989), therefore at the physiological pH (7.4) it is present mainly in its ionised form (Figure 5.2).

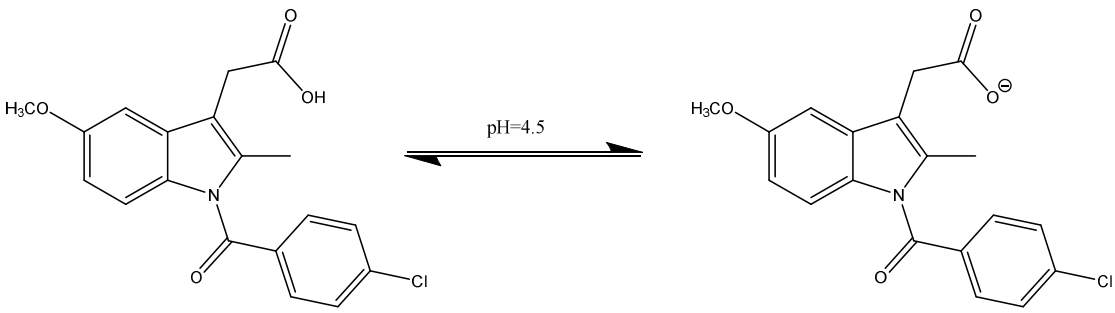


**Figure 5.2: Indomethacin chemical structure. The $pK_a$ is 4.5, therefore it shows its ionised form at pH > 4.5.**

### *5. Pulmonary delivery of poorly soluble drugs. Case study: Indomethacin*

Being a poorly aqueous soluble drug (Class II in the BCS) with acidic properties, it mainly crosses the cellular membrane in its non-ionised form that is more lipid soluble than its ionised counterpart. When the equilibrium is reached, there will be equal concentration of un-ionised form on either side of the cellular membrane, but if there is a pH gradient, the total concentration of un-ionised and ionised forms will be higher on the side with higher pH ("ion trapping" phenomenon). Ion trapping is more frequent in parietal cells due to the greatest pH gradient in the gastrointestinal (GI) tract caused by the secretion of hydrogen ions by these cells, and is the cause of side effects such as gastrointestinal lesions (e.g ulcers and erosions) but also hypersensitivity, hematologic reactions and problems to the renal function that are associated with indomethacin administration (Lucas 2016).

Alternative administration routes have been explored in order to avoid the pH-dependent side effects, and among those is inhalation (Ceschan *et al.* 2015; Onischuk *et al.* 2008). A number of studies have been carried out *in-vivo* proving that the intranasal delivery of indomethacin solution in bicarbonate results in an adequate absorption comparable to that achieved after oral administration. Also, it has been proven that intranasal delivery of indomethacin is as effective on conditions such as joint inflammation as oral delivery even at lower doses, thus providing an additional advantage to the oral delivery, however the dose delivered was low (Onischuk *et al.* 2008; Karasulu *et al.* 2008). In order to improve dose deposition in the deeper airways, novel dry powder formulations of indomethacin have been designed (Ceschan *et al.* 2015).

## 5.1.5. Aim

The first aim of the study presented in this chapter was to investigate the absorption profile of a model poorly water soluble drug (indomethacin) after delivery onto lung epithelial cell layers *in-vitro* either in solution or as a dry powder, and compare it with that of salbutamol sulfate in order to determine whether the system developed was able to discriminate between drugs with different physicochemical properties. In addition, we wanted to verify whether the BCS classification was representative of the behaviour of these two drugs *in-vitro*. In fact, salbutamol is a class III drug of the BCS, therefore characterised by high solubility in water but low permeability (Bur *et al.* 2010), whereas indomethacin is a class II drug in the BCS, therefore characterised by low solubility in water, but high permeability.

The second aim was to investigate the effect of particle properties on indomethacin absorption across the lung epithelium. In order to do so, we wanted to compare the absorption profile after deposition of indomethacin at the air-liquid interface either as micronised dry powder or as a spray dried formulation. The spray dried formulations used in this study were provided by colleagues from the School of Pharmacy, UCL (London), who designed and produced them aiming at improving indomethacin solubility once in contact with the lung epithelium.

## 5.2. Materials and methods

### 5.2.1. Materials

Four different micro-agglomerate formulations of indomethacin nanoparticles (generally referred to as "UCL formulations" or "UCL particles") were kindly provided by Maria Malamatari, a peer Centre for Doctoral Training (CDT) student at the School of Pharmacy of University College London (UCL) (Malamatari *et al.* 2015). The composition of these formulations is reported in Table 5.2:

**Table 5.2: composition of particles provided by UCL.**

| Formulation | Indomethacin content | Stabiliser | Matrix Formers |
|---|---|---|---|
| IND* - F68** | 90 % | F68 (10 %) | N/A |
| IND – TPGS° | 90 % | TPGS (10 %) | N/A |
| IND - F68+MF°° | 40 % | F68 (4 %) | Mannitol (50 %) L-Leucine (6 %) |
| IND - TPGS+MF | 40 % | TPGS (4 %) | Mannitol (50 %) L-Leucine (6 %) |

***IND: indomethacin**
****F68: Pluronic F68; °TPGS: D-α-Tocopherol polyethylene glycol 1000 succinate**
**°°MF: Matrix Formers (mannitol and L-leucine)**

The primary particle size distribution of the UCL formulations is reported in Table 5.3:

**Table 5.3: primary PSD of UCL formulations**

| Formulation | $DV_{10}$ [µm] | $DV_{50}$ [µm] | $DV_{90}$ [µm] |
|---|---|---|---|
| IND* - F68** | 1.17 | 3.83 | 5.82 |
| IND – TPGS° | 1.23 | 3.43 | 8.71 |
| IND - F68+MF°° | 0.83 | 2.50 | 4.68 |
| IND - TPGS+MF | 0.79 | 2.30 | 4.00 |

For the origin of all other materials used refer to Chapter 2 (paragraph 2.1, page 31).

## 5.2.2. Dose released by the PennCentury™ Dry Powder Insufflator

The determination of the doses released by the PennCentury™ Dry Powder Insufflator was carried out following the protocol reported in Chapter 3 (paragraph 3.2.2, page 59).

## 5.2.3. Particle shape and morphology

Particle shape and morphology of micronised indomethacin was determined with SEM as explained in Chapter 3 (paragraph 3.2.3, page 60).

## 5.2.4. Particle size distribution measurements

The particle size distribution of the spray as released by the PennCentury™ insufflator and of the particles landed on the inserts arranged according to the large hexagon geometry (Figure 3.17 (4), page 65) was determined following the protocols in Chapter 3 (paragraph 3.2.5, page 62).

## 5.2.5. Dose delivered study

The dose of indomethacin delivered to individual Transwell® inserts arranged according to the large hexagon geometry (Figure 3.17 (4), page 65) after deposition of either micronised indomethacin or individual UCL formulations was determined as explained in Chapter 3 (paragraph 3.2.6, page 64).

The dose of micronised indomethacin deposited was recovered washing the glass coverslips four times with 50 µL of acetonitrile (AcN, HPLC grade). After evaporation in the JOUAN centrifugal evaporator RCT90, samples were reconstituted in 1.0 mL of HPLC AcN and analysed by HPLC-UV.

### 5.2.5.1. HPLC-UV analysis

For the determination of the best wavelength to use during the HPLC-UV analysis, a 1 mg/mL solution of indomethacin in AcN was analysed by UV-Vis in scan mode from 800 nm to 200 nm using a DU®-800 Series UV-Vis spectrophotometer (Beckman Coulter Inc, UK). Two absorbance maxima at 265 nm and 318 nm were observed in the spectrum (Figure 5.3). The chosen wavelength for indomethacin detection during HPLC-UV analysis was 318 nm.

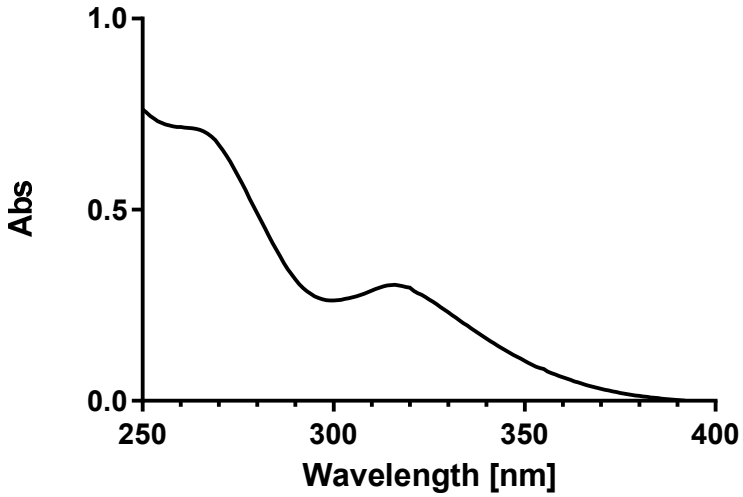


**Figure 5.3: UV-Vis spectrum of absorbance of indomethacin in AcN**

In the case of the UCL formulations, the dose delivered to each insert was recovered with $H_2O$:AcN (50:50), the samples were then evaporated down for one hour and finally reconstituted with 1.0 mL of $H_2O$:AcN (50:50).

HPLC-UV analysis was performed using an Agilent Hewlet Packard series 1100 fitted with a UV microcell for UV-Vis detection. An ACE3 C18 (3µm, 150 mm x i.d. 2.1 mm) column was used. The injection volume was 10 µL, flow rate was 0.2 mL $min^{-1}$ using 0.2 % v/v $H_3PO_4$ in $H_2O$ (pH=2.8) and AcN (20:80) as mobile phases.

The calibration curve used to quantify the amount of indomethacin from the samples produced spraying pure micronised indomethacin was drawn from standard solutions

of indomethacin in AcN at various concentrations ranging from 0.05 to 10 µg $mL^{-1}$ prepared in triplicate (y = 29.66 x, $R^2$= 0.9984, Figure 5.4).

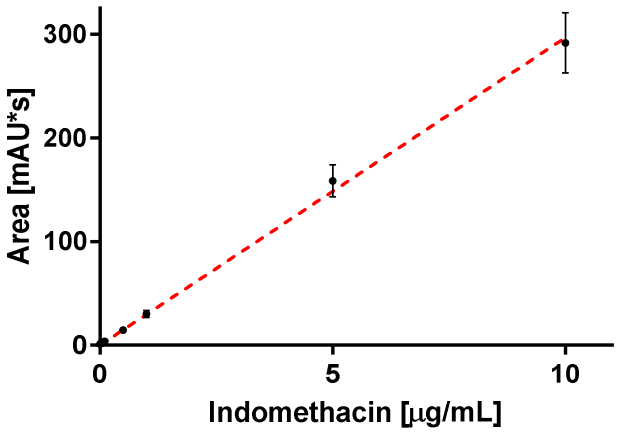


**Figure 5.4: calibration curve for indomethacin in AcN, Range: 0.005 – 10 µg $mL^{-1}$. Y = 29.66 x; $R^2$= 0.9984**

The calibration curve used to quantify the amount of indomethacin from the samples produced spraying UCL formulations was drawn from standard solutions of indomethacin in AcN:$H_2O$ (50:50) at various concentrations ranging from 0.05 to 10 µg $mL^{-1}$ prepared in triplicate (y = 27.43 x, $R^2$= 0.9998, Figure 5.5).

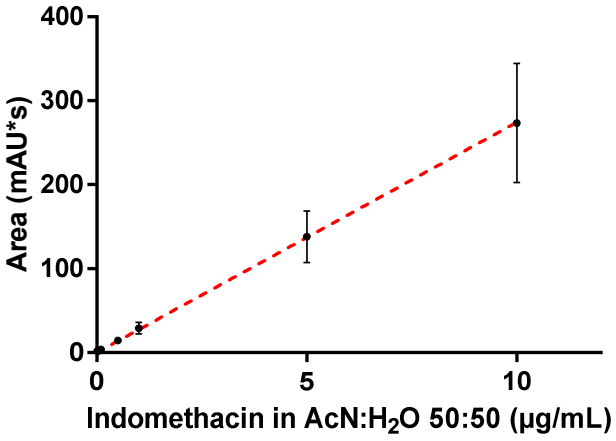


**Figure 5.5: calibration curve for indomethacin in AcN:$H_2O$. Range: 0.005 – 10 µg $mL^{-1}$. Y = 27.43 x; $R^2$= 0.9998**

### 5.2.6. Cytotoxicity of indomethacin and excipients of UCL formulations

For the Calu-3 cell culture protocols (maintenance and propagation of the cell line and 24-well culture plates seeding refer to Chapter 2 (paragraph 2.2.2, page 33).

The cytotoxicity of pure indomethacin, UCL formulations, individual excipients (F68, TPGS, mannitol and leucine) and $Na_2CO_3$ (used to solubilise indomethacin for the transport experiment in solution) was assessed by performing the PrestoBlue® cell viability assay as explained in Chapter 2 (paragraph 2.2.4, page 38).

The cytotoxicity of each compound was assessed for the duration of the transport experiment (240 minutes), at the concentrations reported in Table 5.4.

**Table 5.4: doses of micronised indomethacin, UCL formulations and individual excipients of UCL formulations, and concentrations of $Na_2CO_3$ tested for cytotoxicity by PrestoBlue® cell viability assay.**

| Formulation | Dose tested [µg] | Compound | Dose tested [µg] |
|---|---|---|---|
| Micronised indomethacin | 0.1 ; 2.0 ; 10.0 | TPGS | 0.01 ; 0.1 ; 1.0 |
| IND* - F68** | 0.1 ; 2.0 ; 10.0 | F68 | 0.01 ; 0.1 ; 1.0 |
| IND – TPGS° | 0.1 ; 2.0 ; 10.0 | Mannitol | 0.1 ; 1.0 ; 5.0 |
| IND - F68+MF°° | 0.1 ; 2.0 ; 10.0 | Leucine | 0.01 ; 0.1 ; 1.0 |
| IND - TPGS+MF | 0.1 ; 2.0 ; 10.0 | $Na_2CO_3$ [µM] | 0.05 ; 0.25 ; 1.0 ; 5.0 |

***IND: indomethacin**
****F68: Pluronic F68; °TPGS: D-α-Tocopherol polyethylene glycol 1000 succinate**
**°°MF: Matrix Formers, L-Leucine and mannitol**

### 5.2.7. A→B transepithelial transport experiment

For the Calu-3 cell culture protocols (maintenance and propagation of the cell line and 12-Transwell® plates seeding): refer to Chapter 2 (paragraph 2.2.2, page 33).

For a detailed protocol for the apical to basolateral (A→B) transepithelial transport of indomethacin or UCL formulations: refer to Chapter 2 (paragraph 2.2.3, page 37).

The apical to basolateral (A→B) transepithelial transport of indomethacin was monitored after application of the drug either in solution (0.5 and 1.0 µg doses in HBSS) or as micronised dry powder (1.0 and 2.0 mg loading of the PennCentury™ Dry Powder Insufflator, corresponding to 0.5 and 1.0 µg doses respectively).

The apical to basolateral (A→B) transepithelial transport of the four UCL formulations was monitored only after deposition of the dry powder on the apical surface of the Calu-3 cell layers grown at the air-liquid interface. The initial loading of UCL formulations in the PennCentury™ Dry Powder Insufflator was 2.0 mg, to achieve doses of indomethacin delivered to the individual Transwell® inserts comparable to those of pure micronised indomethacin.

After deposition of the drug either in solution (micronised indomethacin) or as dry powder (micronised indomethacin and UCL formulations), samples were withdrawn from the basolateral chamber at specific time points as explained in Chapter 2 (paragraph 2.2.3, page 37).

TEER measurements and the LY permeability assay were carried out at the end of the transepithelial transport experiment as explained in Chapter 2 (paragraph 2.2.2.7, page 35).

Samples were processed and analysed by LC-MS/MS according to protocol and conditions described in Chapter 2 (paragraph 2.2.5, page 41).

## 5.3. Results and discussion

### 5.3.1. Emitted dose consistency

A preliminary study on the performance of the PennCentury™ dry powder insufflator was carried out also in the case of micronised indomethacin and UCL formulations. In fact, as reported by Hoppentocht *et al.* (2014) the dose emitted by the PennCentury™ insufflator also depends on the powder properties. It is therefore necessary to evaluate the performance of the device every time a new powder/formulation is used.

Based on the information obtained during the system development discussed in Chapter 3 (paragraph 3.3.1, page 69) where it was found that loadings <2.0 mg allowed for more consistent doses emitted, the PennCentury™ device was loaded with varied amounts of powders ranging from 0.5 to 2.0 mg. The powder was aerosolised using 5.0 mL of ambient air. The emitted dose expressed as percentage of the initial loading was determined by difference between the weight before and after the first puff only. Results are showed in Table 5.5.

As it was found for salbutamol sulfate, loadings of the different indomethacin formulations < 2.0 mg allowed for a consistent amount of drug released from the PennCentury™ device after the first puff, with coefficient of variation (CV) < 30% in all cases but the IND – TPGS formulation at 1.0 mg loading for which the CV calculated was 38.7%. This could be due to the powder physicochemical characteristics, in particular its flowability. It must be noted that the variation in amount of powder released by the PennCentury™ Dry Powder Insufflator varied between micronised indomethacin, formulations with only stabilisers (TPGS or F68) and formulations containing also matrix formers (mannitol and L-leucine). In

particular, the formulations containing matrix formers were the most consistently expelled from the device with variations of dose released ≤15%. This is due to the presence of L-leucine in these formulations, that was demonstrated to reduce cohesiveness between the particles, thus preventing agglomeration and enhancing the dispersibility and aerosolisation properties of the powder. This behaviour has been attributed to the ability of L-leucine to modify the surface properties of the single particles, by migrating to the surface of the droplets during the spray-drying process (Seville *et al*. 2007; Chew *et al*. 2005; Boraey *et al*. 2013).

**Table 5.5: percentage of initial loading of micronised indomethacin and UCL formulations emitted after the first puff by the PennCentury ™ device loaded with amounts of powder ranging between 0.5 and 2.0 mg. Data are reported as MEAN ± SD (N=3).**

| Formulation | PennCentury™ loading [mg] | Emitted dose after first puff [%] | CV* [%] |
|---|---|---|---|
| Micronised Indomethacin | 2.0 | 79.5 ± 19.9 | 25.0 |
| | 1.0 | 61.6 ± 16.5 | 26.8 |
| | 0.5 | 49.5 ± 11.3 | 22.9 |
| IND - F68 | 2.0 | 61.4 ± 7.5 | 12.2 |
| | 1.0 | 73.8 ± 21.9 | 29.6 |
| | 0.5 | 80.8 ± 16.8 | 20.8 |
| INF - TPGS | 2.0 | 66.3 ± 7.3 | 11.1 |
| | 1.0 | 70.4 ± 27.3 | 38.7 |
| | 0.5 | 89.1 ± 18.8 | 21.1 |
| IND - F68+MF | 2.0 | 77.5 ± 8.9 | 11.5 |
| | 1.0 | 63.1 ± 9.6 | 15.2 |
| | 0.5 | 100.0 ± 0.0 | 0.0 |
| IND - TPGS+MF | 2.0 | 83.0 ± 11.6 | 14.0 |
| | 1.0 | 84.6 ± 2.1 | 2.5 |
| | 0.5 | 89.4 ± 11.6 | 13.0 |

***CV=coefficient of variation**

## 5.3.2. Particle shape and morphology

Micronised indomethacin dry powder particles released by the PennCentury™ device were visualised using SEM for shape and morphology analysis. Like micronised salbutamol sulfate particles, indomethacin particles look solid and of irregular shape with the presence of plate-like crystals (Figure 5.6).

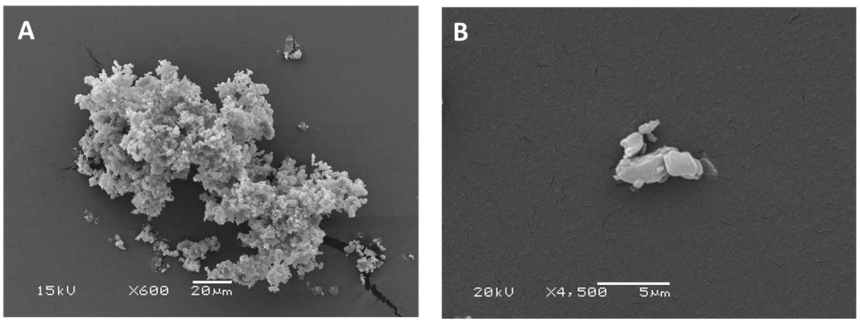


**Figure 5.6: SEM image of micronised indomethacin dry power particles after being sprayed from 20 cm without the needle. A) magnification X600, scale bar: 20 µm; B) magnification X4,500, scale bar: 5 µm**

## 5.3.3. Spray particle size distribution

### 5.3.3.1. Laser diffraction

The size distribution of the particles as they were released by the PennCentury™ Dry Powder Insufflator was investigated by light scattering for all the powders under investigation. The results are showed in Table 5.6 and are expressed as percentiles: $DV_{10}$, $DV_{50}$ and $DV_{90}$, which represent the volume weighted maximum particle size (expressed as diameter [µm]) for a given percentage volume of the sample, in this case 10%, 50% and 90% respectively.

**Table 5.6: particle size (expressed as $DV_{10}$, $DV_{50}$ and $DV_{90}$) of micronised indomethacin and UCL formulations sprays as produced by the PennCentury™ Dry Powder Insufflator. Data are expressed as MEAN ± SD (N=3)**

| Formulation | Loading [mg] | $DV_{10}$ [µm] | $DV_{50}$ [µm] | $DV_{90}$ [µm] |
|---|---|---|---|---|
| Micronised indomethacin | 0.5 | 3.16 ± 0.93 | 8.32 ± 0.49 | 25.19 ± 1.79 |
| | 1.0 | 4.04 ± 0.20 | 14.74 ± 0.20 | 58.24 ± 17.35 |
| | 2.0 | 8.73 ± 1.98 | 51.82 ± 19.19 | 138.42 ± 33.26 |
| IND* - F68** | 0.5 | 3.45 ± 1.17 | 6.45 ± 1.06 | 65.08 ± 78.39 |
| | 1.0 | 3.37 ± 0.43 | 7.32 ± 1.16 | 46.27 ± 6.02 |
| | 2.0 | 3.29 ± 0.71 | 11.12 ± 5.28 | 51.18 ± 18.70 |
| IND – TPGS° | 0.5 | 2.94 ± 0.34 | 6.89 ± 1.69 | 42.79 ± 16.75 |
| | 1.0 | 2.93 ± 0.42 | 7.57 ± 2.12 | 58.81 ± 34.94 |
| | 2.0 | 2.51 ± 0.16 | 7.90 ± 0.24 | 75.59 ± 21.55 |
| IND - F68+MF°° | 0.5 | 1.27 ± 0.12 | 4.26 ± 0.19 | 11.33 ± 0.43 |
| | 1.0 | 1.63 ± 0.32 | 5.13 ± 0.89 | 22.26 ± 15.24 |
| | 2.0 | 1.92 ± 0.46 | 5.92 ± 0.59 | 30.20 ± 21.52 |
| IND - TPGS+MF | 0.5 | 1.57 ± 0.37 | 4.69 ± 0.54 | 15.43 ± 4.22 |
| | 1.0 | 1.60 ± 0.01 | 5.48 ± 0.34 | 21.01 ± 1.46 |
| | 2.0 | 1.75 ± 0.34 | 6.61 ± 0.08 | 25.06 ± 6.12 |

***IND: indomethacin; **F68: Pluronic F68**
**°TPGS: D-α-Tocopherol polyethylene glycol 1000 succinate**
**°°MF: Matrix Formers, L-Leucine and mannitol**

The $DV_{50}$ measured for micronised indomethacin was spanning between 8.32 µm for 0.5 mg loading and 51.82 µm for 2.0 mg loadings, while the $DV_{90}$ was always > 20µm with maximum value of 138.42 µm for 2.0 mg loading. The PSD was dependent on the initial loading of the PennCentury™ device (2-WAY ANOVA/Tukey's test, $p<0.05$), indicating that the higher loading promoted the aggregation of the particles. These data are in agreement with the previous findings about salbutamol sulfate, where the same effect of loading was observed (Chapter 3, paragraph 3.3.4, page 76). However, it must be taken into account that these are results obtained with the spray produced with the first puff after loading, which, in the case of 1.0 and 2.0 mg loading,

was causing a very high obscuration of the laser of the Insitech instrumentation (>10%). This has probably led to an overestimation of the particle sizes due to multiple scattering. For this reason, a second measurement was performed on the residual material remaining in the device after the first puff. In this case, both $DV_{50}$ and $DV_{90}$ were found to be smaller. In particular, the $DV_{50}$ was 5.52 ± 0.28 µm and 5.84 ± 0.52 µm for 1.0 and 2.0 mg loading respectively, whereas the $DV_{90}$ was 13.63 ± 0.99 µm and 26.71 ± 7.24 µm for 1.0 and 2.0 mg loading respectively. Also in this case an effect of the initial loading on the particle size distribution could be observed.

The $DV_{50}$ of UCL particles was always <10 µm, except for 2.0 mg loading of IND – F68 (11.52 µm), while the $DV_{90}$ was spanning between 11.33 µm and 75.59 µm.

The UCL formulation resulted in significantly smaller diameter than micronised indomethacin (2-WAY ANOVS/Tukey's test, $p<0.05$). UCL particles were spray-dried, therefore they were spherical (Figure 5.7), whereas micronised indomethacin particles were irregular in shape (Figure 5.6).

One of the main advantages of producing particles for inhalation by spray drying is the better control over their size and shape. In particular, spray-drying allows to obtain more monodispersed powders in comparison to micronisation. In addition, the round shape characterising the spray-dried particles is responsible for the better dispersibility and flow properties of the resulting powder. In fact, the round shape significantly reduces the contact area between particles, preventing the formation of agglomerates and therefore resulting in higher respirable fraction in comparison to the micronised particles (Kaialy & Nokhodchi 2015).

Moreover, the formulations containing matrix formers (mannitol and L-leucine) showed PSD significantly smaller than their counterparts containing only surfactants

(2WAY-ANOVA/Tukey's test, $p<0.05$). This is due to the presence of L-leucine in these formulations, that was demonstrated to reduce cohesiveness between the particles, thus preventing agglomeration (Seville *et al*. 2007). These data agree with the *in-vitro* aerosol performance characterisation carried out using an NGI by the peer CDT student that provided us with the formulations. In fact, the fine particle fraction (FPS%) was found to reach up to 61.9% and the mass median aerodynamic diameter to be as low as 3.4 µm for the formulations with matrix formers (Malamatari *et al*. 2015).

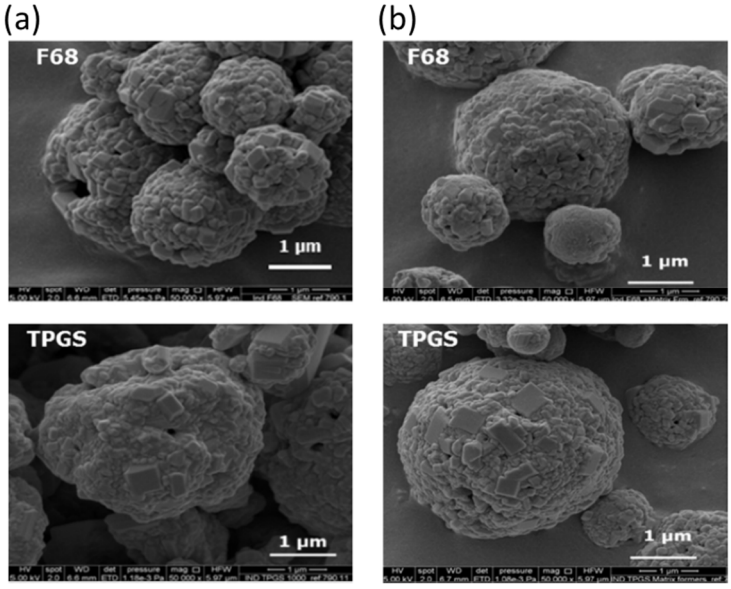


**Figure 5.7: SEM images of UCL formulations nanoparticle agglomerates (a) without and (b) with matrix formers. Figure reproduced from (Malamatari *et al.* 2015)**

### 5.3.3.2. Optical microscopy

The size of the particles reaching the Transwell® inserts arranged according to the large hexagon geometry (Figure 3.17 (4), page 65) after aerosolisation was also determined, as for salbutamol sulfate.

In order to do so, 1.0 mg of powder was sprayed twice onto glass coverslips placed in the Transwell® inserts.

In the case of micronised indomethacin (Table 5.7) the $DV_{90}$ was between 8.30 and 10.81 µm in all inserts, with the only exception for position B and D where a $DV_{90}$ was 12.64 and 13.10 µm respectively. Larger particles could be found as well, with the largest ones being in position O at the centre of the spray (Maximum particle diameter measured = 141.80 µm).

**Table 5.7: descriptive statistics of the particle size distributions of micronised indomethacin dry powder deposited onto seven Transwell® arranged according to the large hexagon geometry (Figure 3.16(4), page 63).**

| *Micronised Indomethacin* | | | | | | | |
|---|---|---|---|---|---|---|---|
| Position | A | B | C | D | E | F | O |
| **Min [µm]** | 0.40 | 0.40 | 0.40 | 0.40 | 0.40 | 0.40 | 0.40 |
| **Max [µm]** | 56.80 | 48.60 | 58.80 | 31.90 | 63.20 | 33.95 | 141.80 |
| **$DV_{10}$ [µm]** | 0.90 | 1.10 | 0.90 | 1.10 | 0.80 | 0.90 | 1.00 |
| **$DV_{50}$ [µm]** | 2.85 | 3.95 | 2.65 | 4.50 | 2.30 | 3.25 | 3.10 |
| **$DV_{90}$ [µm]** | 10.00 | 12.64 | 9.22 | 13.10 | 7.70 | 10.81 | 8.30 |
| **Mean [µm]** | 4.36 | 5.65 | 4.07 | 6.04 | 3.53 | 4.78 | 4.13 |
| **St. Dev [µm]** | 4.39 | 5.27 | 4.05 | 5.31 | 3.65 | 4.61 | 3.73 |

In the case of the UCL formulations, the $DV_{90}$ resulted < 10 µm in all inserts including the centre of the spray (O). However, larger aggregates could also be found with maximum diameter registered in the central position (O) for all formulations (Table 5.8, Table 5.10 and Table 5.11) but for IND – TPGS (Table 5.9). In this case the largest maximum diameter was found in position F (132.50µm), whereas position O was second to last (128.90 µm).

This data is in agreement with what was found in the case of micronised salbutamol sulfate, where the largest particles were detected at the centre of the spray, although no significant difference was found between the PSD in the different positions. This is

confirming our hypothesis that the largest particles, being heavier, are more likely to fall perpendicularly in the central area of the deposition surface in the desiccator chamber, whereas the smaller ones can float around for longer periods and eventually land in more peripheral regions of the desiccator chamber.

In addition, the fact that the $DV_{90}$ of all UCL particles was smaller than what was found in the case of micronised indomethacin, confirmed again the difference in behaviour of the two different kinds of powder, with different aerosolisation and re-dispersion properties.

**Table 5.8: descriptive statistics of the particle size distributions of IND – F68 UCL formulation dry powder deposited onto seven Transwell® arranged according to the large hexagon geometry (Figure 3.16(4), page 63).**

| *IND – F68* | | | | | | | |
|---|---|---|---|---|---|---|---|
| Position | A | B | C | D | E | F | O |
| **Min [µm]** | 0.40 | 0.40 | 0.40 | 0.40 | 0.40 | 0.40 | 0.40 |
| **Max [µm]** | 34.45 | 40.55 | 50.05 | 41.20 | 40.00 | 56.90 | 178.60 |
| **$DV_{10}$ [µm]** | 1.15 | 1.50 | 1.25 | 1.25 | 1.25 | 1.40 | 1.15 |
| **$DV_{50}$ [µm]** | 2.95 | 3.80 | 3.30 | 3.35 | 3.40 | 3.70 | 2.85 |
| **$DV_{90}$ [µm]** | 6.95 | 7.55 | 7.15 | 7.15 | 7.23 | 8.43 | 6.25 |
| **Mean [µm]** | 3.69 | 4.46 | 3.97 | 4.03 | 3.99 | 4.63 | 3.53 |
| **St. Dev [µm]** | 2.98 | 3.39 | 3.05 | 3.15 | 2.80 | 3.81 | 3.20 |

**Table 5.9: descriptive statistics of the particle size distributions of IND – TPGS UCL formulation dry powder deposited onto seven Transwell® arranged according to the large hexagon geometry (Figure 3.16(4), page 63).**

| *IND - TPGS* | | | | | | | |
|---|---|---|---|---|---|---|---|
| Position | A | B | C | D | E | F | O |
| **Min [µm]** | 0.40 | 0.40 | 0.40 | 0.40 | 0.40 | 0.40 | 0.40 |
| **Max [µm]** | 35.85 | 44.00 | 41.05 | 49.90 | 56.80 | 132.50 | 128.90 |
| **$DV_{10}$ [µm]** | 1.00 | 1.45 | 1.35 | 1.30 | 1.00 | 1.10 | 1.10 |
| **$DV_{50}$ [µm]** | 3.25 | 3.35 | 3.10 | 3.00 | 2.30 | 3.10 | 2.90 |
| **$DV_{90}$ [µm]** | 7.95 | 6.90 | 7.00 | 6.55 | 5.60 | 7.90 | 6.75 |
| **Mean [µm]** | 4.09 | 3.93 | 3.82 | 3.62 | 2.99 | 4.20 | 3.60 |
| **St. Dev [µm]** | 3.49 | 2.77 | 2.78 | 2.58 | 2.78 | 4.50 | 3.06 |

**Table 5.10: descriptive statistics of the particle size distributions of IND – F68 + MF UCL formulation dry powder deposited onto seven Transwell® arranged according to the large hexagon geometry (Figure 3.16(4), page 63).**

| *IND – F68 + MF* | | | | | | | |
|---|---|---|---|---|---|---|---|
| Position | A | B | C | D | E | F | O |
| **Min [µm]** | 0.40 | 0.40 | 0.40 | 0.40 | 0.40 | 0.40 | 0.40 |
| **Max [µm]** | 40.55 | 58.35 | 99.25 | 52.5 | 65.05 | 46.50 | 95.70 |
| **$DV_{10}$ [µm]** | 1.75 | 0.90 | 1.60 | 1.85 | 1.10 | 1.30 | 1.30 |
| **$DV_{50}$ [µm]** | 3.85 | 2.60 | 3.75 | 4.20 | 2.80 | 3.35 | 3.20 |
| **$DV_{90}$ [µm]** | 7.85 | 5.90 | 7.85 | 8.85 | 6.50 | 8.90 | 6.90 |
| **Mean [µm]** | 4.47 | 3.16 | 4.48 | 4.98 | 3.51 | 4.51 | 3.85 |
| **St. Dev [µm]** | 2.91 | 2.65 | 3.40 | 3.41 | 2.80 | 3.98 | 2.91 |

**Table 5.11: descriptive statistics of the particle size distributions of IND – TPGS + MF UCL formulation dry powder deposited onto seven Transwell® arranged according to the large hexagon geometry (Figure 3.16(4), page 63).**

| *IND – TPGS + MF* | | | | | | | |
|---|---|---|---|---|---|---|---|
| Position | A | B | C | D | E | F | O |
| **Min [µm]** | 0.40 | 0.40 | 0.40 | 0.40 | 0.40 | 0.40 | 0.40 |
| **Max [µm]** | 44.70 | 37.45 | 75.75 | 56.25 | 67.50 | 59.10 | 83.95 |
| **$DV_{10}$ [µm]** | 1.10 | 1.10 | 0.75 | 0.90 | 1.00 | 1.10 | 1.05 |
| **$DV_{50}$ [µm]** | 3.10 | 2.90 | 3.00 | 3.35 | 2.5 | 2.70 | 2.80 |
| **$DV_{90}$ [µm]** | 7.35 | 6.40 | 7.45 | 8.20 | 5.90 | 6.25 | 6.15 |
| **Mean [µm]** | 4.02 | 3.55 | 3.87 | 4.22 | 3.22 | 3.52 | 3.43 |
| **St. Dev [µm]** | 3.91 | 3.02 | 4.04 | 3.88 | 3.02 | 3.60 | 3.03 |

## 5.3.4. Dose control studies

The PennCentury™ device was loaded with 0.5, 1.0 and 2.0 mg of micronised indomethacin or individual UCL formulation, and 5.0 mL of ambient air was used to aerosolise the powders.

As explained in Chapter 3 (paragraph 3.3.5, page 85), out of all the geometries tested, the large hexagon was giving the best results in terms of reproducibility of dose of salbutamol sulfate delivered, therefore in this set of experiments the dose of indomethacin delivered was investigated for this geometry only.

The doses of indomethacin and UCL-formulations recovered from each insert are reported in Figure 5.8 and in Table I.3 (Appendix II, page 229).

As expected, by increasing the PennCentury™ device loading from 0.5 mg to 2.0 mg, the amount of drug received by each insert was also increased for all the powders under investigation.

Similarly, we expected the inserts positioned at the centre of the spray to receive higher doses of indomethacin compared to the others, and in fact the Transwell® insert in position O was the one receiving the highest dose for all the formulation and all the loadings tested. On the other hand, the Transwell® inserts at the same distance from the centre (O) were expected to receive similar amounts of drug.

In the case of indomethacin, we could deliver between 0.10 and 10.50 µg of drug to the Transwell® inserts depending on their positions and on the initial loading. Averaging between the positions distanced from the centre (A, B, C, D, E and F) we could deliver 0.93 ± 0.31 µg with 2.0 mg initial loading, 0.48 ± 0.12 µg for 1.0 mg initial loading and 0.17 ± 0.06 µg for 0.5 mg initial loading (Table 5.12). These doses were very similar to those found for salbutamol sulfate (Chapter 3, paragraph 3.3.5, page 85) which would be an advantage for a better interpretation of the data of the transepithelial transport studies *in-vitro*, especially when comparing between the two drugs. In fact, both powders being micronised, with similar particle shape and size and deliverable in similar doses, the differences observed in the transepithelial transport behaviour could be attributed solely to the drug characteristics. This could help in the better understanding of how drugs with different chemical properties are absorbed through the lung epithelium.

In the case of the UCL formulations, it was found that the doses of indomethacin that could be delivered were slightly lower than with pure micronised indomethacin (Figure 5.8). This was expected, especially for those formulations containing also matrix formers where the nominal drug content was 40%, whereas the ones with only the stabilisers had a nominal drug content of 90% (Table 5.2). However, as it is possible to notice from Table 5.12, averaging between the six positions away for the

centre (A, B, C, D, E and F), the doses collected after deposition of the spray did not perfectly reflect the proportion of the drug in the formulation if compared to the doses of pure micronised indomethacin leading to doses of deposited drug higher than that expected, especially in the case of the formulations containing matrix formers.

Once again, it is possible to explain this observation by taking into account the nature of the powder. As explained in paragraph 5.3.1 (page 146), the better aerosolisation properties of the spray dried particles, in comparison to the micronised ones, led to a more efficient release of the initial loading from the PennCentury™ insufflator, especially when L-Leucine was introduced in the formulation. The more efficient release of the dose from the PennCentury™ device resulted in higher doses of drug delivered to the Transwell® inserts.

The variability (CV) of the averaged doses delivered to the Transwell® inserts at the edges of the desiccator chamber was higher for all the formulations tested in comparison with that calculated for micronised salbutamol sulfate, spanning between a minimum of 14.65% to a maximum of 45.65%. However, only 2.0 mg loading (CV around 30%) was found to be useful for the following *in-vitro* experiments for all formulations, since this loading allowed for the delivery of doses of indomethacin ranging between 0.49 and 0.81 µg, comparable to the 0.48 µg of drug delivered with 1.0 mg loading of pure micronised powder.

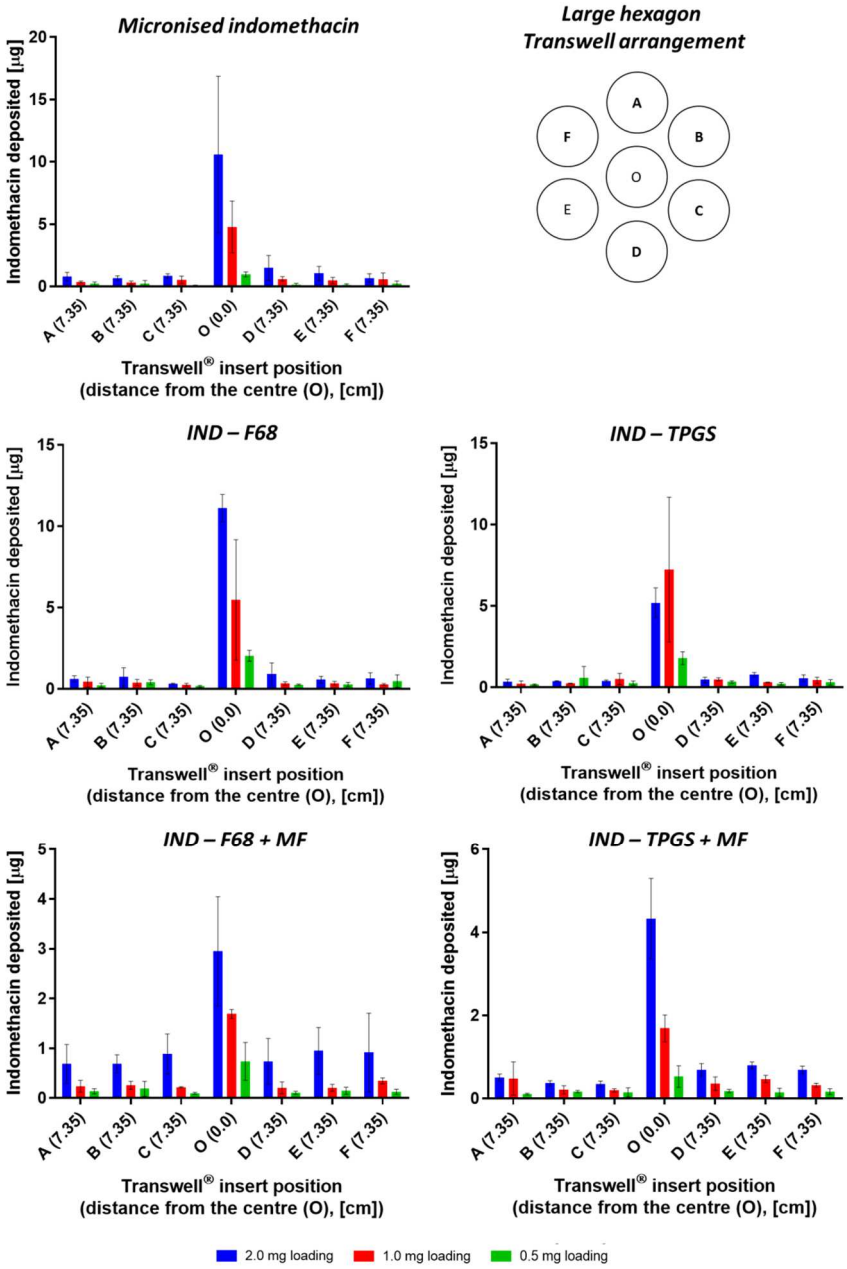


**Figure 5.8: doses of indomethacin deposited on Transwell® inserts arranged according to the large hexagon geometry from a distance of 20 cm from the surface. The PennCentury™ insufflator was loaded with 2.0, 1.0 and 0.5 mg of micronised indomethacin or individual UCL formulation.**

**Table 5.12: averaged doses of indomethacin between positions of the large hexagon geometry at the same distance from the centre of the spray after deposition of micronised indomethacin or individual UCL formulation spray.**

| Formulation | Position (distance from centre [cm]) | Loading [mg] | Indomethacin content [mg] | Dose averaged between positions [µg] | CV [%] |
|---|---|---|---|---|---|
| *Micronised Indomethacin* | A, B, C, D, E, F (7.35) | 0.5 | 0.5 | 0.17 ± 0.06 | 35.94 |
| | | 1.0 | 1.0 | 0.48 ± 0.12 | 25.11 |
| | | 2.0 | 2.0 | 0.93 ± 0.31 | 33.93 |
| *IND – F68* | A, B, C, D, E, F (7.35) | 0.5 | 0.4 | 0.32 ± 0.12 | 37.93 |
| | | 1.0 | 0.9 | 0.35 ± 0.06 | 18.25 |
| | | 2.0 | 1.8 | 0.64 ± 0.20 | 30.24 |
| *IND – TPGS* | A, B, C, D, E, F (7.35) | 0.5 | 0.4 | 0.32 ± 0.15 | 45.65 |
| | | 1.0 | 0.9 | 0.37 ± 0.13 | 34.45 |
| | | 2.0 | 1.8 | 0.49 ± 0.16 | 32.80 |
| *IND – F68 + MF* | A, B, C, D, E, F (7.35) | 0.5 | 0.2 | 0.14 ± 0.03 | 24.03 |
| | | 1.0 | 0.4 | 0.25 ± 0.05 | 21.15 |
| | | 2.0 | 0.8 | 0.81 ± 0.12 | 14.69 |
| *IND – TPGS + MF* | A, B, C, D, E, F (7.35) | 0.5 | 0.2 | 0.15 ± 0.03 | 16.56 |
| | | 1.0 | 0.4 | 0.34 ± 0.12 | 35.78 |
| | | 2.0 | 0.8 | 0.57 ± 0.19 | 32.63 |

As explained in Chapter 3 (paragraph 3.3.5, page 85), although the characterisation of the system was carried out assessing all the positions available in the desiccator chamber, including the central one (O), only the positions at the edges of the chamber were used in the following *in-vitro* studies. In particular, as in the case of salbutamol sulfate, four out of the seven possible positions were employed: B, C, E and F, so to have a symmetrical arrangement of inserts around the centre of the spray.

## 5.3.5. Transepithelial transport of indomethacin

The A→B transepithelial transport of indomethacin across Calu-3 cell layer grown in ALI conditions was monitored after application of the same doses of drug (0.5 and 1.0 µg) either in solution or as a dry powder.

In order to make the solutions of indomethacin in HBSS needed for the transepithelial transport experiment of the drug applied in solution, a 1.0 mg $mL^{-1}$ stock solution was prepared by dissolving indomethacin in 100 mM $Na_2CO_3$, and diluting it immediately in HBSS to the final concentration required (5.0 and 2.5 µg/mL).

In fact, it must be taken into account that indomethacin is a poorly aqueous soluble drug and it is described as practically insoluble in water in the BP (British Pharmacopoeia Commission 2016). It exists as different polymorphs (α, β and γ) characterised by different solubility in water that was found to range between 0.4 µg/mL and 410 µg/mL at 25°C depending on the form the drug was in (Comer *et al.* 2014). In addition, being an acidic drug with $pK_a$ = 4.5, its solubility is also affected by pH. In particular its solubility increases at higher pH, and it is easily solubilised in mild alkali such as sodium carbonate and bicarbonate (Shen & Winter 1977). However, if indomethacin solutions are stable at pH = 7.4, the drug undergoes degradation at pH > 12, and it was found that a solution of indomethacin in 0.1 M $Na_2CO_3$ lost 75% of its content within 80 minutes (Curry *et al.* 1982).

Before applying the indomethacin solutions to the Calu-3 cell layers, the cytotoxicity of indomethacin and $Na_2CO_3$ in the concentrations used during the transport experiments was assessed by performing the PrestoBlue® cell viability assay.

The results are showed in Figure 5.9 and Figure 5.10. Neither the presence of indomethacin or $Na_2CO_3$ affected Calu-3 cell viability in the whole concentration range tested for the period in which the transepithelial drug transport was monitored. It must be noted that the range of doses tested for indomethacin was between 0.1 and 10.0 µg so to include the doses used during the transport experiment (0.5 and 1.0 µg). The same principle was adopted for $Na_2CO_3$ for which the concentrations used in the transport experiments were 0.5 mM and 0.25 mM, therefore the concentration range tested was between 0.05 and 5.0 mM.

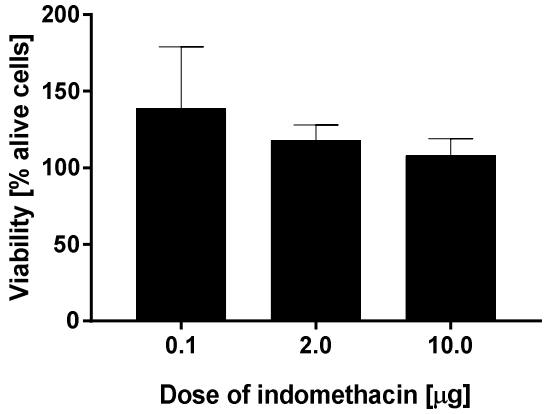


**Figure 5.9: Calu-3 cell viability assessed by PrestoBlue® cell viability assay after a 4 h exposure to indomethacin doses ranging between 0.1 and 10.0 µg in solution. Data are presented as mean ± SD (N=1, n=4).**

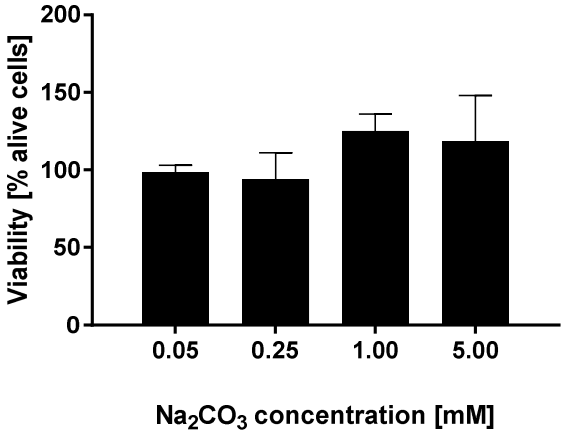


**Figure 5.10: Calu-3 cell viability assessed by PrestoBlue® cell viability assay after a 4 h exposure to solutions of $Na_2CO_3$ ranging between 5.00 and 0.05 mM. Data are presented as mean ± SD (N=1, n=4).**

The TEER and lucifer yellow permeation values registered at the end of the transport experiments were within the acceptable ranges as showed in Table 5.13:

**Table 5.13: TEER and lucifer yellow values registered at the end of the transport experiment after application of indomethacin either in solution or as a dry powder. Data are presented as mean ± sem (N=2, n=between 8 and 12).**

| Dosage form | Dose [µg] | TEER [Ω·cm$^2$] | Lucifer yellow permeation [%] |
|---|---|---|---|
| Solution | 0.5 | 1337 ± 229 | 0.20 ± 0.15 |
| | 1.0 | 1201 ± 382 | 0.11 ± 0.06 |
| Dry powder | 0.5 (1.0 mg loading) | 790 ± 132 | 1.01 ± 0.41 |
| | 1.0 (2.0 mg loading) | 937 ± 182 | 0.83 ± 0.39 |

The A→B transepithelial transport profile of indomethacin applied in solution or delivered as dry powder across the Calu-3 cell layers is shown in Figure 5.11 and Figure 5.12 respectively.

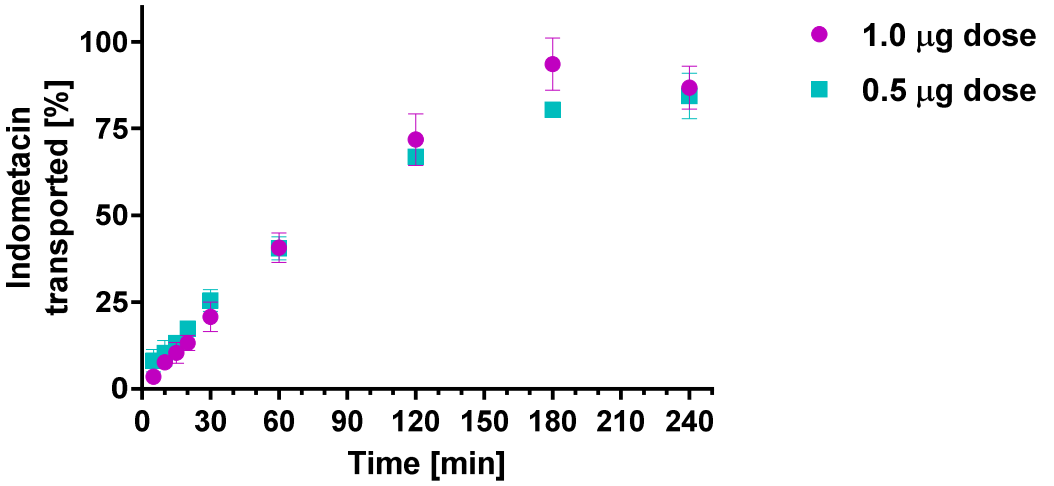


**Figure 5.11: apical to basolateral (A→B) transport profile of indomethacin applied in solution (200 µL of 5.0 and 2.5 µg mL$^{-1}$, corresponding to 1.0 and 0.5 µg doses respectively). Data are presented as mean ± SEM (N=2, n=4).**

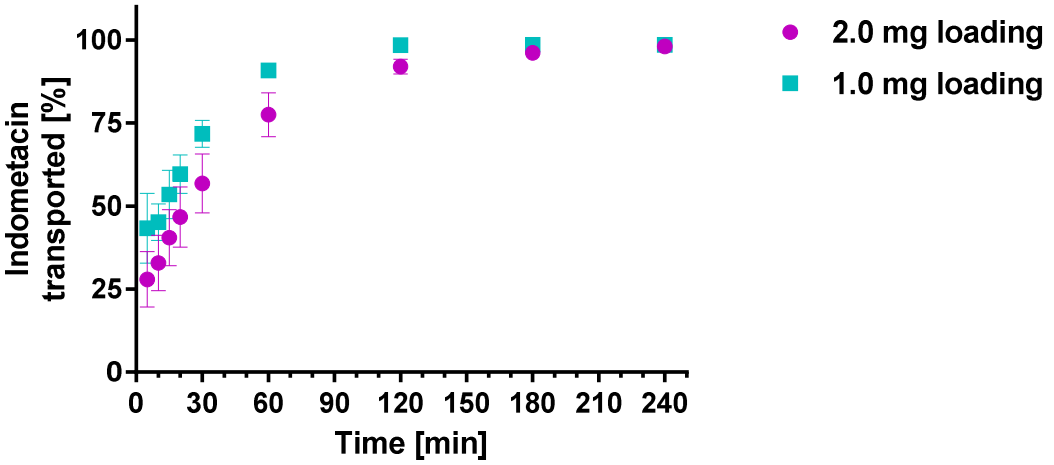


**Figure 5.12: apical to basolateral (A→B) transport profile of indomethacin delivered as a dry powder (2.0 and 1.0 mg PennCentury™ insufflator loading, corresponding to 1.0 and 0.5 µg doses respectively (see paragraph 5.3.4, page 155). Data are presented as mean ± SEM (N=3, n=3-4).**

The percentage of indomethacin transported in solution was not dependent on the initial dose applied for all time-points (multiple t-test, $p>0.05$). The profile followed a linear trend for the first 120 minutes and finally plateaued out reaching about 85%

transport in 240 minutes. The $P_{app}$ calculated in the linear range (up to 120 minutes) was 2.47 ± 0.50 x$10^{-5}$ cm/s and 1.96 ± 0.30 x$10^{-5}$ cm/s for the 1.0 and 0.5 µg dose respectively, indicating as in the case of salbutamol that indomethacin was quicker at crossing the cell layer when the donor solution was more concentrated. However, in this case the flux were found to be statistically not different between the two doses applied and the pooled flux calculated was 0.57 % units/min.

Also in the case of the dry powder the percentage of drug transported was not dependent on the initial dose applied for all time-points (multiple t-test, $p>0.05$). The general trend was similar to that observed for the solution, with an initial burst in the first 5 minutes, followed by a linear increase of the drug transport across the cell layer for the first 60 minutes and a final plateau between 60 and 240 minutes. As in the case of salbutamol (Chapter 4), the high percentage of drug transported in the first 5 minutes suggests a temporary disruption of the cell layer soon after the particle deposition despite the TEER and lucifer yellow permeability values demonstrated that the cell layers were intact at the end of the transport experiment (Table 5.13).

The percentage transported after 240 minutes was higher compared to the solution reaching ≈98%. As observed for salbutamol, also in this case after the 5 minutes' burst two distinct regions can be distinguished for both doses that are characterised by different flux. In particular, between 5 and 60 minutes the flux was not significantly different between the two doses ($p>0.05$) and the pooled flux calculated was 0.89 % unit/min, while between 60 and 240 minutes the flux was found to be significantly different and was found to be 0.05 ± 0.01 and 8.3 ± 0.2 x $10^{-5}$ % unit/min for 2.0 and 1.0 mg loading respectively. Also in this case, as observed with salbutamol, as the drug concentration at the cell layer surface was decreasing, also the flux decreased.

The flux of indomethacin was quicker for the dry powder than for the solution. For the solution the time needed for 50% of the initial dose to cross the cell layer ($t_{50}$) was ≈80 minutes, against a $t_{50}$ < 25 minutes for the dry powder. A similar behaviour was observed for salbutamol sulfate and, as explained in that case, was due to the higher concentration of drug at the cell layer surface when the drug was deposited as a dry powder in comparison to when it was applied already solubilised (Chapter 4, paragraph 4.3.1, page 112).

The $P_{app}$ values calculated for indomethacin applied as a dry powder for the different regions of the curves are reported in Table 5.14. As in the case of salbutamol sulfate, the $P_{app}$ values were not significantly different between the two doses applied (t-test, p>0.05). but a significant difference was found between the $P_{app}$ calculated for the first two parts of the curve (i.e. between 0 and 5 and between 5 and 60 minutes), but not between 5 to 60 minutes and 60 to 240 minutes (2-WAY ANOVA/Tukey's test, p<0.05), confirming the hypothesis of a temporary disruption of the cell layers soon after the particle deposition also in this case.

**Table 5.14: $P_{app}$ values calculated for indomethacin applied as a dry powder on Calu-3 cell layers for the two doses under investigation (0.5 and 1.0 µg, corresponding to 1.0 and 2.0 mg loading respectively) in the three different regions of the transport curves.**

| Time range | $P_{app}$* ($x10^{-6}$ cm/s) |
|---|---|
| Between 0 and 5 minutes | 13.56 ± 2.69 |
| Between 5 and 60 minutes° | 4.70 ± 1.75 |
| Between 60 and 240 minutes°° | 5.98 ± 4.08 |

***$P_{app}$ calculated assuming the volume of fluid coating the cell layer to be 12 µL (volume calculated for 1.12 $cm^2$ inserts from data published by Grainger *et al.* (2009) for 0.33 $cm^2$ insert)**
**°$C_0$ was calculated subtracting the amount of drug transported after 5 minutes from the total dose deposited.**
**°°$C_0$ was calculated subtracting the amount of drug transported after 60 minutes from the total dose deposited.**

Although both the percentage of drug transported and the flux between 5 and 60 minutes were not dependent on the initial dose, it was found that when a higher dose was sprayed onto the cell layers, the $t_{50}$ was also increased (doubled) from ≈12 minutes to ≈24 minutes for 1.0 and 2.0 mg initial loading respectively. A similar trend has been described also in a Copley report for budesonide during the development of a dissolution test for drugs for pulmonary delivery where the dose was reported to have an impact on the dissolution profile of budesonide (poorly aqueous soluble drug, BCS class II) in simulated lung fluids, in particular higher doses corresponded to slower dissolution (Copley & Son 2010).

This could be due to the lipophilicity of the drug, indomethacin in our case (logP = 4.27 (Neuhoff *et al*. 2005)). Before absorption the drug particle must dissolve, and in the case of poorly soluble drugs dissolution could be a limiting step of the absorption process, thus causing poor bioavailability. When a higher dose is deposited on the cell layer surface, one of the consequences could be a longer time required for the dissolution of the particles in the lining fluids. A higher dose corresponded to a larger number of particles deposited, and therefore to a higher density of particles on the cell layer surface (number of particles per $cm^2$). It could be envisaged that dissolving particles that are closer to each other would cause a faster increase of the local drug concentration to the saturation point, that in turn could lead to slower dissolution. In addition, where multiple polymorphs of the drug exist, the local saturation in the liquid film could promote the conversion between a less stable form (e. g. amorphous state) to an energetically more stable form (e.g. crystalline) characterised by lower solubility (Olsson *et al*. 2011) although this is less likely to have occurred in our case since indomethacin used in our studies was in its crystalline form.

Nevertheless, despite being poorly water soluble, indomethacin completely crossed the cell layer, reaching ≈98% transport in four hours for both the doses tested. This data suggested that solubility was not a rate-limiting step in the absorption process.

As explained already, being an acidic drug the solubility of indomethacin is also strongly influenced by the pH. The Merck Index reports a $pK_a$ of 4.5 (Budavari *et al.* 1989), which means that at the physiological pH (7.4) only a portion of the drug would be in its un-ionised form. The pH of the airway surface liquid is considered more acidic and it is reported to be ≈6.6 in healthy lungs, although clinical conditions can cause this value to be shifted towards more acidic (e. g. pneumonia) or more alkaline pH (e.g. chronic bronchitis) (Fischer & Widdicombe 2006). It is possible that the acidic nature of indomethacin could also play an important role in the dissolution of the drug particles, thus favouring the absorption process of the drug across the lung epithelium. In addition, according to its BCS classification into Class II, indomethacin is also highly permeable and is in fact absorbed very quickly across the cell layers (Patton *et al*. 2004), (to be noted that the BCS is based on the GI tract, therefore the absorption profile is intended across the intestinal epithelium). The high permeability due to its lipophilic nature most likely overcome the low solubility. The data obtained in this study suggested that the high permeability may be promoting the dissolution of indomethacin particles by reducing the concentration of the drug in the surrounding fluid. Similar results were obtained by Bur and colleagues (2010) who looked at the transport of budesonide (BCS class II drug) across Calu-3 cell layers.

Confronting the transepithelial transport behaviour of indomethacin and salbutamol sulfate micronised dry powders (Figure 5.13), indomethacin appeared more permeable than salbutamol sulfate.

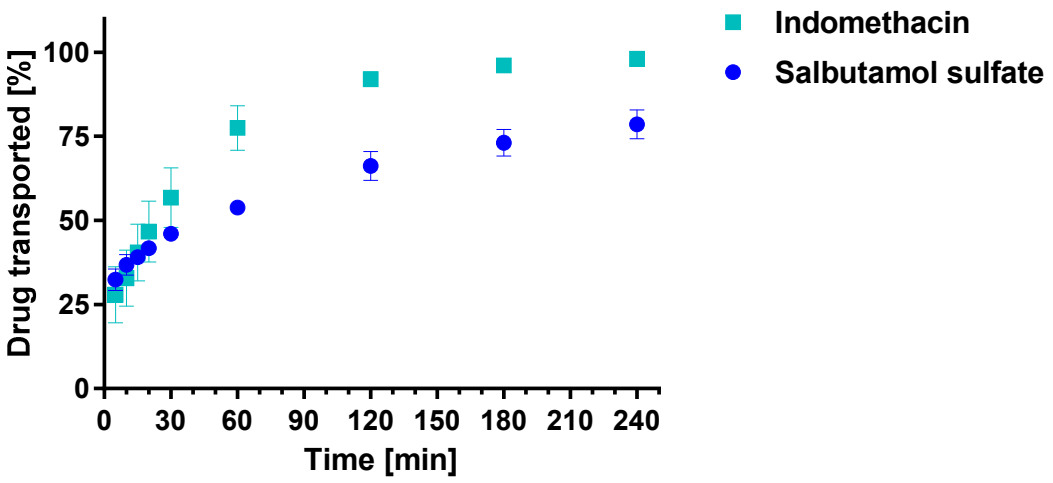


**Figure 5.13: comparison between the A→B transepithelial transport profiles of indomethacin and salbutamol both delivered to Calu-3 cell layers as micronised dry powders (2.0 mg loading of the PennCentury™ Dry Powder Insufflator)**

This is in agreement with the prediction based on the BCS classification as salbutamol sulfate is a Class III drug characterised by high solubility and low permeability (Bur *et al.* 2010).

Being a lipophilic drug, indomethacin could preferentially partition into the phospholipidic bilayer of the cellular membrane. Given that the surface area provided by the cellular membrane is much larger than the surface area available for passive diffusion across the paracellular pathways, this contributes more to the absorption of the drug across the cell layer accounting for the faster absorption of hydrophobic drugs in comparison to hydrophilic drugs (Mathias *et al.* 2002).

In addition to this, it must be considered that the fluid where the particles dissolve is not water, but in the case of the Calu-3 cell layers grown at the air-liquid interface is mucus-like secretions that represent the mucus lining layer in the bronchial region.

Mucus is a gel-like material of varied composition, mainly constituted of water (>90%) but also containing proteins (mucins), lipids and salts (Khanvilkar *et al.* 2001). It can be envisaged that these other components (proteins and lipids in particular) could play a role in the dissolution of indomethacin particles, favouring the wetting of the particles thus increasing the dissolution rate (Olsson *et al.* 2011).

### 5.3.6. Transepithelial transport of indomethacin formulated in UCL particles

The A→B transepithelial transport of indomethacin across Calu-3 cell layer grown in ALI conditions was monitored after deposition of the UCL dry powder formulations. In order to be able to make comparisons between the transport profiles of micronised pure indomethacin and the UCL formulations, 2.0 mg initial loading was selected for the UCL formulations. This would have delivered an equivalent dose of ≈0.5 µg of indomethacin (Table 5.12).

Before applying the UCL particles to the Calu-3 cell layers, the cytotoxicity of the formulations as such as well as of the individual excipients, in the concentrations used during the transport experiments was assessed by performing the PrestoBlue® cell viability assay. The results are showed in Figure 5.14 and Figure 5.15 respectively. The doses ranges tested were chosen to include the doses applied during the transepithelial transport experiment.

None of the UCL formulations and none of the excipients with the exception of L-leucine at a dose of 0.1 µg affected the Calu-3 cells viability over the whole concentration ranges tested and the length of the transepithelial drug transport (Figure 5.14 and Figure 5.15). L-leucine effect on cell viability was however deemed non-significant in the light of the non-cytotoxicity of UCL formulations containing it.

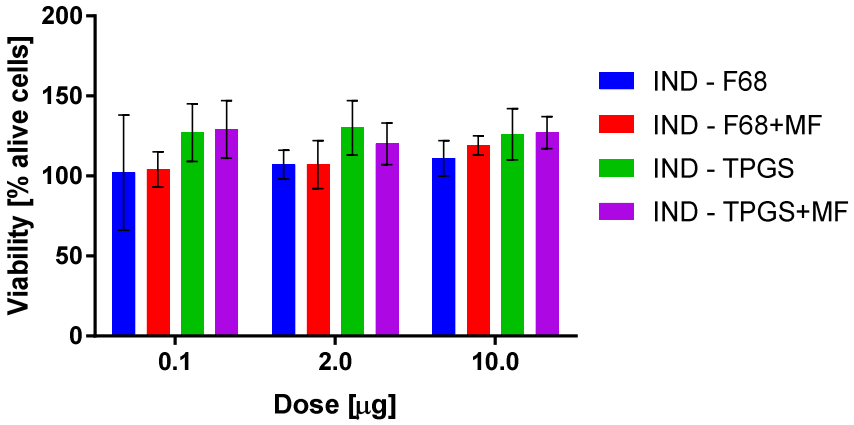


**Figure 5.14: Calu-3 cell viability assessed by PrestoBlue® cell viability assay after exposure of four hours to the UCL formulations (IND – F68, IND – TPGS, IND – F68 + MF and IND – TPGS + MF) in doses ranging between 0.1 and 10.00 µg (in 200 µL of HBSS). Data are presented as MEAN ± SD (N=1, n=4).**

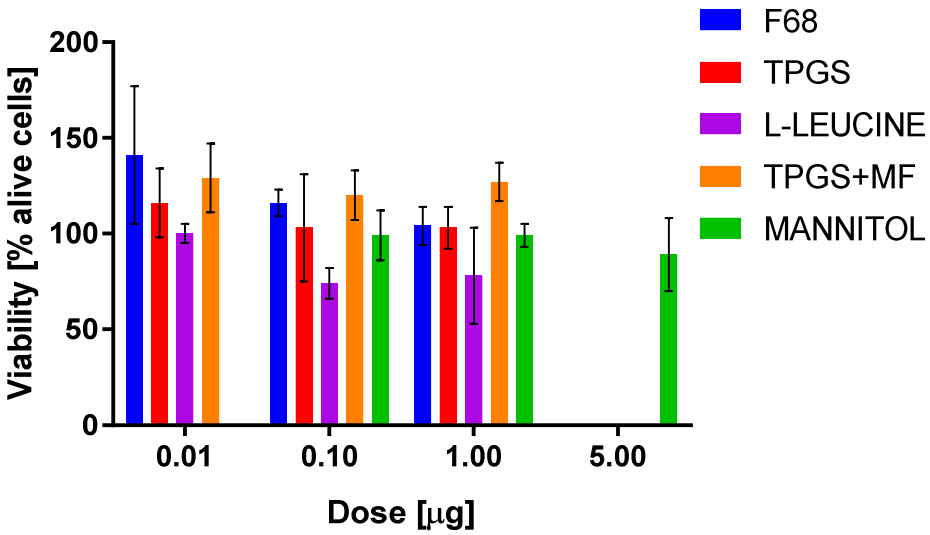


**Figure 5.15: Calu-3 cell viability assessed by PrestoBlue® cell viability assay after exposure of four hours to the individual excipients contained in the UCL formulations (F68, TPGS, mannitol and L-leucine) in doses ranging between 0.01 and 5.00 µg (in 200 µL of HBSS). Data are presented as MEAN ± SD (N=1, n=4).**

The TEER and lucifer yellow permeation values registered at the end of the transport experiments were within the acceptable ranges as showed in Table 5.15:

**Table 5.15: TEER and lucifer yellow values registered at the end of the transport experiment after application of UCL dry powder particles. Data are presented as mean ± SD (N=1, n=4).**

| Dosage form | Dose [µg] | TEER [Ω·cm$^2$] | Lucifer yellow permeation [%] |
|---|---|---|---|
| IND* - F68** | 0.5 (2.0 mg loading) | 805 ± 115 | 1.44 ± 0.14 |
| IND – TPGS° | 0.5 (2.0 mg loading) | 683 ± 96 | 0.83 ± 0.31 |
| IND - F68+MF°° | 0.5 (2.0 mg loading) | 874 ± 195 | 0.92 ± 0.35 |
| IND - TPGS+MF | 0.5 (2.0 mg loading) | 601 ± 100 | 0.69 ± 0.40 |

***IND: indomethacin**
****F68: Pluronic F68; °TPGS: D-α-Tocopherol polyethylene glycol 1000 succinate**
**°°MF: Matrix Formers (mannitol and L-leucine)**

The A→B transepithelial transport profile of indomethacin after deposition of the UCL formulation dry powders across the Calu-3 cell layer is shown in Figure 5.16 and Figure 5.17.

In the case of the UCL formulations containing F68, the transport profile of indomethacin was characterised by an initial burst (≈15% of drug transported in the first 5 minutes), followed by a fast linear trend for the first 30 minutes that was slowed down up to 180 minutes and eventually plateaued out reaching ≈90% transport in 240 minutes. The presence of the matrix formers, mannitol and L-leucine did not have any impact on the transport profile, as no significant difference was observed between the two formulations at all time points (multiple t-test, $p>0.05$).

A similar linear trend could be observed in the case of the formulations containing TPGS, although the initial burst was more intense with ≈35% of the drug transported after only 5 minutes. The transport profile then followed a faster linear trend for 60 minutes that was slower up to 180 minutes when it plateaued out at ≈95% transport

until 240 minutes. Also in this case there was no significant difference between the formulation with matrix formers and the one without (multiple t-test, $p>0.05$).

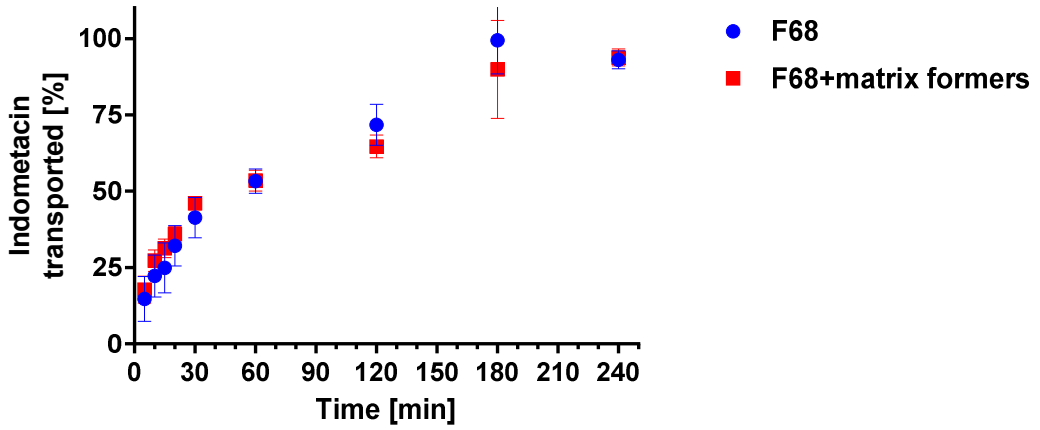


**Figure 5.16: apical to basolateral (A→B) transport profile of indomethacin after deposition of UCL formulations dry powders (IND – F68 and IND – F68 + MF). The PennCentury™ insufflator was loaded with 2.0 mg of individual dry powders corresponding to 0.5 µg dose of indomethacin. (see Table 5.12). Data are presented as mean ± SD (N=1, n=4).**

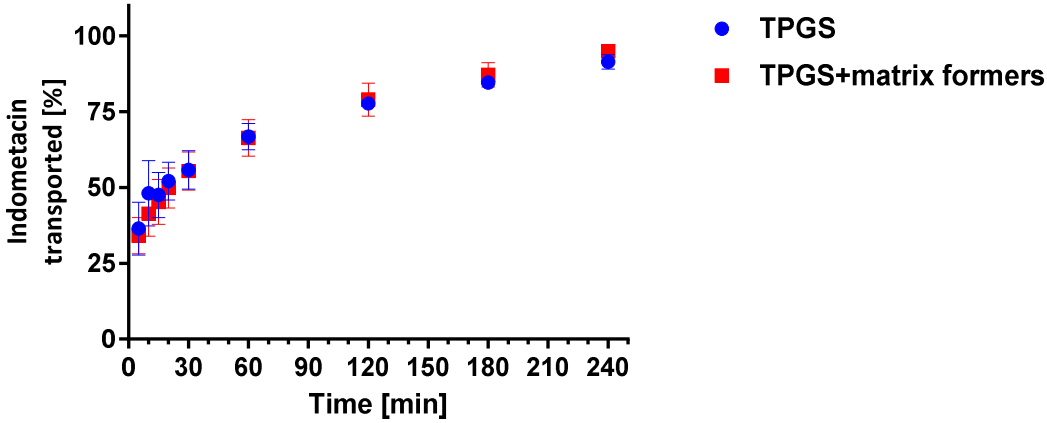


**Figure 5.17: apical to basolateral (A→B) transport profile of indomethacin after deposition of UCL formulations dry powders (IND – TPGS and IND – TPGS + MF). The PennCentury™ insufflator was loaded with 2.0 mg of individual dry powders corresponding to 0.5 µg dose of indomethacin. (see Table 5.12). Data are presented as mean ± SD (N=1, n=4).**

The absorption profile of indomethacin was not significantly improved when it was delivered as a formulation consisting of micro-agglomerates of nanoparticles. Neither the absorption rate nor the percentage transported increased. In fact, the $t_{50}$ calculated was 49 minutes and 20 minutes for the formulations containing F68 and TPGS respectively, which were higher than the $t_{50}$ of micronised indomethacin calculated as

12 minutes for the 1.0 mg loading. It could be envisaged that F68 and TPGS, being surfactant agents, could form micelles upon particle dissolution on the mucus layer of Calu-3 cells. Indomethacin could be entrapped in these micelles and be slowly released from them, with a slower absorption across the cell layer as a result.

This data confirmed what was found after the transport experiment of pure micronised indomethacin: solubility did not limit indomethacin absorption across the lung epithelium, instead its high permeability due to its lipophilic character is reckoned as the driving force of the mechanism of absorption.

## 5.4. Conclusion

The aim of the study described in this chapter was to investigate the absorption profile of a poorly water soluble drug like indomethacin (BCS class II) after delivery onto lung epithelial cell layers *in-vitro* either in solution or as a dry powder and compare it with that of salbutamol sulfate (BCS class III). Ultimately, we wanted to look at the effect of particle properties (micronised particles versus spray dried micro-agglomerates of nanoparticles) on indomethacin transepithelial transport across the Calu-3 cell layers.

As in the case of salbutamol sulfate, it was found that delivering indomethacin as a dry powder increased its absorption rate in comparison to when it was applied as a solution. However, the percentage of drug transported was higher than observed for salbutamol sulfate, therefore the system was able to discriminate between drugs with different permeability profiles according to the BCS. On the other hand, the predictions of indomethacin behaviour based on its BCS classification could not be confirmed in respect to its solubility, demonstrating that the poor aqueous solubility was not limiting its absorption.

The transepithelial transport profile of the UCL formulations revealed that the use of spray-dried micro agglomerates of drug nanoparticles improved neither the absorption rate nor the percentage transported.

## 5.5. References

Amidon, G.L. *et al.*, 1995. A theoretical basis for a Biopharmaceutic Drug Classification: the correlation of in-vitro drug product dissolution and in-vivo bioavailability. *Pharmaceutical Research*, 12(3), pp.413–420.

Boraey, M.A. *et al.*, 2013. Improvement of the dispersibility of spray-dried budesonide powders using leucine in an ethanol-water cosolvent system. *Powder Technology*, 236, pp.171–178.

British Pharmacopoeia Commission, 2016. *British Pharmacopoeia*, London: TSO.

Budavari, S. *et al.*, 1989. *The merck index*,

Bur, M. *et al.*, 2010. Drug transport across pulmonary epithelial cell monolayers: effect of particle size, apical liquid volume and deposition technique. *Journal of Aerosol Medicine and Pulmonary Drug Delivery*, 23(3), pp.119–127.

Ceschan, N.E. *et al.*, 2015. Characterization of indomethacin microparticles for inhalatory administration. *Powder Technology*, 7(8000), pp.51–61.

Chen, L. *et al.*, 2016. Amorphous powders for inhalation drug delivery. *Advanced Drug Delivery Reviews*, 100, pp.102–115.

Chew, N.Y.K. *et al.*, 2005. Effect of amino acids on the dispersion of disodium cromoglycate powders. *Journal of Pharmaceutical Sciences*, 94(10), pp.2289–2300.

Comer, J. *et al.*, 2014. The intrinsic aqueous solubility of indomethacin. *ADMET and DMPK*, 2(1), pp.18–32.

Copley, M. & Son, Y., 2010. Dissolution testing for inhaled drugs. *Pharmaceutical Technology Europe*, 22(11), pp.1–25.

Curry, S.H. *et al.*, 1982. Preparation and stability of indomethacin solutions. *Canadian*

*Journal of Physiology and Pharmacology*, 60(7), pp.988–992.

Eixarch, H. *et al.*, 2010. Drug delivery to the lung: permeability and physicochemical characteristics of drugs as the basis for a pulmonary biopharmaceutical classification system (pBCS). *Journal of Epithelial Biology & Pharmacology*, 3(1), pp.1–14.

Fischer, H. & Widdicombe, J.H., 2006. Mechanisms of acid and base secretion by the airway epithelium. *Journal of Membrane Biology*, 211(3), pp.139–150.

Forbes, B., Richer, N.H. & Buttini, F., 2015. Dissolution: a critical performance characteristic of inhaled products? In *Pulmonary Drug Delivery - Advances and Challenges*. Chichester, UK: John Wiley & Sons, Ltd, pp. 223–240.

Gamsjäger, H. *et al.*, 2008. Glossary of terms related to solubility (IUPAC Recommendations 2008). *Pure and Applied Chemistry*, 80(2), pp.233–276.

Hastedt, J.E. *et al.*, 2016. Scope and relevance of a pulmonary biopharmaceutical classification system AAPS/FDA/USP Workshop March 16-17th, 2015 in Baltimore, MD. *AAPS Open*, 2(1), pp.1–20.

Hoppentocht, M. *et al.*, 2014. In vitro evaluation of the DP-4M PennCentury™ insufflator. *European Journal of Pharmaceutics and Biopharmaceutics*, 88(1), pp.153–159.

Kaialy, W. & Nokhodchi, A., 2015. Particle engineering for improved pulmonary drug delivery through dry powder inhalers. In A. Nokhodchi & G. P. Martin, eds. *Pulmonary Drug Delivery - Advances and Challenges*. Wiley, pp. 171–197.

Karasulu, H.Y. *et al.*, 2008. Permeation studies of indomethacin from different emulsions for nasal delivery and their possible anti-inflammatory effects. *AAPS PharmSciTech*, 9(2), pp.342–348.

Khanvilkar, K., Donovan, M.D. & Flanagan, D.R., 2001. Drug transfer through mucus. *Advanced Drug Delivery Reviews*, 48(2), pp.173–193.

Lucas, S., 2016. The pharmacology of indomethacin. *Headache*, 56(2), pp.436–446.

Malamatari, M. *et al.*, 2015. Nanoparticle agglomerates of indomethacin: the role of poloxamers and matrix former on their dissolution and aerosolisation efficiency. *International Journal of Pharmaceutics*, 495(1), pp.516–526.

Mathias, N.R. *et al.*, 2002. Permeability characteristics of calu-3 human bronchial epithelial cells: in vitro-in vivo correlation to predict lung absorption in rats. *Journal of Drug Targeting*, 10(1), pp.31–40.

Neuhoff, S. *et al.*, 2005. pH-Dependent passive and active transport of acidic drugs across Caco-2 cell monolayers. *European Journal of Pharmaceutical Sciences*, 25(2–3), pp.211–220.

Olsson, B. *et al.*, 2011. Pulmonary drug methabolism, clearance and absorption. In H. D. C. Smyth & A. J. Hickey, eds. *Controlled Pulmonary Drug Delivery: Advances in Delivery Science and Technology*. Springer US, pp. 21–50.

Onischuk, A. a *et al.*, 2008. Anti-inflammatory effect from indomethacin nanoparticles inhaled by male mice. *Journal of Aerosol Medicine and Pulmonary Drug Delivery*, 21(3), pp.231–243.

Patton, J.S. *et al.*, 2010. The particle has landed - Characterizing the fate of inhaled pharmaceuticals. *Journal of Aerosol Medicine and Pulmonary Drug Delivery*, 23(S2), pp.S71–S87.

Patton, J.S., Fishburn, C.S. & Weers, J.G., 2004. The lungs as a portal of entry for systemic drug delivery. *Proceedings of the American Thoracic Society*, 1(4), pp.338–44.

Savjani, K.T., Gajjar, A.K. & Savjani, J.K., 2012. Drug solubility: importance and enhancement techniques. *ISRN pharmaceutics*, 5.

Seville, P.C. *et al*., 2007. Amino acid-modified spray-dried powders with enhanced aerosolisation properties for pulmonary drug delivery. *Powder Technology*, 178(1), pp.40–50.

Shen, T.-Y. & Winter, C.A., 1977. Chemical and biological studies on indomethacin, sulindac and their analogs. In A. B. Simmonds, ed. *Advances in drug research*. Academic Press, pp. 89–245.

Stegemann, S. *et al*., 2007. When poor solubility becomes an issue: from early stage to proof of concept. *European Journal of Pharmaceutical Sciences*, 31(5), pp.249–261.

Tolman, J.A. & Williams, R.O., 2010. Advances in the pulmonary delivery of poorly water-soluble drugs: influence of solubilization on pharmacokinetic properties. *Drug Development and Industrial Pharmacy*, 36(1), pp.1–30.

# Chapter 6
# The role of airway mucus on particle dissolution and drug absorption

## 6.1. Introduction

### 6.1.1. Physicochemical properties of mucus

Mucus is a ubiquitous viscous adherent complex material, produced by specialised cells (goblet cells) in the epithelium. Mucus is continuously secreted and shed or digested, and has the vital function of protecting and lubricating tissues and organs that are exposed to the external environment such as the respiratory system as well as the gastrointestinal tract, the reproductive system or the eyes. Alongside, it also functions as a barrier to pathogens and exogenous materials, while allowing for the exchange of nutrients and gases with the underlying tissues (Bansil & Turner 2006; Cone 2009).

The mucus chemical composition varies depending on its origin, mechanical or physiological role, and presence of any disease condition. However, there are some general features: water is the main component (approximately 95%), followed by proteins (e.g. mucins, lysozyme, growth factors, immunoglobulins) and lipids (0.5-5%), mineral salts (0.5-1%) and free proteins (~1%) (Khanvilkar *et al*. 2001).

Mucins represent the main component of mucus. They are large glycoproteins with molecular weight ranging between 0.5 and 20 MDa. About 20% of mucin molecular

mass is accounted for by its protein core. This is composed of two parts: a central glycosylated region composed mainly of tandem repeats containing serine, threonine and proline (STP repeats); and a poorly glycosylated region rich in cysteine, mainly at the O and N-terminals but also intercalated within the central region. Cysteine moieties are responsible for the formation of disulfide bonds which result in the dimerization of mucin. The remaining ≈80% of the structure consists of carbohydrates (e.g. N-acetylgalactosamine, N-acetylglucosamine, fucose, galactose, and sialic acid). Oligosaccharide chains of about 5-15 units, are attached in a "bottle-brush" configuration around the protein core by means of O-glycosidic bonds to the hydroxyl groups of serine and threonine units (Bansil & Turner 2006).

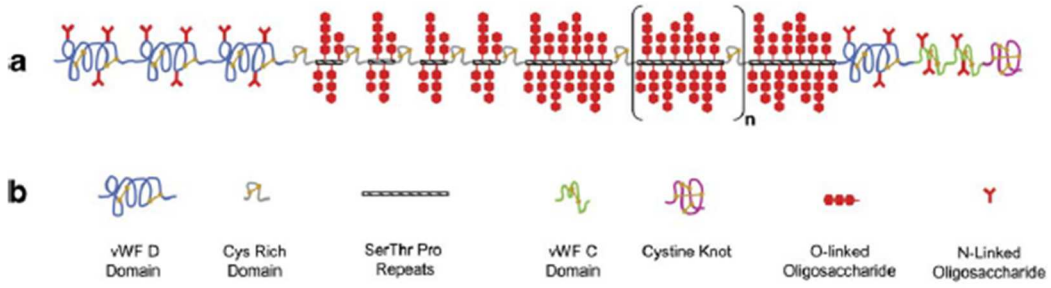


**Figure 6.1: mucin structure reproduced from Bansil and Turner (2006). The symbols in (b) reproduce the domains of the main structure in (a).**

There are two types of mucins: membrane bound and soluble secretory mucins. The membrane bound mucins do not form disulfide bonds but contain a hydrophobic domain that anchors to the cellular membrane. On the other hand, secretory mucins form intermolecular disulfide bonds. Crosslinked, bundled and entangled mucin fibres are responsible for the mucins' tendency to aggregate and form gels, therefore contributing to the viscoelastic properties of mucus (Khanvilkar *et al.* 2001; Thornton *et al.* 2008; Lai *et al.* 2009).

Mucus shows a complex physical behaviour. From a macro-scale point of view, it is commonly referred to as a non-Newtonian fluid, with variable properties ranging

between an elastic solid and a viscous liquid. In particular, it possesses shear-thinning properties (thixotropic), showing decreasing viscosity with increasing shear rates (Lai *et al.* 2009). The macro-rheological properties of mucus are extremely important for its biological functions, ensuring efficient clearance while remaining adherent to the epithelium despite high shear forces such as during blinking, swallowing and copulation. Variations of these properties are very often associated with clinical conditions. For example, severe bronchitis and cystic fibrosis are characterised by the production of very viscous mucus (viscosity >100,000 times that of water) which results in difficult mucus clearance, a condition more favourable to bacterial overgrowth.

The high viscosity (~2,000 times that of water) at low shear rates, would suggest that mucus prevents the transit of various materials (e.g. particles or proteins). However, it is known that nutrients (including proteins) as well as foreign material (e.g. pathogens and particles) can cross the mucus layers. Therefore, the bulk rheology is not sufficient to describe its behaviour and its micro-rheology must also be considered. Mucus is not a homogeneous fluid; it presents various different regions at the nanoscale which are created by the entanglement of the mucin fibres (Figure 6.2). The mesh created is mainly due to non-covalent bonds and was found to be heterogeneous with pore size measured by cryo-SEM ranging from few nano-meters up to several micro-meters in diameter (Kirch *et al.* 2012; Murgia *et al.* 2016). In the interstitial spaces between the entangled mucin fibres the viscosity approaches that of water. Materials with sizes ≤ 55 nm were found to undergo a resistance to their Brownian motion comparable to the viscous drag in water, whereas larger objects (> 500 nm) are found to be significantly slowed down (Lai *et al.* 2009).

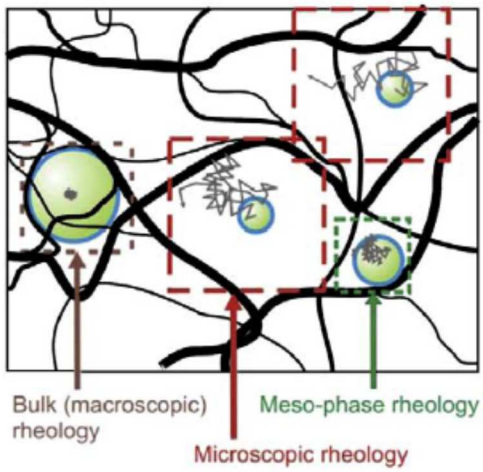


**Figure 6.2: schematic representation of the length-scale dependence viscosity in non-homogeneous fluids (e.g. mucus), reproduced from Lai *et al.* (2009).**

### 6.1.2. Barrier properties of mucus. Implications for drug delivery to the lungs

As previously explained, mucus is present in many organs, lining the tissues in contact with the external environment.

Respiratory mucus can significantly influence particle deposition in the lungs. In fact, in clinical conditions characterised by respiratory mucus overproduction, the peripheral particle deposition is significantly reduced due to the reduction of the lumen of the airways as well as of the airflow (Lethem 1993).

Respiratory mucus functions as a semipermeable barrier that, on one side, allows for the exchange of gases and nutrients, but at the same time has evolved to prevent most bacteria and foreign material (including drug delivery systems) from reaching the epithelium underneath. Mucus exerts its protective role with various mechanisms. For example, components such as immunoglobulins and other antibacterial agents play an important role in the defence of the respiratory system against antigens and bacteria (Lethem 1993). On the other hand, inhaled foreign materials are trapped by the mucus by means of an adhesive mechanism complemented by the mucociliary clearance, by

which mucus is swept towards the upper airways to the throat, to be eventually swallowed (Cone 2009; De Souza Carvalho *et al*. 2014). This efficient mechanism of defence represents an obstacle to pulmonary drug delivery, making the development of inhalable formulations particularly challenging as these would need to overcome the mucus barrier without damaging it in order to preserve its protective properties.

As explained in Chapter 1 (paragraph 1.5.2, page 16), when drug particles deposit in the upper airways they must dissolve first in mucus in order for the free drug molecule to reach the tissues underneath (Olsson *et al*. 2011; Widdicombe 1997). The thickness of the mucus in the airways is estimated to range between 1 and 10 μm in the upper airways and to decrease distally until it is replaced by surfactant (only a few microns thick) in the alveolar region, for a total volume of 10-30 mL (Patton 1996). The thickness of the mucus layer where the drug particles land is very important for their rate of solubility at the air-liquid interface, as it influences the surface area of interaction between the particle and the fluid. In particular, inhaled particles with diameter < 10 μm will typically be immersed in the mucus layer (sink conditions) for dissolution in the upper airways, whereas if deposited deeper in the airways only smaller surface areas will be wetted by the ASL (Airway Surface Liquid) (Olsson *et al*. 2011; Patton *et al*. 2010).

The thickness of the mucus layer is controlled and maintained by a fine equilibrium between the continuous secretion and removal of the mucus. In the tracheobronchial region the main removal mechanism is the mucociliary clearance, by which mucus is moved towards the throat by the continuous beating of the cilia present in the lung epithelium. Respiratory mucus is transported at velocities between 10 and 100 μm/s, thus it is completely replaced within minutes to hours. To guarantee the efficacy of

inhalation therapy, drugs delivered to the lungs have to move "upstream" across the mucus blanket in order to reach the underlying epithelium before the packet of mucus is removed by the mucociliary clearance mechanism.

Two layers of mucus can be distinguished on the lung epithelium, an un-stirred surface gel layer, and a periciliary "watery" layer adherent to the epithelium.

The cilia are immersed for most of their length in the periciliary layer of the mucus characterised by lower viscosity, whereas only the tips move in the viscoelastic upper gel layer. Cilia beating movement is fast enough so that mucus acts more like an elastic material rather than viscous, thus guaranteeing the efficacy of the removal mechanisms (Cone 2009).

Since the top mucus layer is unstirred, drug molecules must be able to diffuse across in order to penetrate.

Mucus can act as a barrier to diffusion for the free drug molecule after particle dissolution has occurred (Olsson *et al.* 2011; Patton *et al.* 2010). In this respect, the chemical nature of the mucus as well as of the drug molecule play an important role. Mucin can show different affinity to drug molecules or particles that could be entrapped in the mucus layer and be slowly released at a rate that is proportional to the binding affinity. For example, it was demonstrated that a number of both polar and non-polar drugs were non-specifically binding to pig gastric mucus, with resulting slower diffusion coefficients. Lipophilic drugs in particular, showed higher affinity for mucus than the hydrophilic ones. However, other studies in the field did not manage to correlate the drug solubility with mucus binding (Sigurdsson *et al.* 2013; Niibuchi & Tsuchiya 1986).

In the case of the lungs, a stronger binding of the drug to the mucus would result in the drug to be released in a different region of the airways (typically upper) or, if the release process is slower than the mucociliary clearance, it could be swallowed.

Mucins being negatively charged, the binding affinity would be higher for positively charged molecules. For example, studies on positively charged, low molecular weight molecules such as β-lactam antibiotics revealed that they bound electrostatically the negatively charged moieties of mucus (Niibuchi & Tsuchiya 1986; Khanvilkar *et al.* 2001). However, the electrostatic interaction would depend on other parameters as well, such as ionic strength and pH that could influence the effective charge of ionisable groups (counter-ion binding/shielding). Also lipophilic drugs tend to bind non-specifically to proteins and/or naked protein regions, and the same could happen when in contact with mucins (Patton *et al.* 2010; Widdicombe 1997; Sigurdsson *et al.* 2013).

If the drug molecule is not trapped by some interactions with mucin molecules, it must overcome the mucin network typical of the mucus structure.

The diffusion of drugs across the network could be slowed down by steric and hydrodynamic hindrance as explained by the steric exclusion model of Anderson and Quinn (1974). For example, it has been demonstrated that the coefficient of diffusion of peptides and proteins across gastric mucus is reduced when the molecular weight is increased (Boegh & Nielsen 2015). Also, other studies reviewed by Khanvilkar *et al.* (2001) have reported a delay in the absorption of drugs due to the presence of mucus in comparison to the diffusion across equivalent un-stirred water layers. However, there is a counterpart literature reporting no significant difference in the diffusion of colloids and particulates through mucus, demonstrating how poorly understood the

interactions between mucus and drug molecules or particles (Khanvilkar *et al*. 2001) still are.

### 6.1.3. Aim

The aim of the work showed in this chapter was to investigate the role of lung mucus on particle dissolution and drug permeation.

Respiratory mucus has proven to play a role in drug absorption, being often referred to as a barrier to foreign material, as previously explained.

The data showed in Chapter 5 on indomethacin transport across the Calu-3 cell layer after particle deposition was surprising considering the drug low solubility in water. It was therefore hypothesised that the mucus could take part in the absorption process of indomethacin, favouring particle dissolution after deposition on the cell layer.

The aim of this study was to clarify the role of mucus in drug absorption in the lungs, in particular of poorly soluble drugs like indomethacin.

Pig tracheal mucus was chosen as *in-vitro* model of the respiratory mucus for the experiments described in this chapter.

The first step was the development of an *in-vitro* system consisting of Transwell® inserts semipermeable membranes coated with pig mucus to allow its exposure to the dry powder spray produced with the PennCentury™ Dry Powder Insufflator. In particular, we aimed at obtaining an even and complete coverage of the microporous membrane of the inserts with mucus, ideally of thickness comparable to that of mucus in the airways (5-10 µm).

## 6.2. Materials and methods

### 6.2.1. Materials

Formaldehyde (16%, methanol free, ultrapure) was purchased from Polyscience Inc (Warrington, PA, USA), acetic acid, activated charcoal and ethanol (EtOH) were from Fisher Scientific (Loughborough, UK), pararosaniline chloride and periodic acid were bought from Acros Organic (New Jersey, USA), sodium metabisulfite was from Scientific Laboratory Supplies (Nottingham, UK).

For the origin of all other materials used refer to Chapter 2 (paragraph 2.1, page 31).

### 6.2.2. Pig mucus collection

Pig tracheal mucus was chosen as the *in-vitro* model to reproduce the mucus layer lining the human upper airways.

Batches of six pig tracheas were obtained from a local abattoir from healthy adult pigs, both males and females. Each trachea (approximate length: 15-20 cm) was cut open longitudinally and the edges were pinned on a support in order to keep them open. The mucus was gently scraped off with a spatula and pooled together in plastic tubes. Samples were stored at -20°C until further use.

### 6.2.3. Pig mucus cleaning

The pig mucus was thawed at room temperature before cleaning.

Mucus aliquots were diluted 1:10 with 0.1M NaCl and stirred at 4°C for 30 minutes. The suspension obtained was centrifuged at 14,000 rpm at 4°C for 15 minutes. The supernatant containing blood residues and debris was discarded. If the mucus did not look clean, the process was repeated again until visibly clean mucus (blood-free and clear) could be obtained. The cleaned mucus was stored at -20°C until further use.

### 6.2.4. Rheological characterisation of the pig mucus

The rheological characterisation of the pig mucus was performed using a Modular Compact Cone-Plate Rheometer MCR302 (Anton Paar GmbH, Germany). The cone used was the CP25-1 with diameter of 24.972 mm, angle of 1.002°, truncation of 51 µm.

Oscillatory tests were carried out in order to obtain information about the mechanical properties of the mucus. Measurements of the storage modulus (G′) and loss modulus (G″) as function of strain γ (0.1 – 100%) were carried out at an angular frequency of 10 rad/s, collecting 5 points per decade. Oscillatory frequency sweeps were performed within the linear viscoelastic (LVE) region, under a strain of 0.1%, and G′ and G″ moduli were measured between 0.1 and 100 Hz.

Viscosity measurements were collected with shear rate increasing logarithmically from 10 to 100 $s^{-1}$.

Mucus samples were analysed in triplicate sampling three different times from the same mucus batch. All measurements were carried out at 37°C.

Rheoplus analysis software (Anton Paar GmbH, Germany) was used for data processing.

### 6.2.5. Transwell® inserts coating with mucus: optimisation of the methodology

Various volumes of mucus ranging from 1.0 µL to 12 µL were tested, in order to obtain a complete and even coating of the semipermeable membrane of the Transwell® inserts.

Before proceeding with the insert coating, mucus was stained with Alcian Blue for a better visualisation of the Transwell® insert coverage. The selected volume of mucus was re-suspended in a solution of 10% Alcian blue (3% acidic acid) in dd-$H_2O$ for a total volume of 300 µL. The suspension obtained was transferred into a Transwell® insert housed in a 12-well cell culture plate. The plate was centrifuged at 1500 rpm for 15 minutes (Multifuge 3S, Heraeus). The supernatant was removed and the images of the insert surfaces coated with mucus were acquired using a Leica microscope MZ16 fitted with a Leica EC3 colour camera using an objective X5.

### 6.2.6. Drug permeation across the Transwell® semipermeable membrane

Four clean Transwell® inserts were transferred to the desiccator chamber in positions B, C, E and F (Figure 3.16(4), page 63). The PennCentury™ Dry Powder Insufflator was loaded with either 2.0 or 1.0 mg of micronised dry powder, and 5.0 mL of ambient air was used to produce the spray. The same protocol as explained in Chapter 2 (paragraph 2.2.3, page 37) was followed in order to carry out the drug permeation study.

After four hours, the apical surface of the Transwell® support was washed once with 200 µL of fresh HBSS.

All samples were processed and analysed using HPLC-MS/MS according to the protocols described in Chapter 2 (paragraph 2.2.5, page 41).

### 6.2.7. Drug permeation across mucus layers

For the drug permeation experiments, 12 µL of mucus was resuspended in 0.1M NaCl for a final volume of 300 µL. The mucus suspension obtained was transferred into four

Transwell® inserts housed in a 12-well cell culture plate. The plate was centrifuged at 1500 rpm for 15 minutes. The supernatant was removed and 500 µL of HBSS was placed in the basolateral chamber. The mucus was left to stabilise and dry from the excess of water overnight.

The following day, the Transwell® inserts coated with mucus were transferred to position B, C, E and F of the deposition chamber (Figure 3.16(4), page 63). The PennCentury™ Dry Powder Insufflator was loaded with 1.0 and 2.0 mg of either salbutamol sulfate or indomethacin micronised dry powders, and particles were aerosolised onto the mucus layers using 5.0 mL of ambient air.

The same protocol as explained in Chapter 2 (paragraph 2.2.3, page 37) was followed in order to carry out the drug permeation study.

After 4 hours, the mucus layer was washed and removed from the insert with 200 µL of HBSS. The suspension obtained was vortexed for 1 minute and centrifuged for 5 minutes at 14,000 rpm. The supernatant was collected for quantification of the residual non permeated drug.

All samples were processed and analysed using HPLC-MS/MS according to the protocols described in Chapter 2 (paragraph 2.2.5, page 41).

### 6.2.8. Mucus removal from Calu-3 cell layers cultured in ALI conditions

Calu-3 cells were cultured as explained in Chapter 2 (paragraph 2.2.2, page 33).

For the removal of mucus, different conditions were tested in order to optimise the method. TEER measurement and lucifer yellow assay were carried out as explained in Chapter 2 (paragraph 2.2.2.7, page 35) before and after removal of the mucus in order to assess whether the cell layer integrity was maintained after the procedure.

*6. The role of airway mucus on particle dissolution and drug absorption*

**a. Method 1:**

N-acetyl cysteine (NAC) was used as a mucolytic agent. On day 21, the medium was removed from the basolateral chamber and 500 µL of 0.3% (w/v) NAC in HBSS and 1.5 mL of pre-warmed HBSS was placed in the apical and basolateral side respectively. Cells were incubated either for 30 minutes once or twice (37°C, 5% $CO_2$, 95% humidity) or for 15 minutes once. Solutions were removed from both the apical and basolateral chambers, and the cell layers were washed twice with pre-warmed PBS.

**b. Method 2:**

The medium was removed from the basolateral chamber and the apical side of the cell layers was washed with 13 mL of pre-warmed PBS dispensed and simultaneously removed with a Pasteur pipette attached to a pump in continuous flow.

**c. Method 3:**

On day 19 medium was removed from the basolateral chamber and 0.5 mL and 1.5 mL of fresh pre-warmed medium was placed in the apical and basolateral chamber respectively. Calu-3 cell layers were kept in LLC for 48 hours before the drug transepithelial transport experiment. On day 21 the medium was removed from both the apical and the basolateral chamber and the cell layers were washed twice with 0.5 mL of fresh pre-warmed PBS.

### 6.2.9. Periodic acid Schiff (PAS) reagent-Alcian Blue assay for mucus staining

The effectiveness of the mucus removal procedures applied to Calu-3 cell layers was assessed by the periodic acid Schiff (PAS) reagent-Alcian Blue assay. The preparation

of the periodic acid and Schiff base solutions necessary for the assay was carried out as follows:

**a. Preparation of periodic acid solution:**

50% (w/v) periodic acid solution was diluted 1:1000 in 7% (v/v) acetic acid in dd$H_2O$.

**b. Preparation of Schiff Base solution:**

Pararosaniline (1.0 mg) was dissolved in 100 mL of boiling water. The solution was cooled down to T=50°C and 20 mL of 1M HCl was added. The solution was mixed twice with 300 mg of activated charcoal, shaken for 5 minutes and filtered on filter paper. The solution was stored in an amber bottle.

Directly before use, 0.1 g of sodium metabisulfite was added to 6 mL of Schiff reagent. The solution was incubated at 37°C for approximately 1.5 h; i.e. until it became pale yellow or clear; then, used in the assay.

Calu-3 cell layers cultured in Transwell® inserts were fixed in 0.5 and 1.5 mL of paraformaldehyde (4% v/v in PBS) in the apical and basolateral chamber respectively, for 10 minutes at room temperature. The cell layers were washed with 500 µL of PBS, and covered with 300 µL of periodic acid solution for 5 minutes at room temperature. The periodic acid solution was removed and the cell layer was washed once with 500 µL of PBS. The Schiff reagent was added (300 µL per well) for 15-30 minutes (until the purple colour was fully developed). The Schiff reagent solution was removed and cells were washed with 500 µL of PBS, and then covered with 300 µL of Alcian Blue solution (1% (w/v) in 3% HCOOH, pH=2.5 adjusted with acetic acid).

After staining the cell layers were mounted on microscopy glass slides for storage. The cell layers were initially dehydrated with consecutive washes with increasing concentrations of EtOH in dd$H_2O$ (50%, 70%, 95% and 100%). The membranes were

then removed from the Transwell® inserts and placed on glass microscopy slides where the mounting medium (clear nail varnish) had been brushed. Glass coverslips were used to cover the cell layers.

The intensity of the purple/blue colour was assessed by eye and comparison between untreated and treated cell layers was carried out in order to assess the effectiveness of the mucus removal procedure.

## 6.2.10. Dissolution of drug particles on mucus

The dissolution of both salbutamol sulfate and indomethacin micronised dry powder particles once landed on the mucus layer was monitored using optical microscopy.

A Transwell® insert was coated with pig mucus as explained in paragraph 6.2.7 (page189). The insert was transferred to position O in the desiccator chamber ((Figure 3.17 (4), page 65) and exposed to the drug dry powder spray produced by loading the PennCentury™ Dry Powder Insufflator with 2.0 mg of material.

Immediately after exposure to the spray, the insert was transferred to a well in a 12-well cell culture plate where 0.5 mL of HBSS was previously placed.

Images of a specific area of the mucus surface were acquired every second using the Imstar - smart imaging system for life optical inverted microscope (Olympus Ix51) fitted with X10 objective, and equipped with an Olympus camera (th400).

Alternatively, images were acquired using an L3001 microscope (GX Microscopes, UK) fitted with a QICAM Fast1394. Since this was not an inverted microscope, the Transwell® insert was modified to allow for the X10 objective to focus on its surface. In particular, the height of the inserts was reduced to 0.2 cm as showed in Figure 6.3:


**Figure 6.3: modification of the Transwell® insert. A: original Transwell® insert; B: modified Transwell® insert (height = 2 mm)**

Due to the modification of the Transwell® insert, it was not possible to leave the mucus layer overnight to stabilise and dry from the excess of water (paragraph 6.2.7, page 189), so the modified Transwell® insert was placed under the microscope immediately after coating. Once the focus was obtained the drug particles were sprayed onto the mucus coated Transwell® using the PennCentury™ Dry Powder Insufflator fitted with a straight needle (7.2 cm long). The dissolution of drug particles deposited on the mucus layer was monitored by acquiring one image every 500 ms for 500 images. The dry powders were sprayed multiple times in order to have a statistically relevant number of particles recorded. The PennCentury™ device was loaded every time with 1.0 mg of dry powder. The acquired images were processed with ImageJ software for the particle size and area reduction analysis.

## 6.3. Results and Discussion

In this study, pig tracheal mucus was chosen as *in-vitro* model to reproduce the respiratory mucus. In reality, crude human mucus would represent the best model, but access to it is limited and also there is a lot of variability due to inter-individual differences. For this reason, several *in-vitro* models of the respiratory mucus have been described in the literature. These include mucin solutions, artificial mucus (reconstituted mucus) and natural mucus. Mucin solutions containing other solutes are the simplest models. However, they are prone to variability especially between different laboratories due to differences in the preparation protocols. The same problems are encountered in the use of reconstituted pig gastric mucus. On the other hand, pig mucus presents several advantages in comparison to other mucus models: it is similar to human mucus and, pigs being large animals, it is possible to collect enough crude mucus from only few individuals. In addition, the collection of the crude mucus directly from the animal trachea allows to obtain a more representative model that contains other components (e.g. lipids and proteins) in addition to only mucin, as opposed to reconstituted mucus or mucin solutions (Groo & Lagarce 2014)

Moreover, since the samples were obtained from a local abattoir, ethical approvals were not required.

### 6.3.1. Rheological characterisation of mucus

The rheological properties of cleaned pig mucus were assessed in order to obtain information about its mechanical properties. Also, since the mucus collected from pig tracheas was undergoing a cleaning step prior to use, it was necessary to make sure

that the resulting mucus was still showing the expected characteristics of a gel like fluid.

The viscoelastic behaviour of mucus was assessed by performing oscillatory measurements. Oscillatory tests provide information about two key parameters, namely the storage modulus (G') and the loss modulus (G''). G' defines the elastic behaviour of the samples, whereas G'' defines its viscous behaviour.

Results obtained are showed in Figure 6.4 and Figure 6.5:

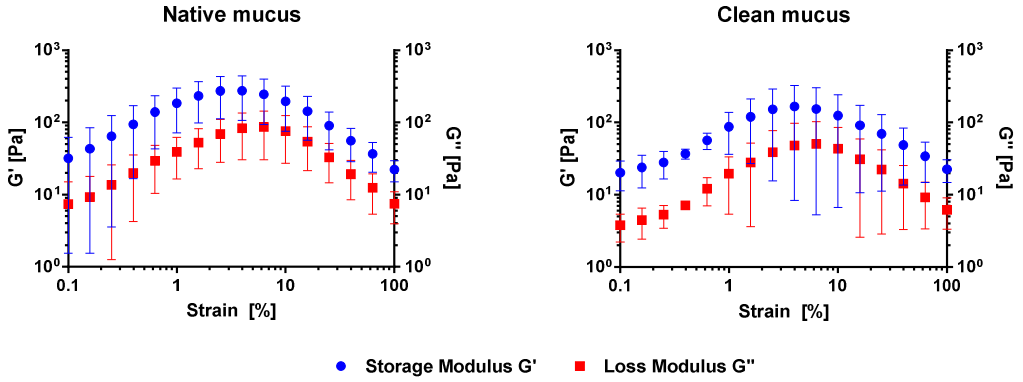


**Figure 6.4: macro-rheology of native (left) and cleaned (right) pig mucus. Storage (G') and loss (G'') moduli measured as a function of deformation (amplitude sweeps experiments). Frequency= 10 rad/s. Results are reported as MEAN ± SD (N=3)**

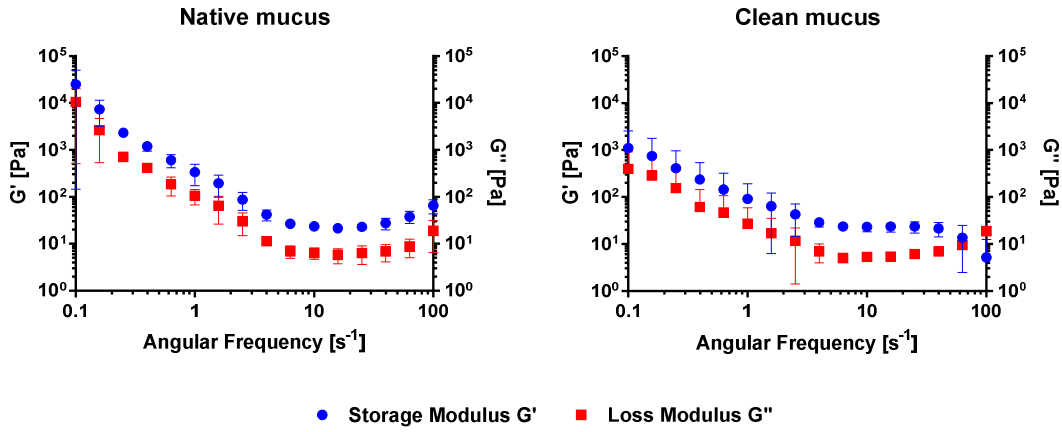


**Figure 6.5: macro-rheology of native (left) and cleaned (right) pig mucus. Storage (G') and loss (G'') moduli measured as a function of frequency (frequency sweeps experiments). Strain=0.1%. Results are reported as MEAN ± SD (N=3)**

As all gel-like materials, the mucus samples under investigation displayed G′ > G″ across the frequencies tested and the resulting G' and G'' curves were almost parallel. Both native and cleaned mucus showed the same viscoelastic behaviour, although the values for G' and G'' were always higher for the native mucus than for the cleaned mucus, probably due to the different level of hydration between the two samples as well as to the presence of blood cells in the native sample. These data demonstrate that the cleaning process did not significantly change the properties of mucus while removing materials (e.g. blood and cell debris) that could have interfered during the following drug permeation experiments.

Another important characteristic of mucus is its viscosity, that is generally reported as a function of the shear rate. It is expressed as the force exerted per unit area of the sliding surface *(F/A)* divided by the shear rate that is measured in units of distance slipped per second divided by the separation distance, therefore it is expressed in $[s^{-1}]$. The results of the viscosity measurements carried out on the mucus samples are showed in Figure 6.6:

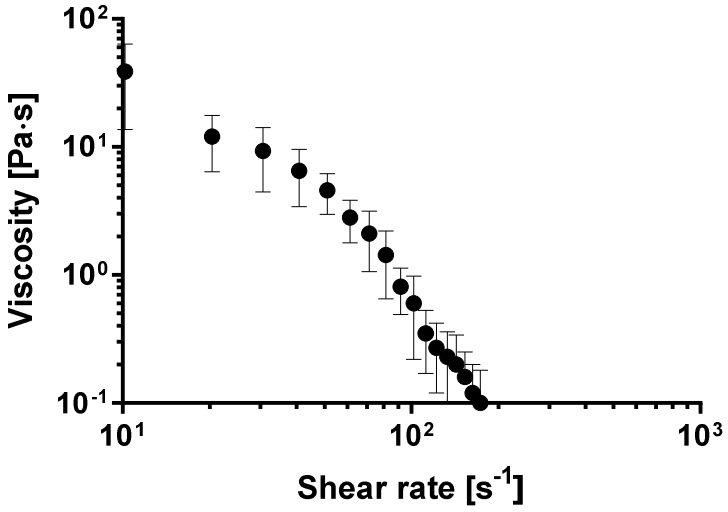


**Figure 6.6: viscosity of clean mucus as a function of shear stress. Results are showed as MEAN ± SD (N=3)**

The viscosity of the mucus samples under investigation decreased with an increase of the shear rate. This is in accordance with the literature where it is widely reported that mucus is a non-Newtonian fluid showing a shear-thinning behaviour. The reduction of the viscosity with the shear rate is due to the disruption of the adhesive interactions between the mucins fibres. The higher shear stress causes the mucin fibres, that are negatively charged to come closer to each other, thus causing a higher repulsion between the individual fibres that would slide one against the other. It is reported that at the maximum physiological shear rate (between $10^3$ and $10^5$ $s^{-1}$) the viscosity of mucus approaches that of water (Cone 2009).

## 6.3.2. Transwell® inserts coating with pig mucus

As extensively reviewed by Grießinger *et al.* (2015) and Groo and Lagarce (2014), several systems have been described in the literature for the *in-vitro* investigation of the role of mucus in drug absorption. These include diffusion chambers (Ussing chamber and modified Franz cells), modified Transwell®/Snapwell® systems and others. Most of these system have been used to study drug or drug-carrier (e.g. nanoparticles) diffusion across the mucus after their application in solution or suspensions, but to our knowledge they have not been used to explore the fate of dry powder particles after deposition onto the mucus layer.

To maintain similarities with the experimental setup used so far in this work, we selected the Transwell® system to carry out our investigation. However, the literature lacks protocols explaining how the mucus was spread onto the insert membrane. In addition, the mucus layer is typically confined in between two semipermeable membranes (Müller *et al.* 2014), and this is not ideal for pursuing our aim, as the membranes could prevent the particles from being properly in contact with the mucus

layer. Friedl *et al.* (2013) developed a Transwell® diffusion system where the mucus layer is in direct contact with the donor compartment. However, they did not provide a detailed protocol of preparation of the Transwell® diffusion system, and in addition report a thickness of the mucus layer of 929 ± 115 µm, that is far too high for our application.

For these reasons, in order to proceed with the *in-vitro* assessment of the role of the mucus on drug particle dissolution and drug permeation, there was a need to develop an *in-vitro* system consisting of Transwell® insert semipermeable membranes coated with pig mucus. The system had to be optimised in order to obtain a complete coverage of the microporous membrane of the inserts with an even mucus layer that could be directly exposed to the dry powder spray produced with the PennCentury™ Dry Powder Insufflator.

The centrifugation of the 12-well cell culture plate housing Transwell® inserts containing mucus suspension was found to be the best way to evenly spread the mucus on the surface of the insert. Different volumes of mucus ranging between 1.0 and 12.0 µL were used in order to find the optimum volume for complete coverage of the Transwell® insert's surface. The results obtained are showed in Figure 6.7:

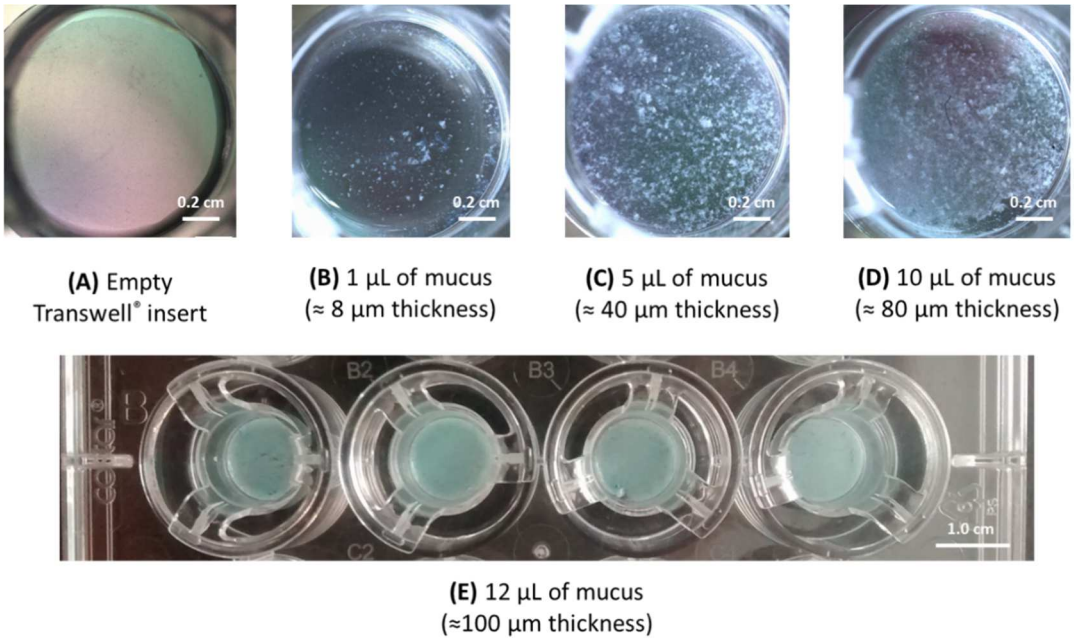


**Figure 6.7: Transwell® inserts coating with pig mucus. (A) Empty insert; (B) Transwell® insert coated with 1.0 µL of pig mucus; (C) Transwell® insert coated with 5.0 µL of pig mucus; (D) Transwell® insert coated with 10.0 µL of pig mucus; (E) Transwell® inserts coated with 12.0 µL of pig mucus.**

The thickness of the mucus layer in the human upper airways varies depending on the region, but it is reported to be between 1 and 10 µm (Patton 1996).

If we approximate the mucus coating to a cylinder with the permeable membrane of the Transwell® insert as base (growth area = 1.12 $cm^2$), 10 µm thickness corresponds to ≈1.0 µL of mucus. As showed in Figure 6.7(B), 1.0 µL of mucus was not sufficient to coat the Transwell® insert with an even layer of mucus. As expected, when increasing the volume of mucus, a larger surface area was coated, but an even and complete coating of the Transwell® insert was only achieved when 12 µL of mucus was used (Figure 6.7(E). However, this volume of mucus, corresponded to a ≈100 µm thickness, which is about 10 times that of the mucus layer lining the upper airways. Grainger *et al.* (2009) quantified the amount of mucin-like secretion of Calu-3 cells grown in ALI conditions and reported a thickness of these fluids to be ≈100 µm, although acknowledging the likelihood of an overestimation of the volume due to the

rehydration of the mucus during TEER measurement. Due to possible errors during the measurements as well as different culture conditions across laboratories, there is no agreement in the literature on the volume of apical fluids secreted by Calu-3 cells. In fact, other researchers have reported values ≤ 2µL (Ramesh Babu *et al*. 2004).

Although both volume and thickness of the mucus layer are recognised to play a significant role in drug absorption, the complete and even coating of the whole surface of the Transwell® insert was considered as important. For this reason, a volume of 12 µL of mucus was selected for the following *in-vitro* experiments.

## 6.3.3. Drug permeation across mucus

In order to understand the role of mucus in drug absorption in the lungs, the permeation of both salbutamol sulfate and indomethacin was monitored across either the semipermeable membrane alone or the Transwell® inserts coated with mucus, and compared to that across Calu-3 cell layers grown at the air-liquid interface.

Before proceeding with the study of drug permeation across the mucus layer, it was deemed necessary to observe the drug permeation across the semipermeable membrane alone. In this way, differences in the permeation profiles could be attributed solely to the physicochemical properties of the drugs.

The permeation profile of salbutamol sulfate across the clean semipermeable membranes of Transwell® inserts is showed in Figure 6.8. As expected, salbutamol sulfate quickly crossed the semipermeable membrane, and after 5 minutes the percentage of drug that had diffused in the basolateral chamber was already ≈75%, reaching ≈95% in four hours. No significant difference was observed in the percentage of drug permeated between the two doses (multiple t-test, $p>0.05$).

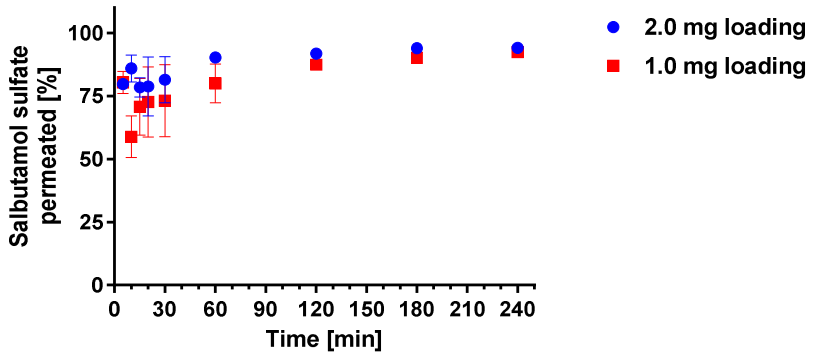


**Figure 6.8: apical to basolateral (A→B) permeation profile of salbutamol sulfate delivered as a dry powder across clean Transwell® inserts (2.0 and 1.0 mg PennCentury™ insufflator loading, corresponding to 1.0 and 0.5 µg doses respectively (Chapter 3, paragraph 3.3.5, page 85)). Data are presented as mean ± sem (N=2, n=4).**

Conversely, as showed in Figure 6.9, indomethacin slowly crossed the membrane following an initial linear trend that plateaued out reaching ≈93% permeation in four hours. Also in this case, no significant difference was observed in the percentage of drug permeated between the two doses delivered to the membrane (multiple t-test, $p>0.05$), and the same was found for the flux that was calculated as 0.45 % units/ min. However, the calculated individual $t_{50}$ was ≈58 minutes and ≈88 minutes for 1.0 and 2.0 mg loading respectively.

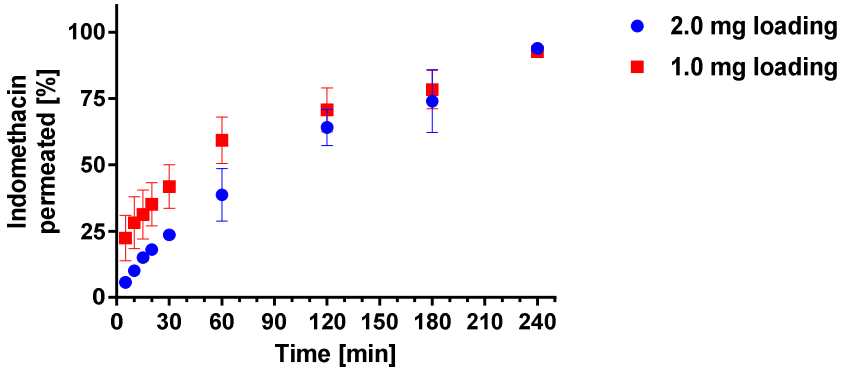


**Figure 6.9: apical to basolateral (A→B) permeation profile of indomethacin delivered as a dry powder across clean Transwell® inserts (2.0 and 1.0 mg PennCentury™ insufflator loading, corresponding to 1.0 and 0.5 µg doses respectively (Chapter 5, paragraph 5.3.4, page 155)). Data are presented as mean ± sem (N=2, n=4).**

As expected from the different solubility in water of the two drugs, salbutamol was more permeable than indomethacin, crossing the semipermeable membrane of the Transwell® inserts nearly quantitatively soon after deposition.

The following step was the inclusion of the mucus layer on the Transwell® insert. With this experimental setup, deviations from the previous permeation profile could be attributed only to the effect of mucus on drug permeation.

The permeation profile of salbutamol sulfate through mucus is showed in Figure 6.10. After deposition, there was an initial burst of drug permeation within the first 5 minutes, when the percentage of drug permeated was already ≈50% of the initial dose applied. The drug permeation increased linearly for the following 30 minutes until it reached a plateau with ≈95% of drug permeated in four hours. The dose applied did not affect either the flux calculated as 1.15 % units/min (between 5 and 30 minutes) or the percentage of permeation for the duration of the experiment (multiple t-test, $p>0.05$).

A different behaviour was observed in the case of indomethacin (Figure 6.11). The permeation profile followed a linear trend slowly increasing from time zero until 30 minutes with a calculated flux of 1.15 % units/min. The linear trend was slower for the following two hours (the calculated flux was 0.21 %units/min) until it plateaued out at ≈90% after four hours. Also in this case, the dose applied did not affect either the flux or the percentage of permeation for the duration of the experiment (multiple t-test, $p>0.05$).

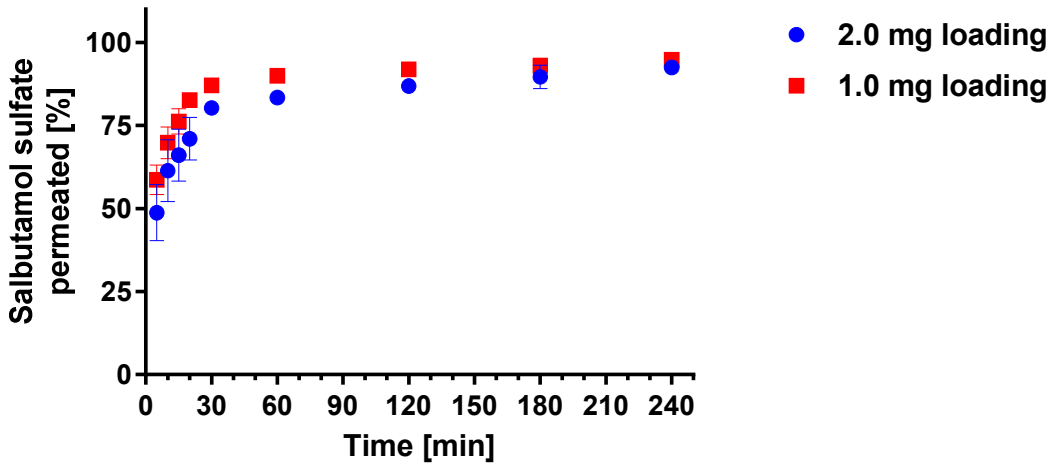


**Figure 6.10: apical to basolateral (A→B) permeation profile of salbutamol sulfate delivered as a dry powder across mucus layer (2.0 and 1.0 mg PennCentury™ insufflator loading, corresponding to 1.0 and 0.5 µg doses respectively (Chapter 3, paragraph 3.3.5, page 85)). Data are presented as mean ± sem (N=2, n=4).**

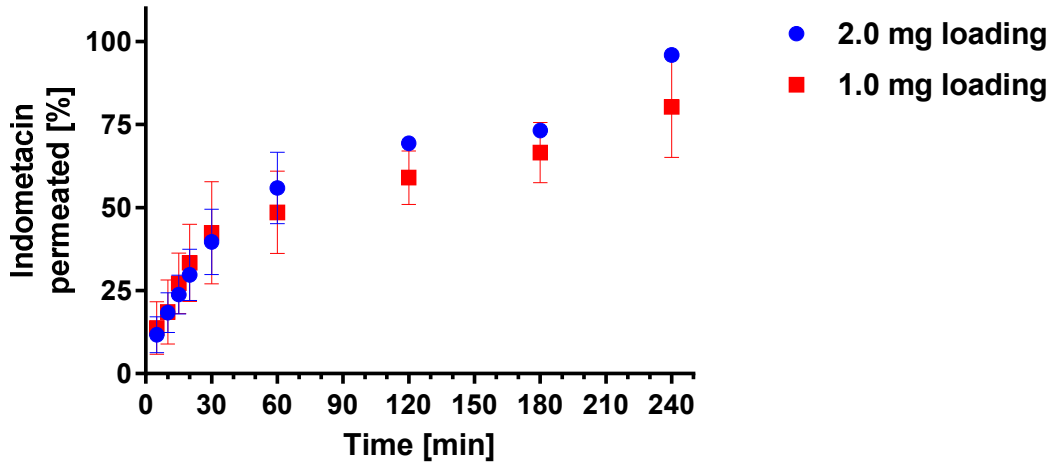


**Figure 6.11: apical to basolateral (A→B) permeation profile of indomethacin delivered as a dry powder across mucus layer (2.0 and 1.0 mg PennCentury™ insufflator loading, corresponding to 1.0 and 0.5 µg doses respectively (Chapter 5, paragraph 5.3.4, page 155)). Data are presented as mean ± sem (N=2, n=4).**

As showed in Figure 6.12, salbutamol sulfate permeated through the mucus layer more quickly than indomethacin, with calculated $t_{50}$ of about 3 minutes and 49 minutes respectively, ranking in opposite order in comparison to what was observed for the transepithelial drug transport across Calu-3 cell layers (Chapter 5, paragraph 5.3.5, page 160).

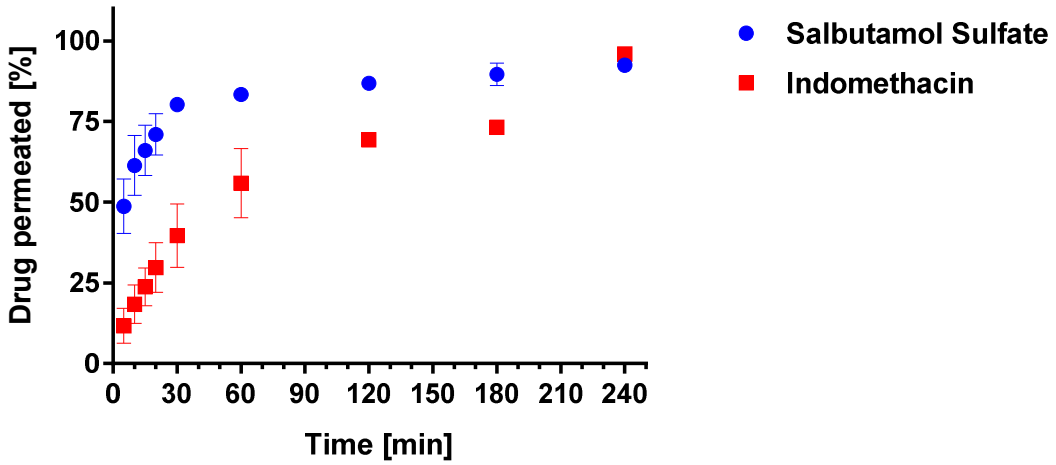


**Figure 6.12: comparison between the A→B permeation profiles of indomethacin and salbutamol both delivered to mucus layers as micronised dry powders (2.0 mg loading of the PennCentury™ Dry Powder Insufflator). Data are presented as mean ± sem (N=2; n=4)**

This could be explained considering the different water solubility and lipophilicity of the two drugs. Salbutamol is more water soluble than indomethacin, which means that after crossing the mucus layer it can easily diffuse in the HBSS aqueous buffer in the basolateral side. On the other hand, indomethacin is a poorly water soluble drug that would more hardly diffuse into the aqueous HBSS buffer. As explained in paragraph 6.1.1 (page 179) mucus is mainly composed of water but also contains proteins and lipids that are believed to favour the dissolution of lipophilic drug particles. In this experimental setup, mucus would represent the sole compartment where indomethacin could preferentially partition, as opposed to the experimental setup where also Calu-3 cells are present with their phospholipidic bilayer of the cellular membrane.

However, as already discussed in Chapter 5, the acidic character of indomethacin is responsible for its intrinsic solubility in water that strongly depends on pH. HBSS being at pH=7.4 (> indomethacin $pK_a$), it is possible for indomethacin to slowly diffuse into the basolateral chamber, and this is probably the reason why it eventually reached ≈90% permeation in four hours.

The effect of the mucus in combination with the chemical properties of the drug is more evident when comparing the drug permeation/transport across Calu-3 cell layers, mucus layers and Transwell® inserts (Figure 6.13).

Figure 6.13 and Table 6.1 summarise permeation profile and the $t_{50}$ calculated for salbutamol and indomethacin for the different experimental conditions used (empty Transwell® semipermeable membrane, mucus layer and Calu-3 cell layer).

The A→B permeation of salbutamol sulfate was slowed down by the presence of the mucus and the effect was even more obvious in the presence of the cell layer. This is in agreement with the theory of the mucus and the epithelium acting as barriers.

A complete opposite trend was observed in the case of indomethacin, for which the permeation across the Transwell® membrane was the slowest. This was faster in the presence of the mucus and of the cell layers. In this case, it is believed that the mucus layer containing lipids and proteins and being at neutral pH would promote the dissolution of indomethacin particles. However, as explained earlier, the diffusion to the aqueous HBSS phase in the basolateral chamber seems to be the limiting step. When the cell layer is added to the system, indomethacin permeation is improved, probably due to the presence of an additional compartment (the phospholipidic bilayer of the cellular membrane) where this lipophilic drug could partition as well.

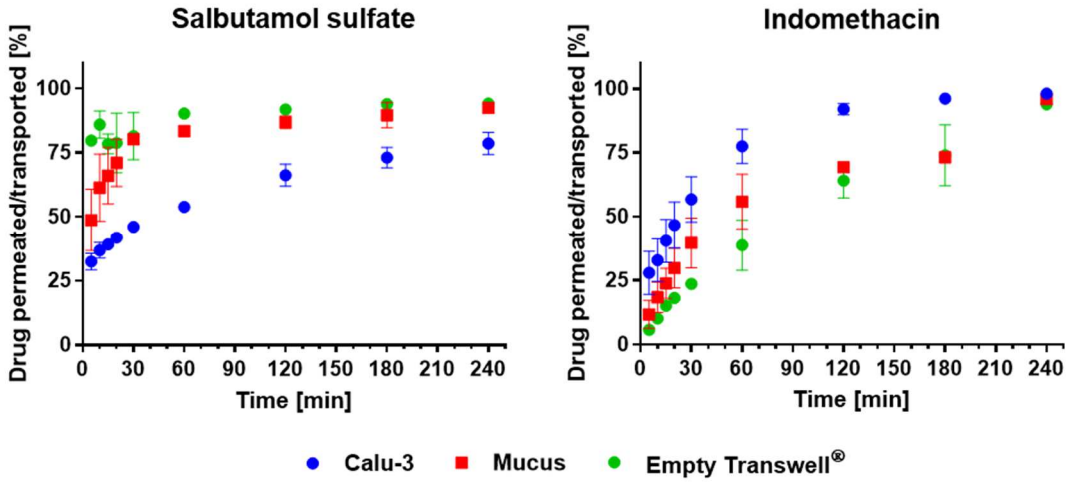


**Figure 6.13: comparison between the A→B permeation profiles of salbutamol sulfate (left) and indomethacin (right) delivered to either Calu-3 cell or mucus layers or clean Transwell® inserts as micronised dry powders (2.0 mg loading of the PennCentury™ Dry Powder Insufflator). Data are presented as mean ± sem (N=2/3; n=4)**

**Table 6.1: $t_{50}$ [min] calculated for salbutamol sulfate and indomethacin across empty Transwell® inserts, mucus layer and Calu-3 cell layers grown in ALI conditions.**

| Drug | $t_{50}$ [min] | | |
|---|---|---|---|
| | Empty Transwell® semipermeable membrane | Mucus layer | Calu-3 cell layer |
| Salbutamol sulfate | <5 minutes | ≈3 | ≈47 |
| Indomethacin | ≈94 | ≈49 | ≈24 |

## 6.3.4. Apical to basolateral (A→B) transepithelial drug transport across Calu-3 cell layers after removal of the mucus

As seen earlier, the drug permeation across the mucus layer for the two drugs under investigation followed an opposite order of permeability (salbutamol >> indomethacin) in comparison to the observations made after deposition of the dry powder particles onto Calu-3 cell layers at the air-liquid interface.

To better understand the mechanisms involved in drug permeation across the lung epithelium, we also looked at the role of the cell monolayer to drug permeability,

without any influence from the mucus. In order to do so, it was necessary to remove the mucus produced by the Calu-3 cells when grown at the air-liquid interface.

The first step was the optimisation of the protocol used to remove the mucus from Calu-3 cell layers. Different methods have been tested involving either the incubation of the Calu-3 cell layers with a mucolytic agent such as N-acetyl cysteine (NAC) for different times (30 minutes twice, 30 minutes once, 15 minutes once) or washing the cell layers with pre-warmed PBS in continuous flow or keeping the cell layers in LLC for 48 hours before the transport experiment.

TEER measurements and lucifer yellow permeability assay were performed before and after to monitor the cell layer integrity. Alcian Blue-PAS staining of the cell layers after mucus removal was used to assess the mucus depletion. Unwashed Calu-3 cell layers were used as reference.

Treatment with NAC was quite efficient in the removal of the mucus layer produced by the Calu-3 cells as showed in Figure 6.14(B, C, D), however it also caused a disruption of the cell layer that resulted in a drop of the TEER values below the 400 $\Omega \cdot cm^2$ threshold as well in an increase of the lucifer yellow flux above 2%.

On the other hand, washing the cell layers with PBS in continuous flow was less efficient in removing the mucus. In fact, the staining remained quite intense although less intense than on the un-treated cell layers as showed in Figure 6.14(E). Additionally, the tightness of the cell monolayer was maintained with a TEER>500 $\Omega \cdot cm^2$ and a lucifer yellow flux<2%.

The last method tested for mucus removal from the cell layers was keeping the cell layers for 48 hours in LLC. In this case, the removal of the mucus was as efficient as

with NAC (Figure 6.14(F)), but with TEER and lucifer yellow values maintained within the accepted thresholds.

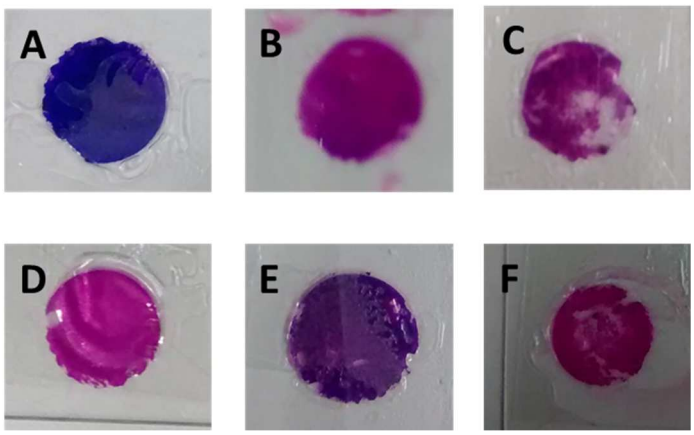


**Figure 6.14: PAS-Alcian blue staining of Calu-3 cell layers after mucus removal. A: Blank; B: NAC 30 mins 2x; C: NAC 30 mins 1x; D: NAC 15 mins 1x; E: PBS wash in continuous flow; F: LLC culture for 48 hours.**

Two of the described methods (namely, washing the cell layers with PBS in continuous flow and keeping the cell layers in LLC for 48 hours prior to the experiment) were selected to remove the mucus from Calu-3 cell layers and carry out the following *in-vitro* experiments.

After mucus removal, the cell layers were exposed to 2.0 mg sprays of either salbutamol sulfate or indomethacin micronised dry powder.

The choice of administering only one dose to the cell layer was due to the fact that, as seen in the previous experiments, the dose did not affect the percentage of drug transported across the cell layers at all time points for both drugs.

The transepithelial transport profiles of the two drugs under investigation across unwashed cell layers or after mucus removal with the continuous flow method are showed in Figure 6.15 and Figure 6.16.

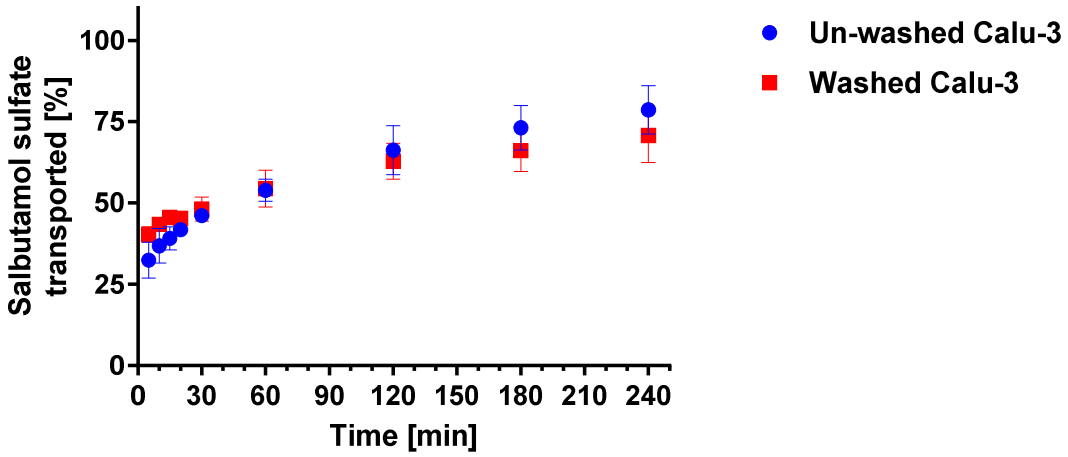


**Figure 6.15: apical to basolateral (A→B) permeation profile of salbutamol delivered as a dry powder across washed and un-washed Calu-3 cell layers (2.0 PennCentury™ insufflator loading, corresponding to 1.0 µg doses (Chapter 3, paragraph 3.3.5, page 85)). Data are presented as MEAN ± sem (N=3/2, n=4).**

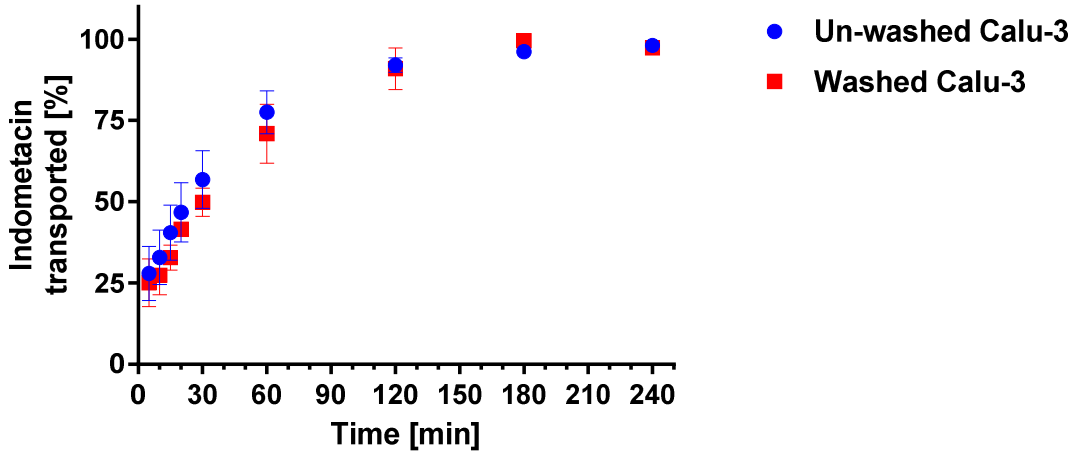


**Figure 6.16: apical to basolateral (A→B) permeation profile of indomethacin as a dry powder across washed and un-washed Calu-3 cell layers (2.0 PennCentury™ insufflator loading, corresponding to 1.0 µg doses (Chapter 5, paragraph 5.3.4, page 155)). Data are presented as MEAN ± sem (N=3/2, n=4).**

No significant difference was observed in the transport profile of both drugs with and without mucus. This could probably be attributed to the fact that the mucus was not completely removed in the washing process. Washing the cell layers with PBS in continuous flow only reduced the mucus thickness. However, only a qualitative analysis was conducted, therefore no information about the percentage of depletion is available.

The other method adopted for the removal of the mucus involved growing the Calu-3 cell layers in LLC conditions only for the last 48 hours before the transport experiment. As discussed before, the mucus removal was much more efficient with this method in comparison to the wash in continuous flow. However, at the end of the transport experiment, both the TEER measurement and the lucifer yellow permeability assay failed, indicating that the cell layers were disrupted. As discussed in Chapter 4, this is most likely due to the protective role of mucus secretion on Calu-3 cell layers.

### 6.3.5. Particle dissolution after deposition onto the mucus layer

In order to confirm the adjuvant role of mucus in drug particle dissolution, especially for indomethacin, monitoring the dissolution of the particles after deposition on the mucus layer was done.

Two different setups were adopted in order to acquire images of the dissolving particles deposited on the mucus layer: an inverted (Imstar) and a normal (L3001) microscope.

The use of the inverted microscope did not allow for the acquisition of meaningful images. In fact, two problems were encountered during the execution of the experiment: the objective being underneath the specimen, the mucus layer was impeding the correct focus on the surface, which resulted in the capture of blurry images. In addition, by the time the focus was obtained, the particles of both salbutamol sulfate and indomethacin had completely dissolved.

The use of a conventional microscope proved more convenient as focussing on the mucus surface was easier. However, it was only possible to monitor particle dissolution in the case of salbutamol sulfate, for which particles completely disappeared from the mucus surface within seconds. As expected larger particles

(d>50 µm) took longer (up to 7 seconds) than small particles to completely disappear (Figure 6.17). However, it is noteworthy that this fast dissolution could have been over-estimated due to the fact that the mucus layer was used immediately after preparation in order to prevent it from drying out if left and therefore it is possible that it contained an excess of water that promoted the particle dissolution.

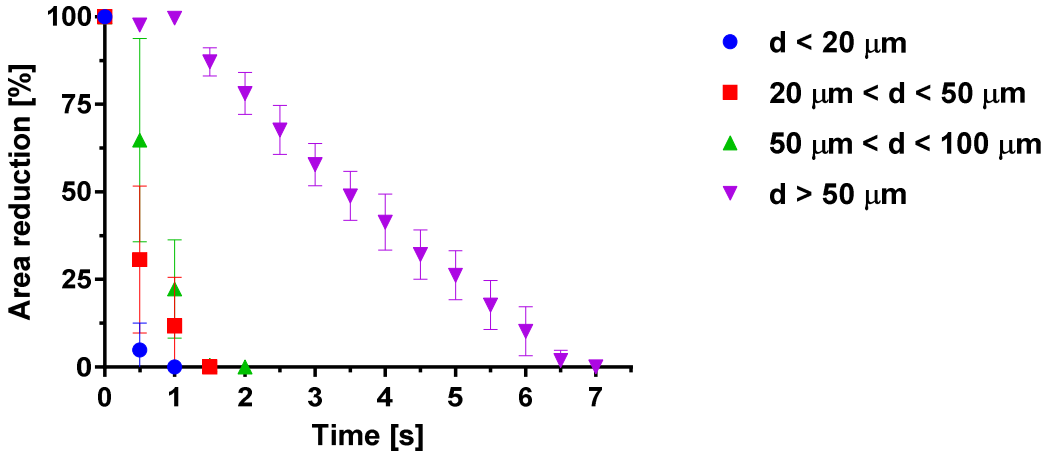


**Figure 6.17: size reduction of salbutamol sulfate micronised particles after deposition on the mucus surface.**

In the case of indomethacin, other technical problems were encountered. After deposition, particles did not dissolve on the mucus layer. This was probably due to the fact that saturation of indomethacin on the mucus layer was reached but there was no place for indomethacin to diffuse to. In fact, as opposed to the other setup on the inverted microscope, in this case the basolateral side was empty, directly touching the surface of the specimen holder. In addition, it is possible that more time was required for the particles to completely dissolve, however it was not possible to observe this as the mucus layer was drying within four hours.

## 6.4. Conclusions

The aim of the study described in this chapter was to investigate the role of mucus on particle dissolution and drug absorption across the lung epithelium.

The permeation of salbutamol sulfate and indomethacin across the three barriers investigated (clean Transwell® inserts, mucus layer and Calu-3 cell layers) followed an opposite order, demonstrating that the mucus was acting as a barrier in the case of salbutamol, but conversely promoted dissolution of indomethacin particles.

On the other hand, it was not possible to clarify the role of the sole cell layer in drug absorption as the two methods used to remove the mucus layer from Calu-3 cells resulted to be non-adequate.

Finally, the methods used to monitor the particle dissolution after deposition on the mucus layer did not provide an additional proof of the ability of mucus to improve solubility of indomethacin due to technical issues. However, it is recognised the dissolution happened quickly, but it was not possible to measure it.

## 6.6. References

Anderson, J.L. & Quinn, J. a, 1974. Restricted transport in small pores. A model for steric exclusion and hindered particle motion. *Biophysical Journal*, 14(2), pp.130–150.

Bansil, R. & Turner, B.S., 2006. Mucin structure, aggregation, physiological functions and biomedical applications. *Current Opinion in Colloid & Interface Science*, 11(2), pp.164–170.

Boegh, M. & Nielsen, H.M., 2015. Mucus as a barrier to drug delivery - Understanding and mimicking the barrier properties. *Basic and Clinical Pharmacology and Toxicology*, 116(3), pp.179–186.

Cone, R.A., 2009. Barrier properties of mucus. *Advanced Drug Delivery Reviews*, 61(2), pp.75–85.

Friedl, H. *et al*., 2013. Development and evaluation of a novel mucus diffusion test system approved by self-nanoemulsifying drug delivery Systems. *Journal of Pharmaceutical Sciences*, 102(12), pp.4406–4413.

Grainger, C.I. *et al*., 2009. The permeability of large molecular weight solutes following particle delivery to air-interfaced cells that model the respiratory mucosa. *European Journal of Pharmaceutics and Biopharmaceutics*, 71(2), pp.318–324.

Grießinger, J. *et al*., 2015. Methods to determine the interactions of micro- and nanoparticles with mucus. *European Journal of Pharmaceutics and Biopharmaceutics*, 96, pp.464–476.

Groo, A.C. & Lagarce, F., 2014. Mucus models to evaluate nanomedicines for diffusion. *Drug Discovery Today*, 19(8), pp.1097–1108.

Khanvilkar, K., Donovan, M.D. & Flanagan, D.R., 2001. Drug transfer through mucus. *Advanced Drug Delivery Reviews*, 48(2), pp.173–193.

Kirch, J. *et al.*, 2012. Optical tweezers reveal relationship between microstructure and nanoparticle penetration of pulmonary mucus. *Proceedings of the National Academy of Sciences of the United States of America*, 109(45), pp.18355–60.

Lai, S.K. *et al.*, 2009. Micro- and macrorheology of mucus. *Advanced Drug Delivery Reviews*, 61(2), pp.86–100.

Lethem, M.I., 1993. The role of tracheobronchial mucus in drug administration to the airways. *Advanced Drug Delivery Reviews*, 11(3), pp.271–298.

Müller, C. *et al.*, 2014. Development and in vivo evaluation of papain-funtionalised nanoparticles. *European Journal of Pharmaceutics and Biopharmaceutics*, 87(1), pp.125–131.

Murgia, X. *et al.*, 2016. Size-limited penetration of nanoparticles into porcine respiratory mucus after aerosol deposition. *Biomacromolecules*, 17(4), pp.1536–1542.

Niibuchi, J. & Tsuchiya, S., 1986. Binding of antibiotics to rat intestinal mucin. *International Journal of Pharmaceutics*, 30(2), pp.181–187.

Olsson, B. *et al.*, 2011. Pulmonary drug methabolism, clearance and absorption. In H. D. C. Smyth & A. J. Hickey, eds. *Controlled Pulmonary Drug Delivery: Advances in Delivery Science and Technology*. Springer US, pp. 21–50.

Patton, J., 1996. Mechanism of macromolecule absorption by the lungs. *Advanced Drug Delivery Reviews*, 19(1), pp.3–36.

Patton, J.S. *et al.*, 2010. The particle has landed - Characterizing the fate of inhaled pharmaceuticals. *Journal of Aerosol Medicine and Pulmonary Drug Delivery*,

23(S2), pp.S71–S87.

Ramesh Babu, P.B. *et al*., 2004. Regulation of apical surface fluid and protein secretion in human airway epithelial cell line Calu-3. *Biochemical and Biophysical Research Communications*, 319(4), pp.1132–1137.

Sigurdsson, H.H., Kirch, J. & Lehr, C.M., 2013. Mucus as a barrier to lipophilic drugs. *International Journal of Pharmaceutics*, 453(1), pp.56–64.

De Souza Carvalho, C., Daum, N. & Lehr, C.M., 2014. Carrier interactions with the biological barriers of the lung: advanced in vitro models and challenges for pulmonary drug delivery. *Advanced Drug Delivery Reviews*, 75, pp.129–140.

Thornton, D.J., Rousseau, K. & McGuckin, M.A., 2008. Structure and function of the polymeric mucins in airways mucus. *Annual Review of Physiology*, 70, pp.459–486.

Widdicombe, J.G., 1997. Airway liquid: a barrier to drug diffusion? *European Respiratory Journal*, 10(10), pp.2194–2197.

# Chapter 7
# General discussion and future directions

## 7.1. General discussion and future directions

The rationale for this PhD project came from the hypothesis that the physicochemical properties of particles for inhalation have an impact on their dissolution, interaction with lung lining fluids and permeability across the lung epithelium. Therefore, the main aim of the study was a better understanding of the relationship between drug particle physicochemical properties and their fate in lung tissue in terms of dissolution and drug absorption.

We successfully assembled a deposition system to apply aerosolised dry powder particles for inhalation, and demonstrated that it is able to homogeneously disperse different types of dry powders (micronised and spray dried), and deliver consistently controlled doses of drug in a narrow particle size range (3-5 µm). However, the system presented a major limitation as no real separation between respirable (<10 µm) and non-respirable (>10 µm) particles could be achieved.

Compared to other systems such as PADDOC (Hein *et al.* 2010), VITROCELL (Kim *et al.* 2013) or TSI (Grainger *et al.* 2009) that can only allocate a maximum of three inserts at a time, our system is more convenient allowing more room to allocate a higher number of inserts. It is also not limited to just one geometry as demonstrated. In addition, compared to the mentioned exposure systems that have been described in

the literature, ours is easier to operate, less costly and allowed to obtain data comparable to those already reported in the literature, proving to be a reliable tool for the investigation of the fate of particles at the air-epithelium interface in the lung. In addition, it only requires a very limited amount of dry powder (1-2 mg) to carry out a single experiment.

The advantages that our system presents over the systems already described in the literature, could make it a useful investigation tool to allow fast screening of new drug candidates or dry powder formulations during the early stage of drug development.

Once the system was obtained, we wanted to investigate the effect of the formulation (solution or dry powder) on drug absorption across the lung epithelium. The drugs used were salbutamol sulfate (BCS class III), and indomethacin (BCS class II).

Using our system, it was possible to discriminate between drugs with different permeability profiles according to the BCS. However, the initial hypothesis of indomethacin limited absorption due to its low water solubility could not be confirmed. Instead, the high permeability of indomethacin could be associated with its acidic character that is believed to promote particle solubility at physiological pH, thus overcoming its lipophilicity.

In the case of salbutamol, we focussed on a better understanding of its mechanism of absorption through the lung epithelium, aiming at evaluating for the first time whether the role of OCT transporters was affected by the physical form of the drug (solution or dry powder). As explained in Chapter 4, the data obtained when salbutamol was applied in solution suggested that OCT transporters are likely to be involved in salbutamol absorption, but it was not possible to draw valid conclusions when salbutamol was delivered as a dry powder, due to the fact that the cell layers failed to pass both the TEER measurement and the LY permeability assay at the end of the

experiment. In this respect, a better characterisation and validation of the Calu-3 cell layers after LPS insult could be useful to determine more appropriate experimental conditions. For example, since the TEER values registered were < 400 $\Omega \cdot cm^2$ only at the end of the experiment, it is not clear when exactly the cell layers were being damaged, so an optimisation of the duration of the experiment is highly recommended. Also, different time spans between the LPS insult and the execution of the transport experiments should be explored. In fact, as demonstrated in Chapter 6, keeping the Calu-3 cell layers in LLC conditions for 48 hours caused the complete depletion of the mucus layer that normally covers the cell layers, thus making the cells more vulnerable to the bombardment of particles released by the PennCentury™ Dry Powder Insufflator. Allowing a time-span of for example 24 hours, could allow for the mucus layer to be restored. However, this new time-span will have to be compatible with the life-time of the extra OCT transporters expressed as a consequence of the LPS insult. Therefore, making sure that the overexpression of the OCT remains unvaried during this time-span is also highly recommended.

A better model to assess the effect of dry powder deposition on OCT activity would be the use of Calu-3 cell layers whose expression of OCT transporters has been genetically modified. To our knowledge, examples of genetically manipulated Calu-3 cells are not available in the literature. While OCT knockdown has been reported in BEAS-2B cells (Nakamura *et al.* 2010), these are unable to form TJs and are thus of limited value for drug absorption studies.

The final aim of this doctoral study was to provide a better understanding of the role of mucus on dry powder particles dissolution and drug absorption after deposition.

Pig tracheal mucus was chosen as *in-vitro* model to reproduce the mucus layer due to its similarity to human mucus and its higher availability. An *in-vitro* model consisting

of Transwell® inserts semipermeable membranes coated with an even thin layer of mucus was successfully developed, although the minimum layer thickness allowed was higher (≈100 µm) than what is found *in-vivo* (≈10µm in the upper airways (Patton *et al*. 2010)). This was considered to be an acceptable compromise since the complete and even coating of the whole surface of the Transwell® insert was essential.

As discussed in Chapter 6, the permeation of salbutamol sulfate and indomethacin across the three barriers investigated (clean Transwell® inserts, mucus layer and Calu-3 cell layers) followed an opposite order, demonstrating that the mucus was acting as a barrier in the case of salbutamol, but conversely promoted dissolution of indomethacin particles. This observation was surprising in the case of indomethacin where we would have expected a more evident effect of the mucus as a barrier, also in consideration of its low water solubility. In fact, as explained in Chapter 6, lipophilic drugs have showed higher affinity with mucus (Sigurdsson *et al*. 2013). However, as already explained, taking into account the acidic character of indomethacin helps in the understanding of these observations. A similar behaviour was reported for other acidic drugs, such as ibuprofen ($pK_a$≈5.2), whose permeation across gastric mucus increased with an increase of pH, and this was attributed to the change in the ionisation of the drug (Shaw *et al*. 2005). In addition, at pH>$pK_a$ indomethacin carries a net negative charge, therefore it would show electrostatic repulsion towards the negatively charged mucin fibres. On the other hand, salbutamol is positively charged at physiological pH, therefore, despite not presenting solubility issues, it would remain trapped in the mucin network because of electrostatic interactions (Sigurdsson *et al*. 2013).

The methods used to monitor the particle dissolution after deposition on the mucus layer presented technical issues, although it is recognised particle dissolution was quite

fast. Other techniques such as atomic force microscopy (AFM) (Danesh *et al.* 2001) or Raman spectroscopy (Tres *et al.* 2015) may be more informative in respect to particle dissolution.

Finally, it was demonstrated that the delivery of dry powder formulation of salbutamol sulfate and indomethacin leads to a faster absorption across the lung epithelium in comparison to the solution counterpart. This could contribute to a faster onset of action of the API, but at the same time could result in a short residence time, and therefore require multiple dosing. However, clinical data revealed no significant improvement of dry powder administration of salbutamol in comparison to nebulisation, which has been attributed to the fact patients are very often not-properly trained in the use of DPI, with a consequent reduction in the drug deposition in the lung (Geller 2005; Raimondi *et al.* 1997). On the other hand, no pharmacokinetics or clinical data is currently available for inhaled indomethacin, therefore it is not possible to compare our findings with the clinical situation.

Due to the high permeability of indomethacin, designing formulations with the intent of enhancing its solubility in the lung is recognised not necessary. Conversely, it may be more interesting investigating opportunities for formulations allowing longer residence times for a prolonged effect.

Although the importance of novel platforms for pulmonary delivery (e.g. UCL formulations) to improve solubility of poorly soluble drugs in water is acknowledged, the choice of indomethacin as a model drug was probably not the most appropriate due to its acidic character that results in a pH-dependent solubility in water. The effect of the UCL formulations on drug solubility may have been more appreciable with a drug exhibiting different physicochemical properties (e.g. alkali or positively charged).

The findings reported in this doctoral thesis are important in the field of pulmonary delivery as they contribute to a better understanding of the fate of particles for inhalation once landed on the lung epithelium surface.

In particular, a contribution in the clarification of the role of the mucus was made with the identification of some of the parameters that affect drug-mucus interaction: ionisation and lipophilicity. Solubility in water does not seem to have the same impact as for oral delivery, but it could be less important than by other properties such as the acidic or basic character of the drug. In this respect, we confirmed that the BCS, which only takes into account drug solubility and permeability, was a non-adequate description for the prediction of the behaviour of indomethacin in the lungs.

The understanding of how the physicochemical properties of particles for inhalation affect their fate in the lungs is extremely important during drug development as it would help in the design of formulations with the desired residence time and bioavailability. For example, while it is possible to target an environment with optimal pH after administration to the GI tract (e.g. by choosing between the fasted or fed state, or using enteric coated tablets that will only dissolve at the higher pH of the intestine), in the case of pulmonary delivery there is no possibility to change the physiological pH of the mucus. This would mean that in order to exploit the effect of ionisation status of the drug molecule to improve its permeation across the mucus layer, the only option is to either chemically modify the nature of the molecule or improve the formulation in order to create a local environment suitable for promoting particle dissolution and increasing the chance of drug absorption.

## 7.3. References

Danesh, A. *et al.*, 2001. An in situ dissolution study of aspirin crystal planes (100) and (001) by atomic force microscopy. *Pharmaceutical Research*, 18(3), pp.299–303.

Geller, D.E., 2005. Comparing clinical features of the nebulizer, Metered-Dose Inhaler, and Dry Powder Inhaler. *Respiratory Care*, 50(10), pp.1313–1322.

Grainger, C.I. *et al.*, 2009. The permeability of large molecular weight solutes following particle delivery to air-interfaced cells that model the respiratory mucosa. *European Journal of Pharmaceutics and Biopharmaceutics*, 71(2), pp.318–324.

Hein, S. *et al.*, 2010. The Pharmaceutical Aerosol Deposition Device on Cell Cultures (PADDOCC) in vitro system: design and experimental protocol. *Alternatives to Laboratory Animals: ATLA*, 38(4), pp.285–295.

Kim, J.S. *et al.*, 2013. Validation of an in vitro exposure system for toxicity assessment of air-delivered nanomaterials. *Toxicology In Vitro*, 27(1), pp.164–173.

Nakamura, T. *et al.*, 2010. Transport of ipratropium, an anti-chronic obstructive pulmonary disease drug, is mediated by organic cation/ carnitine transporters in human bronchial epithelial cells: implications for carrier-mediated pulmonary absorption. *Molecular Pharmaceutics*, 7(1), pp.187–195.

Patton, J.S. *et al.*, 2010. The particle has landed - Characterizing the fate of inhaled pharmaceuticals. *Journal of Aerosol Medicine and Pulmonary Drug Delivery*, 23(S2), pp.S71–S87.

Raimondi, C. *et al.*, 1997. Treatment of acute severe asthma with inhaled albuterol delivered via jet nebulizer, metered dose inhaler with spacer, or dry powder. *CHEST Journal*, 112(1), pp.24–28.

Shaw, L.R. *et al.*, 2005. The influence of excipients on the diffusion of ibuprofen and

paracetamol in gastric mucus. *International Journal of Pharmaceutics*, 290(1), pp.145–154.

Sigurdsson, H.H., Kirch, J. & Lehr, C.M., 2013. Mucus as a barrier to lipophilic drugs. *International Journal of Pharmaceutics*, 453(1), pp.56–64.

Tres, F. *et al.*, 2015. Monitoring the dissolution mechanisms of amorphous bicalutamide solid dispersions via real-time Raman mapping. *Molecular Pharmaceutics*, 12(5), pp.1512–1522.

# Appendix I: ImageJ macros

## I.1. ImageJ batch analysis for surface coverage calculation

```
function ProcessSingleImage(inputFolder,outputFolder,filename)

{
open(inputFolder + filename);
run("Set Scale...", "distance=1358 known=897.6 pixel=1 unit=um global");
run("Colors...", "foreground=white background=black selection=yellow");
originalImage=getImageID();  // Store the original images ID
run("Duplicate...", "title=copyOF" + getTitle);
copyOF=getImageID; // Store the copy's ID
setAutoThreshold("Default");
setThreshold(0, 91);
setOption("BlackBackground", false);
run("Convert to Mask");
run("Remove Outliers...", "radius=2 threshold=50 which=Dark");
run("Set Measurements...", "area centroid center fit shape feret's area_fraction
display add redirect=None decimal=1");
run("Analyze Particles...", "size=0-Infinity circularity=0.00-1.00 show=[Bare Outlines]
display summarize add in_situ");
selectImage(originalImage);
run("From ROI Manager");
save(outputFolder+filename);
close();
}

function Cleanup()
{
        roiManager("Delete");
        close();
}

InputDir = "C:\\";
OutputDir = "C:\\";
format = "JPEG";

setBatchMode(false);
ImagesToProcess = getFileList(InputDir);

for (i=0; i<ImagesToProcess.length; i++)
{
        ProcessSingleImage(InputDir, OutputDir, ImagesToProcess[i]);
        Cleanup();
```

```
        showProgress(i, ImagesToProcess.length);
};
```

## I.2. ImageJ batch analysis for particles size analysis

```
function ProcessSingleImage(inputFolder,outputFolder,filename)

{
open(inputFolder + filename);
run("Set Scale...", "distance=1358 known=448.8 pixel=1 unit=um global");
run("Colors...", "foreground=white background=black selection=yellow");
originalImage=getImageID();
run("Duplicate...", "title=copyOF" + getTitle);
copyOF=getImageID;
run("Enhance Contrast", "saturated=0.35");
setMinAndMax(130, 167);
setOption("BlackBackground", false);
run("Convert to Mask");
run("Remove Outliers...", "radius=2 threshold=50 which=Dark");
run("Set Measurements...", "area centroid center fit shape feret's area_fraction
display add redirect=None decimal=1");
makePolygon(2,0,1136,0,1346,4,1348,226,1158,230,1158,304,1358,300,1356,1018
,2,1018);
run("Analyze Particles...", "size=0-Infinity circularity=0.00-1.00 show=[Bare Outlines]
display exclude summarize add in_situ");
selectImage(originalImage);
run("From ROI Manager");
save(outputFolder+filename);
close();
}

function Cleanup()

{
        roiManager("Delete");
        close();
}

InputDir = "C:\\";
OutputDir = "C:\\";
format = "JPEG";

setBatchMode(false);
ImagesToProcess = getFileList(InputDir);

for (i=0; i<ImagesToProcess.length; i++)
{
        ProcessSingleImage(InputDir, OutputDir, ImagesToProcess[i]);
        Cleanup();
        showProgress(i, ImagesToProcess.length);
};
```

# Appendix II:
# Dose delivered study

**Table I. 1: doses [µg] of salbutamol sulfate deposited in Transwell® inserts after being sprayed from 20 cm without the Quickfit receiver**

| | POSITION | Salbutamol sulfate loading [mg] | | |
|---|---|---|---|---|
| | | 2.0 | 1.0 | 0.5 |
| 12 WELL PLATE | A1 | 1.57 ± 0.57 | 0.73 ±0.09 | 0.31 ± 0.13 |
| | A2 | 4.74 ± 2.10 | 0.80 ± 0.52 | 0.50 ± 0.26 |
| | A3 | 2.90 ± 0.08 | 1.20 ± 0.13 | 0.87 ± 0.08 |
| | A4 | 1.04 ± 0.46 | 0.48 ± 0.23 | 0.17 ± 0.07 |
| | B1 | 3.12 ± 1.50 | 0.49 ± 0.20 | 0.39 ± 0.07 |
| | B2 | 7.25 ± 1.67 | 1.54 ±1.07 | 1.44 ± 0.34 |
| | B3 | 5.61 ± 3.20 | 1.76 ± 1.02 | 0.88 ± 0.41 |
| | B4 | 1.30 ± 0.26 | 0.65 ± 0.08 | 0.26 ± 0.06 |
| | C1 | 3.24 ± 2.50 | 0.40 ± 0.26 | 0.27 ± 0.07 |
| | C2 | 4.89 ± 3.43 | 0.80 ± 0.32 | 0.62 ± 0.23 |
| | C3 | 3.22 ± 1.23 | 1.23 ± 0.88 | 0.33 ± 0.04 |
| | C4 | 1.16 ± 0.03 | 0.43 ± 0.30 | 0.30 ± 0.20 |
| Triangle | V1 | 1.45 ± 0.56 | 0.48 ± 0.12 | 0.37 ± 0.21 |
| | V2 | 1.31 ± 0.65 | 0.45 ± 0.34 | 0.23 ± 0.10 |
| | V3 | 0.98 ± 0.26 | 0.33 ± 0.10 | 0.25 ± 0.14 |
| | S1 | 2.80 ± 1.47 | 1.21 ± 1.24 | 0.47 ± 0.01 |
| | S2 | 3.15 ± 2.05 | 1.35 ± 0.49 | 0.54 ± 0.07 |
| | S3 | 2.09 ± 0.30 | 0.81 ± 0.31 | 0.54 ± 0.08 |
| Hexagon | A | 6.30 ± 0.95 | 0.64 ± 0.07 | 0.35 ± 0.19 |
| | B | 5.54 ± 1.46 | 1.67 ± 1.11 | 0.50 ± 0.12 |
| | O | 24.27 ± 7.26 | 4.31 ± 1.10 | 0.91 ± 0.35 |
| | C | 6.01 ± 2.32 | 1.15 ± 0.28 | 0.32 ± 0.15 |
| | D | 4.29 ± 2.60 | 1.15 ± 0.92 | 0.16 ± 0.01 |
| | E | 5.38 ± 2.70 | 0.79 ± 0.36 | 0.18 ± 0.09 |
| | F | 2.14 ± 0.61 | 0.99 ± 0.53 | 0.42 ± 0.41 |
| Large hexagon | A | 0.70 ±0.05 | 0.41 ± 0.06 | 0.13 ± 0.01 |
| | B | 0.94 ± 0.39 | 0.40 ± 0.22 | 0.45 ± 0.59 |
| | O | 3.19 ± 0.54 | 1.64 ± 0.23 | 0.66 ± 0.22 |
| | C | 0.96 ± 0.30 | 0.32 ± 0.09 | 0.11 ± 0.05 |
| | D | 0.84 ± 0.21 | 0.50 ± 0.11 | 0.15 ± 0.05 |
| | E | 0.83 ± 0.26 | 0.47 ± 0.07 | 0.12 ± 0.02 |
| | F | 0.85 ± 0.43 | 0.36 ± 0.11 | 0.18 ±0.05 |

**Table I.2: doses [µg] of salbutamol sulfate deposited in Transwell® inserts after being sprayed from 20 cm using the Quickfit receiver**

| | | Salbutamol sulfate loading [mg] | |
|---|---|---|---|
| | **POSITION** | **2.0** | **1.0** |
| **12 WELL PLATE** | **A1** | 0.27 ± 0.23 | 0.36 ± 0.35 |
| | **A2** | 0.42 ± 0.32 | 0.47 ± 0.35 |
| | **A3** | 0.29 ± 0.30 | 1.03 ± 1.39 |
| | **A4** | 0.17 ± 0.16 | 0.56 ± 0.90 |
| | **B1** | 0.26 ± 0.22 | 0.26 ± 0.24 |
| | **B2** | 3.20 ± 5.25 | 1.08 ± 0.46 |
| | **B3** | 1.46 ± 1.05 | 2.47 ± 2.04 |
| | **B4** | 0.30 ± 0.18 | 0.34 ± 0.41 |
| | **C1** | 0.26 ± 0.24 | 0.36 ± 0.31 |
| | **C2** | 0.78 ± 0.82 | 0.30 ± 0.19 |
| | **C3** | 0.28 ± 0.20 | 0.75 ± 0.64 |
| | **C4** | 0.24 ± 0.25 | 0.29 ± 0.41 |
| **Triangle** | **V1** | 0.40 ± 0.22 | 0.44 ± 0.44 |
| | **V2** | 0.73 ± 0.68 | 0.58 ± 0.26 |
| | **V3** | 0.44 ± 0.37 | 0.14 ± 0.11 |
| | **S1** | 0.62 ± 0.08 | 0.45 ± 0.23 |
| | **S2** | 1.94 ± 1.90 | 0.78 ± 0.91 |
| | **S3** | 0.78 ± 0.14 | 0.28 ± 0.23 |
| **Hexagon** | **A** | 2.82 ± 2.94 | 1.16 ± 1.18 |
| | **B** | 0.65 ± 0.45 | 0.50 ± 0.67 |
| | **O** | 6.33 ± 1.98 | 5.20 ± 2.59 |
| | **C** | 0.88 ± 0.38 | 0.50 ± 0.41 |
| | **D** | 0.26 ± 0.20 | 0.27 ± 0.17 |
| | **E** | 0.84 ± 0.63 | 0.43 ± 0.41 |
| | **F** | 0.30 ± 0.28 | 1.02 ± 0.22 |

**Table I.3: doses [µg] of indomethacin deposited in Transwell® inserts after deposition of either micronised indomethacin or individual UCL formulations spray**

| | POSITION | Salbutamol sulfate loading [mg] | | |
|---|---|---|---|---|
| | | 2.0 | 1.0 | 0.5 |
| Micronised Indomethacin | A | 0.79 ± 0.35 | 0.37 ± 0.07 | 0.21 ± 0.16 |
| | B | 0.67 ± 0.19 | 0.30 ± 0.15 | 0.24 ± 0.25 |
| | O | 10.59 ± 6.29 | 4.78 ± 2.08 | 0.98 ± 0.20 |
| | C | 0.86 ± 0.17 | 0.54 ± 0.30 | 0.09 ± 0.02 |
| | D | 1.50 ± 1.00 | 0.61 ± 0.18 | 0.15 ± 0.10 |
| | E | 1.05 ± 0.56 | 0.48 ± 0.26 | 0.12 ± 0.10 |
| | F | 0.68 ± 0.34 | 0.58 ± 0.51 | 0.22 ± 0.23 |
| IND – F68 | A | 0.63 ± 0.18 | 0.44 ± 0.30 | 0.24 ± 0.11 |
| | B | 0.75 ± 0.57 | 0.40 ± 0.19 | 0.42 ± 0.15 |
| | O | 11.12 ± 0.84 | 5.49 ± 3.70 | 2.05 ± 0.34 |
| | C | 0.33 ± 0.04 | 0.27 ± 0.08 | 0.18 ± 0.05 |
| | D | 0.92 ± 0.69 | 0.34 ± 0.11 | 0.27 ± 0.04 |
| | E | 0.58 ± 0.21 | 0.36 ± 0.12 | 0.29 ± 0.13 |
| | F | 0.66 ± 0.35 | 0.29 ± 0.05 | 0.50 ± 0.38 |
| IND – TPGS | A | 0.36 ± 0.15 | 0.23 ± 0.18 | 0.17 ± 0.04 |
| | B | 0.38 ± 0.04 | 0.25 ± 0.02 | 0.59 ± 0.70 |
| | O | 5.20 ± 0.92 | 7.25 ± 4.45 | 1.80 ± 0.40 |
| | C | 0.40 ± 0.06 | 0.52 ± 0.35 | 0.27 ± 0.13 |
| | D | 0.47 ± 0.16 | 0.50 ± 0.09 | 0.34 ± 0.08 |
| | E | 0.79 ± 0.13 | 0.31 ± 0.02 | 0.23 ± 0.08 |
| | F | 0.57 ± 0.21 | 0.44 ± 0.19 | 0.31 ± 0.16 |
| IND – F68 + MF | A | 0.69 ± 0.39 | 0.24 ± 0.12 | 0.14 ± 0.05 |
| | B | 0.69 ± 0.18 | 0.26 ± 0.08 | 0.19 ± 0.15 |
| | O | 2.95 ± 1.10 | 1.69 ± 0.09 | 0.74 ± 0.38 |
| | C | 0.89 ± 0.40 | 0.22 ± 0.01 | 0.10 ± 0.02 |
| | D | 0.74 ± 0.46 | 0.21 ± 0.12 | 0.11 ± 0.03 |
| | E | 0.95 ± 0.47 | 0.21 ± 0.07 | 0.15 ± 0.07 |
| | F | 0.92 ± 0.79 | 0.35 ± 0.06 | 0.13 ± 0.05 |
| IND – TPGS + MF | A | 0.51 ± 0.08 | 0.48 ± 0.40 | 0.11 ± 0.02 |
| | B | 0.37 ± 0.06 | 0.21 ± 0.10 | 0.17 ± 0.03 |
| | O | 4.33 ± 0.97 | 1.69 ± 0.32 | 0.53 ± 0.26 |
| | C | 0.35 ± 0.07 | 0.20 ± 0.04 | 0.15 ± 0.11 |
| | D | 0.69 ± 0.15 | 0.36 ± 0.16 | 0.18 ± 0.04 |
| | E | 0.80 ± 0.08 | 0.47 ± 0.09 | 0.15 ± 0.10 |
| | F | 0.69 ± 0.09 | 0.32 ± 0.05 | 0.17 ± 0.07 |